

NO.

89

NTN
TECHNICAL
REVIEW

2022 - 2023

Special Issue

Strengthening the Services and
Solutions Business and
Responding to the Shift to EVs and
Automotive Electrification



NTN TECHNICAL REVIEW

No. 89

Special Issue

**Strengthening the Services and
Solutions Business and
Responding to the Shift to EVs and
Automotive Electrification**

NTN TECHNICAL REVIEW No.89

CONTENTS

Preface	Special Issue “Strengthening the Services and Solutions Business and Responding to the Shift to EVs and Automotive Electrification.” Masaki EGAMI	1
Contribution	The Current Situation of Condition Monitoring and Diagnosis of Machine Systems Tsuyoshi INOUE, Ph.D. Professor, Department of Mechanical Systems Engineering, Graduate School of Engineering, Nagoya University	2
Service and Solution Related Technologies		
	Efforts for Service & Solution Business in NTN Hiroyuki KUREBAYASHI	23
	Development of Remaining Useful Life Prediction Technology for Rolling Bearings Under Flaking Progression Masashi KITAI	29
	Development of Sensor Integrated Bearing “Talking Bearings™” Yasuyuki FUKUSHIMA, Tomomi GOTO, Yosuke TOYOGUCHI, Daigo IKKE, Kohei MATSUBAYASHI	35
	Development of Multi Track Magnetic Encoder Integrated Rolling Bearing Hiroshi OKUMURA, Hiroyoshi ITO, Yasuyuki HAMAKITA	41
	Development of Sensor Integrated Bearing Unit for Machine Tool Spindles Shohei HASHIZUME, Yudai NAKANO, Daichi KONDO, Yoji OHGUCHI, Yohei YAMAMOTO	47
	Bearing Diagnostic Edge Application for Industrial IoT Platforms Yudai NAKANO, Takashi HASEBA	53
EV and Electrification-Ready Technologies		
	NTN’s Activities for Electric Vehicle and Electrification of Automobile Ikuya TATEOKA	58
	Introduction of Rolling Bearings for Electric Drives Corresponding of Automobiles Takashi KAWAI, Tomohisa UOZUMI	65
	Evolution of Fixed Constant Velocity Joint that Contributes to Environmental Protection Masashi FUNAHASHI, Teruaki FUJIO, Ritsuki SAKIHARA	73
	Introduction of Composite Material Products Used in Electrical Auxiliaries for Automobile Ken YASUDA, Shinji KOMATSUBARA	79
Evaluation and Analysis Techniques		
	A Life Estimation Method of Peeling in Rolling Bearings Under Mixed Lubrication Conditions Naoya HASEGAWA, Takumi FUJITA, Michimasa UCHIDATE, Masayoshi ABO	85
	Development of Technical Calculation Systems for Rolling Bearings Tomomi ISHIKAWA, Hiroyasu HIRUKAWA, Mariko IZUMI, Cedric BURNET	91
New Product Introduction		
	Development of Feeder “TRINITTE” for Picking Robots Shuhei MATSUI	96
	Product Introduction of Compact Torque Diode (TDL8) Masayuki OHARA	99
	Application Examples of the Wrist Joint Module “i-WRIST™” Yuzuru TANAKA	102
Award Winning Products		
	Low Friction HUB Bearing III Makoto SEKI	106
	High Speed Deep Groove Ball Bearing for EV/HEV Goro NAKAO, Katsuaki SASAKI, Yukihiro ISHIDA, Kazunori MURANUSHI	107
	Development of Super Long-Life Tapered Roller Bearings for Automobile Hiroki FUJIWARA, Takashi KAWAI, Chikara OHKI	108
	Low Friction Technology of Sealed Ball Bearings for Transmission Tomohiro SUGAI, Katsuaki SASAKI, Takahiro WAKUDA	109
	Estimation Method of Micropitting Life from $S-N$ Curve Established by Residual Stress Measurements and Numerical Contact Analysis Naoya HASEGAWA, Takumi FUJITA, Michimasa UCHIDATE, Masayoshi ABO, Hiroshi KINOSHITA	110
	DLC Coating Spherical Roller Bearing for Wind Turbine Main Shaft Kazumasa SEKO, Takashi YAMAMOTO, Masaki NAKANISHI	111

Special Issue

“Strengthening the Services and Solutions Business and Responding to the Shift to EVs and Automotive Electrification.”



Executive Officer, CTO (Chief Technical Officer)
Masaki EGAMI

Against the backdrop of global warming and climate change issues, global efforts to achieve net-zero greenhouse gas emissions, or carbon neutrality, are gaining pace. **NTN** is committed to contributing to the realization of a carbon-neutral society. We are promoting research and development with a focus on our material issues of realizing a sustainable society powered by natural energy and of reducing energy loss. We also have advanced CAE technology, which aids us as we design our products and study technologies. CAE enhances the reliability of our products and our ability to make proposals to our customers. In this issue, we feature our efforts in the areas of (1) Service and Solution Related Technologies, (2) EV and Electrification-Ready Technologies, and (3) Evaluation and Analysis Techniques. We also introduce three of our new products and six products and technologies that have received external awards.

In Special Feature 1, we introduce technologies and products that contribute to the spread of wind power generation and help improve the productivity of operating equipment. The use of wind power generation systems is expanding globally. Key tasks are to ensure their stable operation and to curb power generation costs. **NTN** has contributed to the stable operation of wind power generation equipment and reduction of operating costs by providing Wind Doctor™. This monitoring service remotely collects and monitors vibration and other data from wind power generation equipment and notifies customers of anomalies and changes, thereby reducing the need for operation management and maintenance. We have also developed technologies and products that contribute to the stable operation of equipment and improved productivity, such as rolling bearings with built-in sensors, including Talking Bearings™, portable vibrosopes, and bearing diagnostics applications compatible with the Edgexcross™ IoT platform. We will introduce these technologies and products here.

In Special Feature 2, we introduce our technologies and products for bearings, hub bearings, and constant velocity joints for automotive electrification. The pursuit of carbon neutrality is driving a rapid shift toward automotive electrification. A key task in this is to stretch the cruising range of EVs. This in turn calls for smaller and more efficient onboard components, including key components such as those used in e-Axles. **NTN** has been contributing to the reduction of energy loss in vehicles by bringing new products to the market that deliver smaller sizes and greater efficiency in bearings, hub bearings, and constant velocity joints. We have also been developing highly functional and efficient modular products that take advantage of our core technologies in tribology, mechanical design, and mechatronics, such as electric ball screw units, electric oil pumps, and the Ra-sHUB™, a hub bearing with a steering mechanism. We will introduce these technologies and products here.

Special Feature 3 introduces Evaluation and Analysis Techniques that use CAE for rolling bearing design and bearing operating life estimation. Proposing, in a timely manner, competitive products aligned to market trends and customer needs calls for greater sophistication and higher efficiency in product design work and product performance evaluation. This paper introduces a newly developed integrated technical calculation system for rolling bearings and a CAE calculation system that semi-automates the design process of hub bearings. In addition, we introduce analysis technology that enables reliable bearing design under conditions where oil film formation is insufficient. This technology addresses the shift toward lower viscosity lubricants which stems from the demand for more efficient machines.

We hope that our technologies and products introduced in this issue will help bring about a carbon-neutral society. Guided by our corporate philosophy “For New Technology Network: Connecting the world through new technologies”, we shall contribute to international society through creating new technologies and developing new products. We will work toward the further development of industry, while coexisting with nature, through research and development activities centered on carbon neutrality.

The Current Situation of Condition Monitoring and Diagnosis of Machine Systems



Tsuyoshi INOUE

Ph.D. Professor, Department of Mechanical Systems Engineering, Graduate School of Engineering, Nagoya University

Recently, condition monitoring and diagnosis technologies for machine systems have been rapidly developing and attracting attention. This paper first reviews the recent trends in condition monitoring and diagnosis of mechanical systems, referring to the standardization activities of ISO/TC 108/SC 5, in which the author has been involved for many years. Subsequently, this paper introduces the recent trends in asset management and condition monitoring, condition monitoring and diagnosis of wind power generation, IoT for predictive maintenance, and condition monitoring and diagnosis using 1DCAE as the latest topics. Finally, some topics regarding condition monitoring and diagnosis of machine systems and bearings at domestic conferences in the past few years have been introduced.

1. Introduction

I have been involved in ISO standardization activities for ISO/TC 108/SC 5 Condition Monitoring and Diagnostics of Mechanical Systems since 2004. I will first briefly review the standardization activities of ISO/TC 108/SC 5 and then give an overview of recent developments in condition monitoring and diagnostics of mechanical systems. The first half of the paper (Chapters 2 and 3) is mainly based on a commentary article¹⁾ written and published in the journal "Nondestructive Inspection" in 2020, with an update based on information from the last two years.

The latter half of the paper (Chapters 4 to 7) will cover recent trends in asset management and condition monitoring, condition monitoring and diagnostics for wind power generation, IoT for predictive maintenance, and condition monitoring and diagnostics using 1DCAE. Finally, we will introduce some content from presentations at domestic academic conferences in the past few years that relate to condition monitoring and diagnostics of bearings.

2. International Trends in Condition Monitoring and Diagnostics of Machine Systems¹⁾

2.1 Scope of ISO TC 108/SC 5

ISO/TC 108/SC 5 is officially called "Condition monitoring and diagnostics of machine systems". The purpose and scope of SC 5 provided on the website²⁾ are as shown below.

Standardization of the procedures, processes and equipment requirements uniquely related to the activity of condition monitoring and diagnostics of machine systems is an important part of all programs with selected physical parameters associated with an operating machine system are periodically or continuously monitored, measured and recorded for the interim purpose of reducing, analyzing, comparing and displaying the data and information obtained to support decisions related to the operation and maintenance of the machine system.

2.2 Working Group for ISO TC 108/SC 5

The working groups (WGs) established in ISO/TC 108/SC 5 as of September 2022 are listed in **Table 1** and introduced individually below.

AG E: This is a working group for discussing the overall strategic plan for SC 5. Here, the overall direction of international standardization of SC 5, how to proceed with the work of each working group, and the establishment and dissolution of working groups are examined and discussed. The initial draft of the preliminary work item (PWI), which assumes that a new working group will be established in the future, is also considered here.

Table 1 Working Group²⁾ of ISO/TC 108/SC 5
(as of September 2022)

WG	Technical field
AG E	Strategic planning
WG 7	Training and accreditation in the field of condition monitoring and diagnostics
WG 11	Thermal imaging
WG 16	Condition monitoring and diagnostics of wind turbines
WG 17	Condition monitoring and diagnostics applications
WG 18	Condition monitoring management

WG 7: This working group focuses on the training and certification of condition monitoring technicians. It has developed a series of standards for training and certification. In addition to ISO 18436-1:2021, which covers the entire range, it has published standards for condition monitoring technicians for individual technologies which include ISO 18436-2:2014 Vibration condition monitoring and diagnostics, ISO 18436-4:2014 Field lubricant analysis, ISO 18436-5:2012 Lubricant laboratory technician/analyst, ISO 18436-6:2021 Acoustic emission, ISO 18436-7:2014 Thermography, and ISO 18436-8:2013 Ultrasound. In Japan, certification of machinery condition monitoring technicians based on these 18436 series, has been in previously in place, details of which are described in Chapter 3.

WG 11 Thermal Imaging: This working group focuses on condition monitoring and diagnostic techniques using thermal imaging. It has published ISO standards for general procedures in ISO 18434-1:2008 and for interpretation of images in ISO 18434-2:2019, where images of bearing anomaly detection are also presented. It is currently considering the standardization of optical gas imaging. In addition to WG11, which focuses on thermal imaging, which were previously in many other working groups on condition monitoring and diagnostic techniques (WG3 Performance monitoring and diagnostics, WG4 Tribology, WG10 Condition monitoring and diagnostics of electrical equipment, WG14 Acoustic techniques, WG15 Ultrasound diagnostics, etc.). However, each of these has finished publishing the ISO standards that are currently required and has therefore been disbanded. Information on these disbanded working groups is shown in **Table 2**. If the need arises for a new ISO standard in the same field, or if a major revision of the current ISO standard becomes necessary, we plan to reopen the Working Groups.

WG 16 Wind turbines, WG 17 Applications: These working groups focus on condition monitoring and diagnostics for individual machines. WG16 has completed the standardization of ISO 16079-1: 2017 General Guidelines and ISO 16079-2: 2020 Monitoring the drivetrain. The latter describes the monitoring and diagnosis of bearings and gears for wind turbines. As its name suggests, WG17 covers a wide range of applications. It has published the standard ISO 19283:2020 Hydroelectric generating units and has started the standardization of reciprocating compressors.

WG 18 Asset Management: This is a new working group launched in 2019 that, as of September 2022, is the most active. The condition monitoring and diagnostics of mechanical systems have traditionally been done mainly by the engineers who directly handle machines. However, the need for standardization that also incorporates the perspective of asset management systems, has been raised at SC 5 international meetings (see Section 2.3) for the past 10 years. Now, under the strong leadership of the current SC5 chairman, the working group has begun studying and vigorously promoting the standardization of asset management systems with a specific focus on mechanical systems. The standards being examined are (1) accreditation of condition monitoring managers, (2) accreditation of condition monitoring auditors, and (3) physical asset management.

2.3 International meetings for ISO TC 108/SC 5

In ISO standardization, international meetings play an important role as forums for reviewing and reflecting ballot comments on draft standardization texts and for considering the next standards. The first international meeting of SC 5 was held in 1994, and 23 meetings were held up to 2019. **Table 3** shows the years and venues of the conference. The 24th meeting was originally scheduled to be held in New York in September 2020 but was postponed (and subsequently canceled) for the first time due to global restrictions on international travel arising from the COVID-19 pandemic that began in March 2020. It was held later in May 2022 as the first online meeting. In 2023, with the pandemic now largely under control, Japan will host the meeting in Kyoto, which will be the first in-person meeting in four years.

Table 2 Working groups established in SC 5^{1) 2)}

WG	Technical field
AG A	Vibration condition monitoring procedures and instrumentation used for diagnostics
WG 1	Terminology
WG 2	Data interpretation and diagnostics techniques
WG 3	Performance monitoring and diagnostics
WG 4	Tribology-based monitoring and diagnostics
WG 5	Prognostics
JWG 6	Formats and methods for communicating, presenting and displaying relevant information and data
WG 8	Condition monitoring and diagnostics of machines
WG 10	Condition monitoring and diagnostics of electrical equipment
WG 14	Acoustic techniques (Acoustic emissions)
WG 15	Ultrasound
For these working groups, items to be discussed to consider future projects or new areas of work are included in each year's meeting. These are examined, along with considering the resumption of activities.	

Table 3 List of SC 5 International Conferences¹⁾

1st	1994	Swansea	UK
2nd	1995	London	UK
3rd	1996	Sydney	AU
4th	1997	Berlin	DE
5th	1998	Tasmania	AU
6th	1999	Copenhagen	DK
7th	2000	Nanjing	CN
8th	2001	Vienna	AS
9th	2002	Minden, NV	USA
10th	2003	Paris	FR
11th	2004	London	UK
12th	2005	Dania Beach, FL	USA
13th	2007	Prague	CZ
14th	2008	Kyoto	JP
15th	2009	Copenhagen	DK
16th	2010	London	UK
17th	2011	Sydney	AU
18th	2013	Berlin	DE
19th	2014	Paris	FR
20th	2016	Sydney	AU
21st	2017	London	UK
22nd	2018	Helsinki	FI
23rd	2019	Copenhagen	DK
24th	2022	Online	
25th	2023	Kyoto (scheduled)	JP

2.4 ISO TC 108/SC 5: Status of activities and outlook

The latest SC 5 activities can be found on the ISO Website. The current chairman is Mr. L. Hitchcock (SA), the fourth chairman. The secretary is Mr. A. Rashid (SA). As of September 2022, the P-members (Participation members) consisted of 23 countries and regions, while O-members (Observer members) consisted of 12 countries and regions.

Fig. 1 shows the status of SC 5 standards as of September 2022. SC 5 has published 28 international standards. Five standards are in the process of being established or revised.

and diagnostics of machines (vibration) has been implemented by the Japan Society of Mechanical Engineers (JSME³⁾) since June 2004. A total of 5 472 persons have been certified by the 37th examination to be held in August 2022. In Category I, the number of qualified personnel is 819. In Category II, it is 4 557. In Category III it is 434. On average, around 10 people receive accreditation in Category I, 100 in Category II, and 20 to 30 in Category III. In addition, 41 people have received accreditation in Category IV, which is positioned as equivalent to a Doctor of Engineering or a professional engineer. This shows the high level of engineers involved in vibration technology in Japan. It is hoped that those who aspire to work internationally as engineers, will take up the challenge of Category III and IV.

The accreditation system for the qualification of technicians who perform condition monitoring and diagnostics of machines (tribology) has been implemented for Categories I - III since FY2009 through joint certification by JSME³⁾ and the Japanese Society of Tribologists (JAST). As of September 2022, a total of 1 421 persons have been certified. (In Category I, the number of qualified personnel is 1 176. In Category II, it is 234, and in Category III it is 11.)

The qualification examinations for technicians who perform condition monitoring and diagnostics of machines (thermography) have been conducted by the Japanese Society for Non-Destructive Inspection (JSNDI) for Category I since FY2016 and for Category II since FY2018. A total of 206 people (173 and 33 for Categories I and II, respectively) have passed the examination as of September 2022.

JSNDI (Certification Division for CM Engineers) and JSME (Japan Society for Machine Monitoring Engineers) have formed a partnership for administering the accreditation of condition monitoring⁴⁾. For example, JSME sponsors meetings of the Condition Monitoring and Vibration Diagnostics Engineer Community. It provides a forum for disseminating information on condition monitoring and for exchange among qualified engineers, including JSNDI's qualified CM engineers and other related parties⁴⁾.

3.2 Workshop on condition monitoring and diagnostics techniques

The ISO/TC 108/SC 5 National Committee organizes and holds a seminar entitled "A Must for Global Engineers! Monitoring and Diagnostics of Mechanical Systems, Fundamentals, Practical Know-How, Application Examples and Standards" (hosted by JSME). The content includes an introduction of the SC5 standards and engineer accreditation for condition monitoring, diagnostics using vibration, lubricant analysis, thermal image analysis, introduction of basic technologies for acoustic emissions (AE), diagnosis of large rotating machinery, diagnosis of wind turbines (mainly bearings), current indication diagnosis (added from 2019), and comprehensive diagnosis (added from 2021). The first seminar was held in Tokyo in October 2007 (30 participants). The

second seminar was held in Osaka in October 2007 (15 participants). After a hiatus following the above two seminars, the third seminar was held in Tokyo in September 2016 (29 participants). The fourth seminar was held in September 2018 (44 participants), and the fifth in September 2019 (53 participants).

A book was written based on the contents of the 5th seminar. Entitled "Condition Monitoring and Diagnostic Techniques for Mechanical Systems", it was published in June 2021 (edited by Inoue and Hyodo, Japan Society of Mechanical Engineers, Corona Publishing).⁵⁾ The 6th seminar was held online in November 2021 (150 participants) using this book as the textbook. In fiscal 2022, this workshop was expanded and held in two rounds in November, one for beginners and the other for intermediate-level students. The last three seminars have been fully booked, highlighting the growing need for and interest in this technology with the arrival of the IoT (Internet of Things) era. We will continue to educate people about this field and introduce the activities of the ISO/TC 108/SC 5 National Committee. I hope that through these seminars and publications, people will learn the fundamentals of technology in this field.

4. Condition Monitoring and Asset Management⁶⁾⁻¹⁴⁾

4.1 Europe: Trends in IoT and Asset Management

Ten years have passed since IoT and Industry 4.0 were proposed in the 2010s, and these terms and concepts have spread widely. In Europe and the United States, these technologies have evolved through deep integration with equipment diagnostics and asset management. This year, Kawai summarized equipment diagnostics and IoT in Europe in comparison with Japan as follows.⁶⁾ In Japan, discussions tend to focus on the use of data obtained from equipment in a single factory or company. In contrast, in Europe, the European Integrated Data Infrastructure Project GAIA-X represents the European Data Economy Area. In recognition of the strategic utility of data, GAIA-X integrates various cloud services of companies on a single system, enabling interoperability through a standardized authentication mechanism that facilitates data exchange across industries (Data Economy Area).

It is expected that manufacturers will evolve to a model of providing services to customers. Globally, the customer's usage environment will become a complex system environment that includes not only their own products but also those of other companies.⁸⁾ Japan will be no exception to this trend. As a result, manufacturers will be required to manage the entire life cycle of the user's usage environment as they provide services. It is thus expected that manufacturers will need to collect data generated from the entire user's usage environment, including competitors' products. In particular, sharing and utilizing data from the operation and maintenance phases, which have not been visualized until now, will become a new and important area of research

and development. It is clear that data collaboration involving users will be key.⁸⁾

Let us briefly touch on the report “Applying the Internet of Things (IoT) to Manufacturing”^{6) 9)} which Siemens has compiled on Industrial IoT (IIoT), the collection and centralization of large amounts of machine data from industrial sites. **Fig. 2** shows the major use cases that manufacturers can implement to maximize the added value and ROI (return on investment) to their businesses, modeled in six levels of IIoT maturity. It is recommended that the IIoT be introduced at the basic level, which is relatively easy to handle, and then gradually expanded to achieve greater value. It is interesting to note that the first asset management and asset maintenance are specifically listed as condition monitoring, asset performance management, and predictive maintenance. We will give an overview of these here.

Asset management condition monitoring uses a centralized IoT system to monitor specific parameters (temperature, vibration, pressure, etc.) and key performance indicators (KPIs). It tracks the operational status of all connected assets and, should a problem occur, takes corrective action before that asset fails, thereby maximizing uptime of critical assets. In this way, condition monitoring ensures transparency into the health and performance of assets at locations around the world.

In asset performance management, KPIs are used to monitor and track the condition and status of machines and identify machines that are not performing adequately in terms of efficiency and productivity. In addition, asset performance management applications using IoT can improve performance by making changes to production lines that deviate from optimal operating conditions. In this way, production is accelerated, and positive effects spill over to resource allocation, time-to-market, and customer satisfaction. In addition, KPIs are fine-tuned each time to identify machine performance more accurately, and machines are continuously adjusted based on real-time data to improve performance. In this way, asset performance management improves overall equipment and corporate profits.

Predictive maintenance in asset maintenance dynamically collects and analyzes machine health and performance data. It then identifies parts that have reached key thresholds, determines when maintenance or replacement is required, and performs maintenance only when necessary. This eliminates the need for scheduled maintenance and significantly reduces unscheduled maintenance. As a result, predictive maintenance can reduce unscheduled downtime, lower maintenance costs, improve quality, productivity, asset uptime, availability, and production, and extend the service life of machines. For more information, including other topics of interest, please refer to the report.

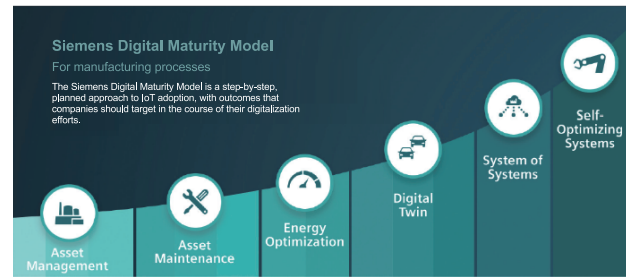


Fig. 2 Siemens Digital Maturity Model^{6) 9)}

Kawai stated that when he attended COMADEM (Condition Monitoring and Diagnostic Engineering Management),¹⁰⁾ a traditional international conference in the field of condition monitoring and diagnosis, he noticed that many of the presentations by Asian researchers were on individual diagnostic techniques, while those by Western researchers were mostly about asset management.⁶⁾ This shows how in Europe and the U.S., research has already expanded in scope to include not only equipment management using diagnostics of anomalies, but also how to realize managerial cost reductions based on such data, taking into consideration the costs of installing diagnostics equipment and conducting diagnostics necessary for that purpose. This point is consistent with the trend of thinking among Western experts, which the author himself has experienced and felt through the standardization activities of ISO/TC 108/SC 5. Japanese engineers and researchers must quickly recognize this global trend so that they can respond appropriately.

4.2 Trends in Japan: Maintenance Optimum Strategic Management System (MOSMS)¹¹⁾⁻¹⁴⁾

In Japan, the Japan Institute of Plant Maintenance (JIPM) has been continuously and actively involved in equipment management. **Fig. 3** shows the history of facilities management in Japan, based on the introduction material of the association¹¹⁾. Facilities management technology continues to expand, as can be seen in the background and history of MOSMS, which integrates these technologies and incorporates asset management.

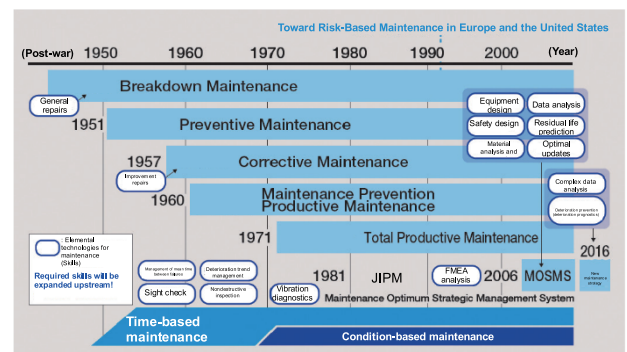


Fig. 3 History of facility maintenance in Japan¹¹⁾

Estimated number of employees (manufacturing and maintenance, thousands)

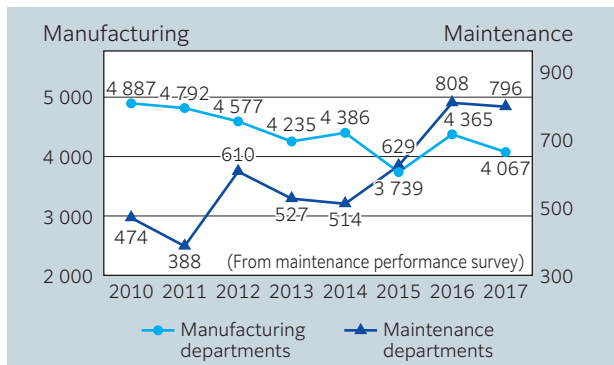


Fig. 4 Number of employees in manufacturing and maintenance departments¹¹⁾

Fig. 4 shows the number of employees in the manufacturing and maintenance departments.¹¹⁾ The results show that the introduction of new equipment has recently decreased. As this has happened, there has been a growing shift toward maintaining and operating existing equipment as well as possible. Therefore, it can be said we are in the age of maintenance.

Given this trend, in 2006, JIPM proposed and started the Maintenance Optimum Strategic Management System (MOSMS).^{12) 13)} Its aim was to build a maintenance system that matched management theory and technology theory through a consistent concept for dealing both with loss (issues that have already occurred) and risk (possibility that such issues may occur in the future). This system clarifies the relationship between the PDCA cycle of management and the PDCA cycle of maintenance (**Fig. 5**). In particular, it emphasizes that in order for maintenance to be integrated with management, a plan must be created that is logical from a management perspective and it must be ensured that maintenance follows the plan (maintenance management).¹³⁾ It is necessary to fully align management and maintenance to create a grand design for maintenance (a maintenance plan offering maximum advantage from a management perspective). MOSMS is a “made in Japan” system that has been developed for this very purpose.

MOSMS lists P (productivity), Q (quality), C (cost), D (delivery time), S (safety), M (motivation), and E (environment) as loss/risk categories, aiming to minimize these loss/risk categories as a result of facility management. The target group is the middle rank (managerial level), which is the same as the target group for asset management in ISO/TC 108/SC 5/WG 18 described in the previous section. To link management and maintenance, as shown in **Fig. 5**, loss/risk management and facility maintenance strategies are incorporated into the P (plan) of the management PDCA cycle. The D (do) of the management PDCA cycle and the P (plan) of the MOSMS PDCA cycle are linked with each other, the C (check) and A (act) of both PDCA cycles are also linked through evaluation of each other.¹⁴⁾ In

this way, the system aims for to align maintenance management, which aims to balance risk and cost, with planned maintenance using technology for continuous improvement.

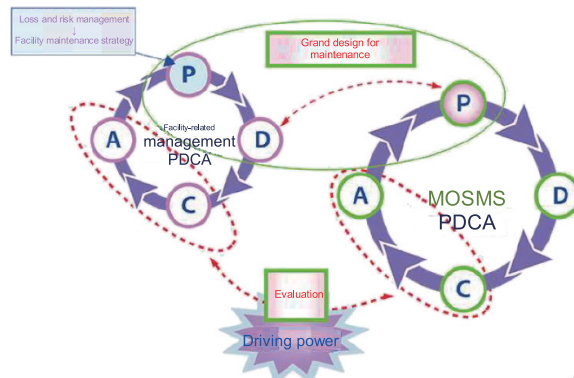


Fig. 5 Linking management and conservation through MOSMS¹⁴⁾

5. Current status of wind power generation and trends in condition monitoring and diagnostics¹⁵⁾⁻²¹⁾

Let us look at wind power generation systems, one of the main systems subject to condition monitoring and diagnostics, and trends in this area.

5.1 Wind power producer trends^{15) 16)}

The following is a summary of a report issued by Accenture^{15) 16)} this fiscal year. Over the past decade, efforts to reduce the Levelized Cost of Electricity (LCOE) of onshore and offshore wind power have expanded and intensified. This has ushered in a digital revolution in the wind power industry. Global onshore wind power generation capacity has risen sharply over the past decade, from 178 GW in 2010 to 594 GW in 2019. Offshore wind power is also growing rapidly, reaching 29 GW of global capacity in 2019.

Fig. 6 shows global offshore wind power capacity and projected short-term growth rates. The power market is investing heavily in offshore wind power, which currently accounts for only about 5 % of global wind power capacity, but with the scale and growth rate of the project, some predict that offshore wind power capacity will nearly triple over the next five years.

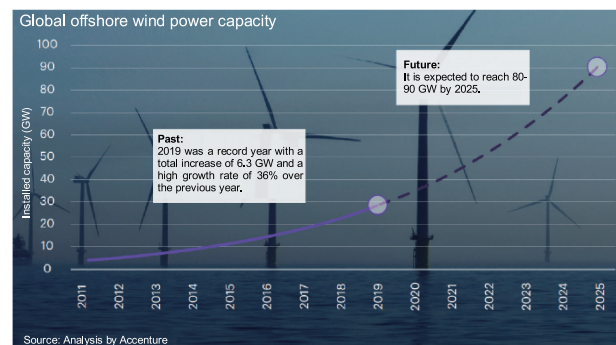


Fig. 6 Global Offshore Wind Power Capacity and Projected Short-Term Growth¹⁵⁾

5.2 Condition monitoring and diagnostics of wind turbines^{15) 16)}

In the wind power business, LCOE has been improved by increasing turbine size (from 2 MW to 12 MW in 10 years in the UK¹⁶⁾), reducing capital investment per MW, and increasing facility utilization (from 30 % to over 40 % in the UK¹⁶⁾). Accordingly, operation and maintenance (Operation & Maintenance, O&M) costs in the LCOE of wind power plants have gradually increased in relative terms and now exceed one-third of the life cycle costs. As a result, there has recently been a growing interest in achieving productivity gains and cost reductions for O&M processes, and digital technology has been identified as one of the key determinants of its success. Accenture has conducted a survey of 11 leading onshore and offshore wind energy companies and identified six key O&M use cases. The results of the study on the impact of advanced digital tools on process improvement for these six key O&M use cases are shown in **Fig. 7**.

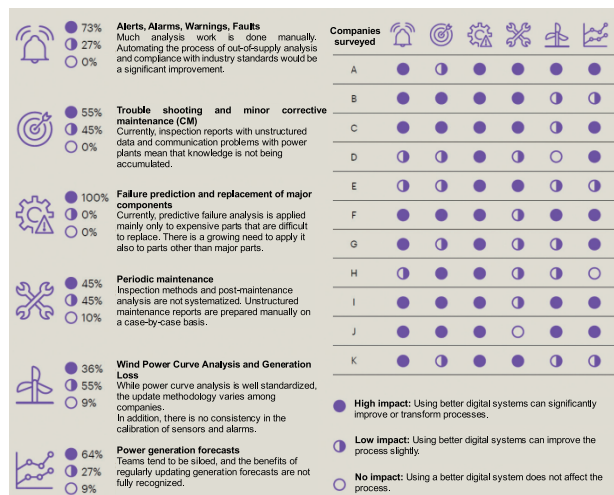


Fig. 7 Degree of impact of advanced digital technologies on key O&M use cases and breakdown of surveyed companies' ratings¹⁵⁾

Three of the six major O&M use cases are related to condition monitoring. Applying advanced digital tools to these three cases offers very high potential for improvement. The following sections provide an overview of three of these use cases individually.

- Alerts, Alarms, Warnings, and Faults: Types of alerts and faults are analyzed to identify trends and patterns for equipment condition analysis, work prioritization, etc. These are incorporated into response time guidelines to minimize loss of generation and cost. The control room monitors alarms and warnings and determines the response. The performance engineering team takes charge of the cause and relevance of alarms and faults, while the asset management team and O&M team identify follow-up actions and prioritize responses.
- Troubleshooting and minor corrective maintenance (CM): The process of investigating and repairing incidents remotely or in the field to reduce

downtime and increase power generation. An operations team monitors plant performance and remotely investigates reported incidents, coordinates field inspections, and handles subsequent activities based on work instructions.

- Failure prediction and major component replacement: Condition monitoring tools and algorithms are used to understand the risk of major component failure within a pre-specified time frame. Setting up an optimally timed major component replacement process reduces downtime and maintenance activities, resulting in cost savings and increased power generation.

In addition, this study comprehensively analyzes the cases above and clarifies the following key findings related to the current role, potential and challenges of digital technology in O&M.^{15) 16)}

Most of the companies surveyed see digital technology as having an important role in fault prediction, alerts and warnings, and trouble shooting. All companies have implemented appropriate custom-built solutions, and many of them would like to develop further functionality. In this regard, a business opportunity has arisen for third-party companies to provide O&M insight services that power producers can implement in their current environments.

- Integrating data of all types throughout the O&M process enables the addition of rich contexts to analytics to create added value. However, because of the low quality of data and the lack of data engineering skills, few companies have achieved this.
- Many companies are willing to improve their O&M processes by learning from past activities and information, such as alert responses and service records. In reality, however, the lack of time and of easy-to-use digital tools makes this difficult to do.
- As for data, data owners, such as owners, power generators, and OEMs (or O&M service providers), are reluctant to share the data and the insights derived from it. Therefore, third-party companies need to clearly define the ownership of the data and consider and provide a partnership model for jointly developing software and tools.

Going forward, based on the abovementioned recognition, advanced digital technologies will be used to devise and build mechanisms for successful data sharing. There will be a rapid global shift to achieve increased productivity and cost reduction for the O&M process of wind power generation. In this regard, condition monitoring and diagnostics will play an important role.

5.3 Wind Power Condition Monitoring and Diagnostics Trends in Japan (from the NEDO Report)¹⁷⁾

In Japan, a few years ago, NEDO summarized its research results in “R&D of Technologies for Wind Power and Other Natural Energies, R&D for Advanced Practical Use of Wind Turbine, smart maintenance technology R&D (analysis) (fatigue prediction, etc.).”¹⁷⁾ The following is a brief overview of the research results.

Fig. 8 shows an example of a basic wind turbine component configuration. In this report, to contribute to the development of maintenance methods for highly efficient rotating (drive train, control equipment) and non-rotating (tower, etc.) systems, data was collected on wind turbine failures and accidents, the circumstances and causes of their occurrence was analyzed, along with analyzing maintenance methods. The report also summarizes the maintenance methods of existing wind turbines in Japan and overseas, as well as the measures taken in response to failure accidents.

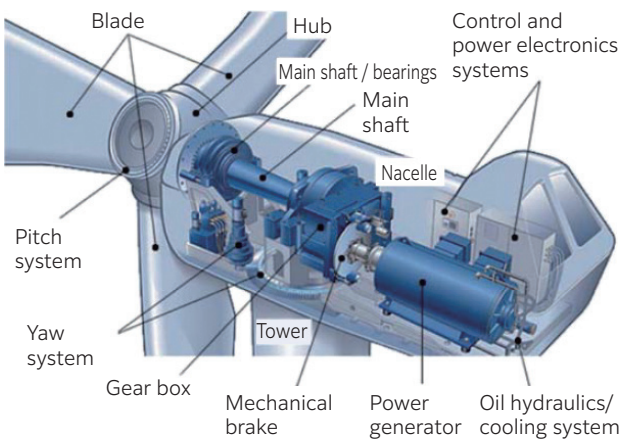


Fig. 8 Example of windmill equipment configuration¹⁷⁾

Fig. 9 shows the trends in the failure and accident rates for the wind turbines cooperating with the survey (the same survey method has been in place since around 2012, and the rates have remained almost constant.)¹⁷⁾ **Table 4** shows a breakdown of the causes of failures and accidents in fiscal 2016. Among the factors related to condition monitoring and diagnosis, “inadequate maintenance” (6.1%), a “human factor”, was relatively common. Compared to past surveys, the “Other” category in the “Cause unknown/other” category, which is related to condition monitoring and diagnosis, has increased significantly. This “Other” category was mainly reported as long-term deterioration. The same trend has continued in recent years, indicating an increase in the number of failures and accidents due to the deterioration of wind turbines after a certain number of years.

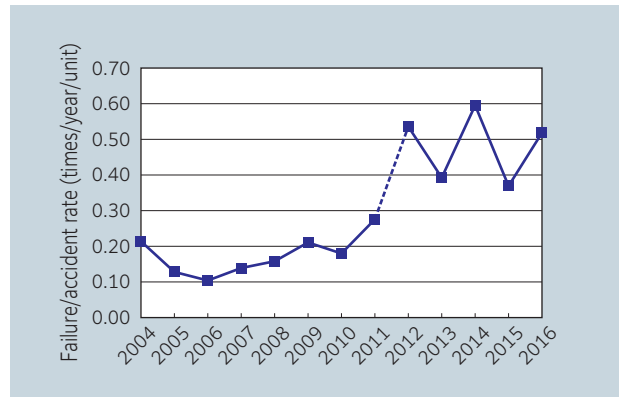


Fig. 9 Trends in wind turbine failure and accident rates¹⁷⁾

Table 4 Breakdown of Failure and Accident Factors (FY 2016)¹⁷⁾

Failure and accident factors	Breakdown of factors	Number of occurrences	Percentage of total
Natural phenomenon	Strong winds	0	0.0 %
	Lightning	34	9.1 %
	Air turbulence	19	5.1 %
	Low temperatures/freezing	0	0.0 %
	Flooding	7	1.9 %
	Other	12	3.2 %
Failure in wind turbine	Design flaw	3	0.8 %
	Manufacturing flaw	17	4.5 %
	Construction flaw	13	3.5 %
Human factor	Inadequate maintenance	23	6.1 %
System failure	System failure	17	4.5 %
Unknown cause/Other	Under investigation	6	1.6 %
	Unable to identify	108	28.9 %
	Other*	115	30.7 %
Total		374	100 %

* “Other” of “Cause unknown/other” is mainly reported as “long-term deterioration”

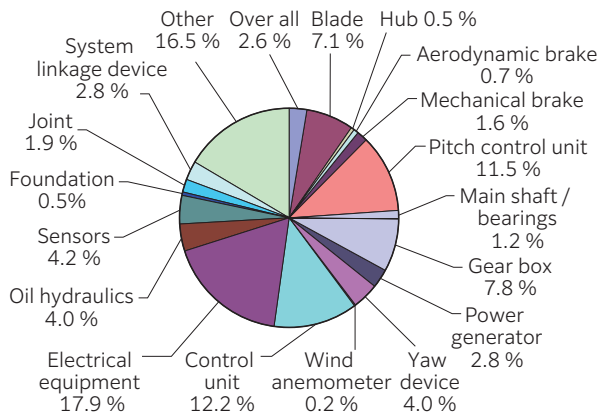


Fig. 10 Summary of wind turbine failures and accidents by site of occurrence (FY2016)¹⁷⁾

Fig. 10 shows a summary of wind turbine failures and accidents by site (FY2016). The most common failure/accident categories were “electrical unit” (17.9%), “other” (16.5%), “control unit” (12.2%), and “pitch control unit” (11.5%). In the evaluation by operation period, “blades”, “pitch control unit”, “gearbox”, “control unit”, and “electrical unit” accounted for a relatively high number of failures of wind turbines that had been in operation for “10 years or longer”. In most cases, the longer the operation period, the greater the number of failures. In the past survey results, the number of failures and accidents tended to increase with the length of operation period for parts with mechanical drive mechanisms such as the pitch control device, gearbox, and yaw device. In contrast, the number of failures and accidents tended to be higher for blades, generators, electrical devices, and control devices regardless of the length of operation period. This is because the former are mechanical devices, while the latter are electrical devices. Mechanical fatigue (including the effect of turbulence) is thought to be the main cause of the former failures, while lightning strikes are often the cause of the latter. The NEDO report also mentions that the data owners are not willing to share their data. The same trend can be seen in the situation in Europe described in the previous section. In addition, a serious shortage of engineers who can work on O&M of wind turbines has been reported worldwide.

5.4 Condition monitoring technology for wind turbines¹⁷⁾

5.4.1 SCADA and wind turbine CMS

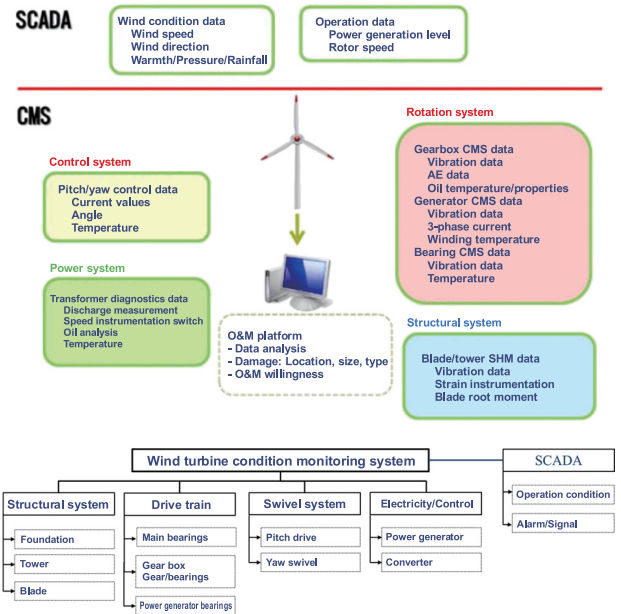


Fig. 11 SCADA and condition monitoring (CMS) system for wind turbines¹⁷⁾

Fig. 11 shows the supervisory control and data acquisition (SCADA) system and condition monitoring system (CMS), which are the core systems for wind turbine operation and control. The actual relationship between CMS and SCADA is organized as an integrated image. Together with the operational status data of each device collected by the CMS, Operational data obtained by the SCADA system is indispensable for evaluating the condition of wind turbine components and equipment. As for the necessity of CMS for wind turbines, the failure rate of gearboxes, generators, and converters, which are major components of wind turbines, is reported to be higher than those of the same type and capacity used in other industries. As the output of a wind turbine fluctuates with wind conditions, the load constantly changes due to turbulence and blade position and deformation. In addition to these load fluctuations, wind turbines with higher output and larger sizes tend to have lighter equipment components, which can increase the probability of failure and accelerate fatigue. It is therefore important to constantly monitor the equipment condition (load and response values) to detect and address anomalies as early as possible (application of condition-based maintenance). It is also important to use digital technology to evaluate and predict the impact of load fluctuations on the equipment and to take measures for operation and maintenance in advance (remaining service life evaluation).

5.4.2 CMS technology for wind turbines

The failure modes of wind turbines and diagnostic techniques are shown in Fig. 12. Most of the monitoring technologies applied to wind turbine CMS are based on existing condition monitoring technologies. The CMS of wind turbines is characterized by the high need for online monitoring because the operation and maintenance of many wind turbines must be performed at a distance from the site. Table 5 shows the results of a survey of detection technologies in the current wind turbine CMS in terms of online monitoring and diagnostic effectiveness. While the development and application of new CMS technology specifically for wind turbines is not necessary, given the shortage of real-world examples there are major obstacles to wind turbine CMS in terms of providing qualified failure diagnosis through online monitoring.

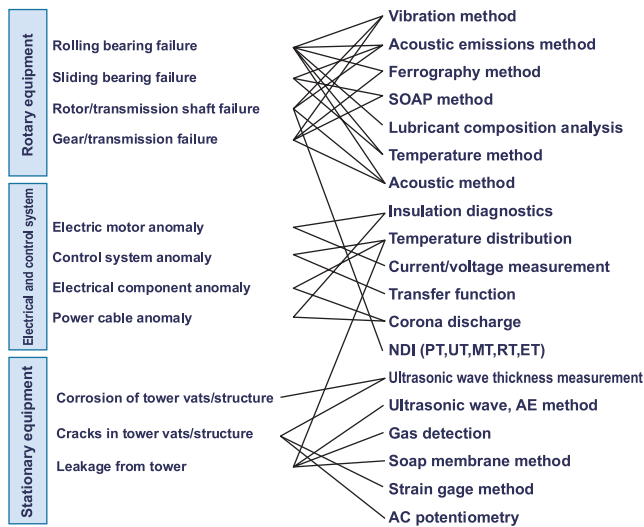


Fig. 12 Failure modes at general plants and applied condition monitoring techniques used for wind turbine CMS¹⁷⁾

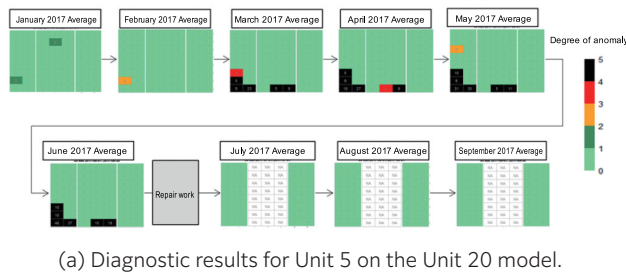
5.4.3 Condition monitoring and prediction of main bearings for wind turbines

As the main bearings of wind turbines are used under low-speed conditions, vibration caused by damage is itself small. In laboratory tests, it is possible to detect changes in vibration levels even in the very early stages of damage. In actual wind turbines, however, peripheral equipment generates vibration at a level that can bring severe damage to the main bearings. Transmission of this vibration from the periphery hinders the detection of damage to the main bearings. A key task in detecting damage to the main bearing is to improve the signal-to-noise ratio by suppressing this vibrational disturbance. To address this issue, this report¹⁷⁾ develops a detection method that highly integrates frequency band splitting, a physical method, and machine learning algorithms, a statistical method. As shown in Fig. 13, we have demonstrated that the method can be used to properly detect and diagnose initial damage to the main bearing.

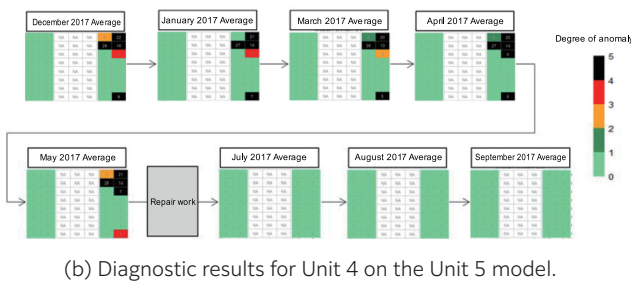
Table 5 Anomaly detection technologies, target sites, and characteristics of wind turbines¹⁷⁾

No	CM technology	cost	online commercial	failure diagnosis	track record	wind turbine components
1	thermocouple	low	○	×	in use	bearing generators converter nacelle transformer
2	particle counter method	low	○	×	in use	gearbox bearing
3	vibration analysis	low	○	○	in use	main shaft main shaft bearings gearbox generator nacelle tower foundation
4	ultrasonic exploration	low to medium	○	×	under testing	tower blade
5	electrical signal (e.g., discharge measurement)	low	○	×	in use	power generator
6	vibroacoustic analysis	medium	○	×	×	blade shaft bearing gearbox generator
7	lubricating oil component analysis method	medium to high	×	○	×	gearbox bearing
8	acoustic emission	high	○	×	×	blade shaft bearing gearbox generator tower
9	twisting vibration (encoder based)	low	○	×	under testing	shaft gearbox
10	optical fiber strain gages	extremely high	○	×	in use	blade
11	thermography	extremely high	○	×	×	blade shaft main shaft bearings gearbox generator converter nacelle transformer
12	shaft torque measurement	extremely high	○	×	under testing	blade shaft main shaft bearings
13	shock pulse method	low	○	×	×	bearing gearbox

The same report¹⁷⁾ also attempted to construct a method for predicting the residual life of wind turbine main bearings. By proposing an equation relating the equivalent distance between wind turbines and the load coefficient that reflects the effect of wakes (areas of lower velocity than the main flow that occur downstream of objects placed in the flow), it is possible to evaluate the bearing-rated life as shown in Table 6.



(a) Diagnostic results for Unit 5 on the Unit 20 model.



(b) Diagnostic results for Unit 4 on the Unit 5 model.

Fig. 13 Damage detection of the main bearing of a wind turbine¹⁷⁾

Table 6 Predicted and actual comparison of rated life¹⁷⁾

Wind turbine	Actual rated life (years)	Distance between equivalent wind turbines (km)	Load coefficient	Predicted rated life (years)
Unit 4	16	0.3	1.55	14
Unit 5	17	0.3	1.51	16
Unit 19	10	0.2	1.72	9
Unit 20	8	0.2	1.75	8

5.4.4 Wind Turbine Tower Anomaly Detection

On March 12, 2013, a wind turbine nacelle fell from the top of the wind turbine support tower at wind turbine No. 3 on the Taikoyama wind farm in Japan. This was due to a fatigue fracture of the tower casing just below the flange. Investigation of the accident revealed that the cause of the fatigue fracture was a stress concentration in the tower casing due to damage to the tower top bolt installed in the flange at the top of the tower. Similar past accidents occurring as anomalies characteristic of wind turbines include: a blade fallout in Falkenberg, Sweden, in 2009; an accident at the Lemnhult wind farm south of Vetlanda, Sweden, in December 2015; and an accident at the Auwahi wind farm on Ulupalakua Ranch on the south coast of Maui, Hawaii, USA in October 2016. In the case of the collapse accident at the Taikoyama wind farm, no anomalies were detected during routine inspections before the accident, and fatigue fracture occurred in a short period. In response to this accident, a method was developed for detecting anomalies in

tower top bolts at an early stage and evaluating axial force.¹⁷⁾ The MT system (Maharonobis-Taguchi) T method (3), a type of multivariate analysis method, was used to detect abnormal bolts. The results of the analysis using the second-order derivative of the strain variation are shown in **Fig. 14**. When the torque was 680 N-m, the value exceeded the threshold value, indicating that it was possible to determine whether the bolt was abnormal or normal, and the accuracy of the determination could be maintained even when the rotor orientation changed (from -45° to 45°).

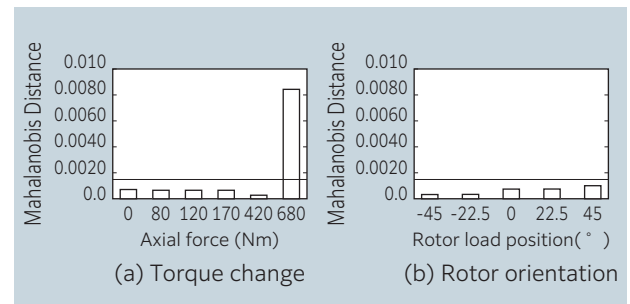


Fig. 14 Early anomaly detection method for wind turbine tower top bolts by Mahalanobis distance¹⁷⁾

5.4.5 Example of standard for wind turbine CMS^{17) 18)}

Here we will introduce the standard for wind turbine CMS using the Guideline for the Certification of Condition Monitoring Systems for Wind Turbines Edition 2013¹⁸⁾ published by GL (Germanischer Lloyd) as an example. The scope and objects of application of the CMS for wind turbines are mainly the drive train, main bearings, gearboxes, and generators. In addition to these, the CMS also covers the tower, blades, main bearings, gearbox lubrication oil, foundations, and other parts of the wind turbine. Monitoring data for wind power generation equipment include load (power generation or torque), shaft speed, temperature in the nacelle, bearing temperature, generator winding temperature, oil temperature, and oil pressure. Other environmental data, such as wind speed, wind direction, and outside temperature, are also required to be measured when available.

Table 4.1 Ref.¹⁸⁾ shows the number of sensors required for a wind turbine CMS. It states that at least six sensors are required to monitor the vibration state of the drive train of a wind turbine equipped with a gearbox. The required frequency bandwidth starts from fairly low speeds and has a wide range. Table 4.2 in Ref.¹⁸⁾ shows a list of methods for using the signals acquired from each sensor in a wind turbine CMS. It requires the application of various analysis methods for each site in order to deal with frequencies, vibration modes, and corresponding anomaly modes.

6. Predictive Maintenance and IoT¹⁹⁾

This is a citation from the article "IoT for Predictive Maintenance" compiled by Mr. Sako, a long-time member of the ISO/TC 108/SC 5 National Committee, in 2020¹⁹⁾.

6.1 Key Points for Building a Predictive Maintenance IoT System

Predictive maintenance is also called condition-based maintenance or condition monitoring maintenance. It is a maintenance method that uses diagnostics techniques to measure and monitor the condition of facilities and equipment to understand or predict the degree of deterioration and take appropriate maintenance measures. The key points of IoT include:

- selection of sensors for detecting anomalies,
- selection of optimal signal processing methods and analysis methods,
- determination of information collection methods,
- determination of monitoring methods,
- and automation of analysis and diagnosis.

Several development items are needed to promote IoT for predictive maintenance. Here, we take "visualization of equipment conditions (as quantitative values)" as an example. Technological development for visualization of facility conditions (as quantitative values) includes expansion of target facilities for anomaly detection, improvement of detection accuracy, and more efficient and easier detection. To this end, it is important to first clarify the equipment to be monitored, the failure mode, the required prediction level (lead time), the difficulty of stopping the equipment, and the time when the equipment can be stopped. At the same time, it is necessary to clarify the measurement location and available sensor types.

The procedure includes identifying a sensing method capable of detecting anomalies through laboratory testing and determining evaluation indices and threshold values for good or bad judgment through field testing using the same method. **Table 7** shows the application status of the diagnostic techniques developed by Sako et al. for rotating equipment¹⁹⁾. The diagnostic techniques have been comprehensively applied to a wide range of objects.

In his contribution¹⁹⁾, Sako further describes in detail the diagnostic technologies for rolling bearings, plain bearings, and motor current symptom analysis (MCSA) for the IoT of predictive maintenance. Here, we will focus on "diagnostic technology for rolling bearings".

6.2 Diagnostics techniques for rolling bearings for predictive maintenance

As shown in **Fig. 15**, rolling bearing anomalies generate vibration and sound in various frequency ranges¹⁹⁾. These can be roughly classified into two categories: structure-borne, such as vibration and AE (acoustic emission), and airborne, such as acoustic. Sound is further divided into audible sounds and inaudible sounds above 20 kHz.

6.2.1 Diagnostics using the vibration method¹⁹⁾

One of the signals used to diagnose anomalies in rolling bearings is vibration acceleration. This acceleration is further divided into two main categories: acceleration in the high-frequency range of 10 k to 30 kHz and acceleration in the low-frequency range of 1 k to 10 kHz.

Fig. 16 shows an example of bearing diagnostic results from the field. This is the acceleration spectrum of a 6310 deep groove ball bearing when false brinelling occurred in the inner ring due to propagating vibration from adjacent equipment. As shown in **Fig. 15**, a frequency of 14 KHz was generated in the zone indicated as high-frequency acceleration. This is an example of how even a small flaw could be detected by acceleration in the high-frequency range.

Fig. 17 compares the trends of acceleration values in the high-frequency range for the six cases that resulted in bearing failure. The average value in the normal state is set to 1.0. The vertical axis shows the ratio of the acceleration to the normal value, and the horizontal axis shows the time elapsed from the time when the condition began to change. Each bearing shows an exponential upward curve. It took three to six months to reach the relative standard of caution (4.0 times), and about six months for the anomaly to arise (8.0 times). When the bearings were replaced after about six months, small defects were observed. It is explained that the variations in the degradation speed of each bearing relates to differences in lubrication conditions and bearing load.

As deterioration progresses from this state, a low-frequency acceleration spectrum in the 2 k to 3 kHz range is generated in addition to the high-frequency acceleration. This is the natural frequency of the bearing outer ring. The explanation for this is that the progressive deterioration of the bearing results in a higher excitation force, which vibrates the entire bearing and generates natural frequencies. The trend of acceleration values in the low-frequency range was also investigated in four cases.¹⁹⁾ As with the high-frequency range shown in **Fig. 17**, an exponential upward curve was drawn, leading to bearing replacement within approximately one to three months after the change was observed.

Furthermore, as bearing deterioration progresses, changes in vibration velocity also occur. A comparison of velocity trends in seven cases of bearing failure due to increased velocity shows an exponential increase curve similar to that in the high-frequency range. The change in velocity value is so rapid, however, about one or two weeks after the vibration velocity begins to increase, the bearing can be said to have reached a terminally degraded state that requires it to be replaced.¹⁹⁾

The conclusion is that although the residual life of bearings can be predicted in several frequency ranges, monitoring using acceleration in the high-frequency range may be essential for critical facilities where continuous operation must not be interrupted.

Table 7 Application of Diagnostic Techniques to Rotating Equipment¹⁹⁾

machine element	type of anomaly (example.)	vibration		lubricant analysis	temperature	AE	acoustics		electric current (MCSA)	applicable equipment	
		vibration velocity	vibration acceleration				audible range	ultrasound			
rolling bearing	medium and high speed rotation	fatigue spalling	x	o	o	Δ	o	o	o	blowers, pumps, compressors, motors, etc.	
		poor lubrication	x	o	o	o	o	o	o		
		wear	x	o	o	o	o	o	o		o
		looseness/rattle	x	o	o	x	o	o	o		o
		seizing	x	o	o	o	o	o	o		o
	low speed rotation (several hundred rpm or less)	fatigue spalling	x	x	o	x	o	x	o	o	agitators, extruders, rolls, paper machines, etc.
		poor lubrication	x	x	o	Δ	o	x	o	o	
		wear	x	x	o	x	o	x	o	o	
		looseness/rattle	x	x	x	x	o	x	o	o	
		seizing	x	x	o	Δ	o	x	o	o	
sliding bearing	seizing	x	o	Keptum	o	o	Δ			turbines, compressors, diesel engines, etc.	
	rubbing	x	o	Keptum	o	o	Δ				
	fatigue	x	o	Keptum	o	x	Δ				
	contamination by foreign matter	x	o	Keptum	o	x	Δ				
	oil whirl	o	x	x	x	x	x	x	x		
gear	pitching	Δ	o	o	o	o	o	o	o	reduction gears, speed increasers, etc.	
	spalling	Δ	o	o	o	o	o	o	o		
	scratching	Δ	o	o	o	o	o	o	o		
	meshing anomaly	Δ	o	x	x	o	o	o	o		
	coupling	misalignment	o	x	x	x	x	x	x		o
belt	slack	o	x	x	x	x	x	x	o		
	overstretching	x	x	x	Δ	x	x	x	o		
blade	imbalance	o	x	x	x	x	x	x	o	blowers, pumps, etc.	
	rotating stall	o	x	x	x	x	x	x		ventilator	
	surging	o	x	x	x	x	x	x		ventilator	
	cavitation	x	o	x	x	o	o	o	o	pump	
	contact	x	o	Keptum	x	x	o	o	x	screw compressor	
axis	bend	o	x	x	x	x	x	x			
	eccentricity	o	x	x	x	x	x	x			
Remarks		• AMD rolling bearing criteria • AMD speed criteria	• AMD rolling bearing criteria • Noise reduction method for inverter motors	• SOAP method, ferrography method • Light transmission method (MD-412L: currently discontinued)	• Thermal imaging camera		• Non-contact measurement • Operation for moving equipment (LM Guide, etc.)		• Application to equipment for which vibration is difficult to measure (screw pumps, axial flow fans, etc.) • Measurement at power supply panels		

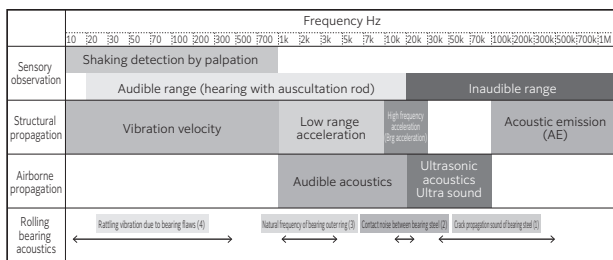


Fig. 15 Vibration and acoustics generated by rolling bearings¹⁹⁾

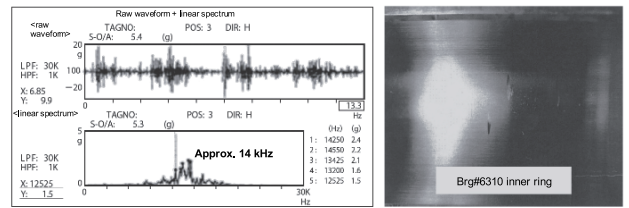


Fig. 16 Acceleration spectrum during false brinelling¹⁹⁾

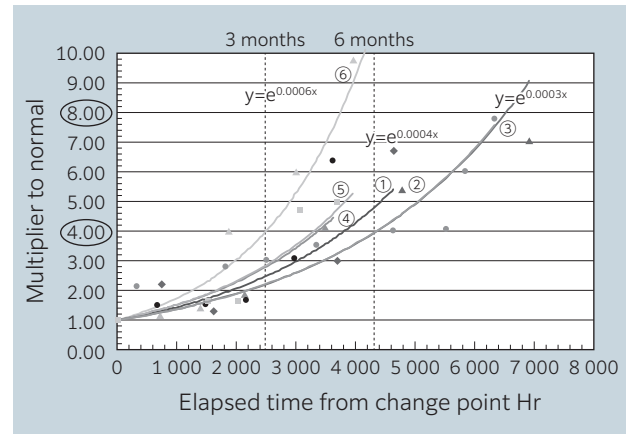


Fig. 17 Bearing degradation curve at high frequency range acceleration¹⁹⁾

6.2.2 Diagnosis by AE method¹⁹⁾

The AE method is the method that enables the earliest detection of anomalies in rolling bearings. **Fig. 18** shows the results of an accelerated life test at 750 rpm. The horizontal axis shows the test time, and the vertical axis shows the event rate for both AE and acceleration of vibration (ACC). AE captures rolling bearing anomalies earlier than the high-frequency accelerations shown in **Fig. 17**. The explanation given¹⁹⁾ for this is that fatigue causes spalling on the bearing steel from its internal starting point, and as it progresses to the surface of the raceway, AE occurs at the time of the spalling occurring whereas acceleration occurs after the rolling elements have begun to collide with the spalling on the orbital plane surface. In the case of spalling with a surface cause such as that due to oil film rupture or indentation, the two occur almost simultaneously.

Fig. 19 compares the AE spectra of the exfoliation propagation and slit cracks. The AE spectrum of the exfoliation propagation has a prominent frequency component between 100 k and 500 kHz, whereas the AE spectrum of the slit flaw has almost no component above 100 kHz. Thus, AE can also capture the difference in anomaly modes of rolling bearings in the early stage.

The AE method is also superior in the low-speed speed range. In the low-speed range, where the product of bearing bore diameter d (mm) and rotational speed N (rpm) (dN value) is less than 2.0×10^4 , the shock signal level of vibration acceleration decreases and is buried in the noise level, making it generally difficult to distinguish between normal and abnormal conditions. In contrast, the AE method

is an effective measurement method because it is independent of rotation speed.

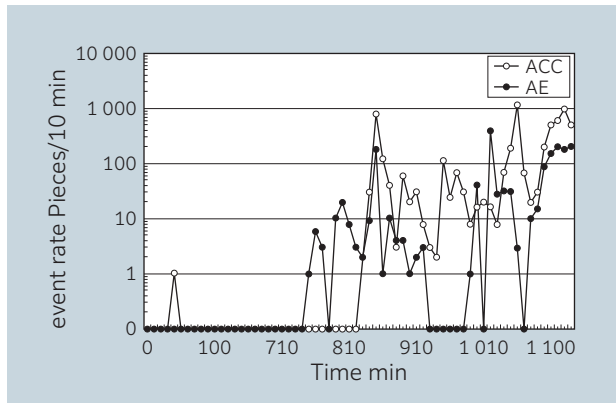


Fig. 18 Accelerated life test results and diagnosis by AE¹⁹⁾

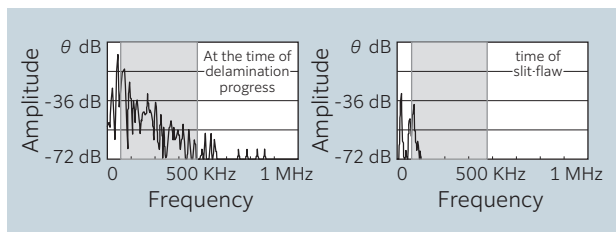


Fig. 19 AE spectra during exfoliation propagation and slit flaw¹⁹⁾

6.2.3 Other¹⁹⁾

The AE method requires a couplant to be applied between the equipment surface and the sensor surface. It is difficult to obtain a stable signal in cases where this is strongly affected by unevenness or curvature of the installation surface. For equipment that has conventionally been difficult to diagnose due to such drawbacks, the authors have developed a non-contact detection method using ultrasonic microphones. Using 20 k to 100 kHz ultrasonic acoustics, it has been shown that bearing separation anomalies can be detected in the same way as with the AE method, even at low rotational speeds of 65 rpm. The ultrasonic acoustic method was applied to detect rolling contact fatigue exfoliation of roll support bearings in a solvent gas environment where AE could not be used due to couplant leakage. In addition, AE is also used to diagnose abnormalities in low-speed rotating equipment, such as contact with the extruder body, pitching of reduction gear gears, and bearing rattling in agitators¹⁹⁾.

7. Trends in Condition Monitoring and Diagnostics Using 1DCAE

Kawai, a leading domestic expert who has been engaged in condition monitoring and diagnosis of machinery for many years in Japan, provides an introduction “On Diagnostic Methods for Equipment Using Physical Models – Application to Digital Twins”²¹⁾ in the opening article of the 2022 JSME Dynamics,

Measurement and Control Division Newsletter. In this article, Mr. Kawai summarizes the process of incorporating 1DCAE software into the equipment diagnosis that he has been working on for many years. 1DCAE is a generic term for CAE methods and tools that have been rapidly spreading and developing in recent years and their design support concepts.²²⁾ It can be applied from the upstream stage of product development because it accurately captures the fundamental nature of the target. It can be expressed in a simple and clear format and can be used for evaluation and analysis. The article explains how modeling the target system with 1DCAE software (in the case of this data, Modelica is used) is useful for equipment diagnosis, and shows examples of system and anomaly modeling (Table 8) that Mr. Kawai has been working on.

As a concrete example, the model of an electromagnetic brake is shown. It is explained that a system such as an electromagnetic brake, which combines complex physical phenomena consisting of dynamics, magnetic circuits, and electric circuits, can be easily modeled by the 1DCAE software (Fig. 20). Here, it is explained that the wear of the armature increases the clearance between it and the plate, and that the resulting effects on other physical quantities can be simulated in a variety of simple ways. Fig. 21 shows the effect of the clearance on the time variation of the current at the start of energization. In the same example, he states that the simulation and experimental results align very well. Thus, he argues, modeling the system and anomalies with 1DCAE software makes it easy to analyze the system behavior when anomalies occur in the system. The interested reader is advised to view the material, which is available free of charge from the department’s website.

Some examples of modeling of mechanical systems using 1DCAE software are shown below. Kashiwase et al.²³⁾ modeled a capacitor motor using the magnetic circuit method and conducted an analysis using 1DCAE software (Modelica). A coupled system (Fig. 22) connecting an electric motor model and a rotating shaft model was used to perform a coupled simulation (Fig. 23) relating the vibration of the rotating shaft and the current of the power supply. This is expected to enable more detailed diagnosis of the electric motor.

Furthermore, Kashiwase et al. constructed a basic model for three-phase induction motors, which are widely used in plants, based on the magnetic circuit method, which consists of a stator, rotor, air gap, and other components, and a model that can be coupled with a rotating shaft²⁴⁾. The validity of the model using 1DCAE software was verified by comparing its electromagnetic behavior with FEM analysis, and the results showed promise for simulation application to electric motor diagnosis. Fig. 24 shows the winding currents in each phase. Although the pulsation of the 1DCAE model (Modelica) is larger, it was confirmed that the overall behavior can be reproduced, according to the report.

Table 8 System and Anomaly Modeling Examples²¹⁾

target system	anomaly
control valve	biting, sensor offset
compressor	leakage
cogeneration system	decrease in efficiency, clogging, and heat transfer coefficient due to debris
crankshaft	bearing rattling
rotational axis system	rotor disproportion, bearing flaw, bearing rattling
coupling	misalignment, miscoupling
journal bearings	wear and its evolution (residual life estimation)
screw compressor	bearing rattling, leakage
electromagnetic brake	wear
gear mechanism	gear wear
3D printer	failure of fan for cooling (control in case of anomaly)

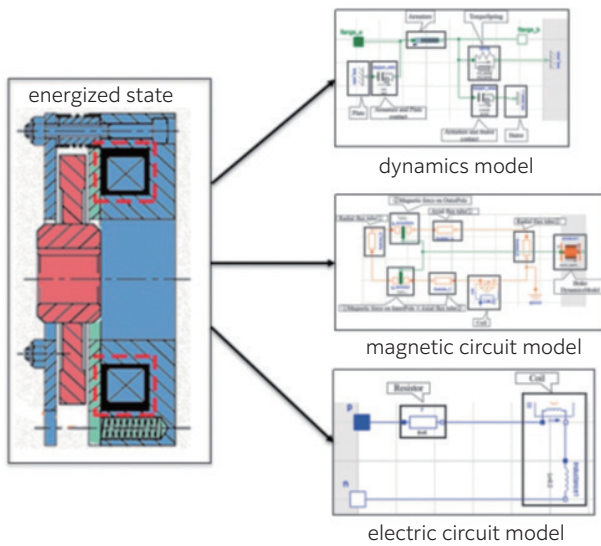


Fig. 20 Electromagnetic brake model²¹⁾

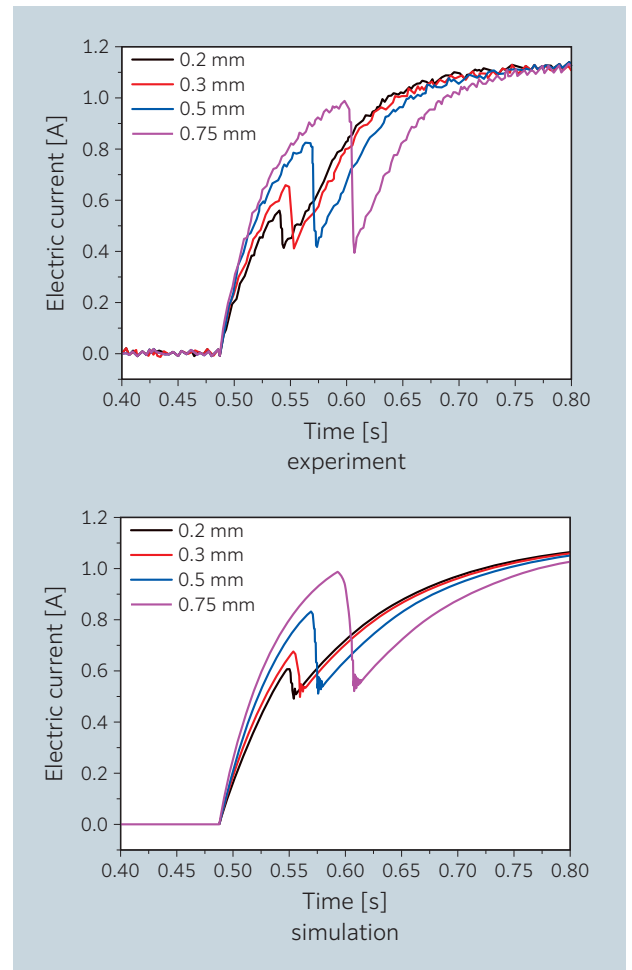


Fig. 21 Current change at the start of energization (effect of clearance)²¹⁾

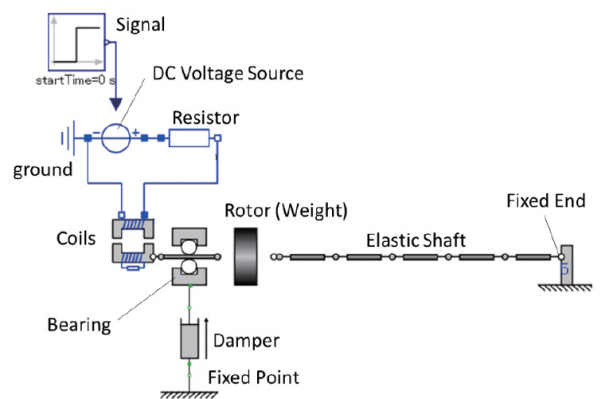


Fig. 22 Modelica model of motor and shaft system²³⁾

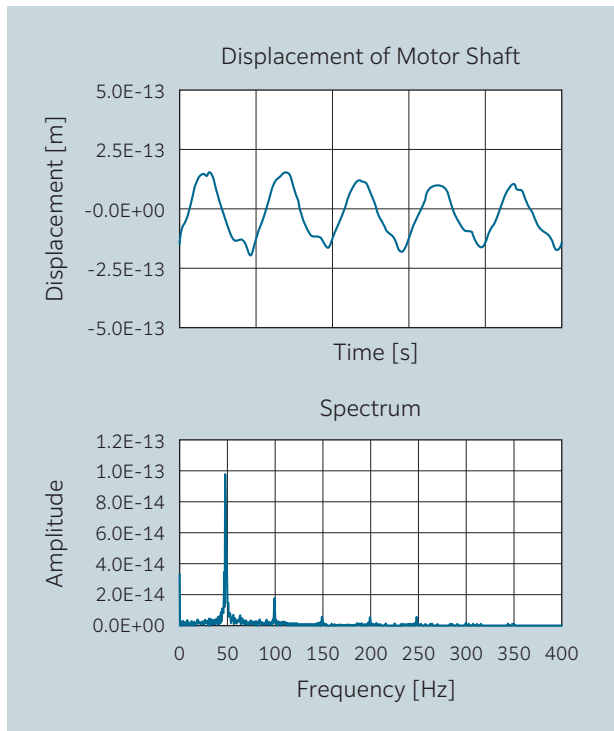


Fig. 23 Vibration analysis results of motor and shaft system²³⁾

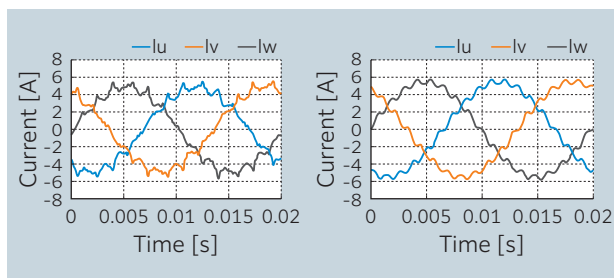


Fig. 24 Stator current (unsteady) (1DCAE and FEM)²⁴⁾

Another study²⁵⁾ modeled gear pairs and gear tooth wear, which are typical power transmission mechanisms, using 1DCAE software (Modelica). The model was used to estimate how the vibration characteristics of the gear pair changed due to wear on the tooth flanks, and also to verify the results using actual equipment.

In this regard, modeling of mechanical systems using 1DCAE software has been used extensively in recent years. The results of 1DCAE modeling of various mechanical systems were presented in a cross-divisional OS organized at the 2022 annual conference of the Japan Society of Mechanical Engineers (JSME). As mentioned above, the use of 1DCAE software as a modeling method for condition monitoring and diagnosis of mechanical systems is expected to advance further.

8. Research Trends in Condition Monitoring and Diagnosis of Bearings in Japan

8.1 National Scientific Conference on Condition Monitoring and Diagnosis

Finally, I would like to review research trends in this field in Japan. In Japan, the representative academic societies for this field are the Japan Society of Mechanical Engineers, the Japanese Society for Non-Destructive Inspection, the Society of Plant Engineers Japan, and the Japanese Society of Tribologists. Among the conferences held by these academic societies are the Dynamics and Design Conference of the Dynamics, Measurement and Control Division of the Japan Society of Mechanical Engineers²⁰⁾ and the Symposium on Evaluation and Diagnosis, which is held jointly by the Dynamics, Measurement and Control Division of the Japan Society of Mechanical Engineers, the Society of Plant Engineers Japan, and the Japanese Society of Tribologists. Numerous condition monitoring and diagnostics research results are published every year.

The following is a list of articles and papers presented at these conferences over the past year or two, focusing on bearing-related topics.

8.2 Examples of AI-based diagnostic techniques

In the field of bearing anomaly diagnosis, there have been recent studies on the use of AI technology for intelligent and automated diagnostics techniques. Deep learning, with its high feature extraction capability has been garnering attention in the equipment diagnosis field in particular. In Japan, Maeda et al. have been working on AI-based bearing diagnosis. In one recent example, after removing noise from vibration signals measured for bearing diagnostics using a statistical information filter, the spectrum of the vibration signal was converted into a quadratic array (equivalent to image information). The method automatically performed feature extraction and state classification using a convolutional neural network (CNN), which is a type of deep learning²⁶⁾. The results of various validation tests showed that the proposed method can achieve highly accurate automatic diagnostics of bearings even in noisy environments.

8.3 Examples of lubricant film evaluation techniques

Takeda et al. have verified the effect of differences in lubricant composition on bearing life by using a thrust ball bearing operating life test machine. The test observed the lifetime until the thrust ball bearing actually failed as a test piece. In addition, the effect of lubricant degradation on bearing life has also been verified by observing the thickness of the lubricant film after bearing failure in new oil and life tests using a lubricant film visualization system. Recently, as a new oil film evaluation method, an ECR (Electrical Contact Resistance) observation circuit was attached

to the lubricant film visualization system (**Fig. 25**) to electrically evaluate and observe the oil film condition, and the observation principle and results were reported²⁷⁾.

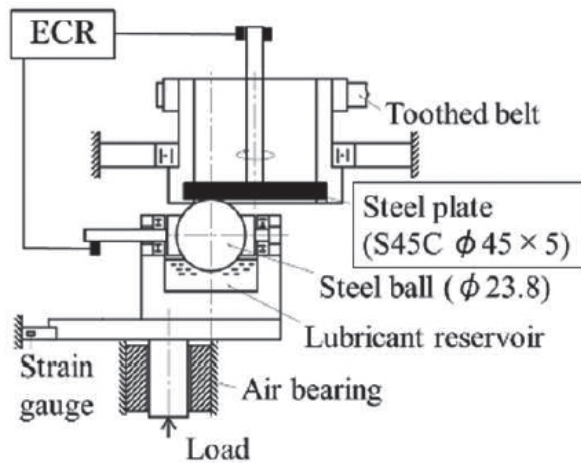


Fig. 25 Equipment for electrical evaluation and observation of bearing oil film condition²⁷⁾

8.4 Examples of diagnostic techniques using ultrasound and acoustics

Wakabayashi et al. reported the efficacy of the ultrasonic echo method for condition monitoring of bearings. They studied the early detection of anomalies in oil-lubricated bearings by applying autocorrelation analysis to the time variation of ultrasonic reflection intensity (URI). The higher the periodicity of the URI waveform, the better the rolling behavior of the bearing. Research has also been conducted recently into the applicability of the ultrasonic echo method to a grease-lubricated bearing (6210 deep groove ball bearing). It was shown that the method can detect rolling behavior inside the bearing during operation and grease removal and replenishment on the orbital plane in the actual working condition by performing two analyses based on autocorrelation for the time variation of the URI. In addition, methods were investigated for extracting periodicity of rolling behavior in URIs with low signal-to-noise ratio (S/N ratio), which is often obtained when diagnosing abnormalities in grease-lubricated bearings by ultrasonic echo method. A comprehensive method and a simplified method were developed as methods to improve multiple analyses by autocorrelation, and it was clarified that they were effective (**Fig. 26**)²⁸⁾.

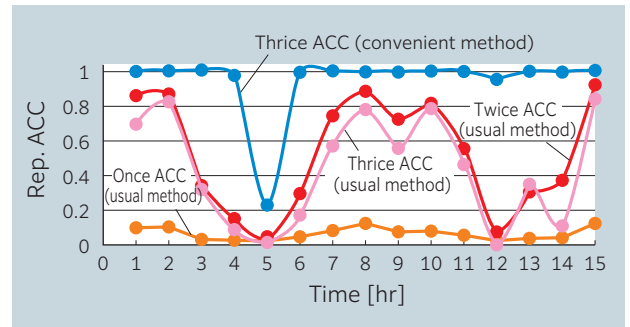


Fig. 26 Analysis of URIs with low signal-to-noise ratios using a simplified method to improve periodicity extraction of rolling behavior²⁸⁾

For highly accurate acoustic diagnosis of bearings, Takada has proposed a new method for improving the signal-to-noise ratio. Recently, he applied this method to failure detection of rolling bearings and confirmed its effectiveness.²⁹⁾ In particular, the effectiveness of this method was demonstrated by applying it to operating conditions with low dN values, which are generally considered difficult to diagnose (**Fig. 27**). Furthermore, the S/N ratio improvement method using an adaptive line enhancer, which is one of the adaptive signal processing methods, was used as a subject for comparison, which shows that the proposed method was effective.

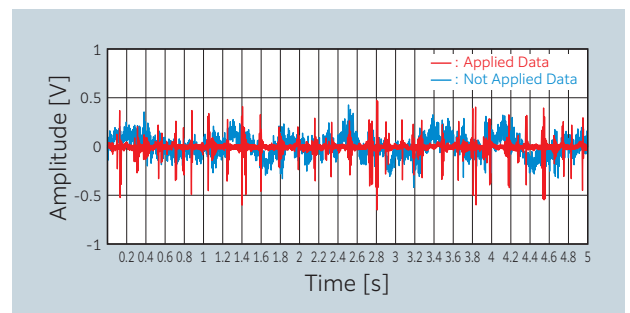


Fig. 27 Time series data obtained by applying the proposed method and an anti-aliasing filter (low-pass filter with a cutoff frequency of 40 [kHz]) to the measured rotating noise of a bearing with outer ring failure²⁹⁾

8.5 Examples of data collection techniques for initial failure processes

Conventional research into the diagnostics of bearings often involves scratching the inner or outer rings beforehand. In actual bearing condition diagnostics, however, it is necessary to detect the earliest signs of any anomalies that could eventually lead to failure. Inoue et al. focused on this point. With the aim of collecting bearing data from the normal state to the occurrence of failure in a time-efficient manner, they created a rotating device with a vibratory mechanism that can apply displacement of any frequency to the rotating shaft. They conducted vibration experiments on deep groove ball bearings as the targets for inducing failure³⁰⁾. Failure progression

was evaluated using acceleration data from the normal state to the occurrence of initial defects (Fig. 28). The degree of failure to the actual bearing was then confirmed by cut-off disassembly inspection.

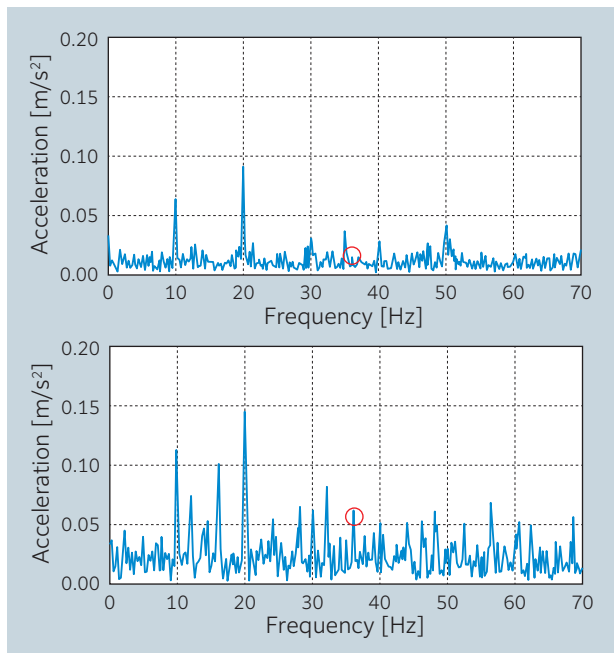


Fig. 28 Envelope spectrum of acceleration signal (upper) before vibration, (lower) after vibration³⁰⁾

9. Conclusion

In this article, entitled “Trends in Condition Monitoring and Diagnosis of Mechanical Systems”, the author first describes the recent activities and trends in ISO/TC 108/SC 5 condition monitoring and diagnosis of mechanical systems with which he is involved¹⁾. Those interested to know more about the historical background to this subject may refer to the series of documents³¹⁾⁻³⁴⁾ compiled by the TC 108/SC 5 National Committee Chairman at that time. Going forward, the international standardization of condition monitoring and diagnosis of bearings is expected to continue. It will develop along with the standardization of condition monitoring asset management in connection with the standardization of individual machines. We look forward to continued cooperation from all parties concerned.

Next, the status of condition monitoring and asset management in Japan and overseas is described, with a focus on the IoT. This field is expected to be one of the biggest areas of development globally in the field of condition monitoring and diagnosis. The paper describes IoT-based condition monitoring and diagnostics and predictive maintenance in wind power generation projects. With the wind power generation business undergoing full-fledged development in Japan with the installation of large floating offshore wind turbines, condition monitoring techniques that involve linkage to a digital twin are being developed.

We look forward to seeing the development of these fields in Japan.

In addition, the author also focuses on the trend of condition monitoring and diagnosis using 1DCAE modeling of target machines in relation to the condition monitoring technology using the digital twin described above. This field is also being actively researched in Japan, and its future trends will be worth watching.

Finally, the research and publication trends in the field of bearing condition monitoring and diagnostics in Japan are described. Recently, the published proceedings of academic conferences have tended to be extremely short. This makes it necessary to actually visit the conference and listen to live presentations. In the wake of social distancing measures adopted during the COVID-19 pandemic, academic conferences are adopting hybrid formats of online and face-to-face meetings. I hope that there will be a resumption in people visiting academic conferences, exploring the latest trends, and engaging in lively exchanges with researchers and technicians in various fields.

The above is an introduction to the trends in condition monitoring and diagnostics of mechanical systems in the direction of this author’s interest and concern, which it is hoped may be of some reference. The author wishes to thank the Japanese Society for Non-Destructive Inspection for granting permission to include the citation in the first half of this paper¹⁾. For providing information in the latter part of this paper, I would like to express my gratitude to Mr. Hitoshi Sakakida, ISO/TC 108/SC 5 committee member and formerly of Toshiba Corporation, Mr. Keita Ishimitsu of JERA Co., Inc, Mr. Takashi Sako, formerly of Asahi Kasei Corporation, to the Japan Institute of Plant Maintenance, and to Professor Tadao Kawai of Osaka Metropolitan University.

References

- 1) Tsuyoshi Inoue and Koji Hyodo, History and Current Situation of ISO Standards on Condition Monitoring and Diagnostics of Machines and Activity of ISO/TC 108/SC 5 (Special issue on trends in condition monitoring and diagnosis technology), Journal of the Japanese Society for Non-destructive Inspection, Vol. 69, No. 9 Sep, (2020) 442-448.
- 2) ISO/TC 108/SC 5 Condition monitoring and diagnostics of machine systems website, <https://www.iso.org/committee/51538.html>
- 3) The Japan Society of Mechanical Engineers (JSME) Certification Program for Machine Condition Monitoring (Vibration, Tribology) <https://www.jsme.or.jp/jotaiweb/>
- 4) Japanese Society for Non-Destructive Inspection Certification System for Machine Condition Monitoring and Diagnosis Engineers (Thermography) <http://www.jsndi.jp/qualification/index12n.html>
- 5) Tsuyoshi Inoue and Koji Hyodo, editors, The Japan Society of Mechanical Engineers, Condition Monitoring and Diagnostic Techniques for Mechanical Systems, Corona, 2021.

- 6) T. Kawai, Equipment Diagnosis in the Continuing IoT Era, *Journal of Economic Maintenance Tribology*, No. 685, (2022) 26-29.
- 7) What is GAIA-X, a European cloud data infrastructure initiative involving GAFAM, *Fintech Journal*, SB Creative, 2021/04
<https://www.sbbit.jp/article/cont1/56622>
- 8) GAIA-X and Catena-X: The Rise of a Huge Ecosystem through Impact Data Linkage—DX in Manufacturing: For Promoting Servitization, *Nomura Research Institute*, Column, 2022/07.
https://www.nri.com/jp/knowledge/blog/1st/2022/iis/fujino/0727_1
- 9) Applying the Internet of Things to manufacturing 8 IoT use cases to boost ROI (IoT (Internet of Things) adoption in the manufacturing industry, 8 IoT use cases to improve ROI), *Siemens website*
<https://resources.sw.siemens.com/ja-JP/e-book-8-industrial-iot-use-cases-for-manufacturing-2>
- 10) COMADEM (Condition Monitoring and Diagnostic Engineering Management)
<http://www.comadem.com/>
- 11) Japan Institute of Plant Maintenance
- 12) Strategic Maintenance Management System (MOSMS), Japan Institute of Plant Maintenance
<https://www.jipm.or.jp/report/?ca=1>
- 13) Maintenance Science for Management, Japan Institute of Plant Maintenance
- 14) Hybrid of "Field Capability" and "Maintenance Management Capability", Utilization of MOSMS "MOSMS", Japan Institute of Plant Maintenance, 2008
- 15) Survey on the use of digital technology in wind power generation, jointly conducted with The Offshore Renewable Energy (ORE), Accenture and ORE Catapult, UK
https://www.accenture.com/_acnmedia/PDF-151/Accenture-210164-ORE-WindCatapult-POV-LCS-JP.pdf
- 16) Using Digital Technology in Wind Power Generation Learning from Overseas Case Studies, *Wind Power Generation / Regional Industry Development and the Use of Digital Technology (Online Seminar)*, Accenture, May 13, 2022.
- 17) New Energy and Industrial Technology Development Organization (NEDO), FY2013-FY2017 Result Report, Research and Development of Wind Power and Other Renewable Energy Technologies, Research and Development of Advanced Practical Application of Wind Power Generation, Research and Development of Smart Maintenance Technology (Analysis) (Fatigue Prediction, etc.), February 2018.
- 18) Service Specification DNVGL-SE-0439, Certification of Condition Monitoring, DNV• GL 2016, GL (Germanischer Lloyd)
- 19) Takashi Sako, On IoT for predictive maintenance, *Plant engineer: Technology for new generation engineers & Information Magazine*, Japan Institute of Plant Maintenance, 52-4, (2020) 32-45
- 20) The Japan Society of Mechanical Engineers (JSME) Dynamics, Measurement and Control Division web page
<https://www.jsme.or.jp/dmc/>
- 21) Tadao Kawai, on a diagnostic method of equipment using physical models - Development to digital twin, *Newsletter of the Japan Society of Mechanical Engineers, Dynamics, Measurement and Control Division*, No. 70 (July 2022) (available from the division website).
- 22) Koichi Ohtomi, and Takehiro Hato, *Design Innovation Applying 1DCAE*, *Toshiba Review* Vol. 67. No. 7, (2012)
- 23) Shoichi Kashiwase and Kenji Ozaki, "Development of a Model-Based Diagnostic Method for Electric Motors", *Dynamics and Design Conference 2021*, September 2021, 442.
- 24) Shoichi Kashiwase, Kenji Ozaki, Hiroaki Makino, *Development of a Model-Based Diagnostic Method for Electric Motors*, 19th Symposium on Evaluation and Diagnosis, 208, 2021
- 25) Tadao Kawai, Yoshihiro Yamamoto, Tatsuro Ishibashi, *Estimation of Gear Wear Using a Physical Model*, *Dynamics and Design Conference 2022*, September 2022, 239
- 26) Linghe Maeda, Haihong Tang, Shanpeng Chen, Keishi Mori, Yuji Yonekura, *Intelligent State Diagnosis of Bearings Using Statistical Information Filter and Deep Learning*, 19th Symposium on Evaluation and Diagnosis, 106, 2021
- 27) Yusuke Takeda, Noriaki Satonaga, Masaya Kano, Takashi Watanabe, Tomoyuki Sonoda, *An Evaluation and Observation Method of Oil Film Condition by Electrical Contact Resistance Method*, 19th Symposium on Evaluation and Diagnosis, 210, 2021
- 28) Toshiaki Wakabayashi, Takahiro Nakatsu, Hideki Yamasaki, *Application of Ultrasonic Echo Technique to Diagnostic Evaluation of Grease Lubricated Bearing - Method of Detecting Periodicity in Rolling Behavior-*, 19th Symposium on Evaluation and Diagnosis, 211, 2021
- 29) Hiroto Takada, Hiromitsu Ohta, Shuji Miyazaki, Daisuke Matsuo, Mirai Ohmori, Satoshi Shimizu, *High Precision Acoustic Diagnosis Method for Low-Speed Rolling Element Bearing*, 19th Symposium on Evaluation and Diagnosis, 202, 2021
- 30) Yuto Inoue, Tsuyoshi Inoue, *Promotion Control of Rolling Bearing Failure*, 19th Symposium on Evaluation and Diagnosis, 203, 2021
- 31) Hitoshi Sakakida, Takuzo Iwatsubo, *The trend of ISO/TC108/SC5 Mechanical Vibration and Shock-Condition Monitoring and Diagnostics of Machines*, *Proceedings of the 1st Symposium on Evaluation and Diagnosis*, (2002) 32-36.
- 32) Hitoshi Sakakida, *The trend of ISO/TC108/SC5 Condition Monitoring and Diagnostics of Machines*, *Proceedings of the 5th Symposium on Evaluation and Diagnosis*, (2006) 7-11.
- 33) Hitoshi Sakakida, *The trend of ISO/TC108/SC5 Condition Monitoring and Diagnostics of Machines*, *Newsletter of the Japan Society of Mechanical Engineers*, (2007) 1.
- 34) Tsuyoshi Inoue, *Present situation and trend of the ISO standards for condition monitoring and diagnostics of machines (TC108/SC5)*, *Turbomachinery* 39(5), (2011) 304-312.

Author Profile

Tsuyoshi Inoue

Ph.D. Professor, Department of Mechanical Systems Engineering, Graduate School of Engineering, Nagoya University

Academic and professional background

1993	Completed master's program in Electronic and Mechanical Engineering, Graduate School of Engineering, Nagoya University
1993-1995	Okuma Corporation
1995-2001	Assistant Professor, Faculty of Engineering, Nagoya University
2000	Doctor of Engineering (Nagoya University)
2001-2005	Lecturer, Graduate School of Engineering, Nagoya University
2004-2012	ISO / TC108 / SC5 National Committee Secretary
2005-2012	Assistant Professor, Graduate School of Engineering, Nagoya University (renamed Associate Professor in 2007)
2012 - Present	Professor, Graduate School of Engineering, Nagoya University
2012 - Present	Chair, ISO / TC108 / SC5 National Committee
2013 - Present	Chairman, Multibody Dynamics Council
2017 - Present	ASME Journal of Computational and Nonlinear Dynamics Associate Editor
2018 - Present	Director, Creation Plaza, School of Engineering, Nagoya University
2018 - Present	Delegate, Turbomachinery Society of Japan
2021 - Present	Vice-Chairman, Standard Project Committee, Japan Society of Mechanical Engineers
2022	Head of the Dynamics, Measurement and Control Division, Japan Society of Mechanical Engineers

Specialties

- Mechanical mechanics, vibration engineering, nonlinear dynamics, vibration control
- Explanation and use of vibration phenomena, in particular those caused by nonlinearity

Academic societies

Japan Society of Mechanical Engineers, Turbomachinery Society of Japan, Japan Society for Design Engineering
The Japanese Society of Tribologists, ASME

Major awards and commendations

Fiscal 2000	Japan Society of Mechanical Engineers Japan Society of Mechanical Engineers Award for Encouragement of Research
Fiscal 2006	The Japan Society of Mechanical Engineers, Dynamics, Measurement and Control Division, Division Contribution Award
Fiscal 2013	Turbomachinery Society of Japan Award (Technology Award)
Fiscal 2016	Turbomachinery Society of Japan Award (Best Paper Award)
Fiscal 2018	Project Award, Tokai Branch, Japan Society of Mechanical Engineers
Fiscal 2019	Turbomachinery Society of Japan Award (Best Paper Award)
Fiscal 2020	Tokai Branch Distinguished Service Award, Japan Society of Mechanical Engineers
Fiscal 2020	25th Engineering Education Award, Japan Society for Engineering Education
Fiscal 2021	Turbomachinery Society of Japan Award (Best Paper Award)
Fiscal 2022	Japan Society of Mechanical Engineers (JSME) Medal for Outstanding Paper (2 papers)
Fiscal 2022	The Japan Society of Mechanical Engineers (JSME) Standard Project Award Contribution Award



Hiroyuki KUREBAYASHI*

Rolling bearings are fundamental mechanical parts working in various equipment that support our life activities. The failures on mechanical parts in the industrial equipment cause a stop of the equipment and induce a considerable amount of profit loss. It is important to monitor the condition of temperature or vibration around the bearings, in order to prevent the unexpected stop of the equipment. NTN develops

bearings with sensing functions and provides condition monitoring service of the bearings. We are willing to provide the service & solution, which is valuable to solve the customer's problems by using the sensing data.

1. Introduction

Machinery and equipment that have rotating mechanisms support the abundant lives of people today. Many of the machines and equipment used to manufacture transport machinery such as automobiles and railroads, as well as air-conditioning equipment and household electrical appliances are equipped with rotating mechanisms. Rolling bearings (hereafter, bearings) are one of the major components used in these rotating mechanisms. Bearings must rotate smoothly while supporting the rotating shaft and be able to operate in a stable manner for long periods of time. Although improvements in bearing performance continue, it is said that bearings are the cause of 30 % of all machinery and equipment failures¹⁾.

Since profit is lost when equipment stops due to defects in machine parts at the production site, it is important to monitor the temperature and vibration around the bearing to prevent defects from occurring. Furthermore, in the automotive sector, bearing condition monitoring will become essential as growth in autonomous driving results in people moving from ownership of automobiles to sharing them, in addition to the development of infrastructure to support autonomous vehicles.

As mentioned above, it is necessary to develop a method (providing services) to use bearings in a stable manner for extended periods of time, not just develop technology (providing products) for the bearings themselves. In response to this, **NTN** provides solutions that combine both products and services that focus on bearing technology:

- High-performance products that integrate sensing functions with bearings (products)
- Services that provide users with information such as bearing condition diagnosis, appropriate methods of use, and replacement periods (services)

Here, I will introduce an overview of the service and solution business that **NTN** is working on and discuss the future prospects. More detailed information about the technology and applicable products will be

introduced separately in other articles in this technical review.

2. Sensing around the bearing

NTN has developed a bearing with a sensor that combines bearing and sensing functions with the aim of responding to the following customer needs:

- (1) Integrated multi-functions for bearings
- (2) Improved reliability for machinery, equipment, and parts as well as support for maintenance

(1) Implementation within compact machines such as motors and pumps. Incorporating a sensing function in the bearing provides an effective method of saving space and reducing the person-hours for assembly, etc. Sensing functions are used to measure such things as the rotational speed, rotational angle, and load around the bearing, and are used to control the operation of machinery.

(2) Implementation within large equipment that must operate in a stable manner and run for long consecutive periods of time. Sensors embedded into the bearing are used to monitor the bearing's operating conditions, and to provide information about bearing condition diagnosis such as whether it is damaged. This aims to prevent unforeseen problems and minimize stoppage time due to failure. To diagnose the condition of a bearing, it is necessary to sense such factors as its temperature, vibration (noise) and lubrication conditions (oil film thickness, grease degradation, foreign object contamination).

If production equipment or infrastructure-related equipment suddenly stops operating, this will have a significant impact on business operators and society. Therefore, there is a strong demand in these sectors for a bearing that will not fail, or at the very least an understanding of a suitable replacement period. **NTN** provides technical services that achieve a high level of accuracy in predicting and detecting when a failure will occur. These services prove useful to customers in preventing equipment-related problems and production downtime.

* Deputy Corporate General Manager, Industrial Business Headquarters

3. Implementation example of a bearing with a sensor

3.1 Rotation sensor bearing

The rotation sensor bearing is constructed by incorporating a magnetic sensor and magnetic encoder in the bearing as shown in **Fig. 1**, and NTN has created a lineup of several standard deep groove ball bearing numbers. Since a magnetic sensor is used, it is resistant to contamination compared with general optical sensors and can also be used in high-temperature environments. This type of bearing is used to control the drive motor on forklifts and for wheel slip prevention control.

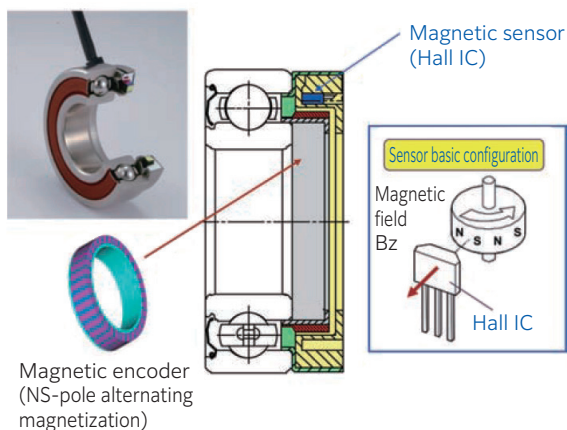


Fig. 1 Rotation sensor bearing²⁾

3.2 Automobile wheel speed sensor

A magnetic sensor to detect the wheel speed is fitted onto the bearings of automobile wheels (hub bearings) and used for controlling ABS (anti-lock braking system). The seal on the hub bearing has a built-in rubber magnetization ring, which provides high durability and prevents deterioration around the wheel over an extended period even in harsh environments. NTN has also developed the Hub Bearing with an Integrated High-Resolution Rotation Sensor²⁾ that uses a magnetic sensor provided with an interpolation function (**Fig. 2**).

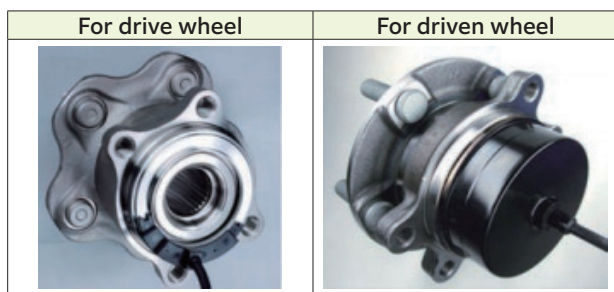


Fig. 2 Hub Bearing with an Integrated High-Resolution Rotation Sensor²⁾

Wheel rotation signals include the impact of tire conditions (such as the air pressure) and road conditions. Analyzing high resolution rotation signals makes it possible for us to detect the differences in tire conditions and road conditions with a greater level

of accuracy. For example, when passing over a section of asphalt road covered in gravel, the rotational speed changes spectrum varies²⁾ as shown in **Fig. 3**. Using this type of high-resolution signal can further enhance the functionality of automotive control.

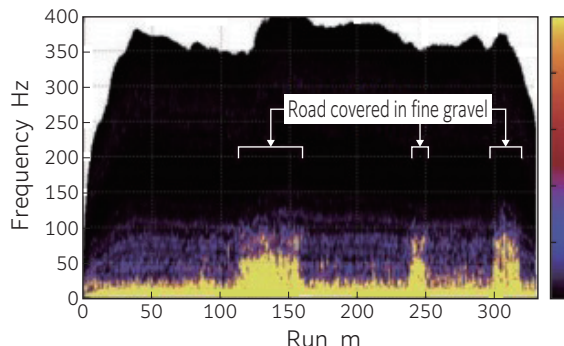


Fig. 3 Variance in speed change spectrum while driving²⁾

3.3 Multi Track Magnetic Ring for absolute angle sensing

NTN has developed the Multi Track Magnetic Ring³⁾ as shown in **Fig. 4**. This magnetic ring is sold as a detection target for use in combination with a magnetic sensor for absolute angle detection. The magnetic sensor's advanced interpolation function and Multi Track Magnetic Ring's highly accurate magnetic pattern make it possible to detect a single revolution (360 degrees) with an angle resolution of over 100 thousand divisions. Since it is magnetic, it has superior environmental resistance when compared to optical sensors, and its compact configuration is suitable for saving space. It is used as a control sensor on robot joints and various types of motors.

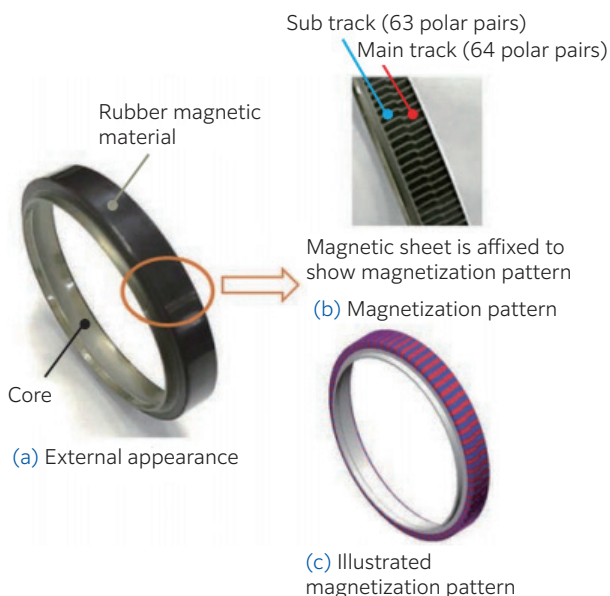


Fig. 4 Multi Track Magnetic Ring: Radial magnetization type³⁾

3.4 Sensor Integrated Bearing Unit for Machine Tool Spindles

The main shaft unit on a machine tool must support condition monitoring and IoT in addition to having the fundamental ability of high speed, high rigidity, and high accuracy, etc. NTN has developed the "Sensor Integrated Bearing Unit" for Machine Tool Spindles, which has various sensors integrated into the outer ring spacer adjacent to the bearing to monitor the conditions inside the bearing and has a load detection function and wireless communication function (Fig. 5)⁴. These sensors detect deteriorating lubrication conditions and signs of damage from vibration and temperature sensing information to prevent defects. Alternatively, they have been proposed for use in adjusting machining conditions by monitoring such factors as forming load and bearing pre-load amount.

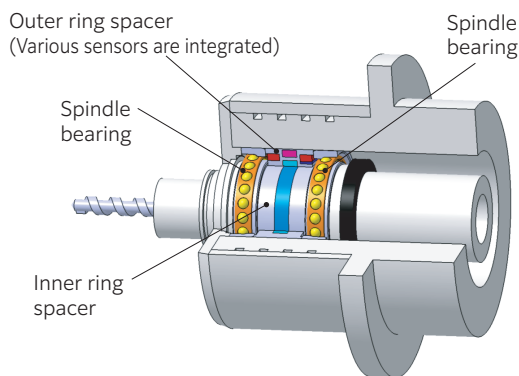


Fig. 5 "Sensor Integrated Bearing Unit" for Machine Tool Spindles⁴

3.5 Talking Bearing™

NTN has developed a "Talking Bearing™" as the ultimate form of a bearing integrated with sensing functions (Fig. 6)⁵. This bearing has the same external dimensions as a standard number bearing but also has vibration, temperature, and rotation sensors as well as a power generator, signal processing circuit and wireless communication unit incorporated into the bearing. The bearing generates power as it rotates and results from sensors are sent wirelessly, allowing the bearing to "talk" and convey information.

Currently, space is required to incorporate the electronic circuit and power generator so there is a limit to the viable bearing size. However, the progress being made in miniaturizing sensor devices and the improvements in power saving will lead to the implementation of much smaller diameter bearings that use this concept in the future.

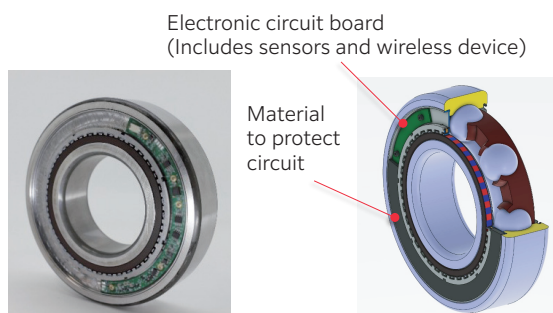


Fig. 6 Talking Bearing™

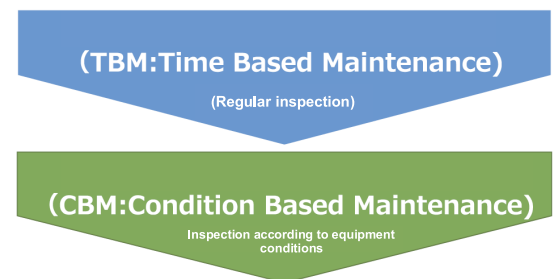
4. Efforts for condition monitoring services

4.1 Trends in condition monitoring

In recent years, the concept of assessment management, which targets the maintenance management and operation of infrastructure such as roads and buildings, is also being expanded to the machinery and equipment sector, and extensively applied to areas from machine condition monitoring to part procurement control. In terms of the equipment maintenance method, there has been a shift towards CBM (condition-based maintenance, predictive maintenance) from the conventional TBM (time-based maintenance, preventive maintenance) method (Fig. 7).

Under such circumstances, efforts to monitor bearing conditions during operation, detect signs of defects and then provide measures before problems arise have attracted a great deal of interest.

The demand for labor-saving and productivity improvements, as well as efficient equipment maintenance is on the rise



Monitor equipment and operational status using IoT
Quickly know about equipment defects and failure to implement planned maintenance

Fig. 7 From time-based maintenance to condition-based maintenance.

4.2 Introducing a condition monitoring system for factory equipment

To operate large machinery and equipment, continuous operation pumps and generators, etc., in a stable manner for extended periods of time it is vital to conduct suitable maintenance work based on bearing condition monitoring, diagnosis technology and the conditions. At large-scale equipment and important production lines, comprehensive condition monitoring systems are introduced while regular inspection and daily maintenance work is conducted constantly together with records for operation and maintenance. In this manner, all companies have established a condition monitoring and operation management system for their entire factory to prevent problems with large equipment.

In contrast, operation management is often conducted individually for each machine when looking at small-scale equipment. This creates the problem of making it difficult to introduce condition monitoring machinery and connect it to a unified system for operation because factories with small-scale equipment use a mix of partially optimized systems throughout the factory.

An IoT platform has been proposed to solve this type of problem. The IoT platform is introduced to each piece of equipment and then applications such as measurement software are run on the equipment

to make it easier for data and communication to be sent between equipment as well as stored data to be managed at a central location and facilitate mutual use of such stored data.

NTN has developed a bearing diagnostic application (Fig. 8) that runs on Edgexcross⁶⁾, which is an IoT platform. This application is provided as a condition monitoring tool that requires no internet connection or detailed settings⁷⁾. See the commentary section for more information about this application.

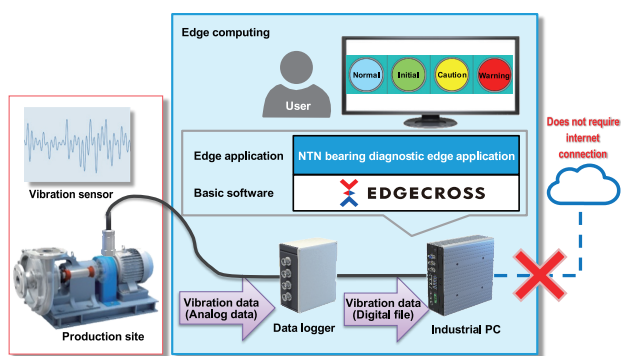


Fig. 8 Bearing diagnostic application

4.3 Portable Vibroscope

When personnel regularly take measurements at fixed points on equipment as they patrol and monitor their worksite where TBM (time-based maintenance) is performed, there is a demand for a measuring instrument that is easy to carry around and that can easily record data. The NTN Portable Vibroscope⁸⁾, as shown in Fig. 9, is a useful tool for this type of application.

Personnel can connect the device to a tablet PC or a smartphone, then measure and record vibrations at the equipment to determine the conditions based on predefined criteria or analyze condition trends. If the observed data needs to be analyzed in more detail, a frequency analysis function is used to enable such things as coupling damage and bearing damage to be diagnosed.



Fig. 9 NTN Portable Vibroscope

4.4 Trends in condition monitoring with large wind turbines

Large wind turbines, as shown in Fig. 10, are installed at a height of over 60 meters above ground level and are often operated in difficult to access locations such as along the coast and in mountainous areas. Weather conditions can also restrict work on wind turbines so it is not easy to know the equipment

conditions and maintenance work cannot be conducted easily. For this reason, remote monitoring using a condition monitoring system (CMS) is necessary, and the use of this type of system has spread throughout Japan.

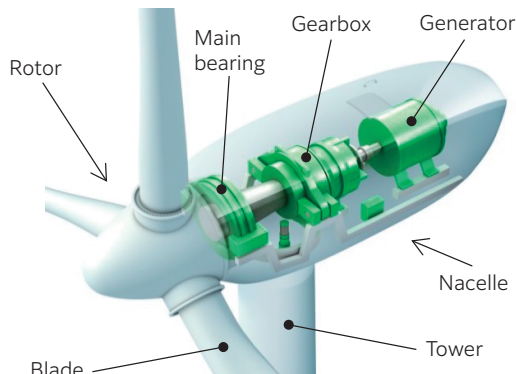


Fig. 10 Large wind turbine structure

Plans are underway in Japan to introduce large wind turbines with the aim of creating offshore wind turbine projects in the region of 10 GW by 2030 and 30 to 45 GW by 2040. One of the technical challenges in this area is reducing the cost of power generation, and targets were indicated to achieve 8 to 9 yen per kWh using seabed-mounted offshore wind turbines. To achieve this, significant importance has been placed on reducing the cost of operation and maintenance (O&M), which accounts for 36 % of the lifetime cost of wind turbines (Fig. 11).

Offshore wind turbine low-cost project (overview)

- To acquire a market share of Asia, which is expected to expand rapidly in the future, it is essential to improve equipment utility factor and reduce costs in response to size increases in wind turbines, while also take into account the development and demonstration results of floating structures to date.
- Therefore,
 - (1) We will continue to take advantage of Japan's strength and develop elemental technologies that conform to the Asian market, such as the weather conditions (typhoons and lightning) and ocean conditions (wave swell) (Phase 1).
 - (2) Conduct demonstrations that integrate related technology for the entire system, while also using these elemental technologies (Phase 2).

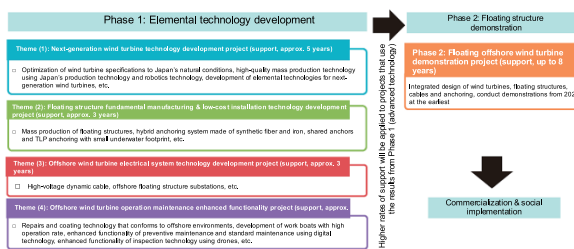


Fig. 11 Lowering the cost of offshore wind turbines (Source: Found in documentation from the Ministry of Economy, Trade and Industry⁹⁾)

4.5 Wind Doctor™, a condition monitoring system for wind turbines

NTN released Condition Monitoring System (CMS) for Wind Turbines "Wind Doctor™" for sale in 2012. Currently, this system is in operation at around 300 wind turbines throughout Japan^{10) 11)}. Wind Doctor™ provides a monitoring service as shown in Fig. 12. Sensors installed on the wind turbine are used to remotely collect and store data such as vibrations on a regular basis for monitoring purposes. If an abnormality or change is detected, the system will promptly send information to the customer.

Customers using this monitoring service can use this information for operation management and maintenance work on their wind turbines.

As discussed above, offshore wind turbines are more difficult to access than those built on land, and remote condition monitoring of key components such as bearings is particularly important for offshore wind turbines. Furthermore, it is believed necessary to evolve and support condition monitoring systems so that they can adapt to the weather conditions unique to Japan, such as typhoons and winter storms over the Sea of Japan, which are said to be the strongest in the world.

NTN has selected the two projects of “next-generation wind turbine technology development” and “offshore wind turbine operation maintenance enhanced functionality” for NEDO Green Innovation Fund Projects¹²⁾ and started activities on these projects from FY2022¹³⁾. These projects promote technological research and development from both sides of “products” and “services” in terms of developing improvements for bearings and enhancing the functionality of CMS.

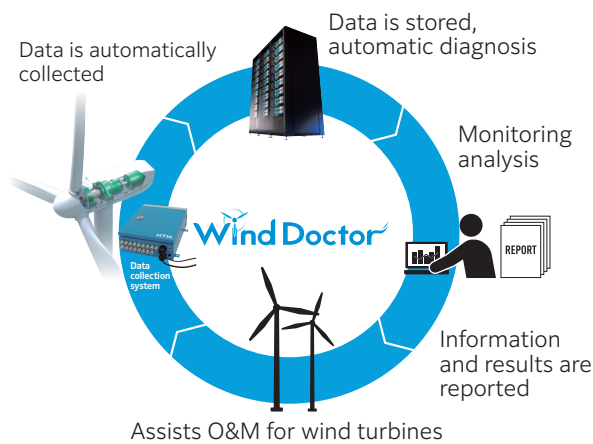


Fig. 12 Wind Doctor™ monitoring service

5. Efforts for the solution business

5.1 Using sensing data

Generally, condition monitoring systems diagnose equipment conditions using diagnosis parameters derived from such things as vibration data measured around bearings. It is possible to calculate many diagnosis parameters, but it is difficult to select parameters that are viable for diagnosis because they are different for each piece of equipment.

If diagnosis parameters have previously been selected through observation and experience, and a large volume of data has been stored that shows the relationship between the measured data and damage, then it is possible to teach an AI system to automatically select viable diagnosis parameters. Also, analyzing cases of observed damage and defects can also improve the design of machinery and equipment and their operation method. The more we can store actual data from the machine, the greater we can improve accuracy in assessing the conditions relating to the equipment.

NTN continues to build a system that stores and

uses observed data from the actual machine and is working on the continuous operation of this system. At the same time, we are focusing on developing sensor devices for collecting sensing information centered on bearings, as well as providing measurement tools, which we consider to be especially important.

5.2 Solutions provided by NTN

The following types of information are required by equipment operation sites to monitor the conditions and sense around the bearing.

- (1) The decision about whether operating conditions are suitable or not
- (2) The estimated progress of damage if it has occurred

Technology shown below is required to provide this information and requires a great deal of time and effort such as expert level training and much experience.

- Fundamental knowledge of bearings and condition diagnosis technology
- Sensing technology and signal processing technology
- Technology to automate condition assessment, such as AI diagnosis
- Expertise in issues unique to bearings

Business operators who run equipment need condition diagnosis information for the entire machine, not just for the bearing condition. Therefore, comprehensive assessment technology that incorporates information from around the machine is required. Furthermore, depending on the unique characteristics of the operated equipment, we may also be able to consider operations that combine information from a wide range of fields. For example, we may be able to use various data such as weather data, financial data, social events, or currency exchange information and apply it to data analysis for equipment operation management through tasks such as considering procurement costs and the timing of repairs.

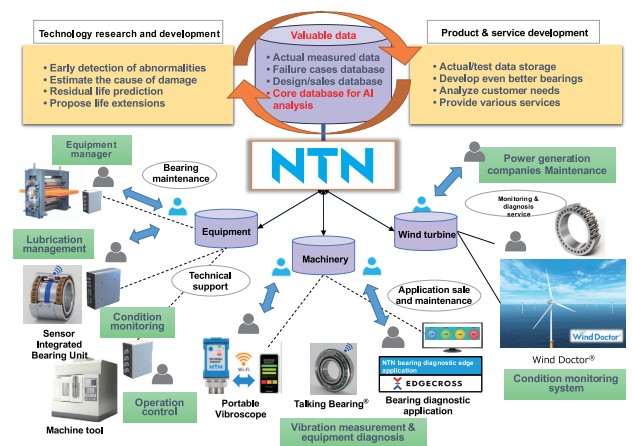


Fig. 13 Service & Solution Business in NTN

Many business operators feel it is important to focus on operation and management that uses collected data rather than spending the effort to build and maintain a monitoring system. As shown in Fig. 13, NTN will continue to develop services that provide solutions that can be used in business

operations, such as equipment maintenance planning, by extracting information beneficial to the customer and information required to resolve problems through activities such as monitoring the condition of bearings incorporated in equipment.

5.3 Development of wind turbine maintenance business

In addition to condition diagnosis based on CMS for wind turbines, NTN is working to optimize operation and maintenance and its use in operation control. In the long term, we will develop long operating life bearings by analyzing CMS data and cases of bearing damage, while promoting the provision of a total service for aftermarket bearings and inspection maintenance to reduce O&M costs for offshore wind turbines.

In the wind turbine sector, NTN has started an initiative¹⁴⁾ in the maintenance business in collaboration with Hokutaku Co., Ltd. By optimizing the operation and maintenance of wind turbines based on CMS information (smart maintenance) and collaborating on the development and procurement of bearings, and operation and maintenance services, as shown in Fig. 14, NTN will achieve bearing life cycle management and continue to contribute to society.

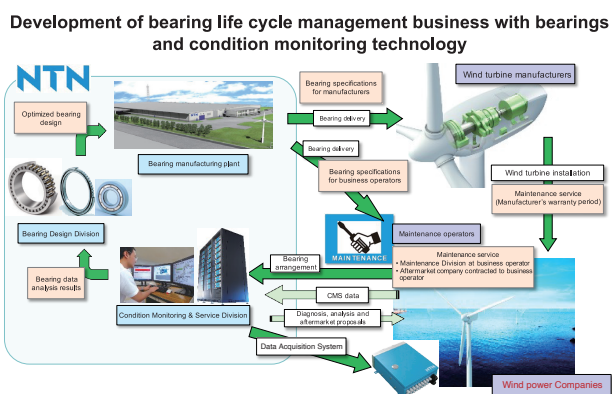


Fig. 14 Bearing life cycle management

6. Summary

NTN not only sells products but also provides services to resolve customer problems. Efforts in this area will be focused on developing software that analyzes sensor signals and software that controls machinery to create new value. Additionally, we will provide aftermarket bearings and develop improvements in new bearings based on collected information and build life cycle management for bearings centered on bearings and their monitoring information.

In the future, we will build a business model that uses this big data and promote service and solution business that will lead to improved NTN brand value.

References

- 1) Japan Lubricating Oil Society, Lubrication Management Optimization Promotion Investigation Report, 1995.
- 2) Kentaro Nishikawa, Toru Takahashi, C. Duret, Hub Bearing with an Integrated High-Resolution Rotation Sensor, NTN TECHNICAL REVIEW, No.81, (2013)52.

- 3) Takashi Koike, Yasuyuki Fukushima, Yusuke Shibuya, Hiroyoshi Itou, Development of Multi Track Magnetic Ring for High Accuracy Absolute Angle Detection, NTN TECHNICAL REVIEW, No.86, (2018) 45.
- 4) Shohei Hashizume, Yusuke Shibuya, Daichi Kondo, Yohei Yamamoto, Hiroyuki Iwanaga, Development of Sensor Integrated Bearing Unit for Machine Tool Spindles, NTN TECHNICAL REVIEW, No.88, (2020) 33.
- 5) NTN, Press Release, NTN Develops Sensor Integrated Bearing "Talking Bearing™". https://www.ntn.co.jp/japan/news/new_products/news202200041.html
- 6) Edgexcross Consortium, <https://www.edgexcross.org/>
- 7) NTN, Press Release, Extension on Period to Provide Free Trial Version of Bearing Diagnostic Application. https://www.ntn.co.jp/japan/news/new_products/news202200022.html
- 8) NTN, Portable Vibroscope, NTN TECHNICAL REVIEW, No. 87, (2019) 106.
- 9) METI, R&D and Public Implementation Plan Formulated for "Cost Reductions for Offshore Wind Power Generation" Projects https://www.meti.go.jp/shingikai/sankoshin/green_innovation/green_power/pdf/001_04_00.pdf
- 10) Makoto Miyazaki, Wataru Hatakeyama, Application of Condition Monitoring System (CMS) for Wind Turbines, NTN TECHNICAL REVIEW, No.86, (2018) 40.
- 11) Katsuyoshi Suzuki, Deployment and Improved Reliability of the Condition Monitoring System for Wind Turbines, NTN TECHNICAL REVIEW, No.88, (2020)111.
- 12) NEDO, Started Green Innovation Fund Project "Offshore Wind Turbine Cost Reduction". https://www.nedo.go.jp/news/press/AA5_101505.html
- 13) NEDO, Business Overview Documentation of "Green Innovation Fund/Offshore Wind Turbine Cost Reduction" Project. <https://www.nedo.go.jp/content/100941539.pdf>
- 14) NTN, Press Release, NTN Starts Maintenance Service for Wind Turbines. <https://www.ntn.co.jp/japan/news/press/news202200031.html>

Photo of author



Hiroyuki KUREBAYASHI

Deputy Corporate
General Manager,
Industrial Business
Headquarters

Development of Remaining Useful Life Prediction Technology for Rolling Bearings Under Flaking Progression

Masashi KITAI*

In recent years, due to aging equipment and the lack of maintenance personnel, there is increasing interest in advanced predictive maintenance, and rolling bearings are attracting attention as a target. In general, rolling bearings are replaced when some kind of damage occurs. However, in some cases where maintenance is not easy, they may continue to be used even after the damage has occurred as long as it does not affect peripheral equipment. This paper introduces a developing AI method for predicting the remaining useful life of rolling bearings under flaking progression.

1. Introduction

Interest is growing for enhanced functionality and automation of maintenance technologies amid the backdrop of increased maintenance costs due to long-term deterioration and the increasing burden on workers due to the lack of maintenance personnel in manufacturing, infrastructure and similar related equipment. In recent years much attention has been given to technology relating to “predictive maintenance”, a method which involves detecting abnormal signs of operation so that maintenance can then be performed. This method is more efficient than “preventive maintenance”, which involves regularly maintaining equipment regardless of its condition or “corrective maintenance”, which involves maintaining equipment after a failure has occurred. NTN has increased activity in this area by introducing these technologies in maintenance using IoT and AI¹⁾.

Rolling bearings are machine elements that is vital to equipment and are a key element in supporting machine rotation. In cases of equipment failure, it is said that roughly 30 % of failures are caused by rolling bearings²⁾. Based on this fact, it is desirable to estimate the condition of rolling bearings and repair or replace them at the proper time to reduce maintenance costs for the entire machine.

Vibration acceleration is often used to diagnose rolling bearings because it can be measured without interrupting the machine and is highly sensitive to damage³⁾. Diagnostic methods that use vibration acceleration predict damage conditions using statistics such as the root mean square value and kurtosis, as well as specifying areas of damage using frequency analysis. There has been much recent activity in R&D development to predict the damage conditions and remaining useful life of rolling bearings in line with the development of AI technology such as deep learning^{4), 5), 6)}.

This paper introduces AI technology⁷⁾ developed to predict remaining useful life up to when it is necessary to replace the bearings and is applicable to rolling bearings after damage has occurred.

2. Development background

Generally, the life of a rolling bearing is often considered to be when some type of damage occurs on the bearing raceway surface, such as flaking or indentation. However, depending on the environment and conditions in which the bearing is used, it is not easy to replace rolling bearings and these bearings may continue to be used even after minor damage has occurred because of the significant maintenance costs involved.

If rolling bearing damage progresses, there will be a sudden increase in vibration, which will cause damage to the machine as well as other elements and will likely lead to increased downtime. Therefore, it is desirable to be able to predict the remaining useful life up to when the bearing needs to be replaced by estimating the extent of damage on the rolling bearing (hereafter, damage condition). However, most research into remaining useful life prediction of rolling bearings mentioned above does not describe the damage condition of rolling bearings.

Therefore, this paper will introduce the technology that was developed with the aim of predicting the remaining useful life with high accuracy, by expressing a regression model of the relationship between the damage condition and remaining useful life for rolling bearings where damage is in progress.

* Advanced Technology R&D Center

3. Flaking progress and vibration acceleration on rolling bearings

Fig. 1 shows the relationship between the operating time and vibration when using a cylindrical roller bearing. Operation continued until the circumferential length of flaking that occurred on the inner ring raceway surface exceeded the rolling element pitch length⁸⁾. The horizontal axis shows the load count while the vertical axis shows the change relative to the root mean square (RMS) initial value of the vibration acceleration (RMS relative value). The figure also shows an external view of the flaking on the inner ring raceway surface for a specific time. Flaking occurred at a load count of approximately 900 thousand times. Flaking on the raceway surface first develops mostly in the axial direction (range A in **Fig. 1**), and when the length of flaking in the axial direction reaches the rolling element contact length, flaking mostly progresses along the circumference after this (the direction in which the rolling element moves) (range B in **Fig. 1**). RMS increases quickly while flaking progresses in the axial direction, and while flaking mostly progresses along the circumference, RMS increases slower and fluctuations follow the same trend. As flaking progresses further, if the length of flaking along the circumference reaches the rolling element pitch length (range C in **Fig. 1**), RMS increases rapidly once again and the fluctuation range also increases.

When this type of vibration increases, displacement between the inner and outer rings of the rolling bearing increases the risk of exceeding the range of acceptable clearance for peripheral components, which will result in damage to the peripheral components. Consequently, it is best to stop operation before the flaking circumferential length reaches the rolling element pitch length. This study regarded the bearing replacement time to be when the circumferential flaking length reaches half of the rolling element pitch length.

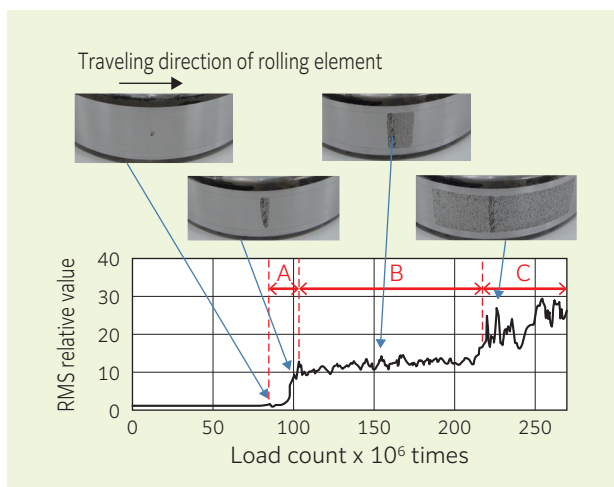


Fig. 1 Relationship between flaking progress and vibration acceleration⁸⁾

4. Characteristics of development technology

This chapter describes the overview for development technology.

4.1 Development technology

Fig. 2 shows an overview of development technology. Development technology consists of a combination of Feature Fusion Network (FFN)⁷⁾ as indicated in section 4.2 and Hierarchical Bayesian Regression, HBR⁹⁾ as indicated in section 4.3. Using a short time Fourier transform (STFT) (see **Fig. 3**)¹⁰⁾ spectrogram to input vibration acceleration time series data, FFN can predict maximum circumferential flaking length (hereafter, flaking size) and remaining useful life (hereafter, SS remaining life) as a snapshot (a single output for a single input data set). Next, from the flaking size and SS remaining life predicted by FFN, HBR can be used to output the remaining useful life regression equation, remaining useful life and its distribution.

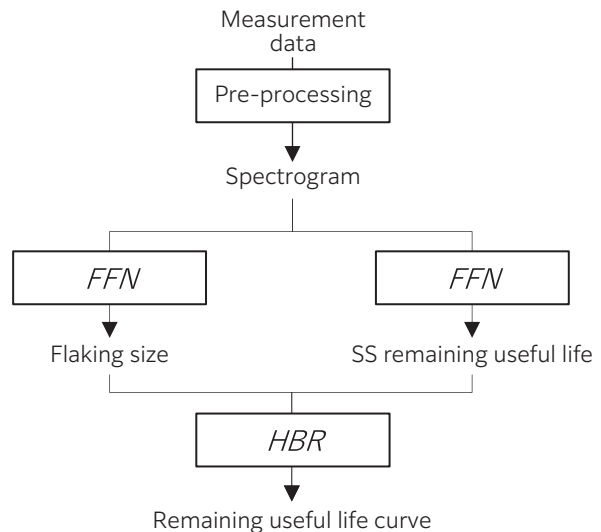


Fig. 2 Development model overview

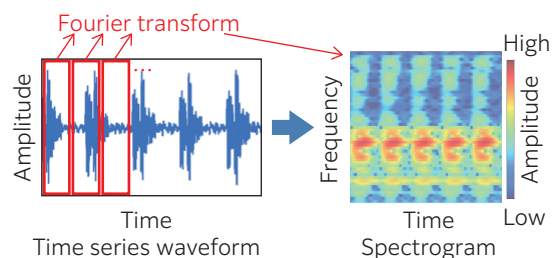


Fig. 3 Illustration of short time Fourier transform

4.2 Feature Fusion Network

FFN is a regression method based on a convolutional neural network (CNN)¹¹⁾ in deep learning and is often used for image recognition. Fig. 4 shows an illustration of FFN. Normal CNN directly predicts corresponding objective variables just from data input at the time of the measurement. FFN calculates a deterioration index (a normalized index in a range of 0 to 1 for the state of deterioration) at each point in time from data input from multiple times in the past. The deterioration index is then vectorized with a measured permutation to create a deterioration index vector, which is then used as an intermediate variable with the aim of improving the prediction accuracy of the objective variables (flaking size and SS remaining useful life).

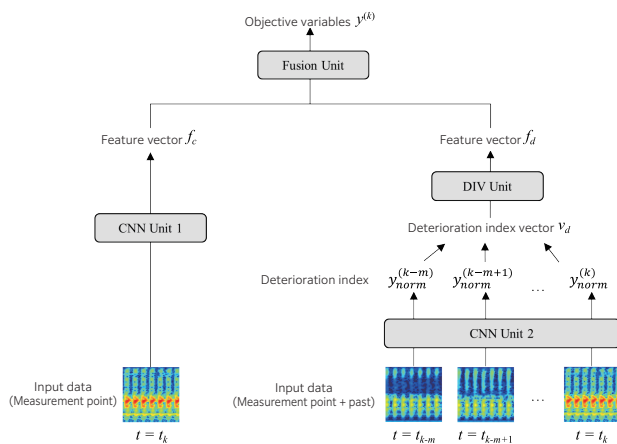


Fig. 4 Feature fusion network overview

4.3 Hierarchical Bayesian regression

Since the previously mentioned SS remaining useful life is predicted with a snapshot, the predicted value changes for each measurement time. In practical use, the regression curve for remaining useful life is defined by a monotonically decreasing function because it is preferable for the remaining useful life predicted value to monotonically decrease as operating time elapses. In addition to the above, HBR was used⁷⁾ as a method to consider variations between individual bearings during this development. HBR uses all past data before the measurement point to obtain the remaining useful life and regression curve. More specifically, differences in individual bearings are assumed to vary based on a probability distribution so that individual remaining useful life regression curves can be handled for each bearing. This enables relatively accurate predictions for remaining useful life output at the end, even for individual bearings whose SS remaining useful life greatly deviates from the average obtained from all learned data.

5. Evaluation test

5.1 Test equipment and measurement data

A schematic drawing for test equipment used to evaluate development technology is shown in Fig. 5, while test conditions are shown in Table. 1⁷⁾. A cylindrical roller bearing (number NU224, bore diameter 120 mm, outer diameter 215 mm) was used as the test bearing. Operation continued until the bearing reached its limit of use after the initial flaking that occurred on the bearing raceway surface, and both vibration acceleration and flaking size were measured at regular intervals. Measurements were taken for a sample of 33 bearings. Fig. 6 shows the relationship between the operating time and RMS from when the initial flaking occurred on each bearing sample until the bearing reached its limit of use. Fig. 7 shows the relationship between the operating time and flaking size. At the end of flaking progress, RMS fluctuated significantly, and this made it difficult to accurately know the flaking conditions. Despite the fact that all 33 bearing samples were tested under the same operating conditions, the remaining useful life, up to when the bearing limit of use was reached, differed significantly among the bearing samples. Therefore, in order to improve the accuracy of predicting remaining useful life, it is necessary to consider fluctuations in feature quantities of vibration acceleration as well as individual differences in remaining useful life.

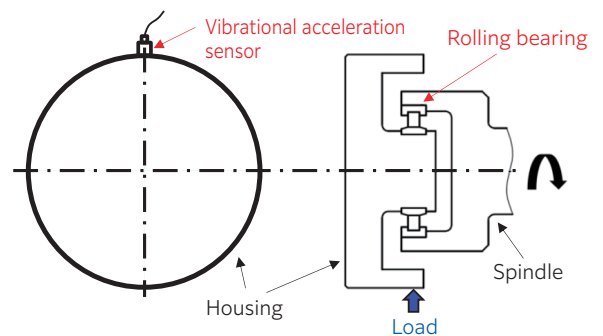


Fig. 5 Test equipment⁷⁾

Table 1 Test conditions⁷⁾

Rolling bearing	Cylindrical roller bearing (number: NU224)
Main shaft rotational speed	500 min ⁻¹
Radial load	90 kN
Measurement data	Vibration acceleration (vertical direction)
Bearing sample quantity	33 pieces

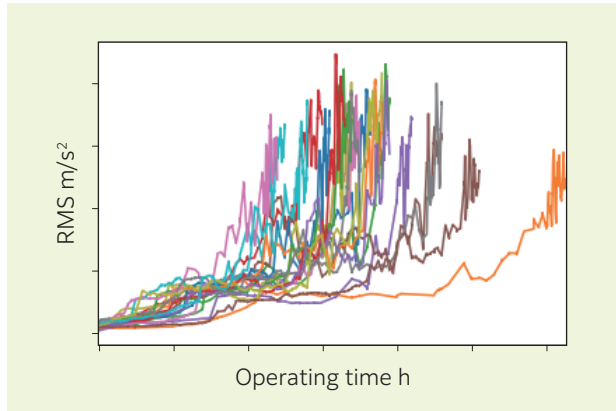


Fig. 6 Relationship between operating time and RMS

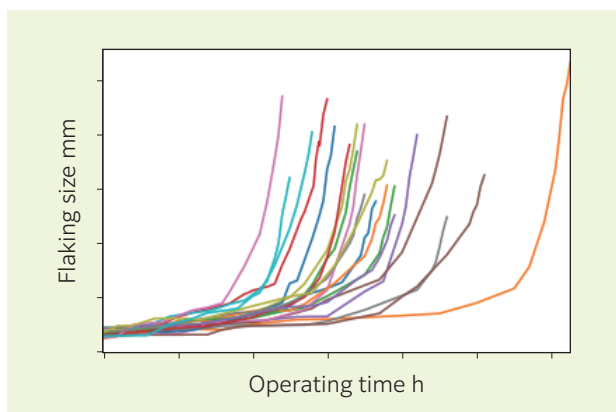


Fig. 7 Relationship between operating time and flaking size

5.2 Evaluation metrics

The coefficient of determination R^2 was used in the evaluation metrics of the development method. R^2 is an indicator of the degree to which a predicted value of the objective variables (flaking size or remaining useful life in this case) matches the actual value (hereafter, true value), and is shown in equation (1) below.

$$R^2 = 1 - \frac{\sum_{k=1}^n (y_k - \hat{y}_k)^2}{\sum_{k=1}^n (y_k - \bar{y})^2} \quad (1)$$

Here, y_k and \hat{y}_k denote the true value and predicted value of the objective variables at measurement time k , respectively. Furthermore, \bar{y} denotes the true value average of the objective variables while n denotes the number of data. R^2 can be a value of 1 or less, and the larger the value (closer to 1), the higher the prediction accuracy. R^2 was calculated for each bearing sample, and both the average and variation of predicted values calculated using leave-one-out cross-validation¹²⁾ were evaluated. Furthermore, the whole range, from when flaking occurred until it was necessary to replace the bearing, was divided into two ranges which were the early stage and late stage. Both of these stages were evaluated. Here, the range in which flaking mostly progressed in the axial direction was taken to be the early stage, while the range in which flaking progressed along the circumference was taken to be the late stage.

5.3 Flaking size and SS remaining useful life prediction results using FFN

This section provides a comparison of FFN with the various regression methods and evaluates the accuracy of predicting flaking size and SS remaining useful life. Kernel Ridge (KR)¹³⁾, Random Forest (RF)¹⁴⁾, Support Vector Regression (SVR)¹⁵⁾, Neural Network (DNN)¹⁶⁾ with 4 hidden layers, and CNN were used as comparison methods. Similar to the development method, CNN inputs the vibration acceleration spectrogram and does not consider past data. Moreover, for KR, RF, SVR and DNN, statistics in the time domain, frequency domain and cepstral domain (RMS, maximum value, peak factor, kurtosis, skewness, RMS after envelope processing¹⁷⁾) were used as inputs after various band pass filtering were applied to vibration acceleration. Hyper-parameters of the development method and comparison methods were then selected as optimal values using 5-fold cross-validation¹²⁾.

Fig. 8 shows a box plot of comparison results for the accuracy of predicting flaking size, while Fig. 9 shows a box plot of comparison results for the accuracy of predicting SS remaining useful life.

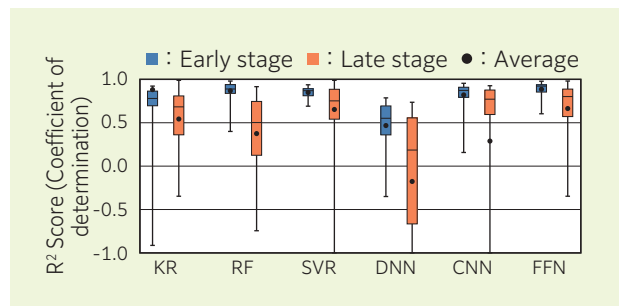


Fig. 8 Flaking size prediction accuracy (w/o HBR)^{7), 17)}

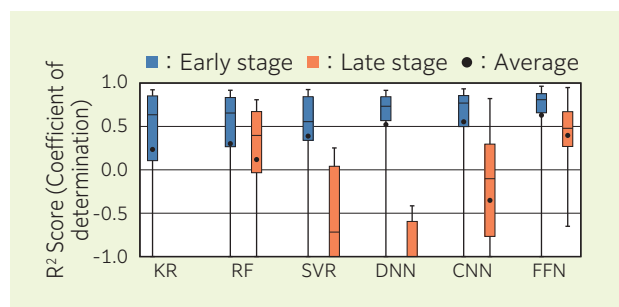


Fig. 9 SS remaining useful life prediction accuracy (w/o HBR)^{7), 17)}

All four methods, excluding KR and DNN, had an average R^2 of 0.7 or higher for the flaking size prediction during the early stage of flaking progression. In particular, FFN prediction accuracy had the highest value. Additionally, the average R^2 for CNN and FFN was high during the late stage of flaking progression. However, because CNN prediction accuracy worsened for specific samples, on average CNN was significantly lower than FFN. Therefore, FFN has the highest prediction accuracy for predicting the flaking size.

The three methods DNN, CNN and FFN have a high R^2 for the SS remaining useful life prediction during the early stage of flaking progression compared with KR, RF and SVR. Among these three methods, FFN had the highest prediction accuracy. All methods had a lower prediction accuracy during the late stage of flaking progression compared with the early stage of flaking progression. However, RF and the development method maintained a comparatively high accuracy out of all the methods.

Based on these results, we can see that FFN maintains a high prediction accuracy for both flaking size and SS remaining useful life in comparison with the other general regression methods.

5.4 Remaining useful life curve using the development method

Fig. 10 shows the relationship for the median and prediction distribution of the remaining useful life curve and damage progression using HBR. In this figure, measured data in the range used for HBR learning is shown to the left of the red dotted line. Measured data in the prediction range is shown to the right of the red dotted line. The black line shows the prediction curve using HBR. Furthermore, the dark grey area shows a 50 % level of confidence range while the light grey area shows a 95 % level of confidence range. The three graphs in the figure show prediction results for remaining useful life at points where 10 %, 20 % and 50 % data was measured out of all measurement data for the bearing from the left, respectively. A dashed line is also shown in the figure to represent the limit of use (life criteria) as defined in chapter 3. The prediction curve approaches the true value and the range for the level of confidence became narrower as measurement data increased with the progression of damage. Therefore, the relationship between remaining useful life and damage progression using HBR can be expressed as a curve with a prediction distribution (reliability of predicted values). Furthermore, increasing measurement data improved the remaining useful life prediction accuracy and increased the reliability of the predicted value.

Fig. 11 shows a box plot of remaining useful life prediction accuracy due to the development method (the combination of FFN and HBR). For comparison, the figure shows the prediction results for RF and HBR combined, CNN and HBR combined, and FFN by itself. During the damage early stage, the development method has improved accuracy in comparison with the other methods. In particular, the interquartile range becomes smaller, confirming that variation in the bearing sample is smaller. This method also has a high prediction accuracy compared with the other methods during the damage late stage, with the only average R^2 exceeding 0.5. Therefore, using the development method can predict remaining useful life with high accuracy more than conventional methods.

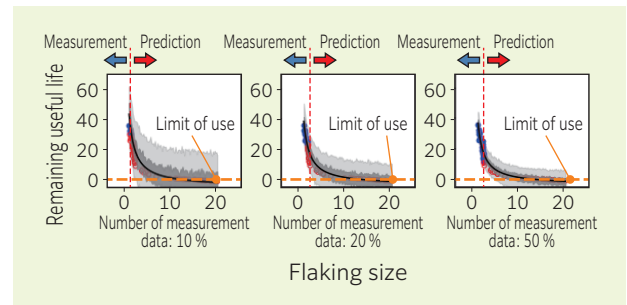


Fig. 10 Relationship between flaking progression and remaining useful life prediction distribution⁷⁾

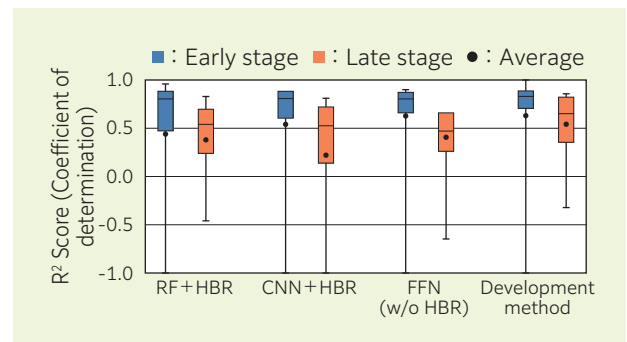


Fig. 11 Remaining useful life prediction accuracy⁷⁾

6. Summary

This paper compared and verified general machine learning methods and their performance for a remaining useful life prediction method developed to target rolling bearings after damage has occurred. It confirmed that using the development method can predict the remaining useful life with high accuracy until the time the rolling bearing needs to be replaced after damage has occurred. Therefore, use of this development method enables us to obtain a guideline for using rolling bearings in the range where the displacement between the inner and outer rings does not exceed the acceptable clearance for peripheral components even when operation is continued after flaking has occurred on a rolling bearing. Equipment such as pumps and fans used in special environments are an example of equipment that continue to be used even after the rolling bearings are damaged. In the future, NTN will continue working on increasing the versatility of this development technology while contributing to the reduction of maintenance costs on various equipment.

References

- 1) METI, "Collection of Advanced Studies in Smart Security", April 2022.
https://www.meti.go.jp/policy/safety_security/industrial_safety/smart_industrial_safety/jireisyu_r3.pdf, (See 2022-8-10).
- 2) Japan Lubricating Oil Society, "Lubrication Management Optimization Promotion Investigation Report", 1995.
- 3) ISO10816-3:2009/Amd1:2017, "Mechanical vibration -Evaluation of machine vibration by measurements on no-rotating parts -Part3: Industrial machines with nominal power above 15 kW and nominal speeds between 120 r/min and 15000 r/min when measured in situ -Amendment 1", (2017).
- 4) Y. Lei, N. Li, L. Guo, N. Li, T. Yan and J. Lin, "Machinery health prognostics: A systematic review from data acquisition to RUL prediction", *Mechanical Systems and Signal Processing*, vol.104, (2018) 799-834.
- 5) S. Ramezani, A. Moini and M. Riahi, "Prognostics and health management in machinery: A review of methodologies for RUL prediction and roadmap", *International journal of industrial engineering & management science*, vol.6, issue 1, (2019) 38-61.
- 6) Z. Xia, Q. Guan, Y. Gao, X. Chen and X. Zhai, "Review on remaining useful life prediction methods of bearing", 2020 11th international conference on prognostics and system health management (PHM-2020 Jinan), (2020) 429-433.
- 7) M. Kitai, T. Kobayashi, H. Fujiwara, R. Tani, M. Numao and K. Fukui, "A framework for predicting remaining useful life curve of rolling bearings under defect progression based on neural network and Bayesian method", *IEEE Access*, vol.9, (2021) 62642-62652.
- 8) M. Kitai, H. Tsutsui, R. Tani and T. Sakaguchi "Investigation into the Relationship between Bearing Damage Progression and Vibration Feature Quantities", *Tribology Congress*, Spring 2019, Tokyo, (2019) 1-2.
- 9) M. S. Hamada, A. G. Wilson and C. S. Reese, "Bayesian Reliability", Springer (2018).
- 10) J. Allen, "Short term spectral analysis, synthesis, and modification by discrete Fourier transform", *IEEE transactions on acoustics, speech, and signal processing*, vol.25, no.3, (1977) 235-238.
- 11) Y. LeCun, L. Bottou, Y. Bengio and P. Haffner, "Gradient-based learning applied to document recognition", *Proc. of the IEEE*, (1998) 1-46.
- 12) C. M. Bishop, "Pattern recognition and machine learning", Springer, (2006) 32-33.
- 13) C. Saunders, A. Gammerman and V. Vovk, "Ridge regression learning algorithm in dual variables", *Proceedings of the 15th international conference on machine learning*, (1998) 515-521.
- 14) L. Breiman "Random forests", *Machine learning*, vol.45, (2001), 5-32.
- 15) V. N. Vapnik, "Statistical learning theory", Wiley, (1998).
- 16) D. E. Rumelhart, G. E. Hinton and R. J. Williams, "Learning representations by back-propagating errors", *Nature*, vol.323, (1986) 533-536.
- 17) M. Kitai, Y. Akamatsu, R. Tani, H. Fujiwara, M. Numao and K. Fukui, "Remaining useful life curve prediction of rolling bearings under defect progression based on hierarchical Bayesian regression", *Proc. European conference on artificial intelligence 2020*, (2020) 2986-2992.

Photo of author



Masashi KITAI

Advanced
Technology
R&D Center

Development of Sensor Integrated Bearing “Talking Bearings™”



Yasuyuki FUKUSHIMA* Tomomi GOTO*
Yosuke TOYOGUCHI* Daigo IKKE*
Kohei MATSUBAYASHI*

There has been a growing demand for equipment condition monitoring using IoT technology to reduce equipment downtime and improve production efficiency. NTN has developed Talking Bearings™ that integrate sensors, a power generation unit, and a wireless device to standard bearings, in order to meet this demand. This paper introduces the features, structure, and performance test results of the developed bearing.

1. Introduction

There has been an increased demand to reduce equipment downtime as much as possible to increase production efficiency¹⁾. Similar strong demands have been made to increase utilization even in power generation facilities and infrastructure. To respond to these demands, it is effective to monitor equipment conditions to prevent sudden equipment stoppages and plan for maintenance and part replacement periods^{2) 3)}.

NTN has developed the “Condition Monitoring System for Wind Turbines (Wind Doctor™)”⁴⁾, the “Sensor Integrated Bearing Unit” for Machine Tool Spindles⁵⁾, the “Bearing Diagnostic Application for Industrial IoT Platforms”⁶⁾, and the “Portable Vibroscope”⁷⁾ as shown in Fig. 1 to meet the needs of condition monitoring at this type of equipment. We have also been releasing devices and analysis software to the market for the purpose of bearing condition monitoring.

It is important to provide devices that are extremely useful and can detect bearing conditions with high sensitivity to achieve a condition monitoring service that will bring a high level of satisfaction to users. Rolling bearings are incorporated into all kinds of machines such as transport machinery, household appliances and industrial machinery to support rotation. Including sensors in rolling bearings is considered to be an ideal data collection element for monitoring the condition of machines.

With this in mind, NTN has developed the sensor integrated bearing “Talking Bearing™” with built-in sensors, a power generation unit and wireless device in a standard bearing^{**}, without changing the bearing size and load carrying capacity. This paper introduces the structure of this developed product, its features, and results from performance tests.

The “Talking Bearing™” detects the bearing condition using sensors and sends the sensor information wirelessly so its name is derived from the fact that we can understand the condition of the bearing as though it is talking to us.

**Rolling bearings that comply with international standards in terms of their boundary dimensions and type



(a) Condition Monitoring System for Wind Turbines [Wind Doctor™]



(b) For Machine Tool Spindles “Sensor Integrated Bearing Unit”



(c) Portable Vibroscope

Fig. 1 Products used for condition monitoring

* New Product Development R&D Center

2. Features and structure

2.1 Features

This section provides the main features of the developed product.

(1) Advanced condition monitoring and abnormality diagnosis

The sensors are built into the bearing so they can detect bearing conditions with greater sensitivity than if the sensors had been installed on equipment. This can diagnose abnormalities early.

(2) Compatibility

Sensors, a power generation unit and wireless device have been built into a standard bearing without changing the bearing dimensions or load carrying capacity. This makes it easy to replace bearings used on existing equipment.

(3) Very convenient

The sensors and wireless devices operate using the power generated by bearing rotation to automatically send sensor information wirelessly. This requires no cables to supply power or transmit data.

2.2 Structure

2.2.1 Overall structure

The structure of the developed product is shown in Fig. 2. A power generator and electronic circuit substrate are arranged at one end of the bearing used at the inner ring rotation. A stator is fixed to the bearing outer ring and coils are held in place by the stator. A rotor (a magnetic ring that is alternately magnetized by the N and S-poles) is also fixed to the bearing inner ring. AC voltage is generated in the coils by the action of electromagnetic induction as the inner and outer bearing rings rotate relative to each other. The electronic circuit substrate, which is mounted with circuits, sensors and wireless devices, is fixed to the bearing outer ring via the stator and also sealed with material that protects the electronic circuit.

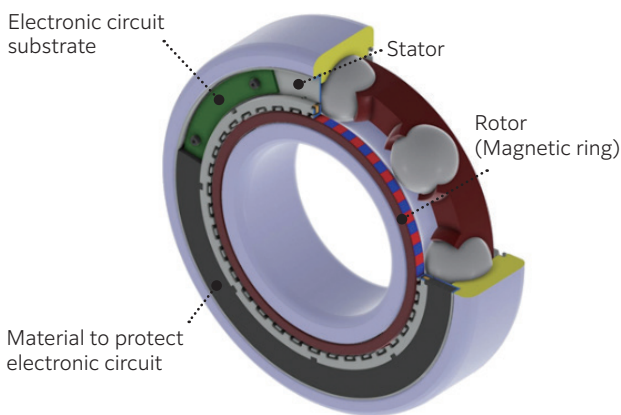


Fig. 2 Structure of Sensor Integrated Bearing “Talking Bearings™”

2.2.2 Electronic circuit

A functional block diagram and power supply circuit block diagram for the developed product are shown in Fig. 3 and Fig. 4, respectively. AC voltage generated by the power generator is input to the power supply circuit. The power supply circuit rectifies AC voltage into DC current, and also steps down any voltage obtained beyond what is required to the designated voltage. Following this, a fixed voltage required for sensor and wireless module operation is obtained using a step-up/step-down DC-DC converter. The fixed voltage activates the sensors, and the obtained sensor signals are sent by radio waves through the wireless device.

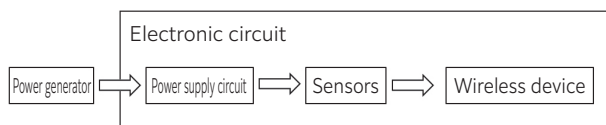


Fig. 3 Functional block diagram for developed product

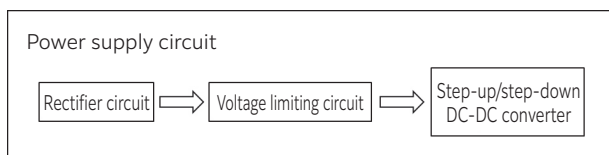


Fig. 4 Power supply circuit block diagram

3. Specifications

Table 1 shows the specifications for the developed product. Such things as acceleration, temperature and rotational speed are provided in the table for items to detect the condition of the bearing. Among these items, rotational speed is obtained by processing the AC current waveform generated by the power generator without using a dedicated sensor. Furthermore, the operating temperature range is set to -40 to 85 °C with consideration for the heat resistant temperature of the electronic components mounted in the circuit.

The wireless device uses Bluetooth Low Energy (2.4 GHz) telecommunication standard. Modes (monitoring mode and analysis mode) are selected based on the application to enable sensing. Monitoring mode assumes that monitoring is performed continuously and over an extended period, and sends data obtained for temperature, acceleration and rotational speed at intervals of 0.1 seconds. During this time, acceleration sent in this mode is the RMS value. Analysis mode acquires and sends acceleration data for a given sample number to enable the frequency to be analyzed by the receiver. In addition, switching between monitoring mode and analysis mode can be done using dedicated software installed on a computer.

Table 1 Specifications for Sensor Integrated Bearing “Talking Bearings™”

Bearing	Type	Deep Groove Ball Bearing
	Number	63-series, bore diameter code 14 or higher
Sensing	Acceleration	Radial detection direction Detection range of ± 50 G Frequency band from 11 kHz (3 dB) Sensitivity 40 mV/G
	Temperature	Detection range of -50 to 150 °C
	Rotational speed	Resolution of 16.7 min ⁻¹
Communication	Standard	Bluetooth Low Energy (2.4 GHz)
	Transmitted data	[Monitoring mode] Temperature, acceleration (RMS value), rotational speed (communication interval: 0.1 second) [Analysis mode] Acceleration
Usage conditions	Allowable rotational speed	Conforms to bearing number
	Rated load	Conforms to bearing number
	Rotational speed that can be transmitted	500 min ⁻¹ or more
	Operating temperature range	-40 to 85 °C

4. Examples of use

Fig. 5 shows communication configuration examples for the developed product. When constantly monitoring the equipment conditions for a long period of time, the amount of received data will be extremely large so it is best to send the data to a device such as a data logger that can store a large volume of data, and configure the device to ensure it can import the data to a computer or similar terminal. Moreover, when wanting to carry a computer or tablet into the workplace each time to check the condition of the equipment, a configuration that allows direct communication with the computer or tablet is effective. The developed product can communicate with devices that comply with telecommunication standards without needing to change the installed communication program, enabling the appropriate usage method to be selected as required.

The use of dedicated software enables the developed product to communicate with a computer or similar device to display sensor data. **Fig. 6**

and **Fig. 7** show examples of displaying data for monitoring mode and analysis mode, respectively. Monitoring mode displays the change over time for acceleration, temperature and rotational speed. Also, when acquired data exceeds a pre-defined threshold, a warning will display. Analysis mode displays the acceleration time waveform and frequency analysis results.

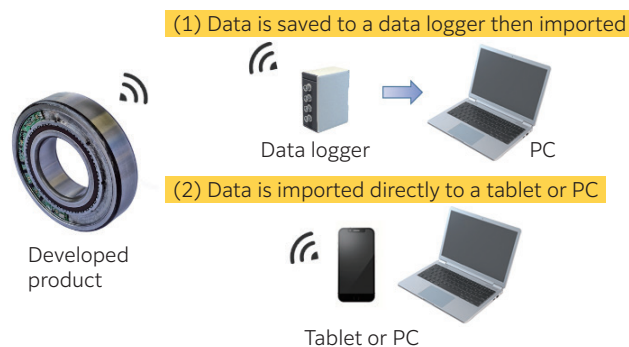


Fig. 5 Communication configuration examples



Fig. 6 Example of data displayed in monitoring mode

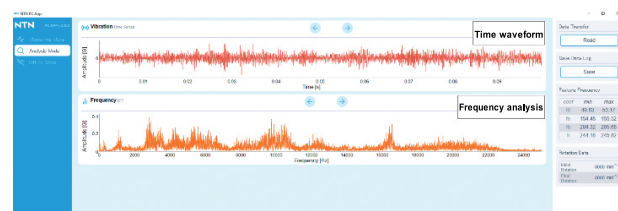


Fig. 7 Example of data displayed in analysis mode

5. Performance test

5.1 Vibration detection performance

To check the vibration detection performance of the developed product, an abnormal bearing with a defect resembling spalling (simulated spalling) on the raceway surface was used. This abnormal bearing was compared with a normal bearing without any defects to observe the vibration detected by the built-in sensor. The vibration detection performance was also compared using the acceleration sensor provided on the outside of the bearing (hereafter, external sensor) and the built-in sensor.

5.1.1 Test machine and test conditions

Fig. 8 shows a schematic drawing of the testing equipment. The bearing being tested is rotated by a shaft fitted to the inner ring of the bearing. A radial load also acts on the bearing being tested through a stand that sways on a pivot point. The external sensor is installed on the stand, and its specifications are provided in Table 2. The external sensor is compared with the built-in sensor (see Table 1), and their detection range is about the same. However, the external sensor has a wider frequency band. The acting radial load was set to 784 N. This load is quite small when compared to the basic dynamic load rating of 115 kN for deep groove ball bearing 6314.

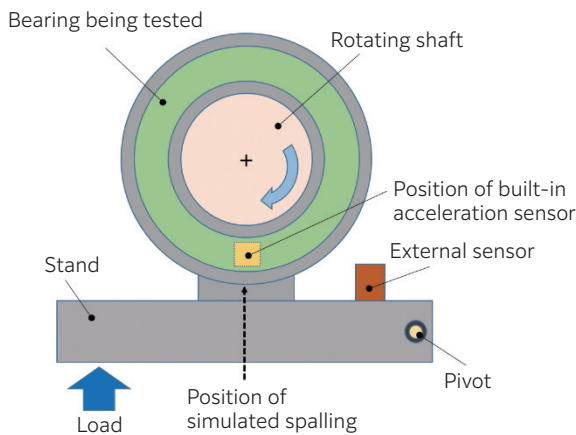


Fig. 8 Schematic drawing of testing equipment

5.1.2 Bearing being tested

Table 3 provides the specifications for the bearing being tested and Fig. 9 shows a schematic drawing of the simulated spalling formed on the bearing outer ring. Cylindrical-shaped simulated spalling was formed at 1 location at the bottom of the groove on the outer ring raceway surface, and its size was set based on the size of the contact ellipse due to elastic deformation of the bearing parts. More specifically, the diameter of the simulated spalling was set to 0.87 mm, which is twice the diameter of the contact ellipse minor axis when the test radial load of 784 N was applied. Fig. 10 shows an external photo of actual spalling that occurred during the damage end stage, as an example of spalling that occurs on a bearing. The size of the simulated spalling was made sufficiently small in comparison to end stage spalling with the aim of evaluating vibration detection performance during the initial stages of damage.

Table 2 Specifications for the external sensor

External sensor	Detection range	±60 G
	Frequency band	3 Hz to 25 kHz (3 dB)
	Sensitivity	100 mV/G

Table 3 Specifications for the bearing being tested

	Normal bearing	Abnormal bearing
Bearing	Deep groove ball bearing 6314	
Seal	Non-contact type (one side)	
Grease	Thickening agent: Urea-based Base oil: Poly-alpha olefin	
Simulated spalling	No	1 location at the bottom of the groove on the outer ring raceway surface φ0.87 × depth of 0.1 mm

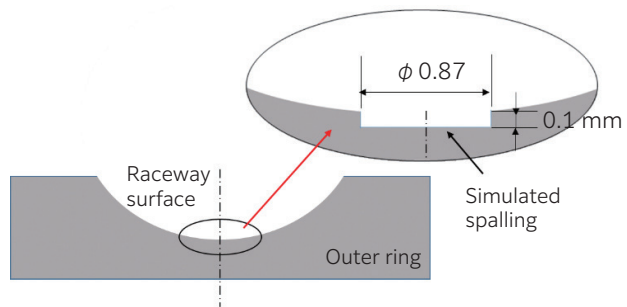


Fig. 9 Schematic drawing of simulated spalling

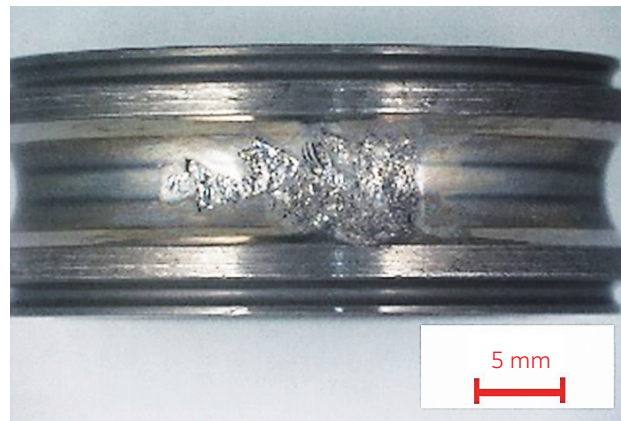


Fig. 10 Example of spalling damage

5.1.3 Test results

Fig. 11 shows the built-in sensor output when rotating the normal sensor and abnormal sensor at 2 000 min⁻¹. Each time the rolling element passes the simulated spalling on the abnormal bearing, an obvious spike in acceleration was detected. If a defect of about the same size as the simulated spalling created this time occurs on the raceway, it would be possible to detect an obvious abnormality with the developed product.

Next, Fig. 12 shows a comparison between the built-in sensor and external sensor for the acceleration measured at the abnormal bearing. Fig. 12 shows the results of conducting envelope processing and frequency analysis (fast Fourier analysis) on the data output in Fig. 13. Finally, Fig. 13 lists the rotational speed (103 Hz) of the rolling element relative to the outer ring and the higher-order rotational speeds. The

sensor output when the rolling element passes the simulated spalling is greater for the built-in sensor in comparison with the external sensor. Frequency analysis also shows that the built-in sensor is more sensitive and can better detect vibration at high frequency.

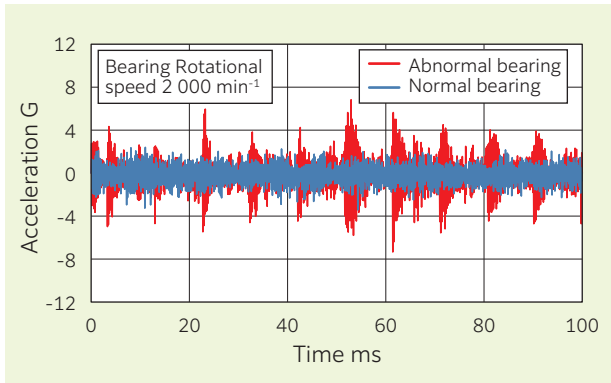


Fig. 11 Comparison of normal bearing and abnormal bearing built-in sensor output

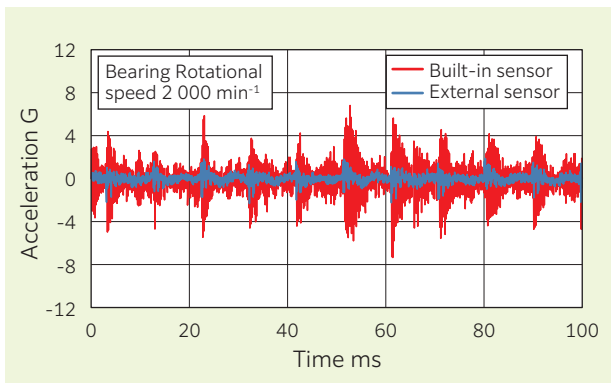


Fig. 12 Comparison of acceleration for built-in sensor and external sensor with abnormal bearing

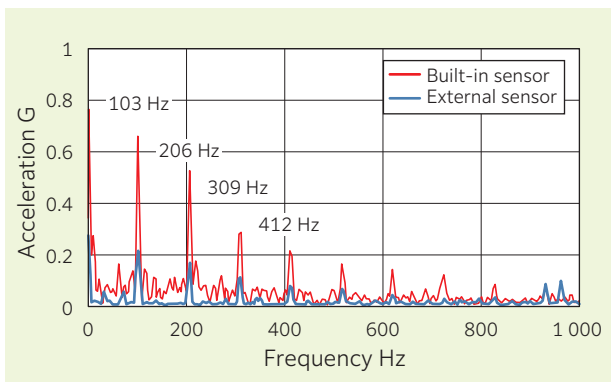


Fig. 13 Comparison of frequency analysis for built-in sensor and external sensor

5.2 Temperature detection performance

Measured values taken from a thermocouple affixed to the outer circumferential surface of the bearing outer ring were compared with measured values taken from the built-in temperature sensor. The bearing being tested was the normal bearing shown in **Table 3**,

and it was measured using the testing equipment shown in **Fig. 8**. The rotational speed was taken as being up to the allowable rotational speed of $4\,600\text{ min}^{-1}$ (value listed in the **NTN** catalog) for deep groove ball bearing 6314 (grease lubrication, non-contact seal). Measurements were taken by repeatedly increasing rotation and holding for two hours at increments of around $1\,000\text{ min}^{-1}$. Measurement results are shown in **Fig. 14**. The results show that there is no significant difference in the values measured with both sensors in either the transient region after rotation was increased or the steady-state region when rotation was held. Thus, the developed product has the same temperature detection performance as when affixing a thermocouple to the bearing outer ring.

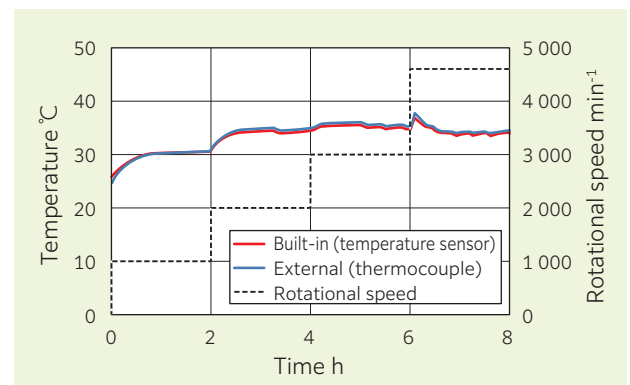


Fig. 14 Comparison of temperature taken with the built-in sensor and external thermocouple

5.3 Temperature increase characteristics

Fig. 15 shows the generated power and running torque of the developed product in relation to rotational speed. Here, the generated power is the sum of the power consumed by the circuit and the power loss from the power generator. Also, the running torque is equivalent to the running torque of the entire bearing with built-in sensor, including the friction loss during bearing rotation and the generated power mentioned above. **Fig. 15** shows the values measured after holding for two hours at each rotational speed. The generated power is small at 1 to 2% in contrast with the power loss of the entire bearing calculated from the running torque and rotational speed, and incorporating the power generator and circuit into the bearing is also estimated to have a minor effect on the bearing temperature.

Fig. 16 shows the results measured for the temperature on the actual bearing. The bearing temperature was measured with a thermocouple affixed to the outer ring outer circumferential surface and the built-in sensor. **Fig. 16** shows the value increase from ambient temperature after holding for two hours at each rotational speed. There was no significant difference between the standard bearing and developed product, showing that the developed product has the same temperature increase characteristics as the standard bearing.

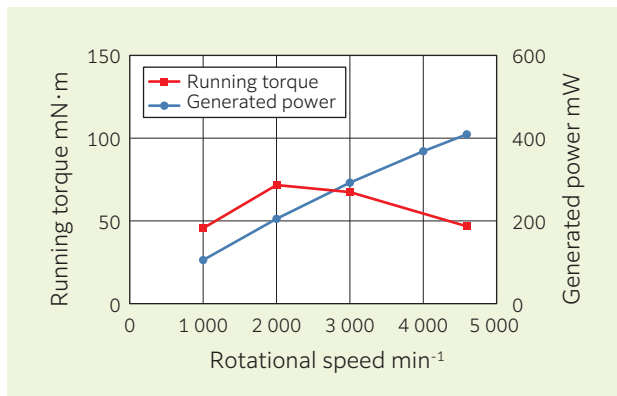


Fig. 15 Generated power and running torque for the developed product

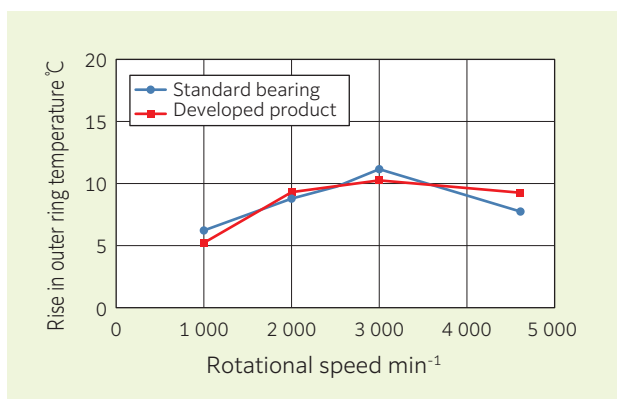


Fig. 16 Temperature increase characteristics for the developed product and standard bearing

6. Summary

To respond to efforts towards reducing downtime at manufacturing sites, **NTN** has developed the Sensor Integrated Bearing “Talking Bearing™” which has sensors, a power generation unit and wireless device built into a standard bearing. The performance of this product was verified in this paper. We predict that demand for equipment condition monitoring will increase in the near future, and further improvements in functionality will be required. **NTN** will continue to develop equipment condition monitoring and contribute towards improving production efficiency through its improvements in the function of “Talking Bearing™” and releasing products in the market.

References

- 1) Japan Institute of Plant Maintenance, 2021 Maintenance Investigation Report Summary (June 2022)
- 2) Sohei Yamada, Shigetoshi Noritake, Investigation to Optimize Manufacturing and Logistics Sites Using Sensing Technology, Journal of The Japan Society of Mechanical Engineers, Vol.123, No.1223(2020)19-21.
- 3) Hou Jinyama, Smart Equipment Condition Monitoring & Diagnosis Technology in the IoT/AI Age, System/Control/Information, Vol.65, No.4 (2021) 113-118.
- 4) Makoto Miyazaki, Wataru Hatakeyama, Application of Condition Monitoring System for Wind Turbines, NTN TECHNICAL REVIEW, No.86, (2018) 40-44.
- 5) Shohei Hashizume, Yusuke Shibuya, Daichi Kondo, Yohei Yamamoto, Hiroyuki Iwanaga, Development of Sensor Integrated Bearing Unit for Machine Tool Spindles, NTN TECHNICAL REVIEW, No.88 (2020) 33-37.
- 6) Hiroyuki Iwanaga, Development of Edge Application for Bearing Diagnosis, Inspection Technology, March 2022 Edition, 32-34.
- 7) Our Line of New Product, Portable Vibroscope, NTN TECHNICAL REVIEW, No. 87 (2019) 106.

Photo of authors



Yasuyuki FUKUSHIMA
New Product
Development R&D
Center

Tomomi GOTO
New Product
Development R&D
Center

Yosuke TOYOGUCHI
New Product
Development R&D
Center

Daigo IKKE
New Product
Development R&D
Center

Kohei MATSUBAYASHI
New Product
Development R&D
Center

Development of Multi Track Magnetic Encoder Integrated Rolling Bearing



Hiroshi OKUMURA*
 Hiroyoshi ITO*
 Yasuyuki HAMAKITA*

The robot industry has been expanding on the back of market demand for improved productivity and labor saving as the countermeasures of diminishing working population. Especially, the demand of small robots such as collaborative robots that work with human labors and service robots has been increasing. Through the recent trend, market requirements for the robots have been getting

higher and more diversified.

NTN has developed the “Multi Track Magnetic Encoder Integrated Rolling Bearing” based on the technology of the “Multi Track Magnetic Ring” for rotary encoders. The bearing is suitable for robot joints and performs high-precision angle detection as well as the shaft support. This report introduces the features, structure, and performance of the bearing.

1. Introduction

The use of robots to perform work instead of humans is on the increase throughout the world in all industrial manufacturing sectors, including for automobile manufacture^{1) 2)}. In recent years we have experienced significant social problems such as the decline in the working-age population ratio due to the decreasing birthrate and aging population as well as slow production activity due to the increase in COVID-19 infections, prompting the increased introduction of robots. Industrial robots installed in production lines, robots that work in locations away from humans, and small robots such as collaborative robots and service robots are on the increase, while the structure of robots and the work they do has become increasingly diverse.

Vertical articulated robots (**Fig. 1**) that move similar to the arms of a human are typical, and such robots must transport a workpiece with high accuracy and speed to a determined position. To achieve this, the joint mechanism must be able to support the motor’s rotating shaft while detecting its rotational speed, rotational direction, and absolute angle with a high level of accuracy to achieve the correct position. In addition to servo motors and reducers, robots use bearings to support rotation and rotary encoders to detect rotational conditions³⁾.

Furthermore, recent joint mechanisms must support the diverse trends as mentioned above, and to be compact, lightweight, be assembled from as fewer parts as possible to reduce man-hours to build them and have a high environmental resistance so they can be used in various operating conditions.

So far NTN has commercialized the highly accurate and compact Multi Track Magnetic Ring for use in

detecting the absolute angle and rotational speed for the robot joint mechanisms⁴⁾. The Multi Track Magnetic Ring, in combination with the magnetic sensor IC, forms a magnetic rotary encoder that provides high environmental resistance.

The application of this technology contributes to greater improved performance for robot joint mechanisms, so NTN has developed a new “Multi Track Magnetic Encoder Integrated Rolling Bearing” (hereafter, developed product) that brings together the bearing, the Multi Track Magnetic Ring, and magnetic sensor IC in a single unit. The developed product supports the rotation of the shaft while detecting the rotational speed, rotational direction and absolute angle as a rotary encoder. Bringing together the bearing and magnetic rotary encoder in a single unit can make the robot joint mechanism more compact and reduce the man-hours required for assembly and setup in the robot manufacturing process. The developed product’s features, structure and test results are introduced below.

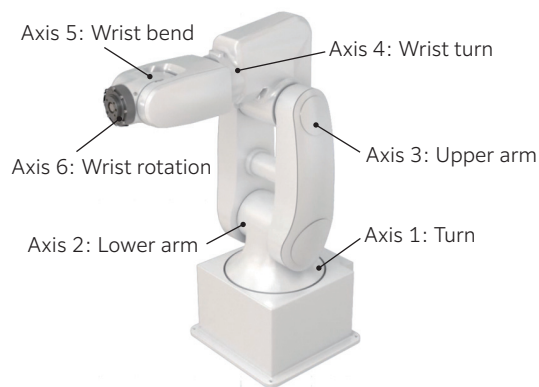


Fig. 1 6 axes vertical articulated robot

* Robotics & Sensing Engineering Dept., Industrial Business Headquarters

2. Developed product structure and features

The developed product is a unit composed of a deep groove ball bearing, Multi Track Magnetic Ring, and magnetic sensor IC (Fig. 2).

The Multi Track Magnetic Ring is attached to the inner ring of the deep groove ball bearing. The magnetic sensor IC is attached to the outer ring of the deep groove ball bearing through the sensor housing. The developed product can be used for joint mechanisms on the robot as shown in Fig. 3. The Multi Track Magnetic Ring rotates as the axis rotates, and to correspond to the rotation the magnetic sensor IC reads the change in magnetic poles. This enables the developed product to detect the rotational speed, rotational direction, and absolute angle. Data detected by the magnetic sensor IC is transmitted to a motor driver prepared by the user, then used for positioning the robot joint mechanisms (Fig. 4).

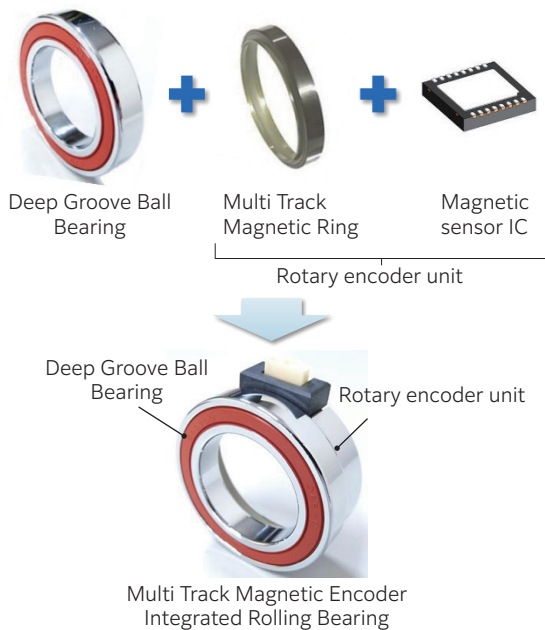


Fig. 2 Configuration of major components for the Multi Track Magnetic Encoder Integrated Rolling Bearing



Fig. 3 Positions where the Multi Track Magnetic Encoder Integrated Rolling Bearing can be used

The developed product is a compact unit that uses technology to integrate the rotation detection unit and bearing that NTN has developed for conventional rotation sensor bearings (Fig. 5), which are well-established for use in transportation machinery⁵. It has the same bearing bore diameter, outer diameter, width, and load rating as a standard bearing without the rotation detection unit, making it compatible with standard bearings. This unit's features are shown in (1) to (4) below. Table 1 also shows the specifications for the developed product using deep groove ball bearing 6907.

(1) Can support shaft rotation and provide high accuracy angle detection.

The developed product detects rotational speed, rotational direction, and absolute angle while supporting shaft rotation. Configuring parameters in the magnetic sensor IC enables a maximum high accuracy output of 20 bits (resolution of approximately 0.00034°).

(2) Contributes towards making the robot joint mechanism compact and lightweight.

Integrating the deep groove ball bearing, Multi Track Magnetic Ring and magnetic sensor IC means that a coupling to connect the joint mechanism and rotary encoder is not needed. This enables a reduction in the joint mechanism shaft length, the use of fewer components, and results in producing a more compact and lighter joint mechanism (Fig. 6).

(3) Can reduce man-hours for robot assembly and setup.

As mentioned above in (2), integrating components can reduce the number of robot components, which reduces man-hours required for assembly. It also means that the user does not have to perform setup such as adjusting output signals required for when assembling the magnetic ring and magnetic sensor, so man-hours can be reduced.

(4) Affected less by the surrounding environment and high environmental resistance.

The developed product is a magnetic rotary encoder that detects the rotational speed, rotational direction and absolute angle using magnetism. In comparison with optical rotary encoders that use light for detection, it is affected less by the surrounding environment such as temperature changes, dust, and oil, and has a high environmental resistance⁶.

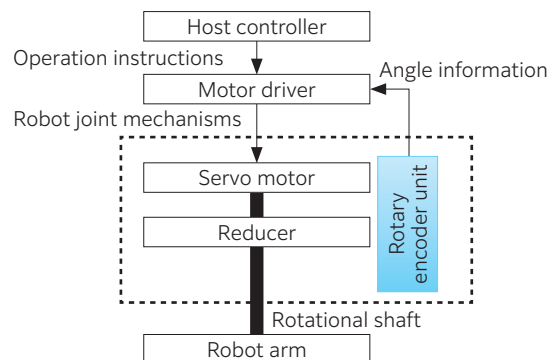
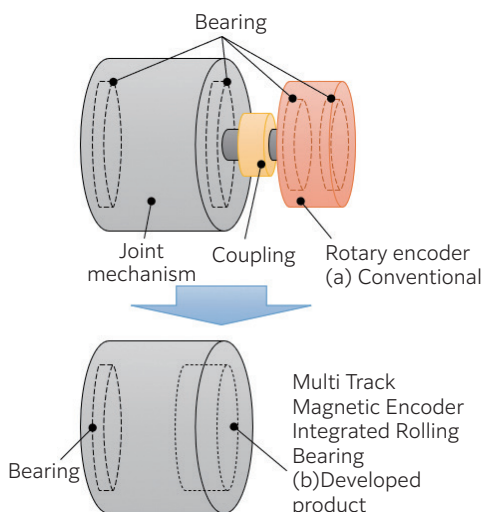


Fig. 4 Schematic drawing of positioning for robot joint mechanisms using the Multi Track Magnetic Encoder Integrated Rolling Bearing



Fig. 5 Rotation sensor bearing (NTN conventional product)



Using the developed product enables the rotary encoder to be integrated into the joint mechanism

Fig. 6 Adopting the Multi Track Magnetic Encoder Integrated Rolling Bearing reduces the number of components required for the robot joint mechanism, and makes it more compact

Table 1 Specifications for the Multi Track Magnetic Encoder Integrated Rolling Bearing (deep groove ball bearing 6907)

Item	Specifications
Deep Groove Ball Bearing	6907 (ID35×OD55×10)
Wiring connector height	6 mm (protrusion amount from bearing outside diameter surface)
Encoder unit width	10.5 mm
Multi Track Magnetic Ring	64/63 polar pairs, 1.28 mm pitch
Magnetic sensor IC	iC-MU
Allowable rotational speed	6 000 min ⁻¹
Angle resolution	Max. 20 bits
Detection information	Rotational speed, rotational direction, absolute angle
Angle detection error	± 0.1°
Power supply voltage	DC 5 V
Current consumption	60 mA
Signal format	ABZ, SPI, BiSS, SSI
Operating temperature range	−25 to +110 °C

3. Absolute angle detection principles and resolution

3.1 Multi Track Magnetic Ring and magnetic sensor IC

The Multi Track Magnetic Ring (**Fig. 7**, **Fig. 8**) is composed of a core press-formed from thin steel plates and rubber material that contains a magnetic material (hereafter, rubber magnetic material). The rubber magnetic material is adhered to the core by vulcanization. Two magnetic tracks with different number of polar pairs for the N-pole and S-pole are formed on the outer diameter circumferential surface of the rubber magnetic material for the radial magnetization type, and the width surface for the axial magnetization type. For a 64/63 polar pair Multi Track Magnetic Ring, the main track is magnetized with N-pole S-pole 64 polar pairs and the sub track is magnetized with 63 polar pairs.

The magnetic sensor IC arranged opposite the Multi Track Magnetic Ring is equipped with two detection units that face the main track and sub track, and an absolute angle calculation unit. For example, IC (iC-MU) manufactured by iC-Haus can be used (**Fig. 9**).

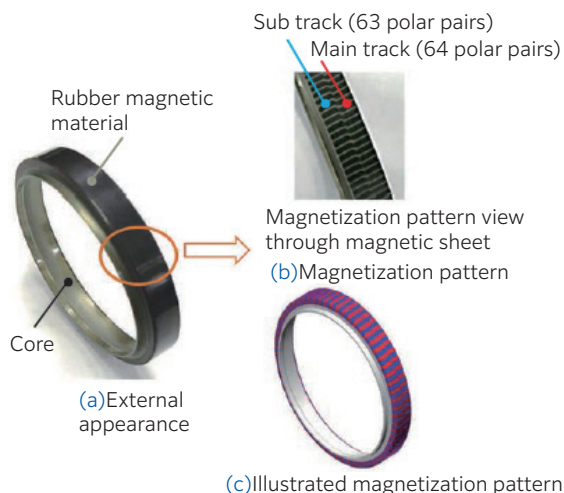


Fig. 7 Multi Track Magnetic Ring: Radial magnetization type

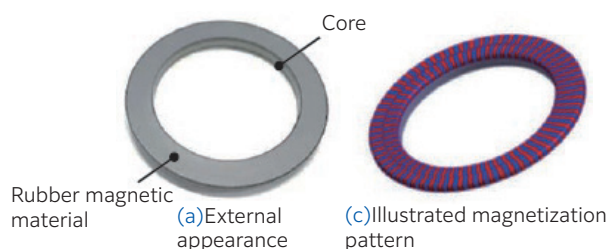


Fig. 8 Multi Track Magnetic Ring: Axial magnetization type



Fig. 9 Illustration of combining the Multi Track Magnetic Ring with iC-MU series (images provided by iC-Haus GmbH)

3.2 Absolute angle detection principles and resolution

This section explains the absolute angle detection principles (Fig. 10) and resolution with the 64/63 polar pair Multi Track Magnetic Ring as an example.

For the 64/63 polar pair Multi Track Magnetic Ring, at each rotation the output signal of the period corresponding to magnetization polar pairs 64 from detection unit 1 of the magnetic sensor IC, and magnetization polar pairs 63 from detection unit 2 are obtained. These output signals have a phase difference of one polar pair for each rotation so calculating this phase difference enables the absolute angle to be detected. Thus, on a magnetic pair with 64 polar pairs, it is possible to detect at what polar pair the position lies.

By accurately reading the magnetic strength between polar pairs with the magnetic sensor IC, 12 bit multiplication is possible. Therefore, angle information for one polar pair can be divided into 2^{12} sections, and together with 64 polar pairs (2^6), 18 bit (resolution of approximately 0.0014°) angle information can be output⁸⁾. Magnetic sensor IC parameters can be configured to also enable up to 20 bit (resolution of approximately 0.00034°) output.

Angle information output from the sensor is dependent upon the magnetic pitch accuracy. To be able to detect the absolute angle and achieve this kind of high angle accuracy, it is necessary to sufficiently magnetize two magnetic tracks with a different number of magnetized polar pairs. NTN has developed original magnetization technology to provide highly precise control of the magnetic pitch for each magnetic pole on the Multi Track Magnetic Ring⁹⁾.

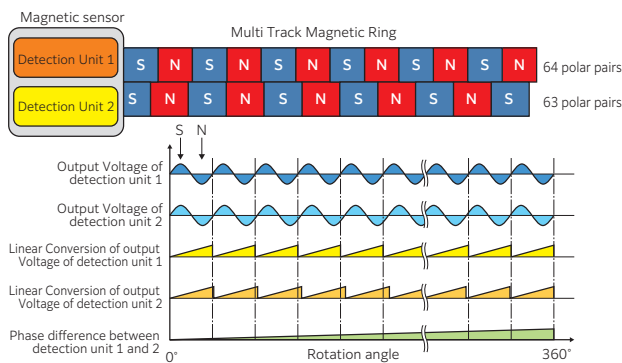


Fig. 10 Absolute angle detection principles

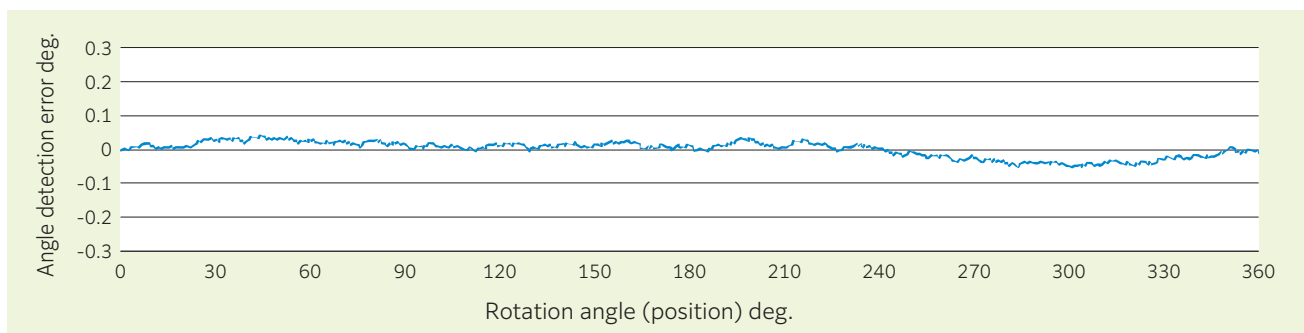


Fig. 11 Absolute angle detection error measurement results of Multi Track Magnetic Encoder Integrated Rolling Bearing

4. Evaluation test

4.1 Absolute angle detection error

The absolute angle detection error was measured for the developed product using deep groove ball bearing 6907. Table 2 shows the measurement conditions and Fig. 11 shows the measurement results. The developed product uses both a Multi Track Magnetic Ring and magnetic sensor IC, and these items are attached to a deep groove ball bearing with good accuracy to achieve high accuracy detection of the absolute angle. Under the measurement conditions shown in Table 2, an absolute angle detection error of $\pm 0.1^\circ$ or less was obtained.

4.2 Resistance to electromagnetic noise

The developed product achieves a compact unit composed of few elements as possible, including a deep groove ball bearing, Multi Track Magnetic Ring, magnetic sensor IC and circuit substrate, and contributes towards a more compact and lightweight robot joint mechanism. To investigate its resistance to various noise assumed at the robot joint mechanism, an electromagnetic noise test was conducted. This test results show that the developed product has resistance to EMC Standards (IEC 61000-6-2) for industrial environments¹⁰⁾ (Table 3, Fig. 12).

Table 2 Absolute angle detection error measurement conditions for Multi Track Magnetic Encoder Integrated Rolling Bearing (deep groove ball bearing 6907)

Item	Conditions
Power supply voltage	DC 5 V
Rotational speed	5 min^{-1}
Measurement angle	360°
Measurement temperature	Room temperature
Number of polar pairs	64/63 polar pairs

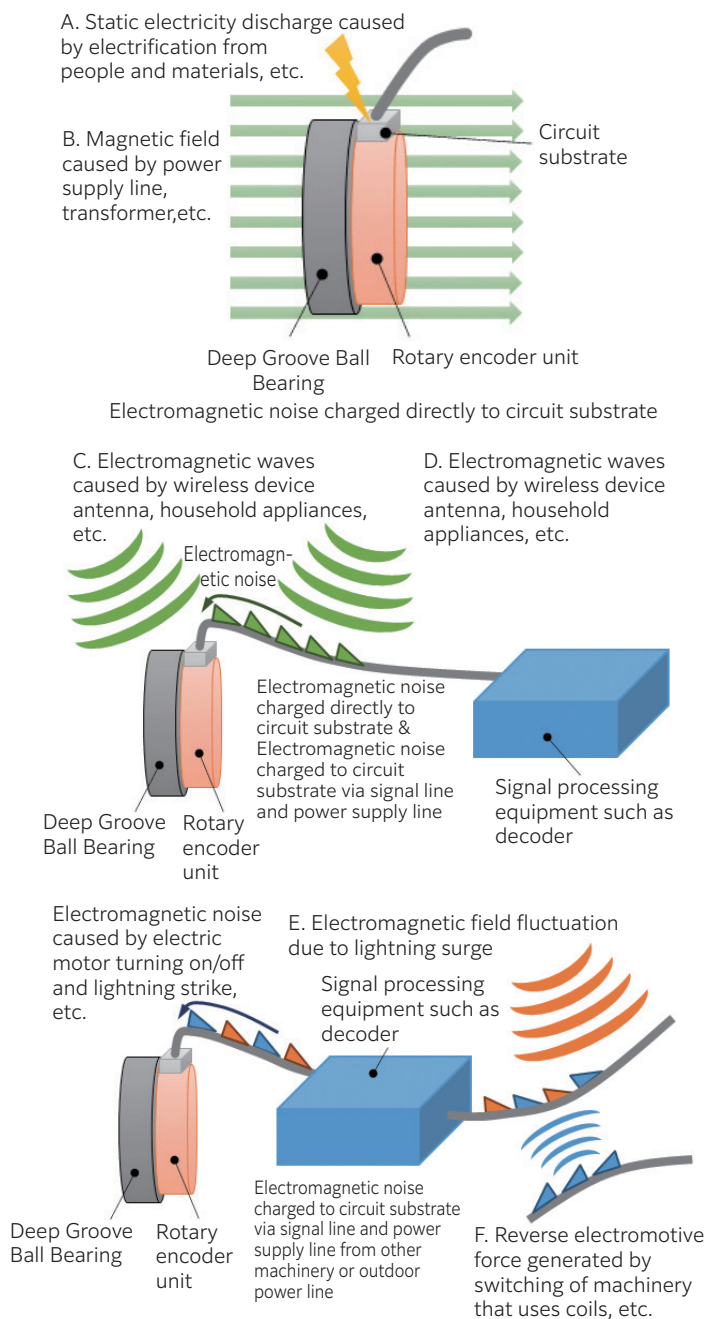


Fig. 12 Types of electromagnetic noise

5. Developed product examples of application

The developed product can be used for compact robot joint mechanisms, such as collaborative robots and service robots using the features introduced in this paper. Additionally, it can also be used in general servo motors by replacing the analog rotary encoders, such as optical rotary encoders and resolvers (**Fig. 13**).

For example, optical rotary encoders require barriers to prevent the intrusion of dust and oil to the light emitter and light receiver, as well as the internal areas of the encoder so it is difficult to make them compact. Furthermore, resolvers require high accuracy arrangement of many coils in the coil unit which is a key component to achieving high resolution, so they have a complex shape, and it is difficult to make them compact. Additionally, resolvers must have an R/D converter to convert the output signal to digital.

In contrast, the developed product only requires a Multi Track Magnetic Ring and magnetic sensor IC to create the magnetic rotary encoder. This produces a simple structure in comparison with an optical rotary encoder or resolver, which can contribute towards making robot joint mechanisms and servo motors more compact and lighter in weight. The developed product also outputs digital signals, so an R/D converter or similar device is not necessary, so it is easy to make the system compact and lightweight.

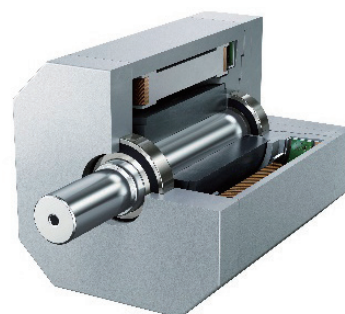


Fig. 13 Servo motor

Table 3 Resistance evaluation test to electromagnetic noise

Test No.	Test standards and name	Assumed electromagnetic noise	Test conditions	Results
1	IEC 61000-4-2 : 2008 Electrostatic discharge immunity test	A in Fig. 12	4 kV	No damage possible to conform with EMC standards (IEC 61000-6-2)
2	IEC 61000-4-4 : 2012 Burst immunity test	F in Fig. 12	1 kV	
3	IEC 61000-4-5 : 2014 Surge immunity test	E in Fig. 12	1 kV	
4	IEC 61000-4-8 : 2009 Power frequency magnetic field immunity test	B in Fig. 12	30 A/m (50 Hz/60 Hz)	
5	IEC 61000-4-6 : 2013 Radio frequency conducted disturbances immunity test	D in Fig. 12	10 V 0.15 to 80 MHz	
6	IEC 61000-4-3 : 2006 Radiated, radio-frequency electromagnetic field immunity test	C and D in Fig.12	10 V/m (80 to 1 000 MHz) 3 V/m (1.4 to 6.0 GHz)	

6. Expanding the developed product series

The developed product can be applied to compact robot joint mechanisms such as collaborative robots and service robots. In addition to using the deep groove ball bearing 6907 introduced in this paper, **NTN** plans to expand the series from bearing bore diameter 15 mm to 45 mm.

7. Summary

The demand for robots, including collaborative robots and service robots, is on the increase, and market demands are becoming more sophisticated and diverse.

To respond to the above needs, **NTN** has developed a Multi Track Magnetic Encoder Integrated Rolling Bearing that integrates a deep groove ball bearing and magnetic rotary encoder using Multi Track Magnetic Ring technology. This enables robots that are more compact and lightweight while also reducing man-hours to assemble and setup the robots.

NTN will continue to work on developing products that contribute to further improvements in performance of industrial machinery, including robots, and support the advancement of technology for further enriching people's lives and technology for protecting the global environment.

References

- 1) Keiichi Ueda, Technical Trend of the Precision Bearings for Machine Tools, Tool Engineer, Vol. 60 No. 16, (2019) 41-43.
- 2) Makoto Oebisu, Hiromichi Kokumai, Yasuyoshi Hayashi, Masato Tsujihashi, Technical Trend and Features of the Bearing for Robot, NTN TECHNICAL REVIEW, No.86, (2018) 34-39.
- 3) Hiromichi Kokumai, Hideaki Tanaka, Kosuke Suzuki, Yuichiro Kawakami, Approach to Development of Robot Joint-related Products, NTN TECHNICAL REVIEW, No.88, (2020) 27-32.
- 4) Takashi Koike, Yasuyuki Fukushima, Yusuke Shibuya, Hiroyoshi Itou, Development of Multi Track Magnetic Ring for High Accuracy Absolute Angle Detection, NTN TECHNICAL REVIEW, No.86, (2018) 45-49.
- 5) Hiroyoshi Itou, Takashi Koike, Bearings with Rotational Sensors, NTN TECHNICAL REVIEW, No. 69, (2001) 108-116.
- 6) Yasuyoshi Hayashi, Development of Robotic Joint-Related Products, Bearing & Motion-Tech Magazine, No.035, (2022) 25-27.
- 7) iC-Haus GmbH, iC-MU off-axis nonius encoder with integrated hall sensors
- 8) Shoji Itomi, Hiroyoshi Itou, NTN Sensor Units for Construction Machine, NTN TECHNICAL REVIEW, No. 76, (2008) 118-125.
- 9) Takashi Koike, Yasuyuki Fukushima, Yusuke Shibuya, High Accuracy Absolute Angle Sensor for Use in Absolute Angle Detection on Robot Joints, Vol. 62 No. 3, (2018) 55.
- 10) Electromagnetic compatibility (EMC) - Part 6-2, Generic standards - Immunity standard for industrial environments IEC 61000-6-2, (2016).

Photo of authors



Hiroshi OKUMURA

Robotics & Sensing
Engineering Dept.,
Industrial Business
Headquarters



Hiroyoshi ITO

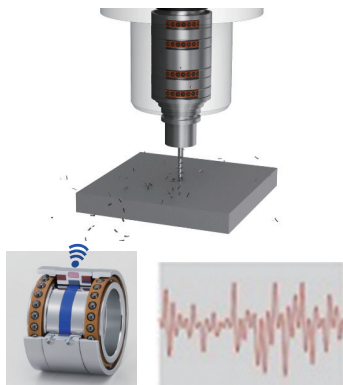
Robotics & Sensing
Engineering Dept.,
Industrial Business
Headquarters



Yasuyuki HAMAKITA

Robotics & Sensing
Engineering Dept.,
Industrial Business
Headquarters

Development of Sensor Integrated Bearing Unit for Machine Tool Spindles



Shohei HASHIZUME* Yudai NAKANO*
 Daichi KONDO** Yoji OHGUCHI**
 Yohei YAMAMOTO***

Machine tools are sometimes called the “Mother Machine” or “Mother of Industry” and have been supporting manufacturing all over the world. They are required for not only fundamental features like high speed, high rigidity, and super precision, but also condition monitoring and “Connected Industries” related technology. In 2018, NTN developed the “Sensor Integrated Bearing Unit for Machine Tool Spindles”, and additionally, applied the load detection function and wireless system to the unit in 2020.

NTN has recently added the data receiver unit which collects the data from the “Sensor Integrated Bearing Unit” in machine tool spindles and the software for data communication. This report introduces the features, structure, and performance of the unit, and offers communication examples between the unit and machine tools.

1. Introduction

Amid significant changes in the global environment and social structure, the industrial world has been tackling various social challenges, such as achieving carbon neutrality to slow down global warming, achieving sustainable development goals (SDGs), and improving production to further enrich people’s lives, by integrating new technology created in the 4th industrial revolution (Industry 4.0) into core technologies developed over many years.

Among these technologies, machine tools¹⁾²⁾ that support manufacturing in various industries, including the automotive, aircraft, medical and IT sectors, are being promoted to further improve basic performance in terms of “high speed, high durability and high accuracy” as a response to energy loss reduction and work force reduction. Productivity improvements and manpower reductions using IoT technology are underway.

NTN has developed the “Sensor Integrated Bearing Unit” for Machine Tool Spindles (hereafter, this bearing unit)³⁾, which has sensors built into the spacer, a component of a bearing unit. This enables sensing of the temperature and vibration around the bearing raceway surface, making it possible for advanced condition monitoring of machine tools. NTN showcased a reference exhibit of this at the 29th Japan International Machine Tool Fair (JIMTOF 2018) held in 2018. A load detection function was also added to this bearing unit together with wireless operation⁴⁾ in 2020.

We have also added a data receiving unit that acquires data detected by the sensors on this bearing unit at the exterior of the spindle as well as

communication software to send and receive the data with the aim of further improving the usefulness of this bearing unit. This bearing unit’s characteristics, structure, performance test results for load and other sensors, and how to connect it to machine tools are described below.

2. Functions and purpose of the sensor integrated bearing unit

Table 1 shows the functions and purpose of this bearing unit. When a bearing that supports the rotation of the spindle (hereafter, spindle bearing), a key component on machine tools, is damaged, operation at the machine tool stops and the spindle must be replaced; this significantly lowers productivity. Due to this fact, there is a growing need to detect this damage early on. Furthermore, it will be even more necessary in the future to increase the productivity of machine tools and to minimize the dependence on individual expertise in machining monitoring in response to the aging of skilled personnel and the decline in the working-age population ratio. This bearing unit is expected to contribute towards these needs while also contributing towards achieving sustainable development goals (SDGs).

For example, if we detect the machine load applied on the spindle, and use this information for machining monitoring, we can optimize the machine conditions such as cutting depth, feed, and rotational speed. This is expected to provide increased machining quality and productivity. Furthermore, this bearing unit detects tool and workpiece collision to reduce

* Robotics & Sensing Engineering Dept., Industrial Business Headquarters ** New Product Development R&D Center
 *** Product Design Dept., Industrial Business Headquarters

Development of Sensor Integrated Bearing Unit for Machine Tool Spindles

Table 1 Functions & purpose of the sensor integrated bearing unit

	Function	Implementation method	Purpose	Connection to SDGs
(1)	Detects preload for spindle bearing (While spindle is rotating and after spindle has been installed)	Load Sensor	<ul style="list-style-type: none"> To see sudden rises in preload that occurs before bearing seizure, and to detect signs of bearing seizure early on To make it easier to manage preload on bearings after the spindle has been installed, and to reduce assembly manhours for the spindle 	<ul style="list-style-type: none"> Improve productivity, and reduce energy loss through optimized production Reduce defective workpieces (waste) Contribute towards automation and manpower reduction 
(2)	Detects external loads applied to the spindle		<ul style="list-style-type: none"> To detect machining load applied to the spindle, and contribute towards improved machining quality and productivity using machining monitoring To detect collisions between the tool and workpiece, reduce damage to the spindle bearing, and use it to investigate the cause of the damage 	
(3)	Monitors temperature changes in the spindle bearing	Temperature Sensor	<ul style="list-style-type: none"> To monitor the bearing raceway surface and lubrication conditions 	
(4)	Monitors vibration changes in the spindle bearing	Vibration Sensor	<ul style="list-style-type: none"> To monitor the bearing raceway surface To detect collisions between the tool and workpiece, reduce damage to the spindle bearing, and use it to investigate the cause of the damage 	
(5)	No need for an externally connected cable or wiring space for power supply	Independent Power supply	<ul style="list-style-type: none"> To reduce man-hours to assemble the spindle 	
(6)	External connection for data transmission No need for cable or wiring space	Wireless Module	<ul style="list-style-type: none"> To eliminate the need to change the structure of the spindle 	<ul style="list-style-type: none"> Reduce energy loss with independent power supply and improved productivity 

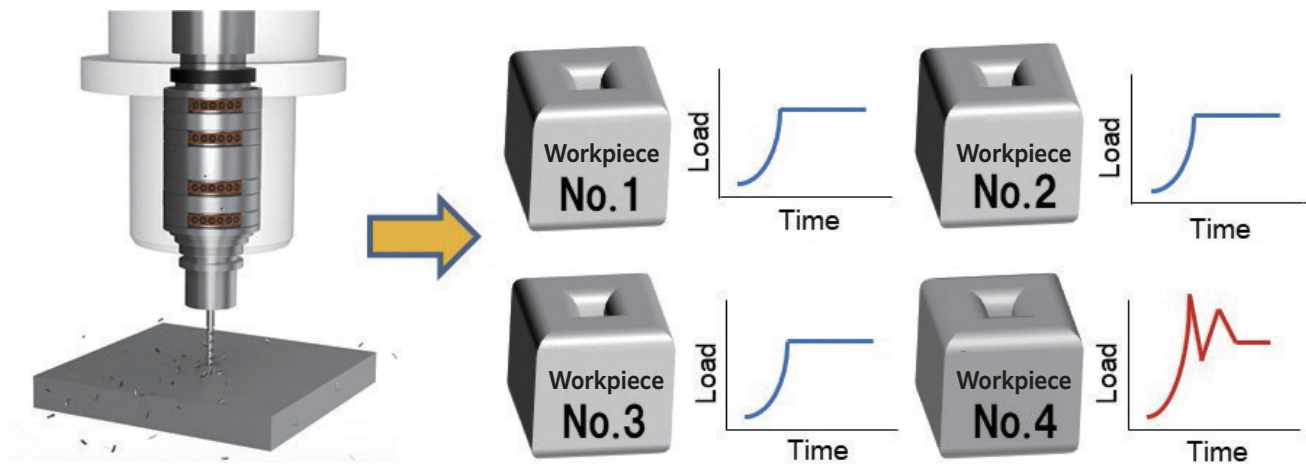


Fig. 1 Illustration of sensor integrated bearing unit application
Example of improving machining quality by linking machining data to each product of a machine tool

damage to the spindle bearing, uses real-time information to determine the cause of the damage, and as shown in **Fig. 1**, links machining data for each manufactured product to both improve machining quality and promptly investigate the reason why a defect occurred.

3. Structure and specifications of the sensor integrated bearing unit

3.1 Structure

Fig. 2 shows a structural illustration of this bearing unit. This bearing unit comprises a set of angular contact ball bearings arranged back-to-back with an outer ring spacer and inner ring spacer provided between the angular contact ball bearings. The outer ring spacer and inner ring spacer are equipped with sensors, circuits to process data detected by the sensors, a wireless module, and an independent power supply.

The independent power supply uses an electromagnetic induction generator. A stator consisting of a coil and yoke is built into the outer ring spacer, and a rotor with alternately magnetized N and S-poles is attached to the inner ring spacer. Electromagnetic induction is generated by the relative rotation of the outer ring spacer and inner ring spacer which generates the power required to run the sensors and circuits.

Fig. 3 shows an example of application for this bearing unit on a machine tool spindle. Factors such as the internal clearance and the difference between the width of the inner ring spacer and outer ring spacer are adjusted to apply preload on the bearing. This maintains high rigidity at the bearing which ultimately improves machining quality. With this structure, bearing preload and the load applied to the tool during machining act on the outer ring spacer so a load sensor is provided on the outer ring spacer of this bearing unit.

The sensors, circuits, and an independent power supply are built into this bearing unit in a compact way; this enables it to achieve the same dimensions as a conventional outer ring spacer without sensors.

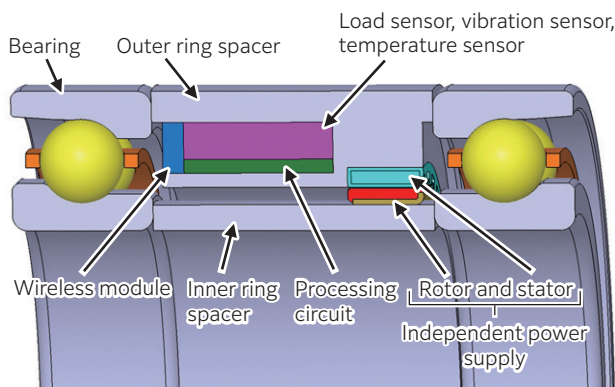


Fig. 2 Structural illustration of sensor integrated bearing unit

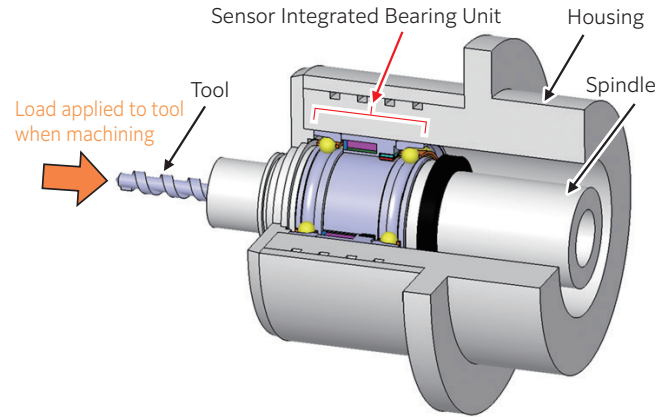


Fig. 3 Example of application for the sensor integrated bearing unit on a machine tool spindle

3.2 Specifications

Table 2 shows the specifications for this bearing unit. It lists load, temperature, and vibration acceleration for sensing items. Bluetooth Low Energy (2.4 GHz) is used for the telecommunication standards to allow for a lower power consumption at the wireless module and to make it more compact. The operating temperature range is set to -20 to 70 °C with consideration for the allowable temperature of electronic components mounted on the module.

Table 2 Specifications for the sensor integrated bearing unit

Bearing	Type	Ultra-high speed angular contact ball bearings with ceramic balls (Equivalent to 5S-2LA-HSE014) Double row back-to-back arrangement
	Bore diameter × outer diameter × width	φ70 × φ110 × 20 (per row) mm
Spacer	Inner ring spacer bore diameter × outer ring spacer outer diameter × width	φ70 × φ110 × 40 mm
Sensing	Load	Maximum detection load: 45 kN
	Temperature	Detection range: - 40 to 125 °C
	Vibrational acceleration	Detection range: ± 50 G Response frequency band: up to 11 kHz
Independent power supply		Electromagnetic induction generator
Communication standard		Bluetooth Low Energy (2.4 GHz)
Operating temperature range		- 20 to 70 °C

4. Connecting to equipment

Fig. 4 shows a schematic example of using the data communication capabilities of this bearing unit. Data detected by the sensors is transmitted wirelessly from the wireless module built into the outer ring spacer to the data receiving unit provided with a USB antenna for data reception. The data receiving unit, the customer's machine tool and server are connected by a LAN cable so that data can be verified.

Data transmitted from the wireless module consists of 3 types of data; these are load, temperature, and vibration detected by each sensor. Since each data type is constantly transmitted to the connected equipment, it is expected that it will be used to control, monitor conditions as the spindle bearing, and provide predictive maintenance to machine tools that require a high level of response.

A separate connection program is required to connect the data receiving unit to dedicated equipment. However, if the system uses an IoT platform, it has the advantage of making the system more versatile and easier to connect. **NTN** provides "Bearing Diagnostic Edge Application" for Industrial IoT Platforms⁵⁾ to support efforts in this area.

This bearing unit has an independent power supply to feed power to the unit and can transmit data wirelessly, which makes it easy to use in an IoT environment.

5. Evaluation test

This section introduces the test results for the load, temperature, and vibration sensor built into this bearing unit.

Fig. 5 shows the evaluated spindle that simulated the machine tool spindle. This bearing unit was assembled onto this evaluated spindle and then the evaluation test was carried out. This bearing unit wirelessly transmitted data detected by the sensors to a receiver installed externally on the spindle using the wireless module.

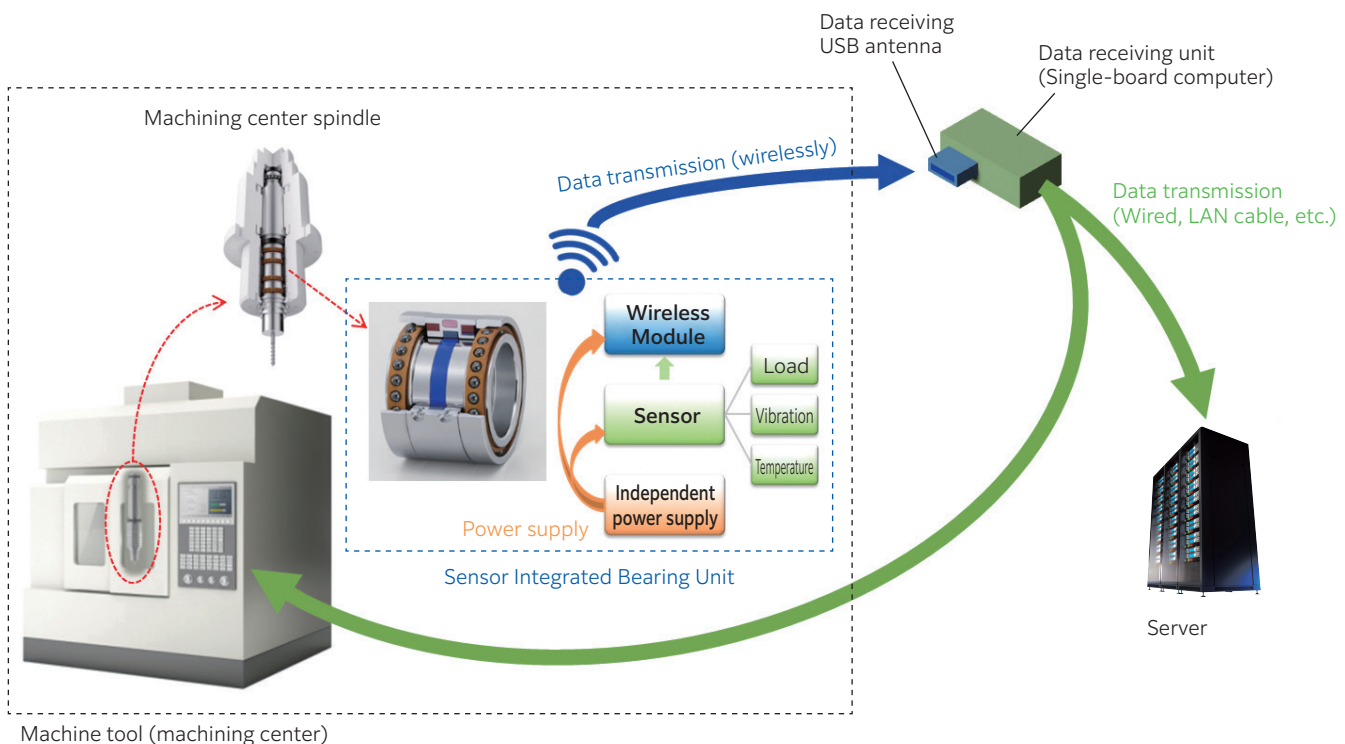


Fig. 4 Example of using the sensor integrated bearing unit

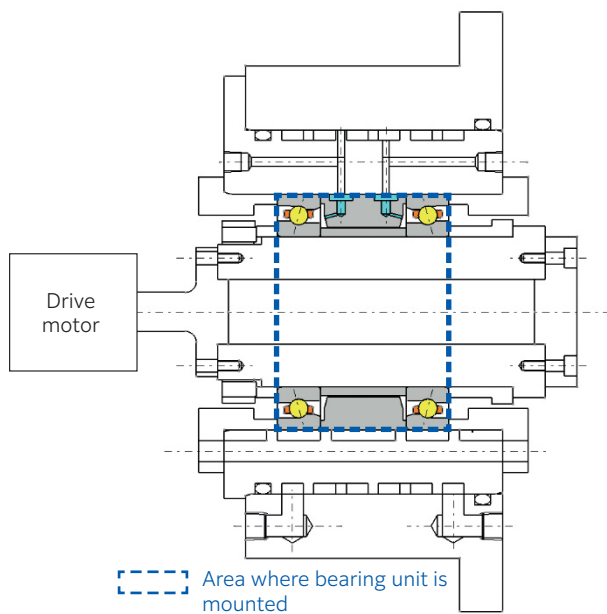


Fig. 5 Structure of evaluated spindle

5.1 Verifying load and temperature responsiveness during an acceleration/deceleration test

An acceleration/deceleration test was carried out in which the rotational speed was changed, assuming the actual operation conditions of a machine tool.

Table 3 shows the test conditions and **Fig 6** shows the test results for load and temperature. It was confirmed that this bearing unit can detect changes in bearing preload and temperature for fluctuations in the rotational speed. It was also confirmed that it has a higher temperature sensitivity than an external sensor.

Table 3 Acceleration/deceleration test conditions

Test bearing	$\phi 70 \times \phi 110 \times 20$ Equivalent to 5S-2LA-HSE014 (Ultra-high speed angular contact ball bearing with ceramic balls)
Preload method	Fixed position preload (preload of 750 N after spindle installation)
Rotational speed	6 000→10 000→6 000→8 000 min ⁻¹
Lubrication method	Air-oil lubrication
Lubricating amount	0.03 mL/10 min
Lubricating oil	ISO VG32
Lubricating airflow rate	30 NL/min
Fluid cooling channel	Yes, room temperature tuning
Axis position	Horizontal axis

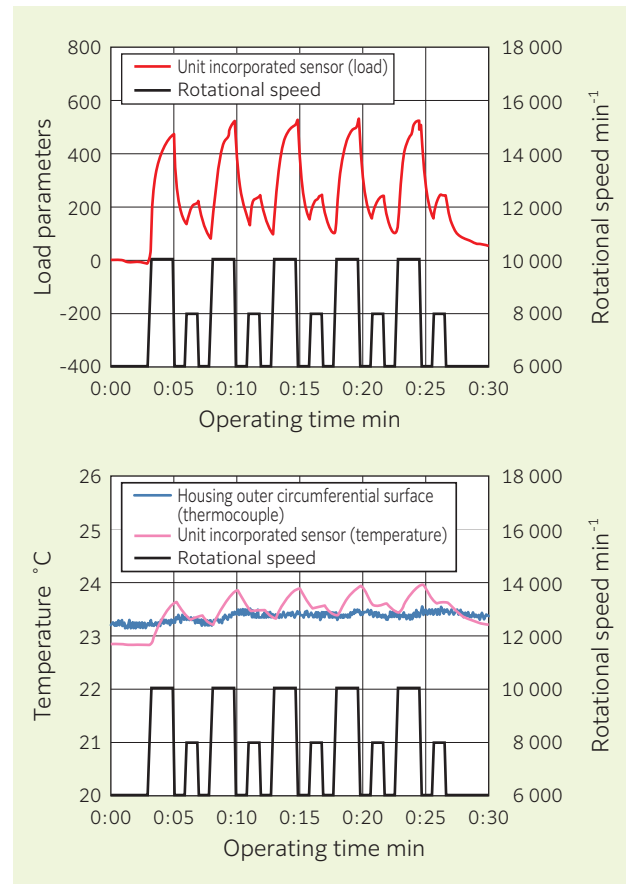


Fig. 6 Acceleration/deceleration test results

5.2 Indentation bearing vibration verification test

To tackle the detection of an abnormality on a bearing that uses a vibration sensor, damage (an indentation) was simulated on the bearing raceway surface. Then a vibration verification test was carried out on the evaluated spindle in **Fig. 5** with the same condition as for the acceleration/deceleration test. **Table 4** shows the test conditions and **Fig. 7** shows a 3D illustration of the simulated damage (indentation) created on the bearing raceway surface. During the test, the vibration on the outer circumferential surface of the evaluated spindle housing was measured at the same time together with the vibration detected by the vibration sensor built into the outer ring spacer, and both measurements were compared. For a vibration of 5 000 min⁻¹ at the test bearing, while checking components with frequency that matches the inner ring damage, feature quantities of the sensor built into the outer ring spacer were greater than at the housing outer circumferential surface, showing that the signal to noise ratio improved (**Fig. 8**). The vibration sensor built into the outer ring spacer is considered to be able to detect damage on the bearing with better accuracy.

Table 4 Vibration verification test conditions

Test bearing	Equivalent to $\phi 70 \times \phi 110 \times 20$ 5S-2LA-HSE014 (Ultra-high speed angular contact ball bearing with ceramic balls)
Preload method	Fixed position preload (preload of 750 N after spindle installation)
Rotational speed	5 000 min ⁻¹
Lubrication method	Air-oil lubrication
Simulated damage (Indentation)	1 location on inner ring raceway surface
	Depth of 6 μ m

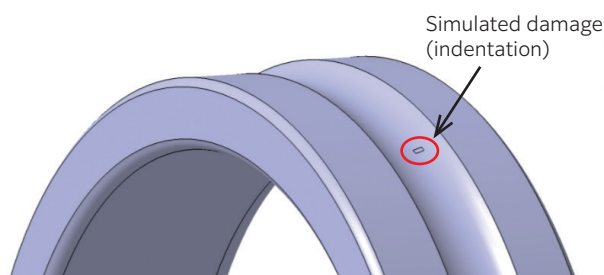


Fig. 7 3D illustration of the simulated damage (indentation) created on the bearing raceway surface

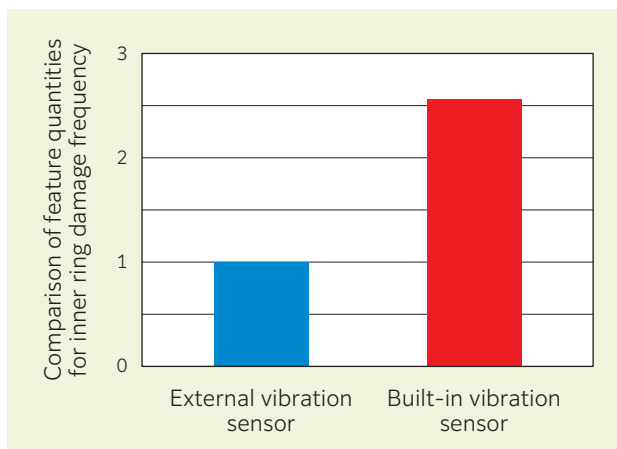


Fig. 8 Indentation bearing vibration verification test results

Photo of authors



Shohei HASHIZUME
Robotics & Sensing Engineering Dept., Industrial Business Headquarters

Yudai NAKANO
Robotics & Sensing Engineering Dept., Industrial Business Headquarters

Daichi KONDO
New Product Development R&D Center

Yoji OHGUCHI
New Product Development R&D Center

Yohei YAMAMOTO
Product Design Dept., Industrial Business Headquarters

6. Summary

Trials are underway to use and introduce sensing technology on machine tools, against the backdrop of the rising demand for condition monitoring and machining monitoring.

To meet this demand, **NTN** is making progress with developing the “Sensor Integrated Bearing Unit for Machine Tool Spindles”, which has a built-in wireless function and can detect load, temperature, and vibration. **NTN** has also made proposals for new methods to connect developed products and machine tools.

We will continue to repeatedly evaluate this bearing unit through operation tests for its practical use and promote further improvements and refinements to its function. Furthermore, we will also work on establishing more advanced condition monitoring and predictive maintenance technology by combining this bearing unit with AI technology. These efforts will support the efficient operation of machine tools.

We intend to work on developing technology that will enrich the lives of people and be ecologically friendly in support of sustainable development goals (SDGs) for the future.

References

- 1) Naoki Matsumori, Keiichi Ueda, Technical Trend of the Precision Bearings for Machine Tools, NTN TECHNICAL REVIEW, No.84, (2016) 40.
- 2) Keiichi Ueda, Technical Trend of the Precision Bearings for Machine Tools, Bearing & Motion Tech, September 2016 Edition, No.002, 33.
- 3) Shohei Hashizume, Yasuyuki Fukushima, Yusuke Shibuya, Yohei Yamamoto, Development of Sensor Integrated Bearing Unit for Machine Tool Spindles, NTN TECHNICAL REVIEW, No.86, (2018) 50.
- 4) Shohei Hashizume, Yusuke Shibuya, Daichi Kondo, Yohei Yamamoto, Hiroyuki Iwanaga, Development of Sensor Integrated Bearing Unit for Machine Tool Spindles, NTN TECHNICAL REVIEW, No.88 (2020) 33.
- 5) Hiroyuki Iwanaga, Development of Edge Application for Bearing Diagnosis, Inspection Technology, March 2022 Edition, Vol.27 No.3, 32.

Bearing Diagnostic Edge Application for Industrial IoT Platforms



Yudai NAKANO*
Takashi HASEBA*

In an effort to realize a smart and efficient factory, IoT-based condition monitoring systems are attracting attention in recent years. Rolling bearings are used to support the rotation of production equipment. We need to monitor bearing conditions to prevent unplanned downtime due to bearing damage.

NTN has developed a bearing diagnostic edge application for industrial IoT platforms to monitor bearing conditions using vibration data. In this article, we introduce the features and application examples of the bearing diagnostic edge application.

1. Introduction

There is a rising demand for predictive maintenance for production equipment, against the backdrop of manpower reduction and improved productivity at production equipment. Manufacturers are preferring to transition to condition-based maintenance from the conventional time-based maintenance implemented at production sites¹⁾.

At the production site, it is necessary to minimize downtime that occurs due to equipment stoppages so that productivity can be improved. Therefore, we must apply monitoring technology that will allow us to quantitatively understand conditions such as equipment deterioration and failure, and quickly detect abnormalities that have occurred so that maintenance can be performed.

A method to achieve this is monitoring the condition of production equipment through the use of an industrial IoT (Internet of Things) platform.

NTN has developed an edge application for industrial IoT platforms that can diagnose production equipment bearings through the use of vibration data. This paper introduces the features of this edge application and examples of its application at production sites.

2. Condition monitoring at the production site

2.1 Industrial IoT platforms

Industrial IoT platforms refer to IoT system infrastructure in the industrial sector. In the manufacturing industry, various equipment at the production site is connected via a network, and the production process is monitored and controlled. This allows improvements to be made to productivity at each step of production.

Fig. 1 shows a schematic drawing of an industrial IoT platform. This schematic drawing shows how the industrial IoT platform, edge application and IT system are linked at the production site.

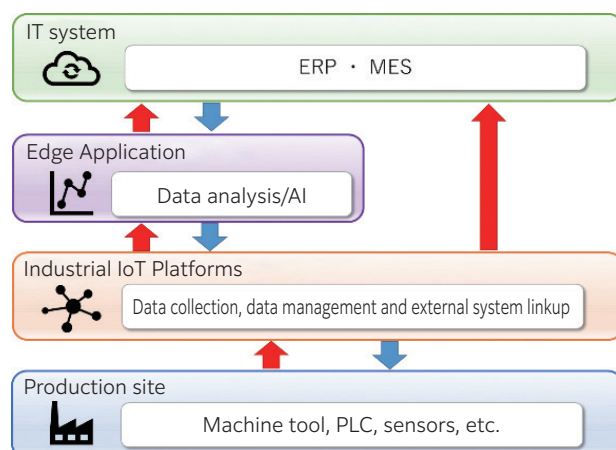


Fig. 1 Schematic drawing of industrial IoT platform

An industrial IoT platform connects to equipment at the production site and collects data relating to equipment operation. An edge application receives the data collected from the industrial IoT platform and analyzes it. The analysis results processed here are then sent to the production site equipment and host IT system. The IT system takes on the role of comprehensively managing the various information for the production site, and systems such as the Enterprise Resource Planning (ERP) system or Manufacturing Execution System (MES) can be used for this task.

Using this industrial IoT platform optimizes management tasks and provides visualization of the production site in terms of monitoring the operation

* Robotics & Sensing Engineering Dept., Industrial Business Headquarters

and conditions of production equipment.

2.2 Monitoring the condition of bearings

Bearings are precision machine parts where high accuracy and quality are critical for proper function and long life. They are installed for use on several types of equipment to support the rotation of machinery.

If a bearing is damaged, the equipment must be stopped to perform inspection and repairs, which lowers productivity. Therefore, it is important to monitor bearing conditions to perform maintenance work at an appropriate time.

A method of diagnosing the bearing using vibration data is often used to monitor bearing conditions²⁾.

Table 1 shows the types of bearing diagnosis using this vibration method. Two types are available to diagnose bearings: simple diagnosis and precision diagnosis.

Table 1 Types of bearing diagnosis

Type	Diagnosis method
Simple diagnosis	<ul style="list-style-type: none"> • Absolute value determination (Evaluated in line with standards/standard values) • Same type comparison (Evaluated by comparing with the same type of equipment/machines under the same conditions) • Trend management (Determine abnormalities by constantly observing trends)
Precision diagnosis	<ul style="list-style-type: none"> • Estimates damage positions on bearing and extent of damage with frequency analysis (FFT, etc.) <p>*Requires various bearing information</p>

Simple diagnosis monitors changes in the condition over time and the degree of deviation from healthy conditions. Methods include absolute value determination in line with predetermined criteria and standards, comparative analysis that involves comparing the same type of equipment and machines, and trend management in which constant observation is implemented. Simple diagnosis is used to properly understand the bearing condition and create maintenance plans for equipment based on diagnosis results, which can prevent such things as unscheduled equipment stoppages due to bearing damage.

Meanwhile, precision diagnosis is performed when further analysis is required based on the results of simple diagnosis. Fast Fourier transform (FFT) and similar can be used to analyze the vibration spectrum to estimate where the bearing is damaged and the extent of the damage. However, to analyze the relationship between the spectrum and the position of damage, various bearing factors such as the rolling element raceway diameter, rolling element diameter, number of rolling elements, and the contact angle, as

well as information about the shaft rotational speed are required.

3. Bearing diagnostic edge application

As a bearing manufacturer, **NTN** has developed a condition monitoring system (CMS) for wind turbines using our knowledge about bearing damage along with sensing technology and diagnosis technology developed over many years and released this for sale as "WindDoctorTM"³⁾. Currently, we are providing a condition monitoring service using this system on over 250 wind turbines throughout Japan. This technology was used to develop a bearing diagnostic edge application using real-time processing functions from Edgexoss⁴⁾, which is an industrial IoT platform (hereafter, bearing diagnostic application).

3.1 Features

The main features of the bearing diagnostic application are shown below.

(1) Realtime diagnosis

The application includes **NTN** proprietary diagnosis algorithms to automatically collect vibration data for analysis and diagnosis purposes. Up to 16 locations are diagnosed within at least 3 seconds using a single bearing diagnostic application license. This enables users to know any changes in the bearing condition that may appear in a short amount of time and can detect abnormalities early on.

(2) Automatic threshold generation

Thresholds are automatically generated to identify the bearing conditions based on learned data. This eliminates work to configure thresholds that require an experienced operator.

(3) Provides diagnosis not limited to certain bearing numbers

It is not necessary to configure such things as bearing factors and rotational speed. Therefore, the application can be used even if you do not know the number of the bearing installed on the equipment or the rotational speed.

(4) Rating scale for bearing health condition

Diagnosis results display 4 ratings (Normal, Attention, Caution, and Warning) in text and color on the display screen of the bearing diagnostic application. Therefore, it is possible to easily know the bearing condition without the operator performing detailed analysis.

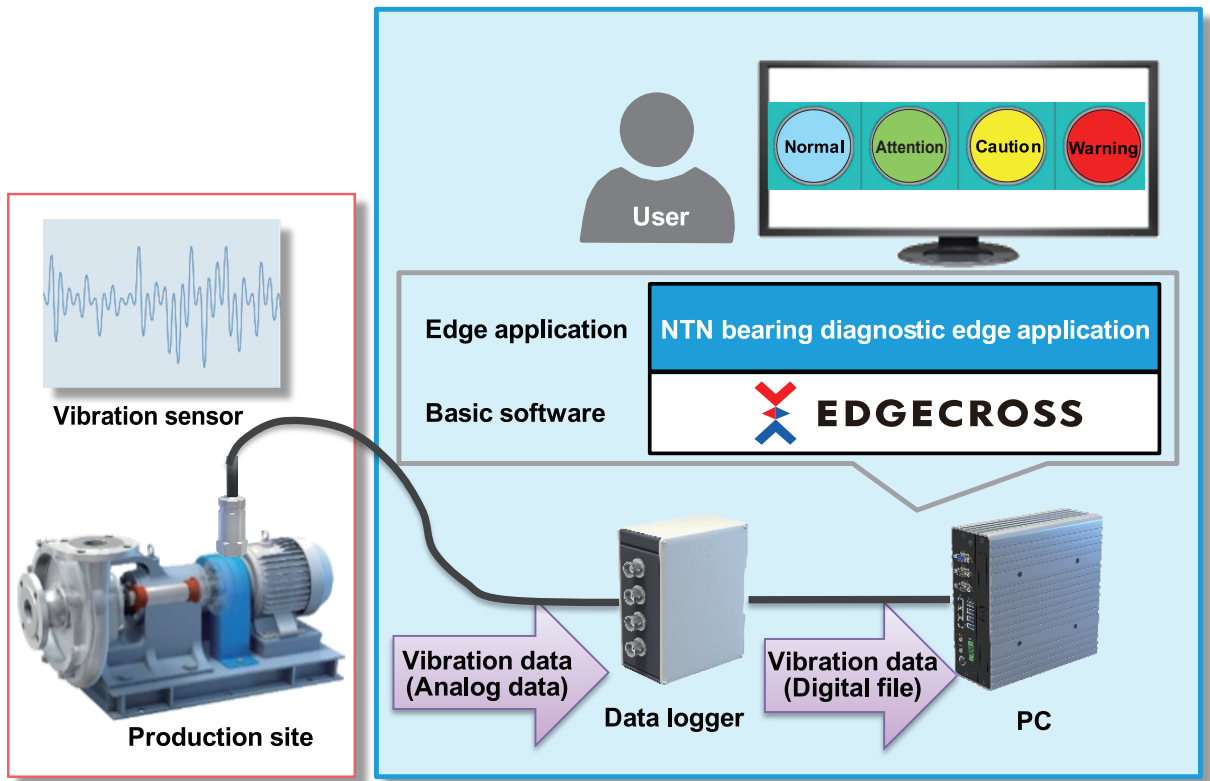


Fig. 2 Device configuration for bearing diagnostic application

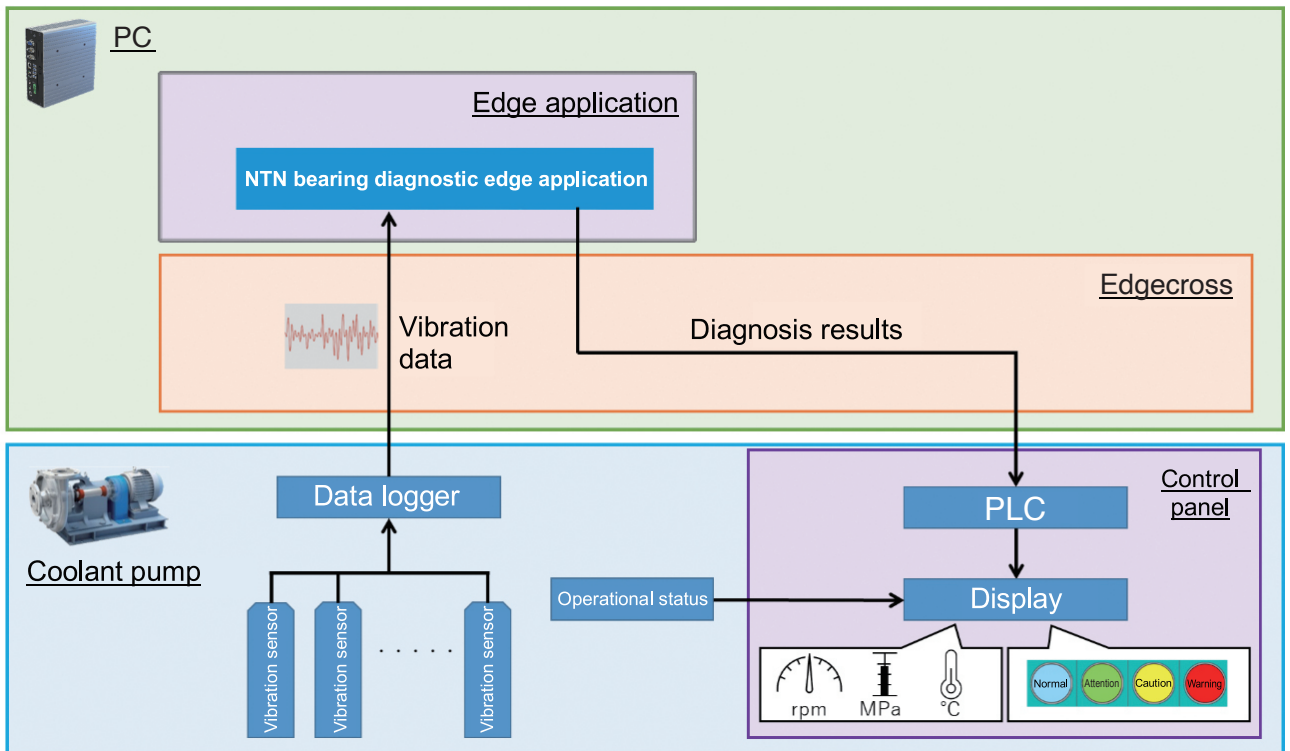


Fig. 3 Coolant pump diagnosis process

3.2 Usage configuration

The devices required to use the bearing diagnostic application are a PC installed with Windows operating system, a vibration sensor, and a data logger. Edgecross basic software and the bearing diagnostic application can be used after installing them onto the PC (Fig. 2).

The bearing diagnostic application can also run in standalone mode for convenience of use at the production site.

4. Example of application on coolant pumps

This section introduces an example of using the bearing diagnostic application to monitor the conditions of a coolant pump at the production site.

4.1 Challenges of inspection work

If a coolant pump that supplies coolant to equipment fails, it will lead to production line stoppages. To mitigate this type of situation, operators either regularly perform inspection work on the equipment or perform such work depending on the situation. However, this inspection work relies on the experience of the operator so there are times when an operator may fail to notice a problem with the coolant pump. To prevent this type of situation, it is necessary to evaluate the bearing conditions automatically and quantitatively (whether damage has occurred and its extent, etc.) based on the operational status of the coolant pump expressed in a numerical format.

4.2 Introducing the bearing diagnostic application

Fig. 3 shows the device configuration and measurement/diagnosis procedure for this example. The bearing diagnostic application is organized such that it links to the coolant pump control PLC and the display via Edgecross. Operation information such as the rotational speed, pressure and temperature are displayed on the coolant pump control panel display in addition to diagnosis results from the bearing diagnostic application.

In this example, operators receive information about the coolant pump operational status at the same time the bearing conditions are checked, which reduces the amount of inspection work the operator must do. Furthermore, the bearing diagnostic application constantly monitors the bearing conditions, enabling any bearing abnormalities or development of damage to be quantitatively evaluated. If any signs of damage are discovered on the bearing, control is switched to lower the load on the coolant pump based on the diagnosis results, which is expected to delay the progress of damage on the bearing.

5. Proof of concept build support service

When introducing the system to the production site, proof of concept (PoC) is performed to validate the effectiveness of introducing the system in advance.

Sensors and equipment used for the PoC step are prepared by the user. However, when introducing the bearing diagnostic application, users were unable to prepare equipment such as vibration sensors and data loggers, and it was sometimes difficult to implement PoC. Due to this fact, NTN provides a "PoC build support service"⁵⁾ in collaboration with Edgecross Consortium⁴⁾, in which the user can borrow a set of the devices that need to be prepared. They are borrowed for a fixed period at no cost to the user.

Fig. 4 shows a flowchart up to the point of starting PoC operation for the PoC build support service. This service includes an interview concerning what equipment needs to be diagnosed and any issues to address, followed by a decision on the PoC implementation details and NTN work support details. For users who are concerned about how to set up the devices, NTN also helps set up peripheral devices and configure the bearing diagnostic application.

This service has been favorably received by users who have used it, describing how they were able to quickly start PoC and were able to understand how it operates. Even after the PoC build support service ended, many users continued to use the bearing diagnostic application.

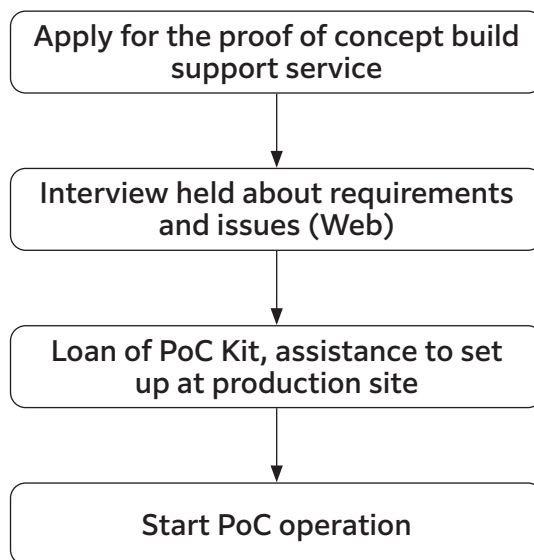


Fig. 4 PoC build support service flowchart

6. Summary

This paper introduced the bearing diagnostic edge application used for industrial IoT platforms. It also showed the introduction of the bearing diagnostic edge application at a production site using an example of application on cooling pumps. The bearing diagnostic edge application is not limited to the example shown in this paper and is used by a variety of users. We will continue to develop products with enhanced functionality in the future, provide service solutions that meet the needs of our users, and contribute towards improving productivity in each industry.

References

- 1) METI, The State of Government Initiatives for Promoting Smart Security, (December 2020)
https://www.meti.go.jp/policy/safety_security/industrial_safety/smart_industrial_safety_symposium/images/medi_goto.pdf
- 2) ISO 20816-1:2016, Mechanical vibration - Measurement and evaluation of machine vibration - Part 1.
- 3) Makoto Miyazaki, Wataru Hatakeyama, Application of Condition Monitoring System for Wind Turbines, NTN TECHNICAL REVIEW, No.86, (2018) 40-44.
- 4) Edgecross Consortium, Edgecross Consortium Official Homepage.
<https://www.edgecross.org/ja/>
- 5) Edgecross Consortium, PoC Build Support Service, Edgecross Consortium Official Homepage.
https://www.edgecross.org/ja/dounyu_kentou/poc.html

Photo of authors



Yudai NAKANO

Robotics & Sensing
Engineering Dept.,
Industrial Business
Headquarters



Takashi HASEBA

Robotics & Sensing
Engineering Dept.,
Industrial Business
Headquarters

NTN's Activities for the Electric Vehicle and Electrification of Automobiles

Ikuya TATEOKA *

With the Paris Agreement of 2015, countries around the world are stepping up efforts to become carbon neutral. Major countries such as Japan, the U.S., and the EU are aiming to achieve carbon neutrality before 2050 by expanding the introduction of clean energy and reforming their industrial structures. The automotive industries are accelerating the development and expansion of sales of electric vehicles that can reduce the generation of exhaust gas. This paper introduces NTN's products for energy-saving and electrification of automobile. The products contribute to carbon neutrality.

1. Introduction

Against the background of global warming, international efforts are accelerating toward achieving a decarbonized society, or, as it also known, carbon neutrality. The Paris Agreement adopted at the 21st Conference of the Parties to the United Nations Framework Convention on Climate Change (COP21) in December 2015 set a long-term goal of limiting global average temperature increase to less than 2 °C above pre-industrial levels, with a further commitment toward a target of 1.5 °C below pre-industrial levels. To achieve this goal, the Paris Agreement targets early limits of greenhouse gas emissions and the achievement of carbon neutrality in the second half of the century. Furthermore, at COP26 in 2021, the 1.5 °C target was stated not as an aspirational target but as a shared global goal.

Based on the Paris Agreement, Japan's Ministry of Economy, Trade and Industry (METI) has led the formulation of a "Green Growth Strategy for Carbon Neutrality by 2050". The strategy calls for 100 % electric vehicles in new car sales by 2035 as one of the green growth strategies in the automotive industry, one of 14 sectors expected to grow in the future. The development and sales of electric vehicles, including EVs, are expected to accelerate in the future as part of efforts toward carbon neutrality. **Fig. 1** shows trends in automobile production and production forecasts for electric vehicles.

The trend of CASE (**Fig. 2**), which collectively refers to Connected, Autonomous, Shared, and Electric (electrification), has come to the forefront as the prominent development trend in the automotive industry. For example, in the field of automated driving, the spread of various systems that support driving and drive control, turning, and stopping, which are the basic functions of automobiles, has been accompanied by a shift toward electrification, mainly through the use of by-wire systems. Against the backdrop of these trends, **NTN** is focusing on

contributing to carbon neutrality and CASE by developing energy-saving and electrification-compatible products.

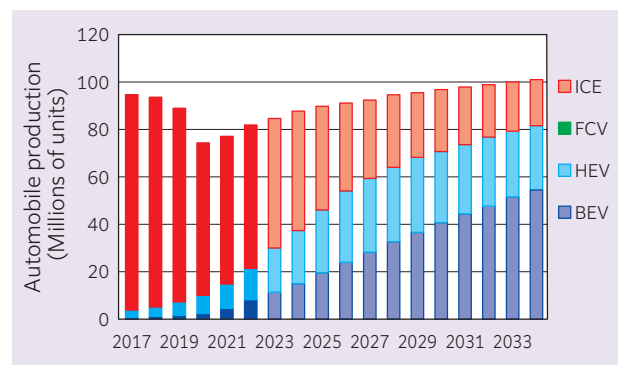


Fig. 1 Automobile production volume forecast¹⁾

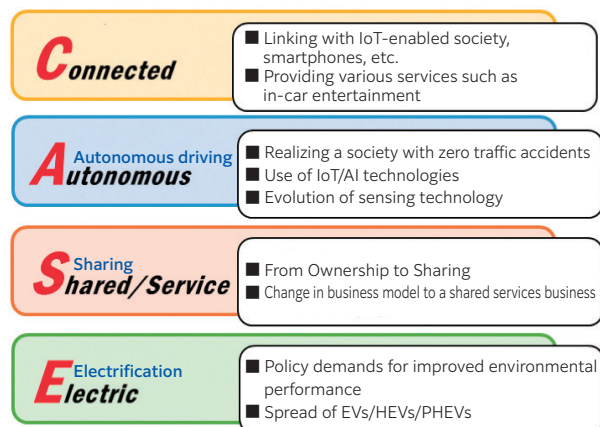


Fig. 2 Overview of CASE automotive trends

* Deputy Corporate General Manager, Automotive Business Headquarters

2. Market Trends and Responding to These Needs with NTN's Research and Development

Table 1 shows market trends in the automotive industry, technological trends, and the products that NTN is developing to respond to market needs. A key challenge in electrification is to extend range while reducing power consumption. This is driving an increase in demand for compact, lightweight, low torque, and high efficiency components. There is also a growing demand for high-speed rotation drive motors to obtain higher motor output with the same size. Furthermore, as the overall weight of the drive unit is reduced and the housing becomes thinner, the rolling bearings are required to suppress creep phenomenon (whereby the mating surfaces of the housing and bearing gradually shift due to deformation of the outer ring caused by the load). In addition, to increase the efficiency of electric auxiliary equipment, there is a trend toward using lower viscosity lubricant and reducing the amount of lubricant supplied. The increasing use of rolling bearings under dilute lubrication conditions can increase the risk of premature bearing failure due to hydrogen embrittlement. NTN has developed long-life technology to prevent early bearing failure due to hydrogen embrittlement by applying new steel materials and special heat treatment technology.²⁾

On the other hand, many automakers expect that as the transition to higher levels of autonomous driving frees people from driving, it will increase demand for roomy, quiet vehicle interior space. This creates a need to improve flexibility in the layout of batteries and electric drive units, and to design components that contribute to the effective use of space. The increasing demand for SUVs in the global market

and the trend toward longer wheelbases to increase battery capacity are increasing the minimum turning radius of vehicles. NTN is developing CVJs with higher angles and rear-wheel steering mechanisms to address this trend. In addition, to pursue safety and comfort, it is necessary to work on drive motors, brakes, suspension, steering, and system control that combines these components. NTN is also working to develop module type products for electrification by utilizing its core technologies in tribology, bearing design technology, mechatronics, and other areas. The following is a list of representative products developed by NTN.

3. Automotive products developed for EV and electrification

3.1 Deep groove ball bearing for high-speed rotation

The market for e-Axles is expanding due to the electrification of automobiles. Deep groove ball bearings, which support the motor shaft of e-Axles and the directly connected motor of reduction gears, are required to support high-speed rotation. As the rotational speed of deep groove ball bearings increases, centrifugal force causes contact between the cage pockets of the resin cage and the rolling elements (balls), which may result in seizure.

In response to this, we developed a high-speed deep groove ball bearing for EV/HEV with a new shaped resin cage that takes into account the deformation of the cage during high-speed rotation. We found conditions where $d_{m,n} = 180 \times 10^4$ operation is possible with oil lubrication³⁾. Here, $d_{m,n}$ is the product of the rolling bearing pitch diameter and rotational speed, and the unit is $\text{mm}/\text{min}^{-1}$.

Table 1 NTN-developed products that respond to market trends/technological trends/market needs for automotive electrification

Market trend	Technology trends	Developed products that meet market needs
Acceleration of electrification and energy saving	Downsizing and lightweighting	<ul style="list-style-type: none"> • Needle bearing unit for planetary gear reducers • Creepless bearings
	Low torque	<ul style="list-style-type: none"> • Deep groove ball bearings with ultra-low friction seals • Low Friction HUB Bearing IV
	Higher efficiency	<ul style="list-style-type: none"> • Higher efficiency fixed constant velocity joint CFJ
	Higher speeds	<ul style="list-style-type: none"> • High Speed Deep Groove Ball Bearing for EV/HEV
	Lower viscosity lubricating oil	<ul style="list-style-type: none"> • Hydrogen Embrittlement Resistant Bearings
Pursuing comfort	Drive stability	<ul style="list-style-type: none"> • Hub Bearing Modules with Rear Steering Function Ra-sHUB™
Pursuing safety	Improving electronic control technology	<ul style="list-style-type: none"> • Ball screw drive modules for electronic hydraulic brakes • Electric oil pumps

The new shape resin cage has the following features. **Fig. 3** shows the appearance of the new shape resin cage.

- (1) Adoption of high-strength materials
⇒ Improved rigidity and hot strength of cage
- (2) Thickening of the pocket bottom to suppress deformation
⇒ Improved rigidity of the cage ring
- (3) Thinned wall between cage pockets (weight reduction)
⇒ Reduction of centrifugal force deformation
- (4) Installation of oil grooves on the inner surface of the cage pockets
⇒ Improved lubricity of cage and rolling elements

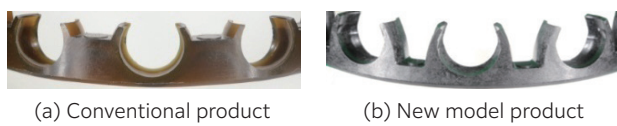


Fig. 3 Exterior photo of resin cage

3.2 Deep groove ball bearing with ultra-low friction seal

We developed a deep groove ball bearing with ultra-low friction seal that reduces running torque by 80 % compared to the conventional contact sealed types by adopting a unique shaped low friction seal.

Rolling bearings used in electric drives such as e-Axles require not only long operating life but also lower torque. The conventional approach to preventing bearing operating life reduction caused by intrusion of hard foreign matter, such as gear wear particles generated in the reduction gears, has been to use contact sealed type bearings. But the problem with this was that the seal comes into contact with the bearing inner ring, which generates drag torque during rotation. In addition, the contact sealed type bearing is difficult to use in recent EV and HEV applications, which require high-speed rotation, due to the limitation of the circumferential speed limit of the seal.

Deep groove ball bearings with ultra-low friction seals employ a newly developed contact seal with arc-shaped (half-cylindrical shaped) micro convexes at equal intervals on the sliding contact zone of the seal lip to reduce running torque by 80 % compared to conventional products. This achieves a low-torque effect comparable to that of ball bearings with non-contact seals. During rotation, the wedge film effect of the micro convexes forms an oil film between the sliding surfaces of the seal and inner ring, significantly reducing seal drag torque despite the fact that it is a contact type seal. Furthermore, since the micro convexes on the seal lip are extremely small, they can prevent the intrusion of hard foreign matter harmful to the bearing, even through the lubricating oil, without the reduction of bearing operating life.

3.3 Needle bearing unit for planetary gear reducers

The needle bearing unit for coaxial e-Axle planetary gear reducers (**Fig. 4**) are compact in the axial direction. Planetary gear reducers with sun and ring gears in parallel on the same axis tend to use small-diameter, long-shaft planetary shafts. The bearings must be durable under high-speed rotation, dilute lubrication, and moment load conditions. Here we introduce needle bearings for planetary gear reducers that meet these needs.

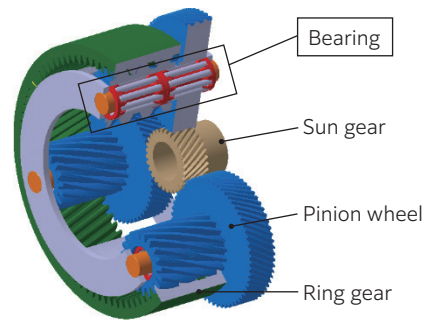


Fig. 4 Structure of co-axial type e-Axle planetary gear reducer

Needle bearing units for planetary gear reducers (bearing unit in **Fig. 4**) consist of rollers, cage, and shaft. The features of each component are as follows.

- (1) Rollers (high carbon chromium steel, special heat treatment)
The crowning shape required for the function was optimized, reducing the maximum contact stress in a moment load environment.
- (2) Cage (low carbon steel, carburized)
Improved cage fatigue strength by changing materials, optimizing weld geometry, and selecting the appropriate heat treatment (an improvement of 1.2 times compared to conventional products)
- (3) Shaft (low carbon steel, special heat treatment)
Plastic deformation is reduced by selecting a material containing a lower amount of alloy components related to hardenability and by optimizing heat treatment (an improvement of 70 % compared to conventional products). The amount of retained austenite in the surface layer and surface hardness were optimized to improve durability.

3.4 Low Friction HUB Bearings

Over the years, NTN has conducted research and development in pursuit of lighter weight, longer operating life, and higher efficiency for hub bearings that support tire rotation. We have promoted the unitization of bearings and peripheral components, contributing to lower fuel consumption and improved ease of assembly through downsizing and lightweighting. We have developed products with longer operating life and lower torque through improvements in areas such as materials, heat treatment, grease, and seal structure. **Table 2** shows the Transition of improvements in low friction HUB bearings.⁴⁾

Recently, to respond to the global demand for improved fuel efficiency of automobiles and stricter CO₂ emission regulations, we have worked to further reduce torque by developing the Low Friction HUB Bearing IV" (**Fig. 5**). The Low Friction HUB Bearing IV features a seal coating grease with a special thickening agent that reduces the running torque of the seal by 38 % compared to conventional grease while maintaining functions such as resistance against environmental contamination and low temperatures. Currently, the seal's performance is being evaluated, and the product will be introduced to the market as soon as possible. Furthermore, by optimizing the internal preload of the bearing and combining elemental technologies up to the Low Friction HUB Bearing III⁵⁾ (**Table 2**) developed in 2019, the bearing running torque was reduced by 67 % compared to Low Friction HUB Bearing I .

Table 2 Transition of Improvements to Low Friction HUB Bearings

Low-torque technology application factor		Low Friction HUB Bearings			
		I	II	III	IV
Bearing	Bearing specifications, preload			○	◎
	Bearing interior grease		○	◎	←
Seal	Seal coating grease		○	←	◎
	Lip design	○	←	←	←
	Lip contact status		○	←	←
	Number of lip contacts		○	←	←

○ : First return improvement, ◎ : Additional improvement

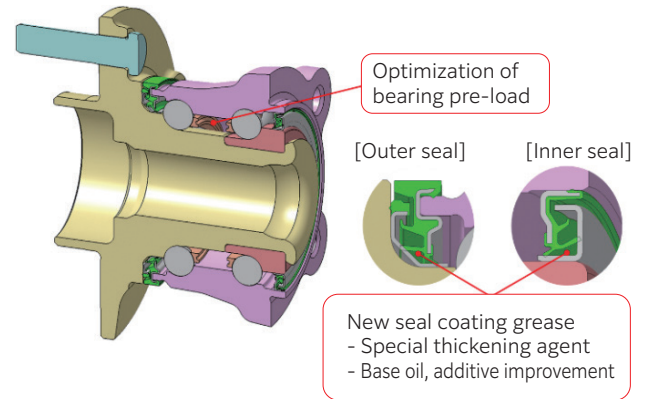


Fig. 5 Low Friction HUB Bearing IV

3.5 Higher efficiency fixed constant velocity joint CFJ⁶⁾

Power from engines and motors is transmitted to the tires via variable speed reducers and differentials through drive shafts. A key challenge for improving fuel efficiency and electricity costs in automobiles will be to reduce the torque loss of these power transmission paths.

The drive shaft consists of two constant velocity joints (CVJ), a fixed type and a sliding type, connected by a shaft, with a typical torque loss ratio of approximately 1 %. Here, we introduce the CFJ, which uses a proprietary spherical cross groove structure to reduce the torque loss ratio by more than 50 % compared to conventional products.

Fig. 6 shows the structure of the CFJ, which consists of an inner and outer ring with raceway grooves (tracks), eight balls that transmit rotational torque, and a cage that holds the balls. The torque loss of the CVJ is caused by energy loss due to friction between the parts. To reduce this internal friction, the CFJ has arc-shaped tracks on the inner and outer rings inclined in the axial direction and adjacent tracks arranged in mirror-image symmetry. In the conventional product, the load (**F1 and F2 in the figure**) of the ball pushing the cage is directed in one direction on all tracks. However, in the CFJ, the above-mentioned structure pushes the cage in different directions, so the internal forces cancel each other out on adjacent tracks, significantly reducing friction between internal parts compared to conventional products.

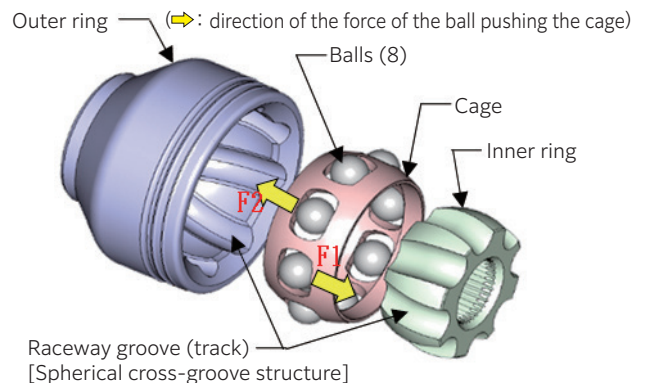


Fig. 6 CFJ structure and internal forces

CFJ achieved a torque loss ratio of less than 0.4 % (a reduction of 50 % or more compared to conventional products) at an operating angle of 9 degrees, enabling world-class transmission efficiency. The difference in efficiency from conventional products is known to yield corresponding improvements in fuel consumption and electricity costs. CFJ, which entered mass production in 2022, is expected to be a new product that can greatly contribute to decarbonization in the future.

3.6 Ball screw and ball screw drive module for electronic hydraulic brake

NTN has a strong track record in ball screws, one of our core technologies, for automotive applications starting in 2004, when mass production began. The features of NTN ball screws include (1) linear motion conversion efficiency of 90 % or higher, (2) high-load capacity (Fig. 7), and (3) improved positioning and position retention due to the high reliability of circulating parts. Table 3 shows examples of applications of NTN ball screws.

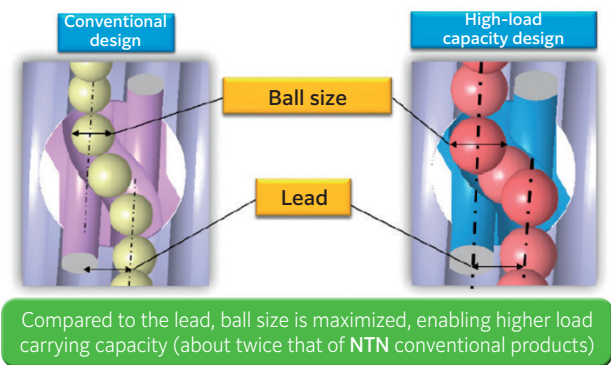


Fig. 7 Features of NTN ball screws

Table 3 Examples of applications of NTN ball screws

Location of application	Ball screw
AMT shift unit	
Variable valve lift mechanism	
Electronic hydraulic brake	Fig. 8

AMT : Automated Manual Transmission

As a modular product using ball screws, we introduce the ball screw drive module for electronic hydraulic brakes shown in Fig. 8. It is used in the brakes of vehicles such as EVs and HEVs as a regenerative mechanism that recovers kinetic energy during vehicle braking as electrical energy. To enable efficient recovery of kinetic energy as electricity, it is important to optimize the distribution of regenerative and hydraulic brakes so that they can instantly respond to changing braking effort. To address this issue, NTN has utilized its ball screw product technology to develop a ball screw drive module for electric hydraulic brakes that uses a motor drive to enable precise control of hydraulic brakes. We began mass production in 2012.

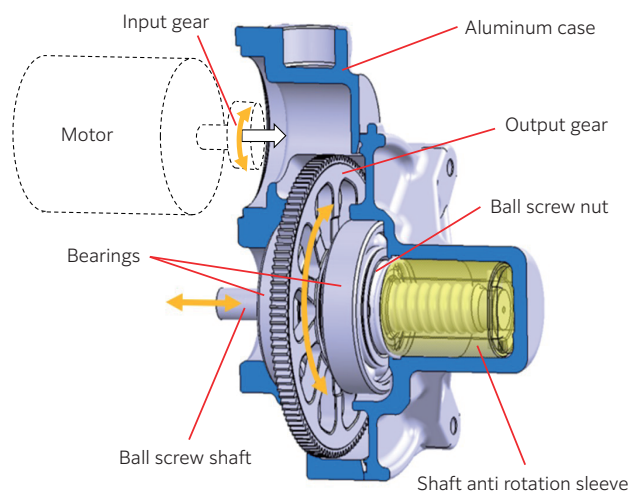


Fig. 8 Structure of the ball screw drive module for electronic hydraulic brake

As automatic braking becomes mandatory and more sophisticated, more responsive brakes will be required. Electric hydraulic brake systems are also being increasingly used to improve fuel efficiency and electricity costs. We believe that there will be a growing need for our ball screws and ball screw drive modules for electronic hydraulic brakes, which can contribute to a higher response of automatic brakes.

3.7 Electric oil pump

In ATs and CVTs, the clutch is operated hydraulically when starting and shifting gears. This hydraulic pressure is normally supplied by a mechanical oil pump driven by the engine. Electric oil pumps are increasingly being used to improve fuel efficiency by reducing oil pump drive loss and to secure hydraulic pressure and lubrication when the engine is stopped in vehicles equipped with a start-stop function. In recent years, the e-Axle, which integrates a motor, inverter, and reduction gearbox, has been used increasingly as a drive motor for EVs. The use of oil-cooled systems for cooling motors is expanding, as they offer a superior cooling effect to water-cooled systems and contribute to higher efficiency and smaller motors. It is expected that electric oil pumps will be increasingly used in electric vehicles. In response to this technological trend, NTN is developing an electric

oil pump that can help enhance vehicle environmental performance (**Fig. 9, Table 4**).

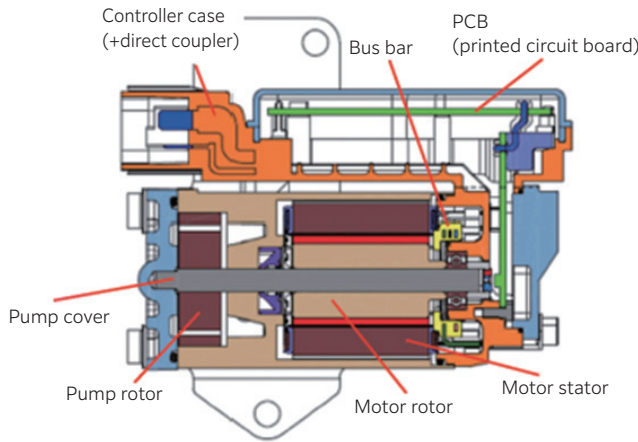


Fig. 9 Electric oil pump structure

Table 4 Electric oil pump specifications

Item	Details
Pump output	(1) 30 W or less (when used for idle stop) (2) 30-300 W (when used for e-Axle, etc.)
Voltage	12 V (to 48 V)
Hydraulic pump	Trochoid pumps (vane pumps)
Control	PWM (CAN compatible)
Features	- Lightweight and compact design achieved by the use of BLDC motors - Aluminum body for improved heat dissipation - Equipped with a rotation sensor to handle various operating conditions (low temperature, low RPM, etc.)

3.8 Hub Bearing Module with Rear Steering Adjust Function “Ra-sHUB™”

The hub bearing “Ra-sHUB™” with rear steering adjust function (**Fig. 10**) utilizes the strengths of our hub bearing base technology. We developed this as a steering system that adjusts to the driving condition of the vehicle, controlling the wheel steering angle and improving turning performance at low speeds and increasing vehicle stability at medium and high speeds.

Although first applied to mass-produced vehicles in the 1980s, rear-wheel steering systems were not widely used at that time because it was widely felt that the vehicle responded unnaturally to the driver’s operation of the steering wheel. In recent years, however, advanced control technology has made it possible to suppress the sense of an unnatural

response. Adoption is increasing, particularly in luxury and sports cars. In addition, EVs tend to have a longer wheelbase and larger turning radius in order to secure battery installation space. There is a limit to reducing the vehicle radius of gyration by increasing the steering angle of the front wheels, and a rear-wheel steering system can assist in this reduction.

Conventional rear-wheel steering systems are limited to undercarriage structures such as multi-link systems. Structurally this made it difficult to achieve a large operating angle. The “Ra-sHUB™” integrates the steering shaft in the hub bearing with the steering mechanism, enabling installation in the same manner as conventional hub bearings, while maintaining a compact design. Regardless of the undercarriage structure that is chosen, it can be mounted on rigid axle structures such as torsion beams, and can be applied to rear-wheel steering systems with independent left and right wheels and large operating angles. Furthermore, the steering function can be housed in the wheelhouse, enabling effective use of space inside the vehicle.

Advantages of the rear-wheel steering system using “Ra-sHUB™” include the following.

- (1) Reduction of vehicle turning radius
- (2) Mounted on the left and right wheels, independent control of the steering angle
- (3) Improved driving safety (vehicle attitude control)
- (4) Improved fuel economy (reduced driving resistance)

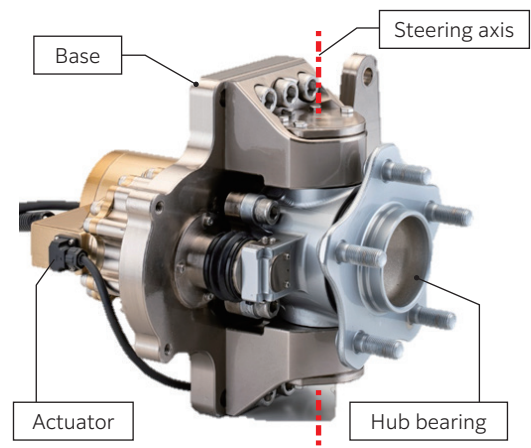


Fig. 10 Ra-sHUB™ (prototype)

4. Conclusion

In the automotive industry, technologies are being developed for carbon neutrality and CASE. This has driven changes in demand for the bearings, hub bearings, CVJs, and electric module products that we offer. NTN has been quick to identify these market trends, developing high value-added products with original technologies that lead to customer satisfaction. In this paper, we have introduced some of our recently developed products and technologies to respond to EVs and electrification in the automotive industry. In the future, we will continue to contribute to the promotion of carbon neutrality and the further development of the automotive industry through the development of new technologies and new products.

References

- 1) S&P Global Mobility Data (January 2023) + NTN Forecast
- 2) NTN website, "Hydrogen Embrittlement Resistant Bearings" developed
https://www.ntn.co.jp/japan/news/new_products/news202100038.html
- 3) NTN website, Nippon Brand Award of 2021 "CHO" MONODZUKURI Innovative Parts and Components Award
<https://www.ntn.co.jp/japan/news/press/news202100067.html>
- 4) Makoto Seki, Low Friction HUB Bearing, NTN TECHNICAL REVIEW, No. 85, (2017) 67-71.
- 5) Makoto Seki, Low Friction HUB Bearing III, NTN TECHNICAL REVIEW, No. 87, (2019) 63-67.
- 6) Teruaki Fujio, Next Generation High Efficiency Fixed Constant Velocity Joint "CFJ", NTN TECHNICAL REVIEW No. 81, (2013) 64-67.

Photo of author



Ikuya TATEOKA

Deputy Corporate
General Manager,
Automotive Business
Headquarters

Introduction of Rolling Bearings for Electric Drives Corresponding of Automobiles

Takashi KAWAI *
Tomohisa UOZUMI **

Continued electrification of automobiles has introduced the need for electric drive bearings with new and diverse performance capabilities. This article introduces the efforts made at NTN to design rolling bearings specifically to meet these requirements.

1. Introduction

The automotive industry is undergoing an unprecedented transition from gas powered to fully electric vehicles. The shift to electric vehicles (EVs) is accelerating worldwide as one solution on the path to achieving carbon neutrality¹⁾. Rolling bearings, which support power transmission in electric drives, are a key component. They must respond to the demand for higher speeds in addition to smaller size, lighter weight, and lower torque. Here NTN introduces rolling bearings for electric drives that have been designed specifically to meet these requirements.

2. Performance Requirements of Rolling Bearings for Electric Drives

There are two main types of rolling bearings for automobiles: deep groove ball bearings and tapered roller bearings. These rolling bearings consist of the four parts shown in Fig. 1 (inner ring, outer ring, rolling elements [balls and tapered rollers], and cage) and sometimes seals. With the recent shift to electric vehicles, bearings are required to have new performance characteristics to meet the operating conditions.

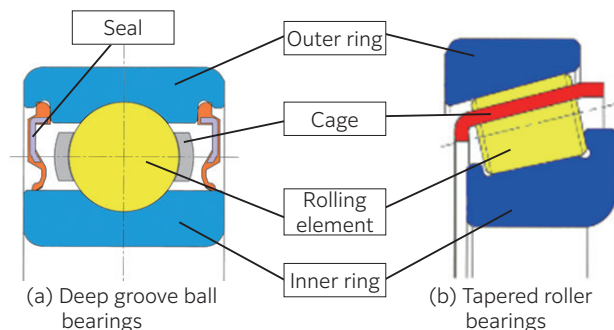


Fig. 1 Rolling bearing cross-section and part names²⁾

Fig. 2 shows an example of an “e-Axle”. An e-Axle is a drive unit which integrates a motor, inverter, and reduction gear for electric vehicles (EVs). An e-Axle with a parallel three-axis structure uses two bearings for the motor and six bearings for the gear reducer. Fig. 3 shows a typical example of a parallel triaxial e-Axle with a rolling bearing arrangement supporting the motor and reduction gearbox. Since the combination of the motor torque and reduction ratio affects the bearing load on each axis of the reducer, deep groove ball bearings and tapered roller bearings are used on the second and third axes, depending on the load.

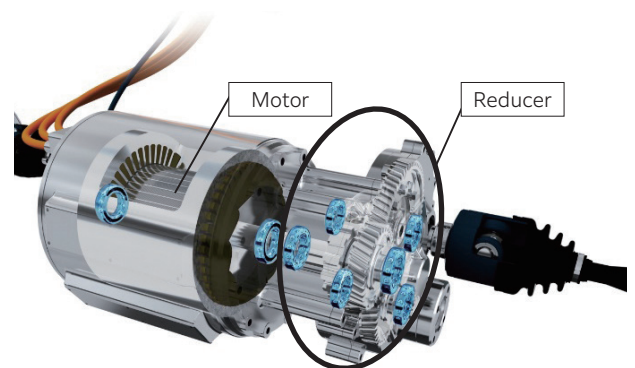


Fig. 2 Example of e-Axle structure and arrangement of rolling bearings³⁾

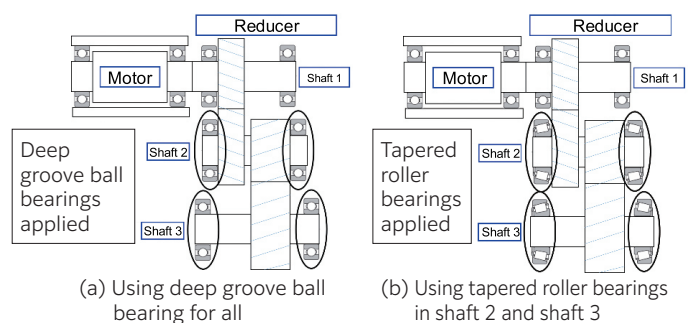


Fig. 3 Example of rolling bearing arrangement in a simplified cross-sectional view of an e-Axle (motor and reduction gear)⁴⁾

* Automotive Bearing Engineering Dept., Automotive Bearing Products Unit, Automotive Business Headquarters

** NTN BEARINGS (UK) LTD.

The rolling bearings used in each of the e-Axle's axes are required to have the following performance characteristics.

- (1) To meet the demands for higher power output and downsizing of the e-Axle, driving motors are operating at higher speeds. The deep groove ball bearings that support the motor shaft and the directly connected motor shaft of the first reducer shaft are required to offer high-speed performance.
- (2) As bearing raceways become thinner due to the e-Axle becoming smaller, creep (a sliding phenomenon in which the outer ring rotates relative to the housing) is more likely to occur on the outer diameter of the outer ring. Each reduction gear shaft must therefore have anti-creep measures.
- (3) The high voltage of the batteries used in e-Axle motors requires countermeasures against electrical pitting of the bearings (a phenomenon in which electrical discharge occurs in the bearing, causing microscopic melting of the raceway surface) in the motor shaft and the first shaft of the reduction gear.
- (4) To improve the efficiency of the e-Axle under low viscosity lubricating oil, the tapered roller bearing supporting the second shaft of the reducer requires heat generation countermeasures at the area of sliding contact on the large end rib.
- (5) The increased bearing load associated with the higher output of the e-Axle requires the tapered roller bearings supporting the second and third shafts of the reducer to have a higher load carrying capacity than conventional bearings.

Table 1 summarizes the performance requirements for e-Axle rolling bearings.

Table 1 Performance Requirements for e-Axle rolling bearings

Market trend	Technology trends	Performance requirements for rolling bearings
Environmentally friendly technology Motor-driven electrification Shared	Higher efficiency	Low torque 3.1 Deep groove ball bearing with ultra-low friction seal 4.1 Low temperature rise and low torque tapered roller bearing
	Higher speed	Support for high-speed 3.2 Deep groove ball bearing for high-speed rotation
	Downsizing and lightweighting	Improved creep resistance 3.3 Creepless bearings
	Higher voltage Higher frequency	Preventing electrical pitting 3.4 Ceramic rolling element deep groove ball bearings
	Lower viscosity and smaller volume of lubricating oil	Lower temperature rise 4.1 Low temperature rise and low torque tapered roller bearings
	High reliability	Long operating life 4.2 Tapered roller bearings with long operating life

3. Introduction of high-performance deep groove ball bearings

This section introduces the technology NTN has developed for deep groove ball bearings to meet the performance requirements for e-Axles as shown in **Table 1**.

3.1 Deep groove ball bearing with ultra-low friction seal

Due to increased demand for higher efficiency and more compact e-Axles, the deep groove ball bearings used in these applications are required to have both high operating life and low operating torque. Optimizing e-Axle bearing operating life requires preventing hard particulate material present in the lubricating oil of the application from contaminating the bearing rolling surfaces. Although contact seals can prevent the intrusion of particulate contamination, it is difficult to optimize both bearing life and operating torque with this seal type because sliding torque (which accounts for most of the running torque for deep groove ball bearings with contact seals) is generated at the contact area between the seal lip and the inner ring.

NTN's newly developed ultra-low friction seal⁵⁾ employs a contact-type seal with arc-shaped (half-cylindrical shaped) microscopic convexes at equal intervals on the sliding contact area of the seal lip, as shown in **Fig. 4**. During rotation, the wedge film effect of the microscopic convexes forms an oil film (**Fig. 5**) between the sliding surfaces of the seal and inner ring, significantly reducing seal drag torque compared to a more conventional contact-type seal. Furthermore, because the clearance between the seal and the inner ring sliding surface is extremely small, the intrusion of particulate contamination of a size that would affect bearing operating life can be prevented.

Under the conditions shown in **Table 2**, NTN compared running torque between the ultra-low friction seal and conventional contact/non-contact seals. As shown in **Fig. 6**, The running torque of the ball bearing with ultra-low friction seals was 80 % lower than that of the ball bearing with contact seals due to the wedge film effect of the micro convexes on the seal lip. Running torque of the ball bearing with ultra-low friction seal was also equivalent to that of the ball bearing with non-contact seals.

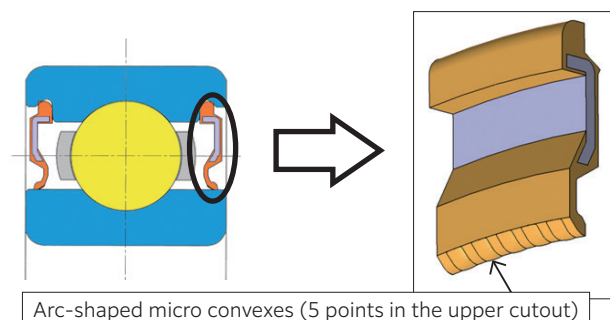


Fig. 4 Cross section of deep groove ball bearing with ultra-low friction seal⁵⁾

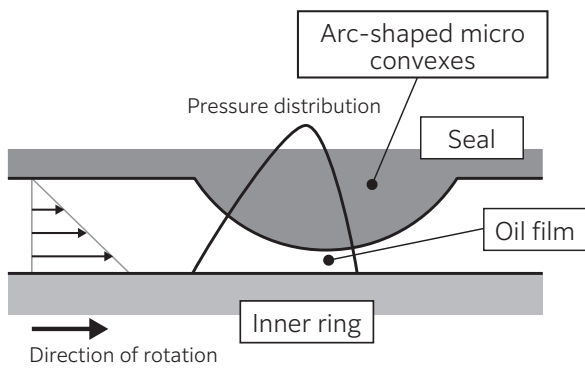


Fig. 5 Diagram of wedge film effect⁵⁾

Table 2 Test condition⁵⁾

Test bearing	6010 equivalent
Radial load	Basic dynamic load rating of 5 % (JIS B 1518:2013)
Rotational speed	1 500 min ⁻¹
Bearing temperature	35 to 120 °C
Lubricating oil	CVTF

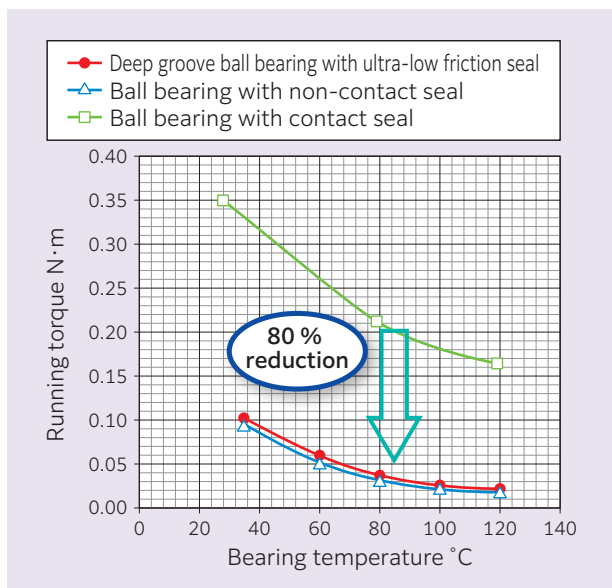


Fig. 6 Relationship between running torque and bearing temperature⁵⁾

3.2 Deep groove ball bearing for high speeds

By adopting a new shape of resin cage that takes into account the deformation of the cage during high-speed rotation, **NTN** found operation was possible under oil lubrication at $d_m n^{*1} = 180 \times 10^4$. Here **NTN** introduces a high-speed deep groove ball bearing for EV/HEV that uses high-speed rotation technology.^{6) 7)}

*1 Bearing rolling elements pitch diameter and rotational speed mm min⁻¹

Deep groove ball bearings, which support the motor shaft of e-Axles and the directly connected motor of first axis reduction gears, are required to support high rotational speeds. As the rotational speed of deep groove ball bearings increases, centrifugal force causes contact between the cage pockets of the resin cage and the rolling elements (balls), which may result in seizure.

In response to this, **NTN** developed high-speed deep groove ball bearings for EVs and HEVs by adding improvements (1-4) to the resin cage.

Fig. 7 shows a comparison between the conventional and improved resin cage.

- (1) Adoption of high-strength materials
⇒ Improved rigidity and strength of cage
- (2) Thickening of the pocket bottom to suppress deformation
⇒ Improved rigidity of cage ring
- (3) Thinned wall between cage pockets (weight reduction)
⇒ Reduction of centrifugal force deformation
- (4) Installation of oil grooves on the inner surface of the cage pockets
⇒ Improved lubricity of cage and rolling elements

A temperature rise qualification test (oil lubrication) was conducted on high-speed deep groove ball bearings for EVs and HEVs under the conditions shown in **Table 3**. **Fig. 8** shows the test results. The outer ring temperature of the high-speed deep groove ball bearings could be operated stably below the upper temperature limit for $d_m n$ values up to 180×10^4 .

Table 3 Test condition²⁾

Tested bearing characteristics	Basic dynamic load rating = 16 800 N (JIS B 1518:2013)
Radial load	264.5 N
Axial load	147 N
Rotational speed	$d_m n$ 160 to 180×10^4

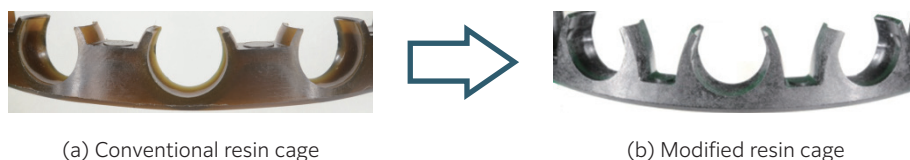


Fig. 7 Exterior of resin cage for high-speed deep groove ball bearings for EV/HEV⁴⁾

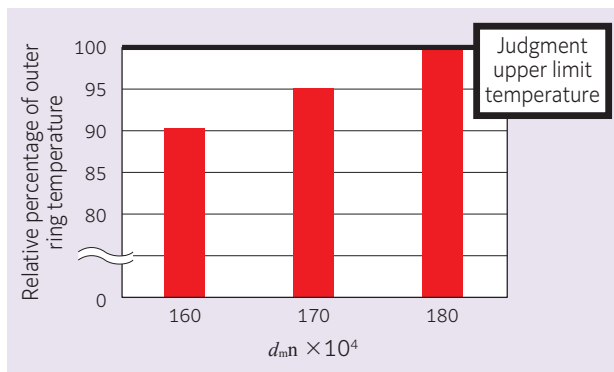


Fig. 8 Relationship between d_{mn} and outer ring temperature²⁾

Recently, by optimizing the lubrication conditions and the internal elements of the bearing, NTN has confirmed that the deep groove ball bearing can support high-speed rotation with a d_{mn} value of 220×10^4 8).

3.3 Creepless bearing⁹⁾

As bearing raceways become thinner due to the demand for smaller and lighter e-Axles, the rigidity of the outer ring decreases, increasing the likelihood of rippling deformation on the outer ring outer diameter surface as the rolling element passes through. This repetition results in a progressive wave that causes the outer ring to rotate relative to the housing (progressive wave type creep).¹⁰⁾

The structure of the creepless bearing that NTN has developed is shown in **Fig. 9**. As shown in **Fig. 10**, by providing a full-width arc-shaped relief area on a portion of the outer ring outer diameter surface, the housing inner diameter surface and outer ring outer diameter surface lose contact when the undercut of the outer ring is positioned in the load-bearing zone, thereby blocking the transmission of traveling waves. This suppresses creep. Although creep occurs when the undercut of the outer ring is positioned in the non-load-bearing zone, creep stops at that position when the undercut of the outer ring moves to the load-bearing zone. Therefore, when the bearing is assembled into the housing, there is no need to align the undercut with the load-bearing zone. The only design change is in the undercut of the outer ring outer diameter, making it easy to replace an existing bearing.

Creep rate evaluation tests were conducted on creepless bearings and standard deep groove ball bearings¹¹⁾ under the conditions shown in **Table 4** in a testing machine for inducing creep. The test results are shown in **Fig. 11**. The creep rate of the standard deep groove ball bearing tended to increase with increasing load. By contrast, it was confirmed that creep did not occur in the creepless bearing under any of the loading conditions due to the effect of the outer ring undercut.

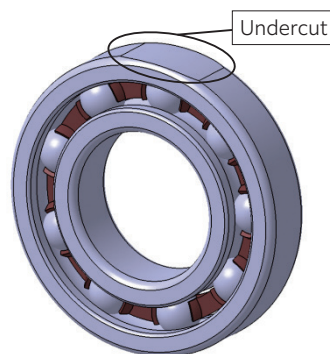


Fig. 9 Cross section of creepless bearings⁹⁾

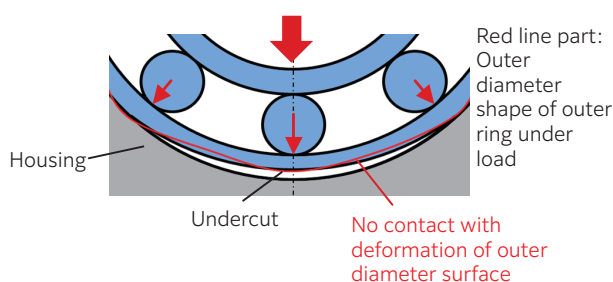


Fig. 10 Relationship between creepless bearing outer ring shape and housing⁹⁾

Table 4 Test condition⁹⁾

Bearing number	6208
Radial load	Basic dynamic load rating (JIS B 1518:2013) 10% - 40%
Inner ring rotational speed	6 000 min ⁻¹
Lubricating oil	CVTF
Bearing outer ring temperature	50 °C

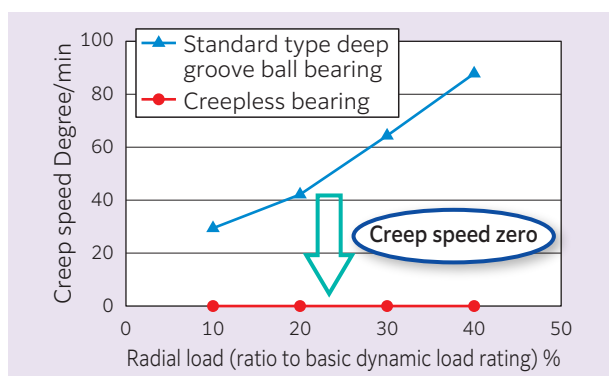


Fig. 11 Creep speed evaluation test results⁹⁾

3.4 Ceramic rolling element deep groove ball bearings



Fig. 12 Ceramic rolling element deep groove ball bearings

Inverter-driven motors are shifting toward higher power output and smaller size, and the drive power supplies are becoming higher voltage. In the case of inverter drives, a potential difference is generated between the shaft and housing. The oil film that forms between the bearing raceways and rolling elements is known to break down, causing damage due to electrical discharge.^{12) 13)} The higher the voltage, the greater the potential difference generated, which increases the risk of bearing damage due to dielectric breakdown. This leads to acoustic deterioration and a shorter operating life. As a countermeasure, a ceramic rolling element deep groove ball bearing (**Fig. 12**) using silicon nitride ceramic balls as rolling elements can be applied to insulate the inner and outer ring raceways and prevent the occurrence of electrical pitting.

Rolling tests were conducted under the conditions shown in **Table 5** on the test machine shown in **Fig. 13** to investigate bearing spalling life in an energized environment. The results are shown in **Table 6**. Compared to standard ball bearings using steel balls, the ceramic rolling element deep groove ball bearing can suppress the occurrence of spalling on the rolling element surface due to electrical pitting.

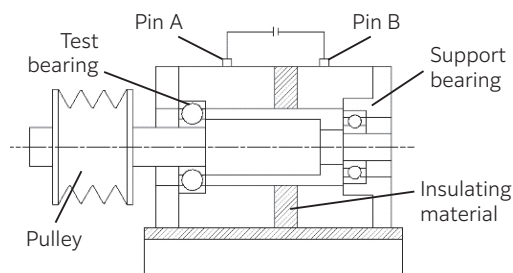


Fig. 13 Rolling life test machine

Table 5 Test condition¹⁴⁾

Bearing being tested	Deep Groove Ball Bearing (6203)	
Rolling element	Steel ball	Ceramic ball
Grease	Non-conductive grease	
Amount of grease injected (g)	0.86	
Rotational speed (min ⁻¹)	0-20 000 (rapid acceleration/ deceleration)	
Atmosphere	Room temperature	
Pulley load (N)	1 617	
Bearing load (N)	2 332	
Current (A)	0.5	-
Stopping conditions	Vibration 10 times initial level	

Table 6 Rolling life test results for energized state¹⁴⁾

	Life (h)	Spalling area
Deep groove ball bearings (steel balls)	19.6	ball
Deep groove ball bearings (ceramic balls)	>200	None

4. Introduction of high-performance tapered roller bearings

Fig. 14 shows the structure of a tapered roller bearing. Compared to ball bearings, tapered roller bearings can support higher radial and axial loads, but also generate more torque. NTN has developed a tapered roller bearing that achieves both low torque (low temperature rise) and long operating life by optimizing the geometry of the rolling surfaces and the inner ring large end rib face.¹⁶⁾

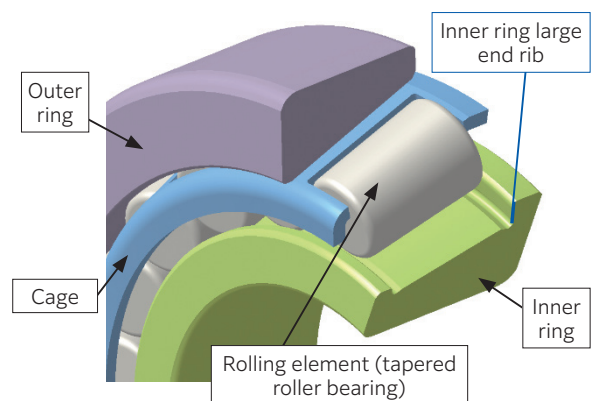


Fig. 14 Structure of tapered roller bearing¹⁵⁾

4.1 Low Temperature Rise and Low Torque Tapered Roller Bearing

The lubricating oil used in e-Axles is becoming lower in viscosity and volume in order to achieve higher efficiency in automobiles. When standard tapered roller bearings are used under these conditions, it becomes difficult for an oil film to form in the sliding contact area of the bearing rib, increasing the risk of rapid temperature rise. Our newly developed Low

Introduction of Rolling Bearings for Electric Drives Corresponding of Automobiles

Temperature Rise and Low Torque Tapered Roller Bearing improves anti-galling and reduces torque by making the design changes described in (1) to (4) below (Figs. 15 and 16).



Fig. 15 Exterior of Low Temperature Rise and Low Torque Tapered Roller Bearing¹⁶⁾

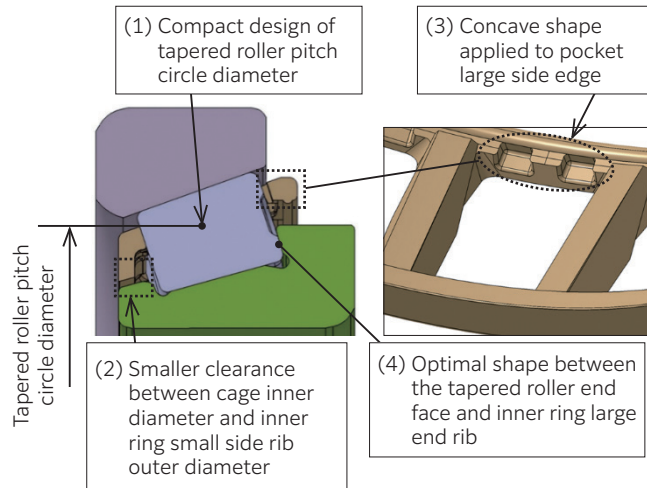


Fig. 16 Structure of "Low Temperature Rise and Low Torque Tapered Roller Bearing"¹⁶⁾

- (1) Compact size and low torque enabled by tapered roller and reduced pitch diameter
- (2) Reduced clearance between cage inner ring and inner ring cone front face rib outer diameter reduces torque caused by agitation of lubricating oil
- (3) Recessed shape added to large diameter end of cage pocket improves lubricity
- (4) Optimal shape of tapered roller end face and inner ring large end rib face improves lubricity

A rotary torque test was carried out under the conditions shown in **Table 8** to compare performance between a conventional tapered roller bearing¹¹⁾ and the Low Temperature Rise and Low Torque Tapered Roller Bearing shown in **Table 7**. The test results are shown in **Fig. 17**. The Low Temperature Rise and Low Torque Tapered Roller Bearing achieved a significant torque reduction of 66 % compared to the conventional design.

Temperature rise characteristics were evaluated for the two types of bearings shown in **Table 7** under the conditions shown in **Table 9**. In this test, to simulate an oil starved environment in the e-Axle, the bearings were operated after only an extremely small amount of lubricating oil was applied to the bearing surface. The bearings were tested until the outer ring temperature reached 100 °C. The test results are shown in **Fig. 18**. The time to reach 100 °C for the Low Temperature Rise and Low Torque Tapered Roller Bearing was approximately 10 times longer when compared to the standard tapered roller bearing.

Table 7 Test bearing¹⁶⁾

	Standard tapered roller bearing 32007X	Low Temperature Rise and Low Torque Tapered Roller Bearing
Scale drawing of bearing cross-section		
Size	φ35×φ62×18	φ34×φ58.5×13.5
Dynamic load rating	46 000 N	28 500 N
Cage	Standard steel plate cage	New shape resin cage

Table 8 Test condition¹⁶⁾

Axial load	3 000 N
Rotational speed	5 000 min ⁻¹
Lubrication conditions	Oil bath ATF (50 °C)

Table 9 Test condition¹⁶⁾

Lubricating oil conditions	ATF (25 °C)
Inner ring large end rib plane contact stress	Approx. 200 MPa
Inner ring large end rib plane sliding velocity	Approx. 2.5 m/s

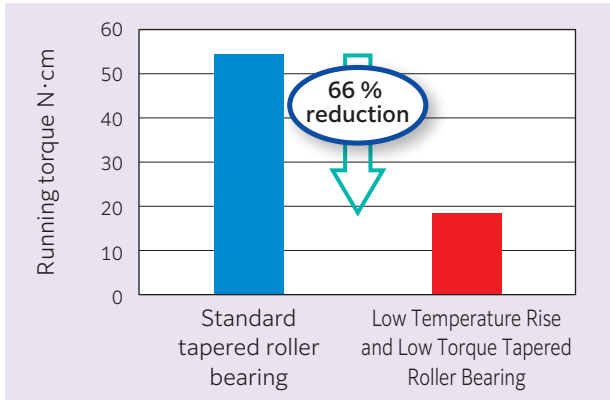


Fig. 17 Tapered roller bearing running torque test results¹⁶⁾

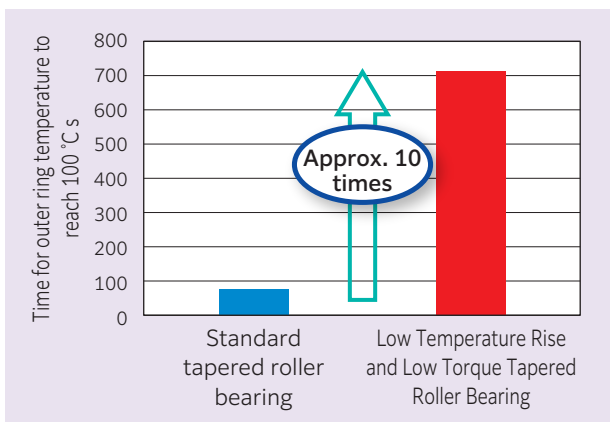


Fig. 18 Tapered roller bearing temperature rise evaluation test results¹⁶⁾

4.2 Long operating life tapered roller bearings

Here we introduce ULTAGE Tapered Roller Bearings,¹⁵⁾ which feature an optimized internal bearing design to achieve high load capacity and high-speed rotational performance (Fig. 19).



Fig. 19 ULTAGE Tapered Roller Bearing¹⁵⁾

ULTAGE Tapered Roller Bearings use optimized tapered roller surface geometry to maximize bearing operating life. (This technique, which involves reducing the diameter of tapered rollers toward the end in micrometer increments, is known as “crowning.”) Roller crowning allows for uniform contact stress between the rolling elements and the raceways when an unbalanced load is applied. This design technology has enabled ULTAGE Tapered

Roller Bearings to achieve a dynamic load rating which is 1.3x higher than conventional product and a rated life which is 2.5x higher.²⁾ The geometry of the contact area on the inner ring large end rib surface was also optimized to improve the allowable rotational speed by approximately 10 %³⁾.

*2: Comparison with tapered roller bearings to which the basic dynamic load rating is applied according to Japanese Industrial Standards B 1518:2013.

*3: Comparison with tapered roller bearings in NTN Corporation Ball and Roller Bearings Catalog (CAT.No.2203/J 20.08.199 NI/NI)

Fig. 20 compares the contact stress distribution of ULTAGE Tapered Roller Bearings and a conventional tapered roller bearing design.¹¹⁾ The ULTAGE Tapered Roller Bearings do not have excessive stress (edge stress) at the edge of the contact area due to the optimized crowning geometry.

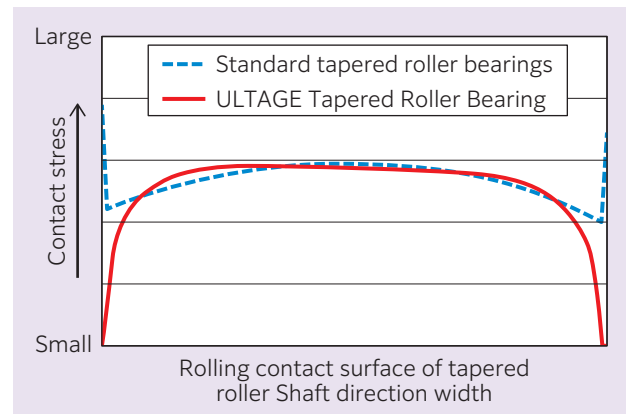


Fig. 20 Contact stress distribution on the raceway surface of a tapered roller bearing¹⁵⁾

Service life tests were conducted under the high misalignment (0.002 rad) conditions (Table 10) assumed for e-Axle. Fig. 21 shows the test results. The ULTAGE Tapered Roller Bearings achieves a long operating life approximately 16 times longer than that of standard tapered roller bearings due to the uniformity of the contact stress distribution.

Table 10 Test condition¹⁵⁾

Test bearing size	φ23×φ55×20
Bearing material heat treatment	Standard bearing steel heat treatment
Test load	Basic dynamic load rating of 26 % (JIS B 1518:2013)
Misalignment	0.002 rad
Rotational speed	4 000 min ⁻¹
Lubricating oil	ISO VG100 gear oil equivalent
JIS basic rating life	73 hours

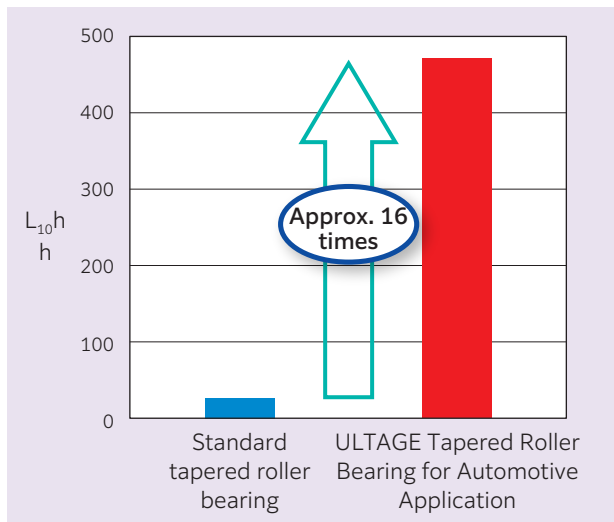


Fig. 21 Clean oil life test results for tapered roller bearings under high misalignment conditions¹⁵⁾

5. Conclusion

As the shift to electric vehicles (EVs) continues as part of the pursuit of carbon neutrality, the functions required of bearings are becoming more diverse. In this article, **NTN** introduced rolling bearings for electric drives that can meet the technical requirements of e-Axes. Looking towards the future, **NTN** will continue to develop technologies that anticipate the evolving needs of the automotive market.

References

- 1) Ministry of the Environment website, Decarbonization Portal, https://ondankataisaku.env.go.jp/carbon_neutral/
- 2) Takashi Kawai, Introduction of Recent Rolling Bearings for Automotive Applications, *Automotive Technology*, Vol. 9, No. 10, (2022) 43-50.
- 3) NTN Corporation to expand mass production and delivery of high-speed deep groove ball bearings for EVs and HEVs, 2020 https://www.ntn.co.jp/japan/news/new_products/news202000044.html
- 4) Takashi Kawai, Introduction of Rolling Bearings for EVs (Electric Vehicles), *Journal of Economic Maintenance Tribology*, No. 692, (2022) 37-44.
- 5) Katsuaki Sasaki, Takahiro Wakuda, Tomohiro Sugai, Ultra-low Friction Sealed Ball Bearing for Transmission, *NTN TECHNICAL REVIEW*, No. 85, (2017) 62-66.
- 6) Katsuaki Sasaki, Technical Trend of High-Speed Deep Groove Ball Bearings for Motors, *Monthly Tribology*, No.404, (2021) 12-15.
- 7) NTN Corporation wins Nippon Brand Award of 2021 "CHO" MONODZUKURI Innovative Parts and Components Award, 2021 <https://www.ntn.co.jp/japan/news/press/news202100067.html>

- 8) NTN Corporation achieves high-speed rotation of 2.2M with deep groove ball bearings for EVs and HEVs, 2022 https://www.ntn.co.jp/japan/news/new_products/news202200027.html
- 9) Hayato Kawaguchi, Toshiki Masuda, Marina Nagata, Toshitaka Kawai, Creepless Bearings, *NTN TECHNICAL REVIEW*, No. 88, (2021) 66-70.
- 10) Tsuyoshi Niwa, A Creep Mechanism of Rolling Bearings, *NTN TECHNICAL REVIEW*, No. 81, (2013) 100-103.
- 11) NTN Corporation Ball and Roller Bearings Catalog (CAT.No.2203/J 20.08.199 NI/NI), 2020
- 12) Shoji Noguchi, Electric Pitting Prevention Technology for Rolling Bearings, *Monthly Tribology*, No.320, (2012) 18-20.
- 13) Yoshinori Isomura, Tatsuo Maetani, Akihiko Watanabe, Keisaku Nakano, et al., A Study of Electrical Pitting for Small Ball Bearing of PWM Inverter Drive (Part 2), *The Tribologist*, Vol. 58, No. 1, (2013) 46-51.
- 14) Takayuki Kawamura, Hiroki Fujiwara, and Koya Ohira, New Technology of Rolling Bearings contributing to Low Fuel Consumption of Automobiles, *NTN TECHNICAL REVIEW*, No. 87, (2019) 85-91.
- 15) Yasuhito Fujikake, Takanori Ishikawa, Susumu Miyairi, ULTAGE Tapered Roller Bearing for Automotive Application, *NTN TECHNICAL REVIEW*, No. 85, (2017) 51-55.
- 16) Yasuhito Fujikake, Takanori Ishikawa, Low Temperature Rise and Low Torque Tapered Roller Bearings, *NTN TECHNICAL REVIEW*, No. 88, (2021) 71-76.

Photo of authors



Takashi KAWAI

Automotive Bearing Engineering Dept., Automotive Bearing Products Unit, Automotive Business Headquarters

Tomohisa UOZUMI

NTN BEARINGS (UK) LTD.

Evolution of Fixed Constant Velocity Joint that Contributes to Environmental Protection



Masashi FUNAHASHI *
Teruaki FUJIO *
Ritsuki SAKIHARA *

In 1963 NTN commercialized the constant velocity joint for the first time in Japan. Since then, NTN has continued to develop new products in order to adapt to the environmental policy which changes with the times. This article looks back on the evolution of NTN's fixed constant

velocity joints and explains about two types of high efficiency fixed constant velocity joints applied for the evolving EV market of the future.

1. Introduction

Drive shafts used for power transmission in automobiles can be divided into two types. Fixed constant velocity joints ("fixed CVJs") are attached to the tire side and can take a large angle as the tire rolls. Sliding constant velocity joints ("sliding CVJs") are attached to the powertrain unit side and can take an angle and slide with vertical movement of the vehicle body (**Fig. 1**). NTN has been developing drive shafts that are compact, lightweight, high-angle, low-vibration, and has made continuous improvements using tribology, materials, mechanical design and other technologies. On the other hand, as abnormal weather conditions have occurred due to global warming caused by increased CO₂ emissions, the impact of human activity on the environment is being taken up as a social problem making it increasingly important to find a new approach to environmental conservation. Since the Kyoto Protocol was established in 1997, the international community has worked to advance global warming countermeasures. To achieve the global average temperature increase target set in the Paris Agreement of 2015, efforts to realize a decarbonized society by 2050 are accelerating around the world. Against that background, in recent years the use of high-efficiency (low heat generation) drive shafts has been attracting attention.

This paper focuses on fixed CVJs, for which there is a greater need for improvement from the market. We introduce the evolution of CVJs that NTN is continuously developing in response to the changes in automobiles associated with environmental protection.

2. Market trends/needs

As the drive toward decarbonization continues, each year countries around the world are tightening their standards for CO₂ emissions and fuel efficiency of automobiles. There is a continuing need for lightweighting and higher efficiency of all components used in automobiles. In addition, the automotive industry is rapidly shifting from conventional internal combustion engine vehicles to electric vehicles (EVs) which are expected to have a longer cruising range. In addition, changes in vehicle layout such as changes in the position of the powertrain unit and extension of the wheelbase are expected in order to provide space for large capacity batteries. (**Fig. 2**)

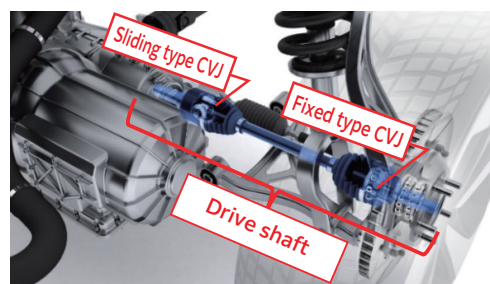


Fig. 1 Arrangement of fixed CVJs at the drive shaft

* CVJ Development Dept., CVJ Products Unit, Automotive Business Headquarters

Evolution of Fixed Constant Velocity Joint that Contributes to Environmental Protection

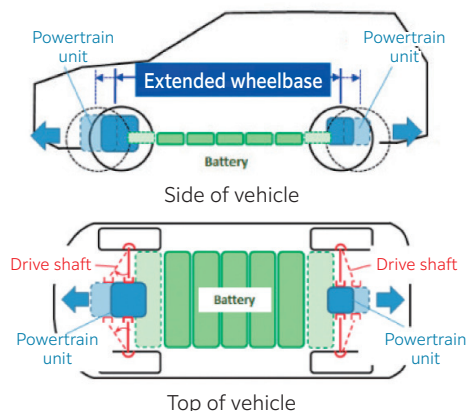


Fig. 2 Image of EV drive shaft arrangement

In this context, the functions required of drive shafts are (1) higher efficiency, smaller size, and lighter weight to help reduce fuel consumption and electricity costs, and (2) a higher operating angle (higher steering angle) to control the increase in turning radius due to an extended wheelbase and a higher working angle due to the need to secure battery space. One particular issue has been that fixed CVJs are less efficient than sliding CVJs in terms of the required functions and structure. NTN is continuously developing fixed CVJs to meet these market trends and needs.

3. Evolution of NTN fixed CVJs¹⁾²⁾⁴⁾⁵⁾

3.1 Development of CVJs in Japan

Before the 1960s, automobiles developed mainly as rear-wheel drive (FR) vehicles, while front-wheel drive (FF) and four-wheel drive (4WD) vehicles were also developed to improve comfort and driving performance, etc. In FF and 4WD vehicles, power from the engine is transmitted to the front wheels. Drive components are therefore required to be able to transmit power at constant speed even if the tires are steered. The cardan joint (cross shaft coupling, **Fig. 3**) used at that time was an unequal-velocity joint that caused large rotational fluctuations between the input and output shafts when the operating angle increased, resulting in unstable steering operation during driving.

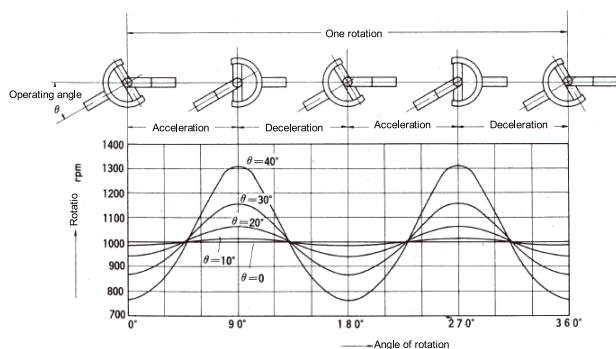


Fig. 3 Cardan Joint (cross shaft coupling)

In 1956, Hardy Spicer (U.K.) developed a fixed CVJ that could transmit power at constant velocity even when the operating angle was increased. This enabled the front wheels of a car to have both steering and driving functions. NTN formed a technology alliance with Hardy Spicer in 1962, through which we developed the BJ (maximum operating angle 42.5 degrees) for the Suzulight Van FE (Suzuki Motor Corp., **Fig. 4**). In 1964, the first vehicle equipped with a fixed CVJ that was successfully mass-produced in Japan was introduced to the market (**Fig. 5**). This greatly improved handling stability, which had been a problem for FF and 4WD vehicles, and contributed greatly to the popularization of automobiles in Japan.

Later, to meet the rapidly expanding demand for fixed CVJs and the increasing need for higher steering angles in vehicles, NTN developed BJ-L (**Fig. 6**), which expanded the maximum operating angle from 42.5 degrees to 46.5 degrees while maintaining the outer diameter. NTN achieved this by changing the fixed CVJ outer ring material from carburized steel to induction hardened midcarbon steel, and by making an optimal high angle design. Mass production of the BJ-L fixed CVJ began in 1982, is still used as the basic design today, and continues to evolve to capture the market needs of small size, lightweight, high efficiency, and high angle.



Fig. 4 Suzulight Van FE (Suzuki Motor Corp.)



Fig. 5 Exterior of CVJ mounted on Suzulight Van FE



Fig. 6 BJ-L exterior

3.2 The shift towards more compact, lightweight, high-efficiency CVJs

The evolution of fixed type CVJs is shown in Fig. 7.

The first evolution was to change the lubricant sealed inside the CVJ from lithium-based grease to urea-based grease, thereby achieving a longer operating life. The fixed CVJ (BJ-L compact) is 4 % smaller and 8 % lighter than the BJ-L while maintaining the maximum operating angle of 46.5 degrees. Mass production began in 1992.

The next evolution was the E-series fixed CVJ (“EBJ”; Fig. 8), which achieved further downsizing and weight reduction. To reduce the size while maintaining the same load carrying capacity as the BJ-L, the outer diameter size was reduced and the number of balls was increased from six to eight. The EBJ is 13 % smaller and 20 % lighter than the BJ-L, and it improved the torque loss ratio by 30 % (higher efficiency). Mass production of the EBJ began in 1998. The torque loss ratio was further improved by 20 % with the EBJ-S, by optimizing the internal clearance and applying low-friction grease to the EBJ. Mass production of the EBJ-S began in 2020.

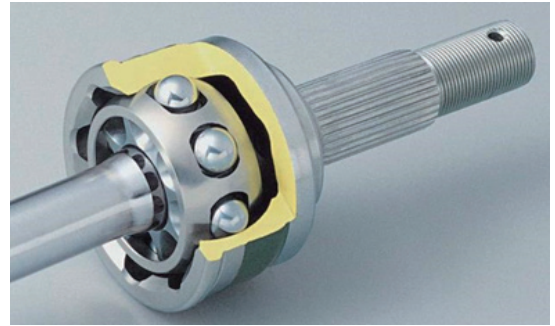


Fig. 8 Exterior of EBJ, EBJ-S

In 2022, NTN began mass production of the high-efficiency fixed CVJ “CFJ”.³⁾ This was the first CVJ to adopt NTN’s proprietary spherical cross groove structure (the “proprietary structure”) as a further evolution of the EBJ. The same outer diameter and mass as the EBJ were maintained while the torque loss ratio was improved by more than 50 %. CFJs will be introduced in detail in Chapter 4.

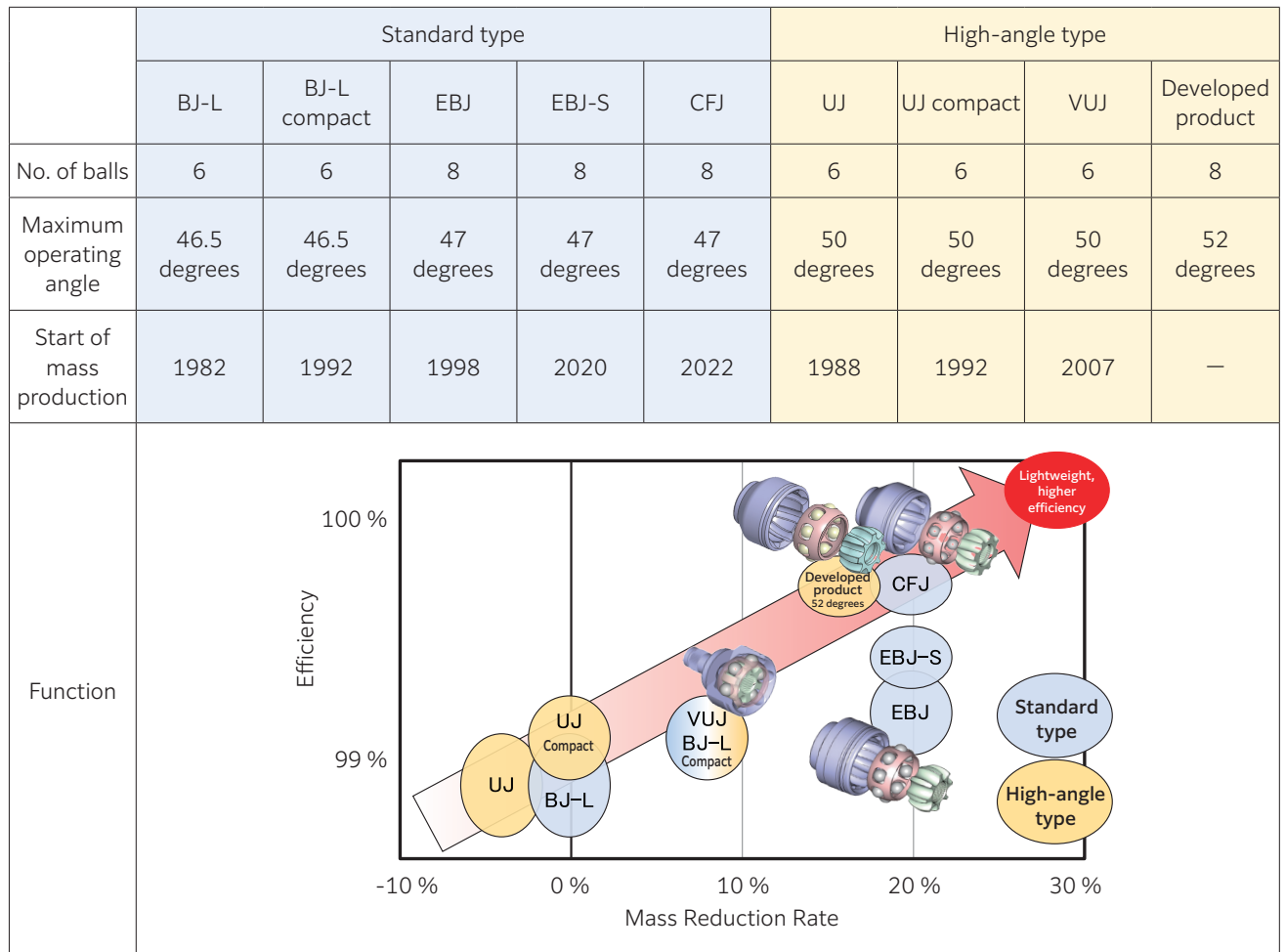


Fig. 7 Evolution of fixed type CVJs

3.3 Increasing the operating angle of CVJs

As FF vehicles became larger in the 1980s and 4WD vehicles increased in number, the need to reduce the minimum turning radius drove demand for fixed CVJs with a high operating angle. In 1988, **NTN** began mass production of UJ, which has a maximum operating angle of 50 degrees. To ensure high angle functionality, mass production of UJ began with a 4 % increase in diameter and an 8 % increase in mass compared to BJ-L. In 1992, UJ (small size) was developed that achieved an outer diameter and mass equivalent to BJ-L by applying urea-based long-life grease (**Fig. 7**).

In 2007, **NTN** began mass production of VUJ, which has the same six balls as UJ, but is smaller and lighter due to the optimized strength of each part and the application of long-life grease. In 2022, **NTN** completed basic development of a 52-degree high-angle fixed CVJ [developed product] based on CFJ technology. Compared to the UJs (compact type) developed since the 1990s, the VUJ is 4 % smaller and 8 % lighter, while the 52-degree high-angle fixed CVJ [developed product] is 10 % smaller and 16 % lighter, with a torque loss ratio improvement of over 50 % (**Fig. 7**).

4. Helping to reduce environmental impact with higher efficiency fixed type CVJs

To meet vehicle requirements, **NTN** offers two types of fixed CVJs: a standard type and a high-angle type with different maximum operating angles, as shown in **Fig. 7**.

This chapter introduces the standard high-efficiency fixed CVJ “CFJ” and the high-angle type 52-degree fixed CVJ [developed product] to show how improvements in the efficiency of fixed CVJs can help to reduce environmental impact.

4.1 High-efficiency fixed CVJ “CFJ”³⁾ (standard type)

The CFJ is a fixed CVJ with a maximum operating angle of 47 degrees that achieves the world’s highest level of efficiency through the adoption of a unique structure (**Fig. 9**) with the aim of reducing automobile CO₂ emissions and improving fuel efficiency. The torque loss ratio is reduced by 50 % or more while maintaining the same outer diameter and mass as the EBJ (conventional product), which has achieved the world’s highest levels of compactness and lightweight.

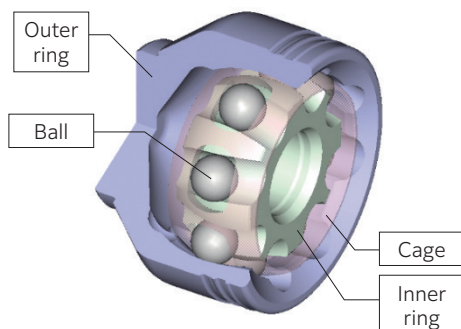


Fig. 9 Configuration of CFJ

4.1.1 Features

- (1) Arc-shaped tracks on the inner and outer rings are inclined in the axial direction, with adjacent tracks arranged in mirror-image symmetry (**Fig. 10**).
- (2) The slopes of the inner and outer ring tracks cross each other and the ball is placed at the intersection (**Fig. 11**).

The torque loss of a CVJ is equivalent to the energy lost due to the frictional forces that occur between the parts during torque transmission. In the case of EBJ, among the internal forces of the CVJ that occur during torque transmission, the direction of the force of the ball pushing the cage is the same for all balls. The cage is pushed in one direction and contacts the outer and inner rings. On the other hand, the unique structure of the CFJ causes the force of the ball pushing the cage to be in the opposite direction for adjacent balls, which cancels out the force on the cage and significantly reduces the contact force with the outer ring and inner ring (**Fig. 12**). This reduces the frictional force between the cage and the outer and inner rings, resulting in the world’s highest level of efficiency.

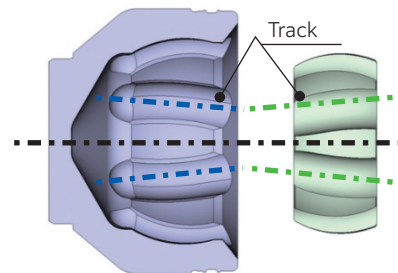


Fig. 10 Image of track shape

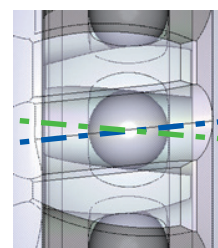


Fig. 11 Arrangement of track and ball

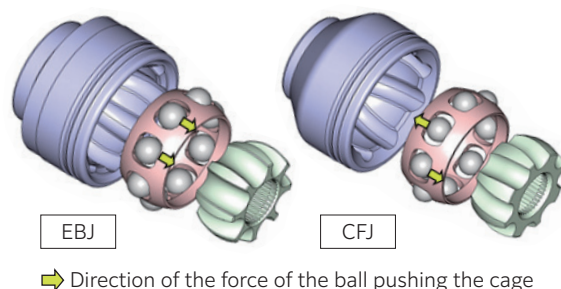


Fig. 12 Comparison of internal force

4.1.2 Function

Fig. 13 shows the measurement results of torque loss ratio. The torque loss ratio was reduced by more than 50 % compared to the conventional product not only during normal driving, but also during the regenerative driving that occurs in vehicles such as EVs.

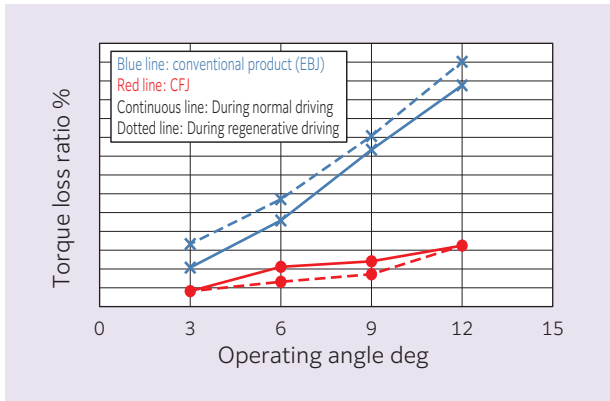


Fig. 13 Comparison of torque loss ratios

4.1.3 Efficiency of Fixed CVJs and Estimated Effects on Vehicles

The efficiency of the drive shaft, the component that transfers power from the engine to the tires, directly affects the fuel efficiency and electricity consumption of a vehicle. In addition, it has an even greater impact on hybrid vehicles and EVs that have regenerative braking for recovering energy during deceleration.

Performing a detailed calculation for CFJ, we find that in the case of a gasoline vehicle, fuel efficiency improves by 0.62 % and CO₂ emissions decrease by 0.96 g/km compared with EBJ (fuel efficiency: 17.6 km/L) when the vehicle weighs approximately 1.5 tons and the drive shaft is installed at a 9-degree angle under the WLTP (Worldwide Harmonized Light Vehicle Test Procedure) conditions. BEV (electric power consumption: 155 Wh/km) improves electric power consumption by 0.90 % (**Table 1**).

Table 1 Effects on automobiles (EBJ ratios)

	Fuel and electricity cost Improvement rate	CO ₂ Emission Reduction
Gasoline vehicle	0.62 % UP	-0.96 g/km
HEV	0.76 % UP	-1.12 g/km
BEV	0.90 % UP	—

<Test conditions>

Setting angle: 9 degrees

Vehicle: fuel efficiency 17.6 km/L; power consumption 155 Wh/km

Vehicle weight: approx. 1.5 tons; driving conditions: WLTP

4.2 52 degrees fixed type CVJ (high-angle type) [developed product]

This product is a high-angle, high-efficiency fixed CVJ. As well as offering a high operating angle that is larger than the maximum operating angle of the VUJ (maximum operating angle: 50 degrees), it offers high efficiency and is compact and lightweight.

4.2.1 Features

By adopting a unique structure similar to that of the CFJ, it is possible to reduce the force generated inside the CVJ during torque loading (internal force) and to improve the load carrying capacity at high operating angles. In addition, NTN changed the track shape in the area where the ball moves toward the outer ring aperture at high operating angles. This secured the rolling path length of the ball to align with the contact point between the ball and the track at operating angles exceeding 50 degrees. The cage, which is the weakest part of the fixed CVJ at high operating angles, was made smaller yet higher angle was achieved by optimizing the shape and changing the material. As a result, a 6 % reduction in size and an 8 % weight reduction were achieved while increasing the maximum operating angle by 2 degrees compared to the VUJ (**Fig. 14**).

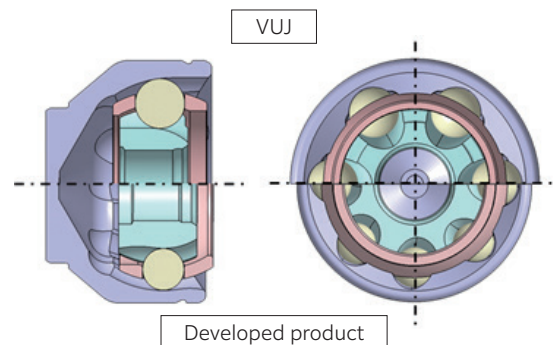


Fig. 14 Design comparison

4.2.2 Function

- Efficiency (torque loss ratio)

By adopting a unique structure, the torque loss ratio was improved by more than 50 % in all angular regions compared to the VUJ (**Fig. 15**).

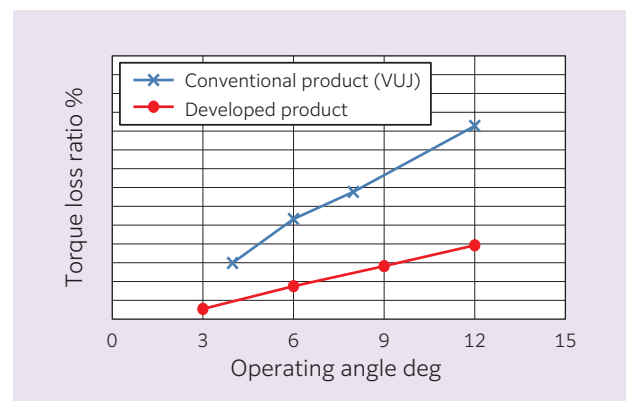


Fig. 15 Comparison of torque loss ratios

Evolution of Fixed Constant Velocity Joint that Contributes to Environmental Protection

- Strength at high operating angles

By using a unique structure, modifying the track shape, optimizing the cage shape, and changing the materials, we achieved a 6 % reduction in size and 9 % reduction in weight compared to the VUJ, while achieving the same strength at high operating angles (**Fig. 16**).

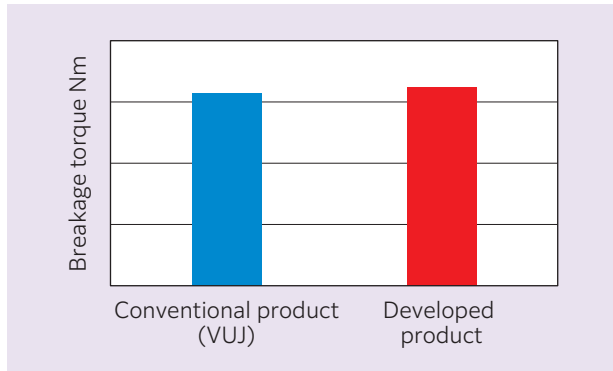


Fig. 16 High angle static torsional strength comparison

5. Summary

This paper touched on the evolution of fixed CVJs that contribute to reducing environmental impact, and introduced products **NTN** has developed in response to the changing times and their effectiveness. To realize a global decarbonized society, automobiles are undergoing a once-in-a-century transformation. CVJs are required to provide enhanced functions to respond flexibly to this transformation. As a constant velocity joint manufacturer, **NTN** will target demand for EVs, which will continue to expand going forward so that we can contribute to the realization of a decarbonized society and reduce environmental impact. We will continue to develop CVJs that are small, lightweight, high-performance, and have excellent quietness with optimal strength and durability tailored to the locations of their application and to vehicle characteristics.

References

- 1) Takeshi Ikeda, History of CVJ Design for Automobiles and Recent Technology, NTN TECHNICAL REVIEW, No. 70, (2002) 8-17.
- 2) Shin Tomogami, Technical Trends in Constant Velocity Universal Joints and the Development of Related Products, NTN TECHNICAL REVIEW, No. 75, (2007) 10-15.
- 3) Teruaki Fujio, Next Generation High Efficiency Fixed Constant Velocity Joint "CFJ", NTN TECHNICAL REVIEW, No. 81, (2013) 64-67.
- 4) Shinichi Takabe, History of Constant Velocity Joints, NTN TECHNICAL REVIEW, No. 85, (2017) 40-45.
- 5) Tatsuro Sugiyama, History of Development of Constant Velocity Joint Aiming at Low Fuel Consumption, NTN TECHNICAL REVIEW, No. 87, (2019) 59-62.

Photo of authors



Masashi FUNAHASHI
CVJ Development
Dept.,
CVJ Products Unit,
Automotive Business
Headquarters

Teruaki FUJIO
CVJ Development
Dept.,
CVJ Products Unit,
Automotive Business
Headquarters

Ritsuki SAKIHARA
CVJ Development
Dept.,
CVJ Products Unit,
Automotive Business
Headquarters



Ken YASUDA *
Shinji KOMATSUBARA **

The Composite Material Product Division at NTN has developed bearings, mechanical parts, and module products. These products make full use of tribology and are made of multi materials such as: resins, sintered metals, magnetic materials. In this article, we mainly introduce products for thermal management in automobiles.

1. Introduction

In recent years, the automotive industry has been in development of various technologies focused on the keyword of CASE. For example, motors and other power sources, inverters, and DC-DC converters are being developed for electrification. Meanwhile, cameras, sensors, and ECUs that integrate and control these accessories and their parts, are being developed for autonomous driving. As these accessories become smaller and lighter to improve the fuel efficiency and power consumption of automobiles, heat dissipation has become more difficult to manage due to the rise in heat generation of new automobile components. The addition of electrical and electronic devices that generate large amounts of heat due to high-speed, large-capacity communications (such as 5G) have made thermal management of the entire automobile an important theme for ensuring reliability. The shift to electric vehicles has also created new market demand for a quiet vehicle interior that offers a recreational environment free from the noise of a conventional engine.

This paper introduces examples of applications for composite material products and how they contribute to higher efficiency of accessories as they relate to thermal management of automobiles, and to improved cabin comfort.

2. Elastomer main shaft seal for electric compressors

The accessories related to thermal management are critical to the range and battery life of electric vehicles. This has led to the increased market demand for energy-saving and high-efficiency performance.

These accessories contain various sliding parts made of high polymer materials (elastomers and resins) and their tribological properties are important.

While conventional internal combustion engine vehicles use belt-driven compressors powered by the engine, electric vehicles such as HEVs, PHEVs, and EVs use electric compressors. Electric compressors are used for cooling the cabin in HEVs and PHEVs, and for temperature control for batteries and other components – in addition to air conditioning in EVs. There are two types of compressors: scroll type and swash plate type.

Scroll type compressors are used because of their superior quietness. Scroll compressors use a main shaft seal that seals the refrigerant and refrigerating machine oil. NTN has developed a low-torque, low-leakage, BEAREE TP5300 main shaft seal that contributes to power savings and higher efficiency.

2.1 Structure of electric scroll compressors

A cross section of an electric scroll compressor is shown in **Fig. 1**. The refrigerant is compressed by the gyrating motion of the movable scroll, which is opposed to the fixed scroll. The movable scroll is driven by the rotation of the main shaft, and is supported by ball bearings. The main shaft seal has an inner diameter of about 20 mm with lips on both the inner and outer circumference to reduce leakage of refrigerant and refrigerating machine oil to the rotor side.

In EVs, electric compressors are used not only for heating and cooling, but also for the temperature management of batteries and other components. As a result, they operate for longer durations than in internal combustion engine vehicles. This has led to the need to improve the durability of electric compressors.

* Plastics Engineering Dept., Composite Material Product Division

** Hydrodynamic Bearing Engineering Dept., Composite Material Product Division

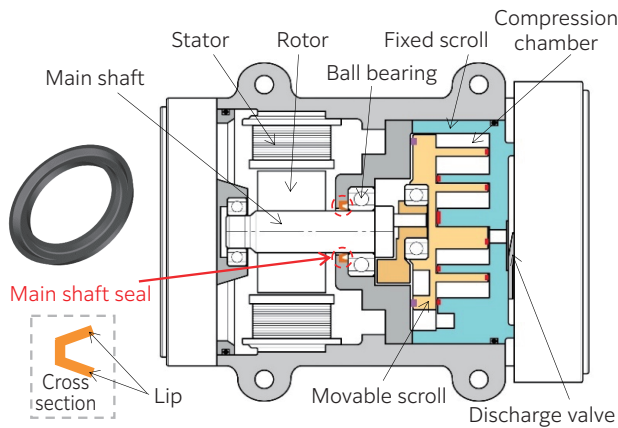


Fig. 1 Cross section of electric scroll compressors

2.2 Features of the BEAREE TP5300 main shaft seal

NTN's BEAREE TP5300 main shaft seal is made of a composite material that is formulated with a filling material in a thermoplastic elastomer – offering excellent friction and wear characteristics. Its flexibility (low elasticity) offers advantages such as low torque and low leakage. The lip reaction force caused by the interference with the shaft is small, and the lip tip (inner and outer sides) easily follow the shaft and housing. Further torque reduction is achieved by optimizing the lip design (thickness, angle, length, etc.).

Table 1 shows a performance comparison with a conventional polytetrafluoroethylene resin (PTFE) shaft seal. While conventional PTFE shaft seals are machined, the BEAREE TP5300 shaft seals can be injection molded, offering better design flexibility and reduction in manufacturing costs.

Table 1 BEAREE TP5300 and PTFE main shaft seal performance comparison

Item	BEAREE TP5300 main shaft seal	PTFE main shaft seal (Conventional product)
Base resin	Thermoplastic elastomer	PTFE
Processing method	Injection molding	Compression molding + machining
Flexibility of shape design	◎	△
Torque	◎	○
Leak	○	○
Durability	◎	△
Cost	◎	△

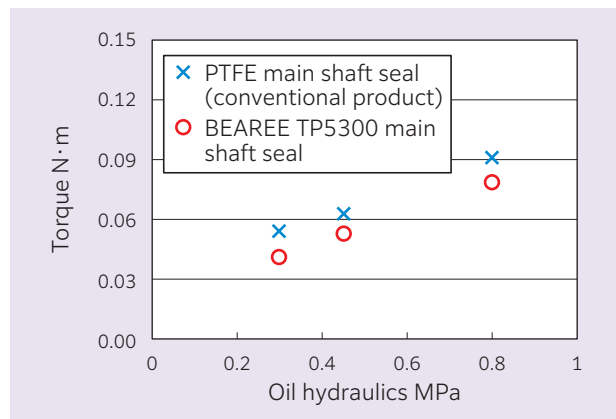
◎: Excellent ○: Good △: Acceptable

2.3 Friction and wear characteristics

Fig. 2 shows the torque measurement results of the shaft seal in refrigerating machine oil. The torque of the BEAREE TP5300 shaft seal is 15 % to 25 % lower than that of the PTFE shaft seal, and the TP5300 seal has lower oil leakage. The oil leakage of the TP5300 seal is equivalent to the PTFE seal (less than 1 mL/min).

Fig. 3 shows the results of a wear test for BEAREE

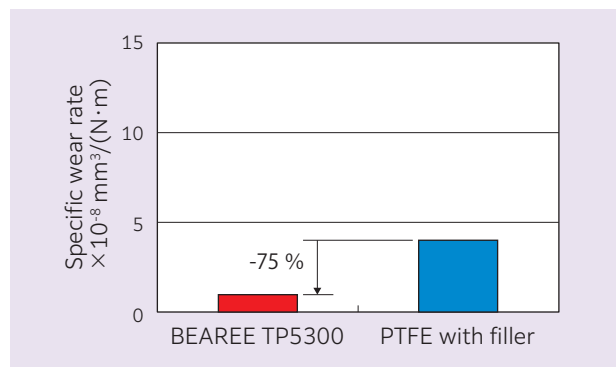
TP5300 and PTFE with filler, on a disc type testing machine. The BEAREE TP5300 has specific wear rate that is approximately one-fourth that of PTFE with filler.



<Test conditions>

- PAG oil, Oil temperature 100 °C
- Oil hydraulics 0.3 to 0.8 MPa
- Rotation speed 7 500 min⁻¹, Steel main shaft

Fig. 2 Torque measurement results



<Test conditions>

- Ring on disc type testing machine, PAG oil, Room temperature
- Surface pressure 0.3 MPa, Speed 1 m/s
- Opposing material SUJ2, 50 h

Fig. 3 Wear test results

3. Low torque plastic sliding bearings for electric water pump

Electric vehicles are equipped with an electric water pump that circulates cooling water, and an electric compressor for thermal management. Sliding bearings used in these pumps require even lower friction coefficients for lower fuel and power consumption.

NTN has developed a low torque plastic bearing with a significantly reduced friction coefficient in cooling water. This bearing features special lubrication grooves on the thrust surface of a PPS sliding bearing. This bearing is made of a proprietary composite material⁽¹⁾⁽²⁾ that combines materials such as polyphenylenesulfide (PPS), polytetrafluoroethylene resin (PTFE), and carbon fiber (CF).

3.1 Role and structure of electric water pump

Electric water pumps are classified by high-flow, medium-flow, and low-flow types, with each type having a different purpose in a vehicle. The high-flow type electric water pump is used for engine cooling, the medium-flow type is used for cooling the batteries, motors, and inverters, while the low-flow type is used for cooling and heating intercoolers and exhaust gas recirculation equipment.

Fig. 4 shows a cross section of a typical electric water pump. The rotor includes: the impeller, magnet, and sliding bearing, and is found in the pump housing. Meanwhile, the stator is arranged opposite the magnet and is freely supported by the shaft through the sliding bearing. The magnetic field generated by the energization of the stator causes the rotor to rotate about the shaft. Since the impeller is integrated with the rotor, the impeller rotates as the rotor rotates, and the cooling water is sucked into the pump housing.

The inner diameter of the sliding bearing is about 4 to 10 mm. During rotor rotation, radial and axial loads are generated. This causes the inner diameter surface and shaft of the sliding bearing, and the thrust surface and the thrust pad, to slide in the cooling water. The sliding bearing is pressed against the thrust pad on the impeller side, and the axial load is larger than the radial load. The frictional resistance of the thrust surface is thus greater than that of the inner diameter surface of the sliding bearing. To reduce the frictional resistance of the sliding bearing, it is therefore necessary to reduce the frictional resistance of the thrust surface.

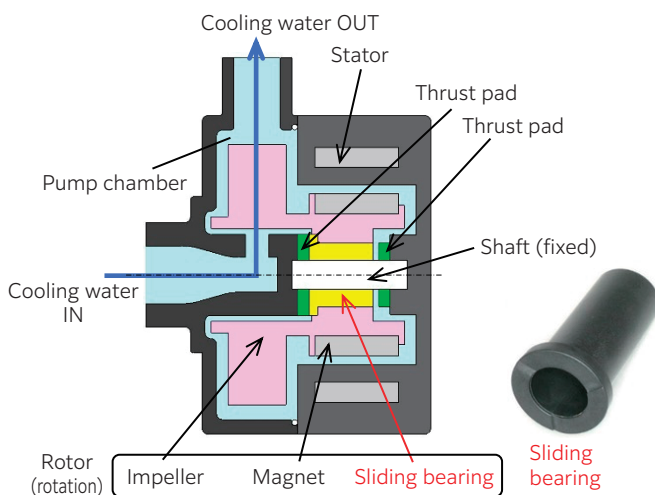


Fig. 4 Structure of electric water pump

3.2 Bearing thrust surface lubrication groove shape

Sliding bearings in electric water pumps maintain low friction and low wear under good lubrication conditions (high speed and low load). However, during startup, shutdown, and when there is localized water film loss during operation, the friction coefficient increases due to contact between the sliding bearing and the thrust pad – increasing the likelihood of wear. As a countermeasure, lubrication grooves are included on the thrust surface of the sliding bearing.

In general, a rectangular lubrication groove shown in **Table 2(b)** is used as a lubrication groove on the thrust surface in sliding bearings for electric water pumps. This rectangular lubrication groove penetrates radially from the bearing bore to the outer diameter. The cross section has a simple rectangular shape, so it is conventionally applied to machined products such as the carbon sliding bearings used in water pumps.

NTN's low torque plastic bearings instead have special lubrication grooves on the thrust surface of the PPS sliding bearing, as shown in **Table 2(a)**. These special lubrication grooves have a shape that enables material transfer during injection molding. As shown in **Fig. 5**, the special lubrication grooves are designed so that the grooves gradually become shallower in the counter-rotational direction of the bearing. This causes cooling water to be forced into the shallower grooves during bearing rotation, and generate pressure by the hydrodynamic effect. As a result, the cooling water can easily penetrate the thrust sliding surfaces of the bearing.

Fig. 6 shows the dynamic friction coefficient in cooling water for three types of PPS sliding bearings with three shapes of thrust surface: one with special lubrication grooves, one without lubrication grooves, and one with rectangular lubrication grooves on the thrust surface. The dynamic friction coefficient of the PPS sliding bearing with special lubrication grooves is 65 % lower than that without lubrication grooves, and 30 % lower than that with rectangular lubrication grooves.

Table 2 Shape of lubrication grooves on thrust surface of each thrust bearing

Item	(a) Special lubrication groove	(b) Rectangular lubrication grooves	(c) No lubrication grooves
Thrust surface lubrication groove shape	Rotational direction of bearing 		
Sliding area ratio	0.88	0.95	1 (reference)
Pressure, MPa	1.06	1.00	0.93

Note: Surface pressure is the value in the test (load 128 N) described below.

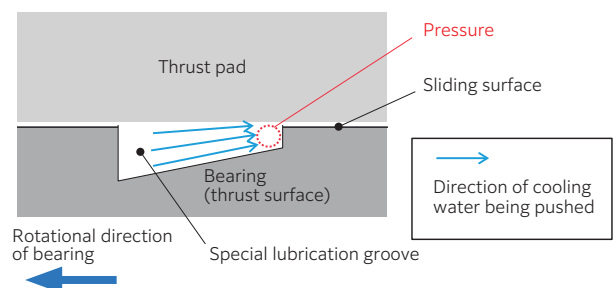
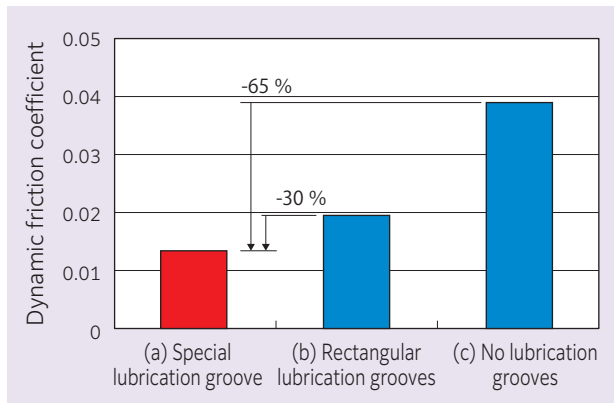


Fig. 5 Hydrodynamic effect from special lubrication grooves



<Test conditions>

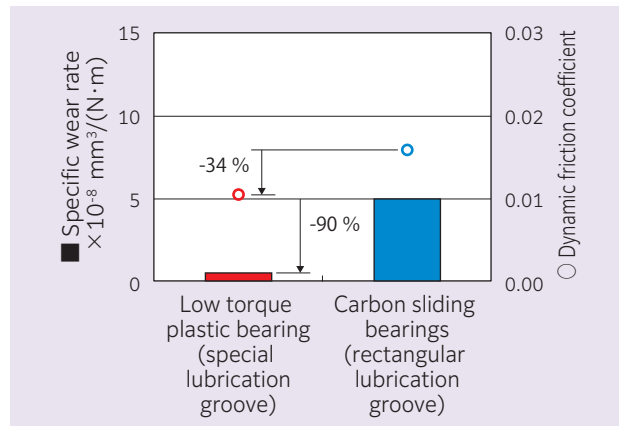
Ring on disc type testing machine cooling water (ethylene glycol 50 % concentration), Room temperature, 128 N load (surface pressure approx. 1 MPa), Speed 125 m/min, Opposing material SUS304

Fig. 6 Relationship between shape of lubrication grooves on thrust surface and dynamic friction coefficient

3.3 Friction and wear characteristics

Fig. 7 shows the results of friction and wear tests in cooling water for a low torque PPS sliding bearing, and a conventional carbon sliding bearing with three rectangular lubrication grooves as shown in **Table 2 (b)**. The low-torque plastic bearing (with special lubrication grooves) had a 34 % lower coefficient of dynamic friction and 1/10 th the specific wear rate as compared to the carbon sliding bearing (rectangular lubrication grooves). This difference in the dynamic friction coefficient is similar to the results for the rectangular lubrication groove and the special lubrication groove shown in **Fig. 6**.

Low torque plastic bearings are made of PPS composite material with fillers suitable for sliding in cooling water. These bearings have special lubrication grooves on the thrust surface, which provide lower friction and wear characteristics compared to carbon sliding bearings (rectangular lubrication grooves). Low-torque plastic bearings have various other excellent properties, as shown in **Table 3**.



<Test conditions>

Ring on disc type testing machine, Cooling water (ethylene glycol 50 % concentration), Room temperature, 128 N load (surface pressure approx. 1 MPa), Speed 125 m/min, Opposing material SUS304, 50 h

Fig. 7 Friction and wear characteristics of each type of sliding bearing

Table 3 Comparison of properties of each type of sliding bearing

Item	Low torque plastic bearing (special lubrication groove)	Carbon sliding bearings (rectangular lubrication groove)
Processing method	Injection molding	Machining
Chemical resistance	⊙	⊙
Impact resistance	○	△
Flexibility of shape design	⊙	△
Friction properties (in cooling water)	⊙	○
Wear resistance (in cooling water)	⊙	○
Cost	⊙	△

⊙: Excellent ○: Good △: Acceptable

4. Sintered hydrodynamic BEARPHITE headlight cooling fan

In conventional internal combustion engine vehicles, the sound from interior accessories is typically less noticeable due to the noise of an internal combustion engine. With no more engine noise, the electrification of automobiles has led to a growing demand for quieter interior accessories reliable over a wide range of temperatures.

In recent years, energy-saving and long-life LED lights have entered the mainstream for headlights.

These require higher current to provide a visible light intensity, but subsequently result in a large amount of heat generated in the LED circuit board. The need for thermal management is therefore increasing, and the cooling fan motor used for heat dissipation (**Fig. 8**) must have stable performance over a wide temperature range, from low temperatures (- 40 °C) to high temperatures (100 °C).

NTN has developed a hydrodynamic bearing, Hydrodynamic BEARPHITE (**Fig. 9**), that meets these requirements and is quiet over a wide temperature range.

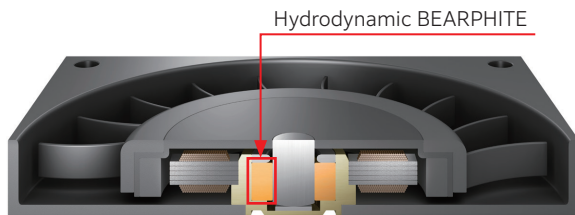


Fig. 8 Cooling fan motor



Fig. 9 Hydrodynamic BEARPHITE

4.1 Excellent quietness

Hydrodynamic BEARPHITE is a type of oil-impregnated sintered bearing manufactured by powder metallurgy and has herringbone-shaped hydrodynamic grooves on the bearing inner diameter (**Fig. 10**). The hydrodynamic effect generated by shaft rotation forms an oil film in the bearing clearance and supports the shaft without contact.

Fig. 11 shows the results of determining the presence or absence of contact between the shaft and Hydrodynamic BEARPHITE by the electrical resistance method. This is done to confirm the difference in oil film formation depending on the presence or absence of hydrodynamic grooves. Based on the detected voltage, the oil film formation rate was set to 0 % for the contact state and to 100 % for the non-contact state. These results indicate that hydrodynamic grooves can support the shaft without contact.

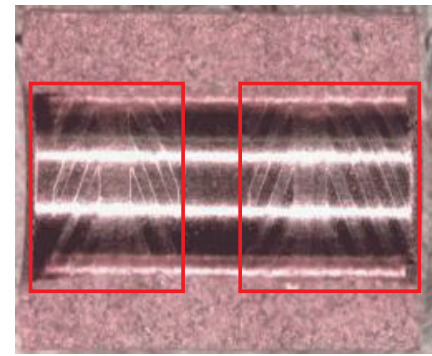


Fig. 10 Hydrodynamic BEARPHITE inner surface (red outlined areas: hydrodynamic grooves)

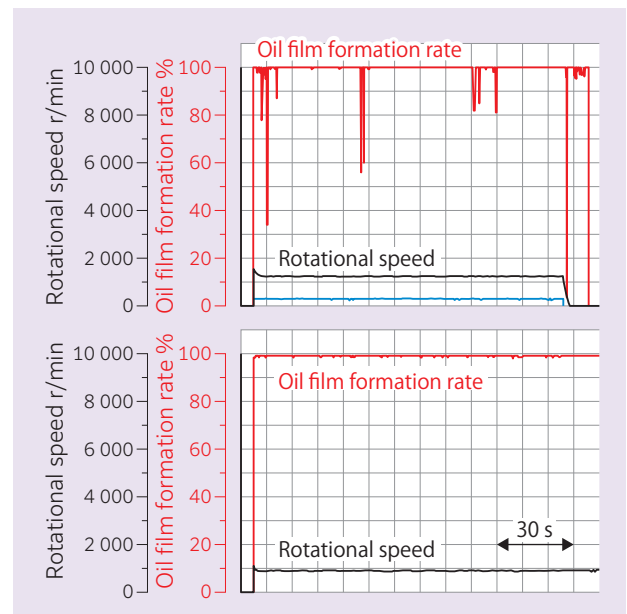


Fig. 11 Difference in oil film formation depending on presence or absence of hydrodynamic grooves (upper: no hydrodynamic grooves; lower: with hydrodynamic grooves)

Where a drop in oil film pressure is a concern³⁾, Hydrodynamic BEARPHITE generally remains quiet at low rotational speeds. This is why it is popularly used in cooling fan motors for information equipment, such as thin-type notebook PCs and mobile terminals. It is also being used in cooling fan motors for headlights because of its excellent quietness over a wide range of rotational speeds, from low to high speeds.

4.2 High reliability over a wide temperature range

In headlights, the bearing performance remains stable because of the minimum change in lubricant viscosity expected, over the wide temperature range required for headlights. A significant drop in lubricant viscosity at high temperatures reduces the hydrodynamic pressure effect generated by shaft rotation. However, the Hydrodynamic BEARPHITE, which applies a less viscous lubricating oil that decreases at high temperatures, offers excellent temperature characteristics when compared to conventional products. (**Fig. 12**)

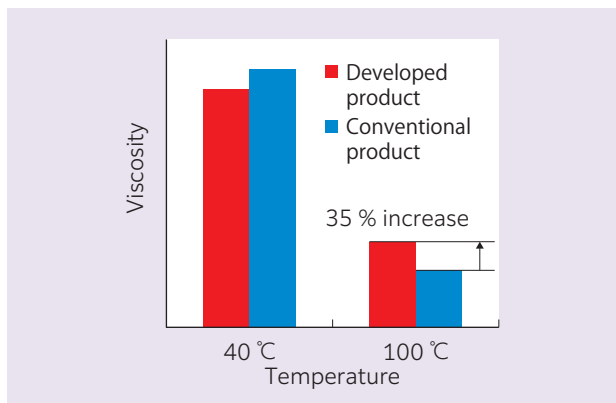


Fig. 12 Relationship between lubricating oil temperature and viscosity

Fig. 13 shows the eccentricity ratio calculation results of the shaft at high temperatures (100 °C). The eccentricity ratio is the ratio of shaft center displacement to radial clearance, and a lower eccentricity ratio means a larger minimum film thickness. The Hydrodynamic BEARPHITE can significantly reduce the eccentricity ratio as compared to conventional products, ensuring better bearing reliability over a wide range of temperatures.

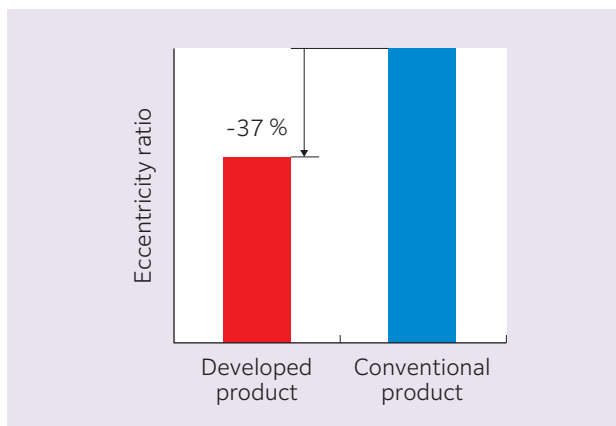


Fig. 13 Eccentricity ratio calculation results

Furthermore, as a feature of the powder metallurgy process, Hydrodynamic BEARPHITE can retain ample lubricant in the pores on the bearing surface layer and inside the pores (**Fig. 14**). Therefore, even if the assumed operating temperature range is exceeded, there is an effect of suppressing seizure due to the contact between the shaft and the Hydrodynamic BEARPHITE.

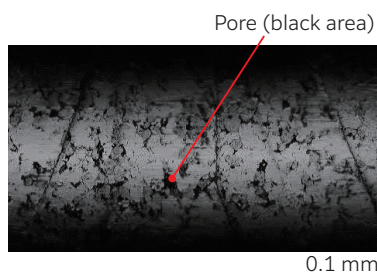


Fig. 14 Surface condition of Hydrodynamic BEARPHITE

5. Conclusion

This paper introduces a case in which NTN’s bearings and elemental parts made of resin, sintered metal, and other materials were adopted to save energy in automobiles and provide a comfortable cabin interior.

Thermal management has become vital to the development of vehicle electrification, autonomous driving, and connected automobiles. The UN-R51 international standard for four-wheeled vehicle noise has entered Phase 3 and is becoming stricter. In Phase 3, tire noise is taken into account, and the noise level during driving is required to be reduced from the level of a vacuum cleaner in Phase 2 to that of a washing machine. In addition, in a future where autonomous driving frees drivers from driving operations, it is expected that the demand for a quieter interior space will rise.

We will continue developing products and technologies that are key to improving thermal management and vehicle interior habitability, thereby contributing to the development of a mobile society with vehicles at its core.

References

- 1) Takuya Ishii, Ken Yasuda, The Latest Technology of Resin for Automobiles and Aircraft, Technical Information Institute (2016) 167.
- 2) Ken Yasuda, Technology of Plastic Sliding Bearings for Electric Water Pumps, Monthly Tribology, May 2021, No. 405 (2021) 32.
- 3) Shinji Komatsubara, Hydrodynamic BEARPHITE Bearings for Thin Cooling Fan Motors, NTN TECHNICAL REVIEW, No.88 (2021) 44-45.

Photo of authors



Ken YASUDA
Plastics Engineering
Dept.,
Composite Material
Product Division

Shinji KOMATSUBARA
Hydrodynamic
Bearing Engineering
Dept.,
Composite Material
Product Division

A Life Estimation Method of Peeling in Rolling Bearings Under Mixed Lubrication Conditions

Naoya HASEGAWA *
Takumi FUJITA **

Michimasa UCHIDATE ***
Masayoshi ABO ****

Peeling, which consists of spalls and cracks with the size of about 10 μm , is one of the failures of rolling bearings under boundary and mixed lubrication conditions. In the past, we introduced a life estimation method of peeling which is applicable to boundary lubrication and rolling conditions without slip. In this report, we introduce an updated life estimation method which is applicable to mixed lubrication conditions. The updated method applies a contact analysis based on the load-sharing theory of Johnson et al. This enables us to estimate peeling lives with consideration of the effect of oil film on supporting the load under mixed lubrication conditions. We evaluated the accuracy of the updated method by rolling contact testing. The accuracy of life estimation by the updated method was improved as compared with that of the previous method.

1. Introduction

International efforts toward carbon neutrality are expected to further accelerate the use of low viscosity lubricating oil for reducing friction in machinery and automobiles. Low viscosity lubricating oils will increase opportunities for use in boundary lubrication of rolling bearings (hereafter “bearings”) and mixed lubrication conditions (hereafter “severe lubrication conditions”). Improving the reliability of bearings under these conditions is thus expected to be an important technical issue in the future.

Peeling is a typical example of bearing failure that occurs under dilute lubrication conditions. It refers to a dense area of spalling and cracks of about 10 μm in size.¹⁾ Peeling tends to occur under certain conditions, such as severe lubrication conditions, where the rolling surface oil film parameter λ (the ratio of the minimum film thickness of the rolling area determined by EHL theory to the square root of the root-mean-square roughness of the two surfaces) is low. The cause is thought to be cyclic stress acting on the direct contact area of the surface roughness (hereafter “the real contact area”). In addition, the authors’ research^{2,3)} shows that the initial notches of peeling occur because of notch formed by plastic deformation due to the action of the cyclic stress mentioned above.

To examine the reliability of bearings under dilute lubrication conditions, it is necessary to estimate the life as affected by peeling (hereafter the “peeling life”). If the peeling life can be estimated, the surface roughness and lubricant of the bearing can be selected appropriately. In addition, it can also be applied to the design of the surface roughness and lubricating oil viscosity of the bearing necessary to balance reliability

and low torque, which can also help reduce friction for bearing users. In the previous report, the authors introduced a peeling life estimation method⁵⁾ that they independently developed,⁴⁾ but its application was limited to boundary lubrication conditions. In this paper, we present a peeling life estimation method applicable to mixed lubrication conditions, along with the results of validating its estimation accuracy.⁵⁾

The term “peeling” is customarily used by Japanese domestic bearing manufacturers, while the term “micropitting” is commonly used outside Japan.

2. Conventional peeling life estimation method⁵⁾

2.1 Procedure for life estimation

Fig. 1 shows the procedure for estimating peeling life. In Step 1, rolling fatigue tests are carried out under various operating conditions to obtain a history of peeling life (hereafter “stress history”) and the stress acting on the rolling surface (von Mises stress acting on the depth of 0.5 μm directly below the true contact area, hereafter “surface stress”). Surface stress is reduced during operation by decreasing the surface roughness of the rolling surface and generating compression residual stress (hereafter “running-in”). The surface stress is thus estimated using the results of contact stress analysis and residual stress measurement using the surface roughness measured for each constant load.

The von Mises stress at a depth of 0.5 μm was used for life estimation as the von Mises stress tended to be highest at a depth of 0.5 μm regardless of the test conditions.⁵⁾ In Step 2, the peeling $S-N$ curve (Stress-Number of cycles to failure) was obtained from the

* Advanced Technology R&D Center ** Product and Business Strategic Planning Dept.

*** Faculty of Science and Engineering, Iwate University **** School of Engineering, University of Hyogo

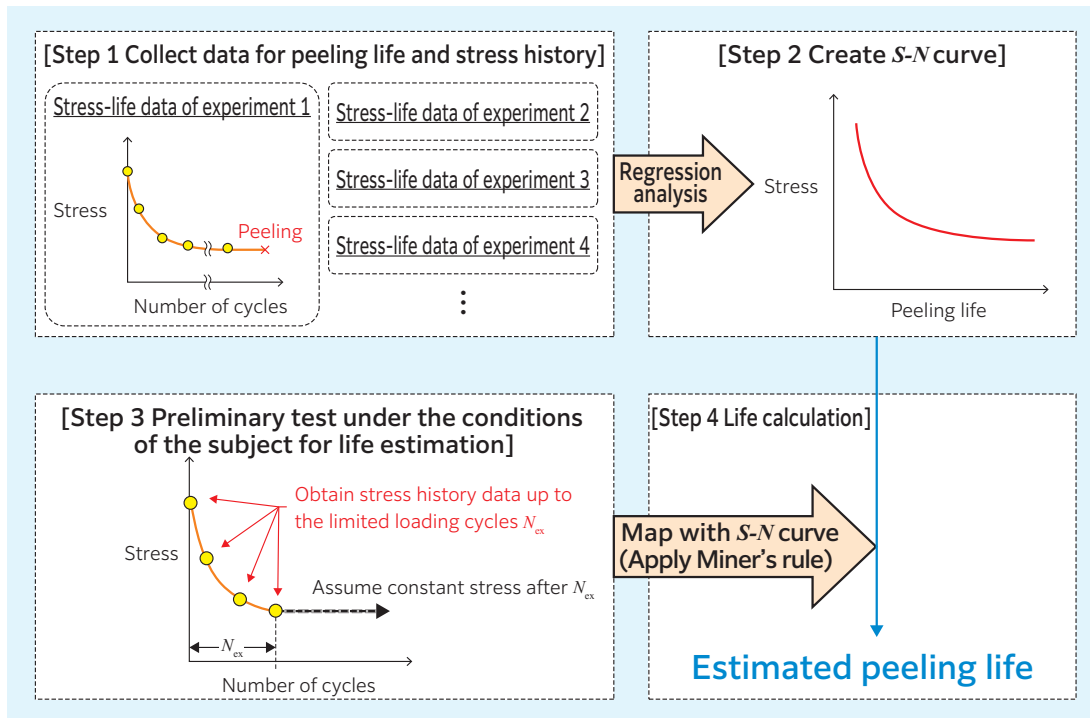


Fig. 1 Flow of the estimation method of peeling life⁴⁾

peeling life and stress history data obtained in Step 1 by regression analysis. In Step 3, a rolling fatigue test simulating the operating conditions to be estimated (hereafter the “preliminary test”) is conducted to estimate the peeling life under arbitrary conditions, and the stress history under those conditions is obtained. The preliminary test is conducted up to the number of loading cycles when the flexibility stops, N_{ex} (about 10^4 cycles). It is assumed that the surface stress does not change after that time. Finally, in Step 4, the peeling life is estimated using the stress history and $S-N$ curve obtained in Step 3.

In Steps 2 and 4 of this procedure, the degree of fatigue (the ratio of the total number of loads to the lifetime) is calculated using Miner’s law from the stress history. The concept adopted is that peeling occurs when the degree of fatigue reaches 100 %.

For surface stress, the average value of von Mises stress acting at a depth of $0.5 \mu\text{m}$ below the individual real contact area is used. To obtain this, the normal stress component $\hat{\sigma}_j$ and the shear stress component $\hat{\tau}_{jk}$ of the triaxial stress acting substantially at a depth of $0.5 \mu\text{m}$ below the true contact area are first determined by the following equations (1) and (2).

$$\hat{\sigma}_j = \sigma_{j, \text{con}} + \sigma_{j, \text{res}} \quad (1)$$

$$\hat{\tau}_{jk} = \tau_{jk, \text{con}} + \tau_{jk, \text{res}} \quad (2)$$

$$(j = x, y, z, k = x, y, z, j \neq k, \tau_{jk} = \tau_{kj})$$

Here, the subscript “con” indicates the contact stress obtained by contact stress analysis, and “res” indicates the residual stress obtained by residual stress measurement. In addition, x represents the circumferential direction, y the axial direction, and z the depth direction in the rolling surface. The triaxial stress components obtained in equations (1) and (2)

are then substituted into equation (3) below to obtain the von Mises stress at a depth of $0.5 \mu\text{m}$ at the real contact area, and the surface stress is obtained as the average of these values.

$$\sigma_{vm} = \sqrt{\frac{1}{2} \{(\sigma_x - \sigma_y)^2 + (\sigma_y - \sigma_z)^2 + (\sigma_z - \sigma_x)^2 + 6(\tau_{xy}^2 + \tau_{yz}^2 + \tau_{zx}^2)\}} \quad (3)$$

Although this estimation method requires preliminary testing, the life can be estimated in a few hours, including preliminary testing. By using the data from the preliminary tests, it is possible to perform a life estimation that accurately reflects running-in behavior under a wide variety of conditions that are difficult to simulate. Another feature of this method is that it takes into account the effect of residual stress on the life. The $S-N$ curves should be prepared for each steel grade and heat treatment of rolling parts.

3. Improved method of contact stress analysis for application to mixed lubrication conditions

3.1 Overview of contact stress analysis

Under mixed lubrication conditions, the effect of load support by the oil film cannot be ignored. In this paper, to apply the peeling life estimation method described above to mixed lubrication conditions, the contact stress analysis for estimating surface stress was enhanced to a method⁷⁾ that can consider the effect of load support by the oil film. In this analysis, the load sharing theory⁸⁾ of Johnson et al. is applied. The load on the rolling parts is considered to be shared by the oil film and the true contact area at a certain ratio, as shown in Fig. 2. The pressure distribution on the rolling surface is therefore obtained as the sum of

the pressure distributions of the oil film and the true contact area. The pressure distributions of the oil film and the true contact area are determined separately by convergence calculations with the load sharing ratio of the oil film as an unknown quantity. The convergence condition here is that the mass of the oil film in the clearance between two rough surfaces is equal to the mass of oil film formed between two smooth surfaces when the sharing load of oil is applied.

Hereafter, the procedure of this analysis is described with reference to **Fig. 3**. In Step 1, the load sharing ratio of the oil film to the load W on the rolling area is set as α . Then, the central oil film thickness h_c , the distribution of oil film pressure $P_f(x, y)$, and the elastic deformation of the two surfaces are calculated under the condition in which the sharing load of oil αW is applied to smooth surfaces. An arbitrary initial value is set for α in this calculation. The central oil film thickness h_c is calculated with the formula⁹⁾ of central oil film thickness of Chittenden et al, and the correction coefficient¹⁰⁾ due to shear heating. The oil film pressure $P_f(x, y)$ and the elastic deformation are assumed to be equal to them when the two surfaces contact with the load αW , and are obtained by the contact calculation program¹¹⁾ using the boundary element method. This is based on the fact that the spike of oil film pressure under high pressure conditions (several GPa) is small and negligible.¹²⁾ Besides, the lubrication regime of rolling bearings is generally the E-V (Elastic-Variable viscosity) regime in which the viscosity of the oil increases with the rise in pressure and the deformation of the rolling surface due to hydraulic pressure cannot be ignored. However, under conditions where α is close to 0, the lubrication regime is not E-V regime. In that case, the Chittenden et al. formula cannot be applied. Nevertheless, the error of analysis due to applying the formula of Chittenden et al. may be small as the influence of the oil film on the load support is small when α is close to 0. In Step 2, the three-dimensional roughness data of the rolling surface actually measured in advance is added to the shape of the two surfaces after the elastic deformation obtained in Step 1, and the rough surface shape of the deformed state due to the action of hydraulic pressure (hereafter, the rough surface

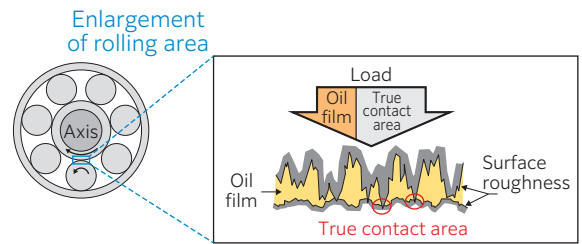


Fig. 2 Concept of load sharing theory

shape after hydraulic action) is created.

In Step 3, the remaining load $(1 - \alpha)W$ is applied to the rough surface shape after the hydraulic action, and the distribution of pressure $P_a(x, y)$ at the true contact area and the average clearance $h_{m, rough}$ of the two surfaces are calculated using the same contact calculation program as in Step 1. The average clearance $h_{m, rough}$ is calculated by the following equations.

$$h_{m, rough} = \int_A h_{rough}(x, y) dx dy / A \quad (4)$$

In the formula (4), A is the area of the region where the oil film pressure $P_f(x, y)$ is greater than 0 in Step 1. In addition, the clearance at the true contact area is set to 0. In Step 4, we examine whether the central oil film thickness h_c found in Step 1 is equal to the average clearance $h_{m, rough}$ found in Step 3. If it is not equal, we return to Step 1 and correct α . This is the convergence condition of the contact stress analysis, and is based on the idea that the mass of the lubricating oil drawn in between the two surfaces does not change regardless of the surface roughness of the two surfaces (law of conservation of mass). In Step 5, the pressure distribution $P(x, y)$ on the rolling surface when the total load W is applied is determined as the sum of $P_f(x, y)$ and $P_a(x, y)$, then the elasticity solution of Boussinesq¹³⁾ is applied to the obtained pressure distribution. In this way, the distribution of internal stresses (triaxial stress components) below the rolling surface is calculated.

3.2 Validity of contact stress analysis

The value of the load sharing ratio α and surface stress of the oil film obtained by this analysis method was verified to match the index of oil film formability obtained in the rolling fatigue test and the residual stress

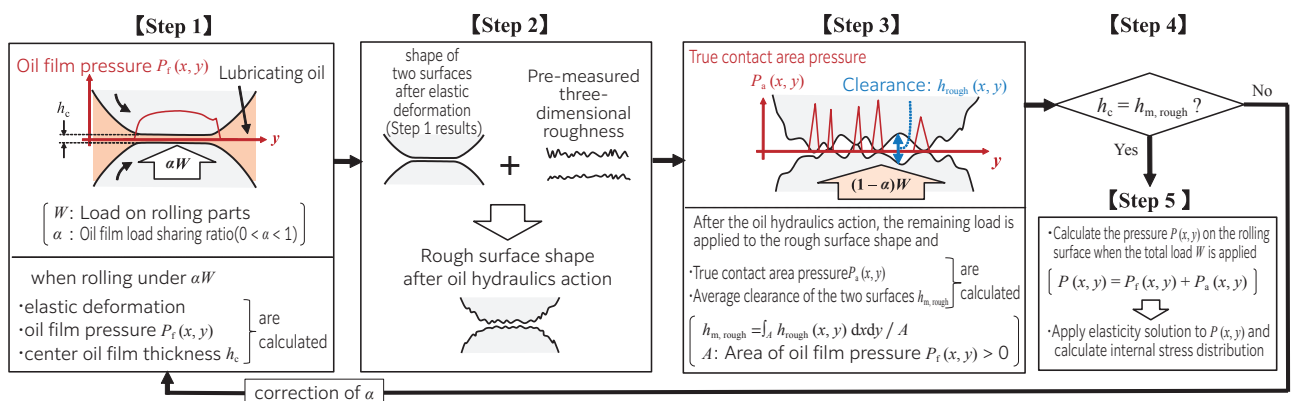


Fig. 3 Contact Stress Analysis Procedure⁷⁾

change of the test piece.⁷⁾ Although details are omitted in this paper, it has been confirmed that the analytical values of α and surface stress are generally consistent with the test data. **Fig. 4** shows, as an example of the results of the study, the relationship between the estimated value of the surface stress of the rolling surface and the measured value of the residual stress in the rolling fatigue test.

The rolling fatigue tests were conducted in a two-roller testing machine, as described below, with a gradually decreasing rotational speed starting at 900 min⁻¹. The test was interrupted each time when the rotational speed was changed, and the three-dimensional roughness and residual stress of the rolling surface were measured at each interruption. From these measurements, the surface stress during the test at each rotational speed was estimated. **Fig. 4** shows that the surface stress (estimated value) during operation exceeded the yield stress of the test piece at a rotational speed of 125 min⁻¹. The residual stress (measured value) increased during operation at a rotational speed of 125 min⁻¹. These results are consistent with the prediction of the contact analysis that the rolling surface shows plastic deformation at 125 min⁻¹ and the validation of the residual stress measurements.

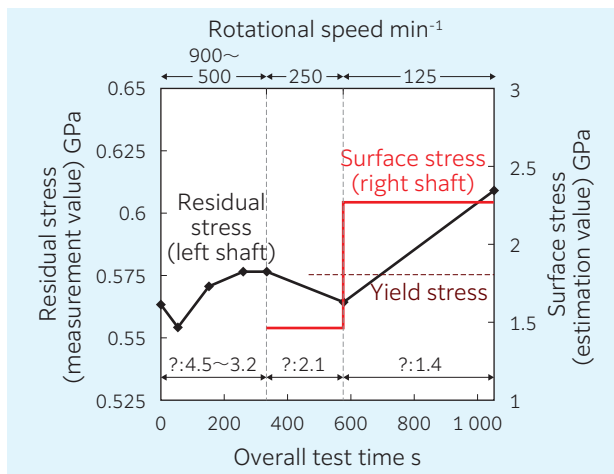


Fig. 4 Relationship between surface stress estimated by contact stress analysis and measured residual stress⁷⁾

4. Life estimation overall accuracy verification

4.1 Rolling fatigue test

To verify the accuracy of the new life estimation method, rolling fatigue tests were carried out with the two-roller testing machine shown in **Fig. 5**. The drive roller and the driven roller were cylindrical with an outer diameter of ϕ 40 mm and a thickness of 12 mm. A radius of 60 mm was applied to the drive roller only in the axial direction. A felt pad impregnated with lubricating oil was used to lubricate the roller test piece by contacting it from below. The material of the roller test piece was SUJ2, which was subjected to standard quench-hardening and tempering so that the surface hardness was about 63 HRC. **Table 1** shows the test conditions. Testing was carried out under varying conditions in terms of the surface roughness of the rolling surface, the rotation speed, the maximum hertzian contact surface pressure, and the lubricating oil type. The λ of Nos. 6 and 7 tests is more than 0.5, which corresponds to the mixed lubrication condition. Since it is easy for peeling to occur in the driven roller, which has low surface roughness, the life was determined from the occurrence of the peeling on the driven roller. In principle, each test was interrupted at 10² cycles, 10³ cycles, 5 × 10³ cycles, 10⁴ cycles, and 10⁵ cycles at load. At these interruptions and before the test, the three-dimensional roughness measurement of the drive roller and the driven roller and the residual stress measurement of the driven roller were performed. The stress history of the driven roller was obtained from the collected data. In addition, the occurrence status of the peeling of the driven roller was observed with an optical microscope at the time of interruption. The total number of loads when the ratio of the area of the occurrence of micro spalling and cracks to the area of the observation field of view (hereinafter referred to as the peeling area ratio) reached 0.5 % or more at six different places in the rolling surface was taken as the actual life L_{act} of the peeling. If the peeling area ratio was less than 0.5 % at 10⁵ cycles, the test was continued until 0.5 % was reached.

Table 1 Test conditions of the two-roller test⁶⁾

Test No.	Surface roughness (R_a) μ m		Rotational speed min ⁻¹	Maximum Hertzian contact pressure GPa	Lubricant	Dynamic viscosity (40 °C) mm ² /s	Oil film parameter λ	
	Drive roller	Driven roller						
1	0.75	0.02	2 000	2.3	Synthetic oil (PAO)	6.2	0.11	
2							0.12	
3							0.06	
4							0.17	
5	0.50	0.02	2 000	2.3	Mineral oil	32.6	0.52	
6	0.75		2 000				47.7	0.87
7	0.40		500				2.3	6.8
8		1 000	Synthetic oil (PAO)	6.2	0.17			
9					0.24			
10	0.35	0.02	2 000	2.3	Synthetic oil (PAO)	6.2	0.17	
11			0.24					

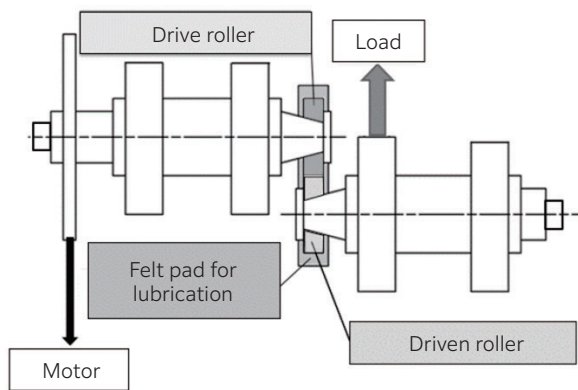


Fig. 5 Two-roller testing machine²⁾

4.2 Method for verification of overall estimation accuracy

Peeling life was estimated for the two-roller testing machines Nos. 1 to 11 shown in **Table 1** by the procedure shown in **Fig. 1**. The life was estimated with and without considering the load sharing theory in the contact stress analysis, and the accuracy of the life estimation was compared between the two cases. The estimated peeling life L_{est} for each test was calculated from the stress history up to 10^4 cycles. For the life estimation with load sharing theory, $S-N$ curves were generated using the test data except for Nos. 7 and 8, which were used for the calculation of L_{est} . In the case of life estimations where the load sharing theory was not considered, L_{est} was calculated using the $S-N$ curve that had already been created in a previous report.⁵⁾ The overall accuracy of the life estimation was examined using the life ratio (L_{act} / L_{est}) between L_{est} and the actual life of the peeling, L_{act} , which was finally obtained in the test.

5. Results

Fig. 6 shows the relationship between the estimated life L_{est} and the actual life L_{act} . The median, minimum, and maximum values of the life ratio (L_{act} / L_{est}) are

also shown in the figure. In the case of **Fig. 6** (a) without consideration of load sharing theory, the overall accuracy of life estimation for tests Nos. 6 and 7, which were conducted under mixed lubrication conditions, was lower than that of the other tests, and the error in estimated life relative to actual life (the error is calculated as the largest value or the reciprocal of the minimum value of L_{act} / L_{est}) was 20 times. On the other hand, when the load-sharing theory is taken into account in **Fig. 6** (b), the error in the estimated overall accuracy for tests Nos. 6 and 7 is less than five times, indicating that the overall accuracy of life estimation under mixed lubrication conditions is improved. Considering that the life of bearings generally varies by a factor of 10 or more under the same conditions¹⁴⁾, the overall accuracy of the life estimation in the case of the load sharing theory is considered to be at a sufficiently high level for practical use.

6. Summary

This article has presented an improved peeling life estimation method applicable to mixed lubrication conditions and the results of validation of the overall accuracy of the life estimation.

- 1) In this estimation method, a method of contact stress analysis that applies load sharing theory is employed, and the effect of lubrication conditions on peeling life is considered.
- 2) The maximum error of the peeling life obtained by this estimation method is less than 5 times of the actual life, and the accuracy of the peeling life estimation under mixed lubrication conditions is improved compared to the conventional method. The overall accuracy of the above is sufficiently high for practical use as a peeling life estimation method for bearings.

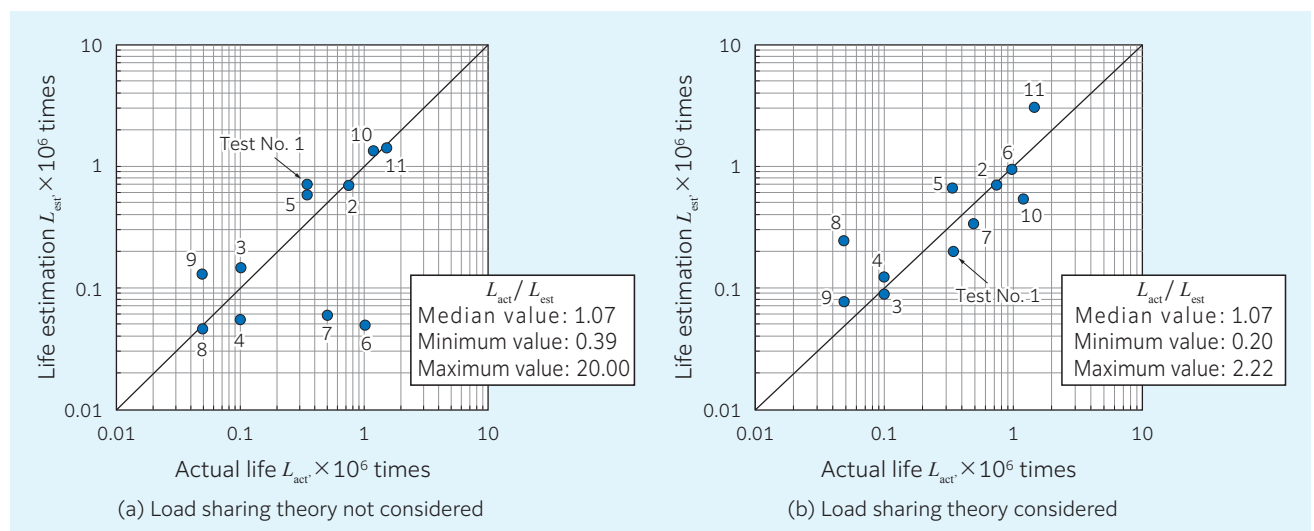


Fig. 6 Relationship between estimated peeling lives and actual peeling lives⁶⁾

It should be noted that the scope of application of this estimation method is currently limited to pure rolling conditions. Going forward, we will work to further improve the accuracy of the estimation and extend it to conditions where there is slip on the rolling surface. This estimation technique will be used to provide customer value in the form of improved bearing reliability and higher machine efficiency.

This paper summarizes the content of the presentation “Estimation Method of Micropitting Life from *S-N* Curve Established by Residual Stress Measurements and Numerical Contact Analysis, 2nd Report” in the Proceedings of Tribology Congress 2021 Spring Tokyo, which was organized by the Japanese Society of Tribologists and the presentation “Validation of Contact Stress Analysis of Rolling Surface under Mixed Lubrication” in the Proceedings of Tribology Congress 2022 Spring Tokyo. (Some figures and tables have been translated into Japanese and rearranged.) We thank the Japanese Society of Tribologists for their kind permission to publish this paper.

References

- 1) Noriyuki Tsushima, Hirokazu Nakashima, Hiroshi Kashimura: Typical Failures of Bearings, NTN TECHNICAL REVIEW, No. 57 (1990) 59.
- 2) Naoya Hasegawa, Takumi Fujita, Michimasa Uchidate, Masayoshi Abo: Mechanism for Initiation of Peeling in Rolling Contact and the Effect of Black Oxide Treatment on the Suppression of Peeling (Part 1), The Tribologist, 63, 8, (2018) 551.
- 3) Naoya Hasegawa, Takumi Fujita, Michimasa Uchidate, Masayoshi Abo, Mechanism for Initiation of Peeling in Rolling Contact and the Effect of Black Oxide Treatment on the Suppression of Peeling (Part 2), The Tribologist, 63, 9, (2018) 618.
- 4) N. Hasegawa, T. Fujita, M. Uchidate, M. Abo, and H. Kinoshita: Initiation Mechanism of Peeling in Rolling Bearings, and Its Life Estimation Method, NTN TECHNICAL REVIEW, No. 88, (2021) 77.
- 5) N. Hasegawa, T. Fujita, M. Uchidate, M. Abo & H. Kinoshita, Estimation Method of Micropitting Life from *S-N* Curve Established by Residual Stress Measurements and Numerical Contact Analysis, Tribology Online, 14, 3, (2019) 131.
- 6) N. Hasegawa, T. Fujita, M. Uchidate, and M. Abo: Estimation Method of Micropitting Life from *S-N* Curve Established by Residual Stress Measurements and Numerical Contact Analysis, 2nd Report, Proceedings of Tribology Congress 2021 Spring Tokyo, (2021) B22.
- 7) N. Hasegawa, T. Fujita, and M. Uchidate: Validation of Contact Stress Analysis of Rolling Surface under Mixed Lubrication, Proceedings of Tribology Congress 2022 Spring Tokyo, (2022) F11
- 8) K. L. Johnson, J. A. Greenwood & S. Y. Poon, A Simple Theory of Asperity Contact in Elastohydrodynamic Lubrication, Wear, 19, (1972) 91-108.
- 9) R. J. Chittenden, D. Dowson, J. F. Dunn & C. M. Taylor, A Theoretical Analysis of the Isothermal Elastohydrodynamic Lubrication of Concentrated Contacts, II. General Case, With Lubricant Entrainment Along Either Principal Axis of the Hertzian Contact Ellipse or at some Intermediate Angle, Proc. Roy. Soc. Lond., A, 397, (1985) 271-294.
- 10) M. K. Ghosh and R. K. Pandey, Thermal Elastohydrodynamic Lubrication of Heavily Loaded Line Contacts-An Efficient Inlet Zone Analysis, Trans. ASME, J. Tribol., 120-1, (1998) 119-125.
- 11) M. Uchidate, Comparison of Contact Conditions Obtained by Direct Simulation with Statistical Analysis for Normally Distributed Isotropic Surfaces, Surface Topography: Metrology and Properties, 6, 3, (2018) 034003.
- 12) H. Takada and R. Aihara, Life and Reliability of Rolling Bearings, Nikkan Kogyo Shimbun, (2005) 161.
- 13) K. L. Johnson, Contact Mechanics, Cambridge University Press, Cambridge, (1985) 51.
- 14) Rolling Bearing Operating Life Study Group, Influence of Load and Lubricant on the Life of Rolling Bearing, The Tribologist, 61, 9, (2016) 607

Photo of authors



Naoya HASEGAWA

Advanced
Technology R&D
Center



Takumi FUJITA

Product and
Business Strategic
Planning Dept.



Michimasa UCHIDATE

Faculty of Science
and Engineering,
Iwate University



Masayoshi ABO

School of
Engineering,
University of Hyogo

Development of Technical Calculation Systems for Rolling Bearings

Tomomi ISHIKAWA *
Mariko IZUMI *

Hiroyasu HIRUKAWA *
Cedric BURNET **

The performance requirements for rolling bearings are diverse, and the pace of this diversification has accelerated in recent years due to environmental concerns and other factors. The use of Computer-Aided Engineering (CAE) technology is indispensable for NTN to respond quickly to these requirements. Two technical calculation systems developed by NTN to improve the efficiency and sophistication of rolling bearing design will be introduced in this technical review.

1. Introduction

Introduce a wide variety of competitive bearing products to the market that consider market trends and customer needs in a timely manner, it is necessary to improve the sophistication and efficiency of product development work. To this end, NTN is promoting the use of Computer-Aided Engineering (CAE) technology. In October 2018, NTN established the CAE Research and Development Center¹⁾ to accelerate our research and development of CAE technology.

In the past, NTN used both commercial software and the NTN-proprietary CAE system for bearing product development work. There were several challenges for efficient design, such that engineers were required to select and use multiple, unlinked subsystems repeatedly based on their specific applications to derive design values that met the design requirements. Furthermore, even routine Finite Element Method (FEM) analysis had to be carried out by a Computer-Aided Engineering (CAE) specialists.

To improve the efficiency of the entire development process, NTN developed two systems: SharcNT, an integrated technical calculation system for rolling bearings that consolidates existing calculation systems with additional features, and ABICS, an integrated calculation automation system that automates the design work of third-generation (GEN3) hub bearings. This paper describes an overview of these systems.

2. Integrated technical calculation system for rolling bearings

2.1 Background

Rolling bearings are an essential machine element used in mechanical systems. They require a long operating life, low torque, high stiffness, high precision, and other performance capabilities. In recent years, energy saving and decarbonization have

been advanced to achieve carbon neutrality. This has led to greater diversity in rolling bearing design to meet required specifications and performance needs. For example, electrified automobiles and various industrial machines require smaller, lighter bearings with ultra-high speed specifications, while wind power generation requires larger bearings with long operating lives as wind turbines become larger and are used offshore. NTN must adapt to these market trends and customer needs; there are strong demands for highly reliable, high-performance bearing designs and shorter design lead times. The use of CAE technology is essential to meet these demands.

In the initial stage of designing rolling bearings, life and internal bearing load calculations based on theoretical calculations are used as the primary performance evaluation. In recent years, calculation models have become larger, more complex, and more sophisticated. Calculations of entire applications, including power transmission mechanisms, and calculations considering elastic deformation around the bearing are essential.

NTN developed SharcNT (Shaft, Housing and Roller Coupling with NTN Technology), NTN's proprietary integrated technical calculation system for rolling bearings, to enable designers to design reliable, high-performance bearings quickly using CAE technology.

2.2 Global integration of calculation systems

In the past, NTN conducted design studies by utilizing multiple calculation systems according to the design requirements of rolling bearings. However, making full use of multiple systems required a certain level of experience. Therefore, SharcNT was developed by combining the main calculation functions of NTN's conventional calculation systems (Fig. 1) based on a system developed and used by NTN subsidiary company NTN-SNR.

* CAE R&D Center

** NTN-SNR ROULEMENTS Research, Innovation & Development

In addition to the calculation functions required for performance evaluation such as bearing operating life, bearing load, load distribution, contact stress, bearing stiffness, and bearing torque, SharcNT can construct a multi-axis calculation model in which bearings are arranged using an intuitive graphical user interface (GUI) (Fig. 2).

Integration of multiple systems made it possible for designers to perform a wide variety of calculations within a single system and acquire skills and experience more easily.

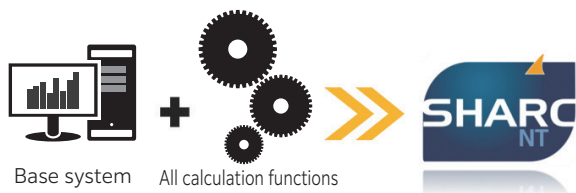


Fig. 1 Integration of calculation systems

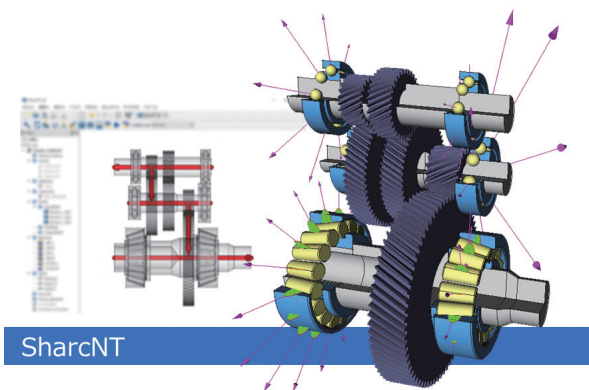


Fig. 2 Integrated technical calculation system SharcNT

2.3 Calculation for entire applications

In recent years, gearbox manufacturers have diversified their products to cater the wider needs of the markets, for example to meet the varying requirements of the automobile market which provides gasoline vehicles, hybrid vehicles, and electric vehicles, ranging from simple structures to multi-stage and complex structures. When bearings used in more complex structures are examined throughout their application, the calculation model becomes complex. It is not only difficult to understand and verify the calculation results, but it is also difficult to do so in a short period of time. Even in the case of complex structures, one must accurately and quickly grasp the bearing characteristics.

To enable complex gearbox construction, SharcNT makes it possible to create a calculation model with many parallel and orthogonal axes to analyze the bearing in detail while taking into account the power flow (power transmission path). In addition, the overall life of the bearing can be determined by setting the duration of time that the bearing spends at each operating condition. In addition, advanced calculations that consider elastic deformation around the bearing, which will be discussed in the next section, can be completed in a short time.

To understand the internal load of the bearing obtained by calculation, it is necessary to confirm how the shaft displaces with deformation due to conditions such as gear load and bearing position. Depending on the structure, it may be extremely difficult to verify the calculation results using only the numerical information shown for each power flow.

Fig. 3 shows an example of a calculation for the gearbox. The calculation model is displayed in a 3D model, and the vector of the internal load and the displacement of the axis on the model can be confirmed visually. In addition, detailed results for each bearing are output as various graphs and numerical data. These improvements make it easier for the user to grasp the characteristics of the calculation conditions.

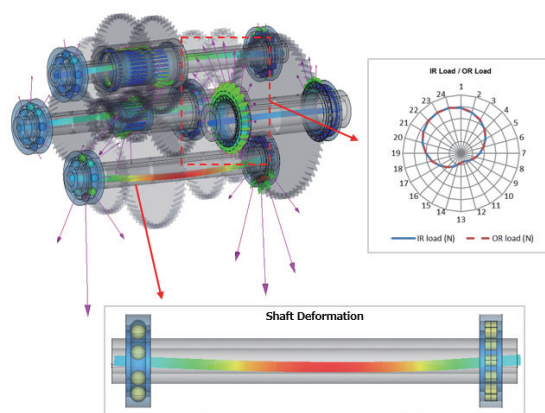


Fig. 3 Calculation for entire applications

2.4 Calculation that considers bearing elastic deformation

Normally, the internal bearing loads are calculated on the assumption that the contact between the rolling element and the raceway surface will cause infinitesimal deformation. However, in some applications, the stiffness of the housing is low (due to thin thickness, aluminum alloy, etc.), and the internal load of the bearing cannot be accurately determined unless the elastic deformation of the outer ring and the housing is considered. In this case, although it is possible to use FEM to perform calculations that consider the elastic deformation of the outer ring and housing, high-precision calculations demand expertise and involve a series of calculations, which takes time. SharcNT has a function²⁾ that can consider elastic deformation of the outer ring and the entire housing as a contracted stiffness matrix (“virtual spring”), which can be combined with the contact calculation between each rolling element and a raceway with relevant degrees of freedom. This function allows calculation that takes elastic deformation of the outer ring and housing into account at higher calculation speeds when compared to FEM.

Calculations can also be performed that consider elastic deformation of the inner ring and shaft using the “virtual spring”. However, the fit between the inner ring and the shaft is usually highly rigid when

compared to the fit between the outer ring and the housing, and it is often sufficient to consider only the deflection of the shaft. In such cases, the calculation time can be shortened by modeling the shaft with the beam element³⁾.

3. Integrated calculation automation system for hub bearings

3.1 Background to development

Hub bearings are used in automobile undercarriages to support the rotation of the vehicle's wheels. Since the late 1970s, hub bearings have evolved into unit products incorporating peripheral components.⁴⁾ This was done in response to market demands for easier bearing assembly into vehicles, bearing downsizing, reducing bearing weight, and higher bearing performance (load-carrying capacity, low-torque performance, resistance against muddy water, stiffness, strength, etc.). Currently, the predominant hub bearing is the 3-generation hub bearing called GEN3 shown in **Fig. 4**.

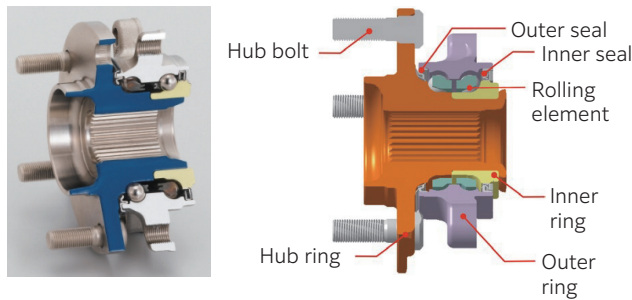


Fig. 4 GEN3 hub bearing

In the design of unitized GEN3 hub bearings, automobile manufacturers require a balance between long bearing operating life and high stiffness on the one hand and compactness and light weight on the other. While a larger bearing size is required to reduce contact stress and increase stiffness to improve bearing life and steering stability, smaller bearing size and lighter weight is optimal for vehicle fuel efficiency. In addition to these bearing design optimization tasks, CAD and FEM analyses are also required in the design process. All of these tasks are performed by human workers and required a long time to complete.

To solve these problems, **NTN** developed an integrated calculation automation system Axle Bearing Integrated Calculation System (ABICS) for hub bearings that automates each area of design work and shortens the design and lead time.

3.2 System overview

To automate the various tasks required for the design study of hub bearings, **NTN** developed the ABICS (**Fig. 5**), which has the following four primary functions.

- Search function for optimal bearing specifications
- Automatic creation of 3D shape models
- Automatic execution of FEM analysis
- Data management

The use of this system enables designers to perform tasks that were previously performed by separate people in charge of each task. This further reduces design and lead time through automation. Details of each function are described in the following sections.

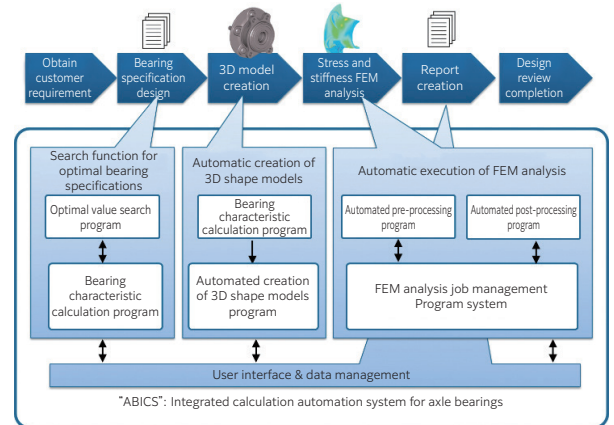


Fig. 5 ABICS system overview

3.3 Search function for optimal bearing specifications

In the past, when determining the bearing characteristics of a hub bearing, the **NTN** designer would repeatedly change each parameter and calculate the characteristics until the required characteristics (life, internal mass (mass within a certain area around the rolling element), internal stiffness, torque, etc.) had been met (**Fig. 6** left). Multiple calculation tools for each characteristic were used for the characteristic calculation. The human work therefore required time for both the search for optimal results and the calculations.

In ABICS, **NTN** has created a bearing characteristic calculation program that combines these calculation tools. An optimal value search function (**Fig. 6**, right) has been developed to automatically select desired values for specifications.

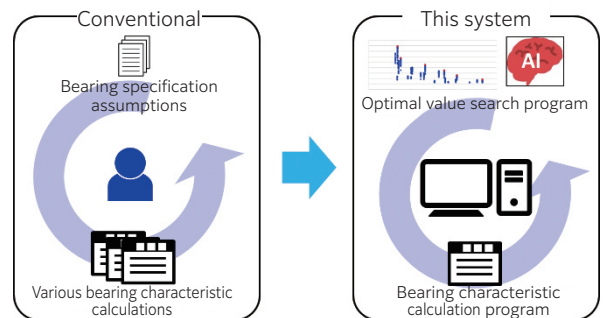


Fig. 6 Optimization of bearing specifications

The optimal value search program employs a genetic algorithm (GA), which is classified as AI. For the search, the desired bearing characteristics to be optimized are set as the objective function and the design parameters that affect the characteristics of the objective function are set as explanatory variables. Under these conditions, the explanatory variables selected by the GA are sent from the optimal

value search program to the bearing characteristic calculation program, where bearing characteristics are calculated. The characteristic values are returned to the optimal value search program, and the GA selects new explanatory variables. This iterative process results in optimal values.

An example of an optimal value search is shown in **Fig. 7**. The objective function is set to the conflicting properties of life and internal mass, and the explanatory variables are the three design parameters related to these two properties. **Fig. 7** shows the results of the search. The Pareto solution for the bearing life relative to the mass (marked in red) determines the candidates of optimal values. Based on the results, the designer selects the value that meets the customer's required characteristics. In this example, about 34 000 calculations are required to find the optimal value by exhaustive search, where the search for the optimal value is completed in about 300 calculations (marked in blue) with GA. In addition to the computational cost, automation of the search also reduced the work time required of personnel.

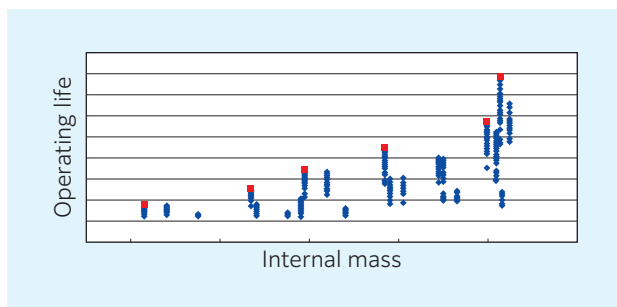


Fig. 7 Example of optimal value search

3.4 Automatic creation of 3D shape models

In the past, a CAD specialist created the 3D shape model required for FEM analysis and drawing (**Fig. 8**, top) based on previously-determined bearing specifications. Since CAD work was done manually by dedicated personnel, model creation was time consuming. In addition, there was time spent waiting for preliminary meetings with designers and for the completion of work in progress.

In the ABICS, an automatic 3D shape model creation program has been developed to automate this model creation process (**Fig. 8**, bottom). The program has a variety of shape templates and automatically creates a 3D shape model by automatically inputting dimensions derived from bearing characteristics obtained from the optimal value search function and the bearing characteristic calculation program described in the previous section. In the case of shapes for which it is difficult to create templates, the program automatically creates a similar shape and then allows manual modification.

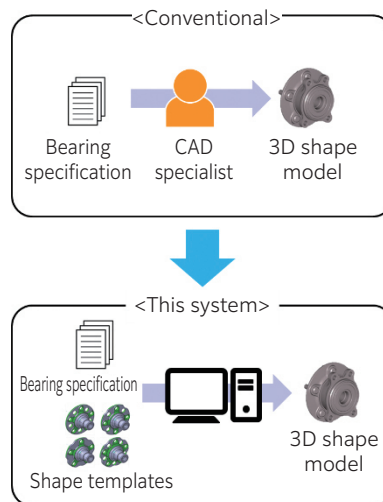


Fig. 8 Creation of 3D shape model

3.5 Automatic execution of FEM analysis

In the past, based on a previously-created 3D shape model, a CAE specialist would perform the pre-processing, calculation execution, and post-processing required for FEM analysis stress and stiffness characterization⁵⁾ (**Fig. 9**, top). As with the other tasks described above, time was required to complete these tasks due to the skill level of the specialist, prior discussions with the design engineer, and waiting time before starting the work.

A program and system were created to automate these tasks, and an automatic FEM analysis execution function (**Fig. 9**, bottom) was developed. Details of each program are shown below.

- Automated pre-processing program
Automatically create a mesh for each part of the 3D shape model to be analyzed, combine the peripheral components necessary for analysis, and set the boundary conditions.
- Automated post-processing program
The system automatically obtains characteristic values of stress and stiffness from calculation results, obtains contour plots, checks calculation logs, etc.
- FEM analysis job management program / system
Computers to execute each of the above programs and FEM calculation jobs are automatically assigned according to the computer utilization status. **Fig. 10** shows this job management system. Jobs are distributed from the ABICS server to the job management computer (the computer executing this program) based on the input information of the user computer. From the job management computer, jobs are allocated according to the usage status of multiple computers prepared for pre-processing, calculation execution, and post-processing. This system reduces the waiting time for jobs and improves the availability of computers and software licenses used for FEM analysis.

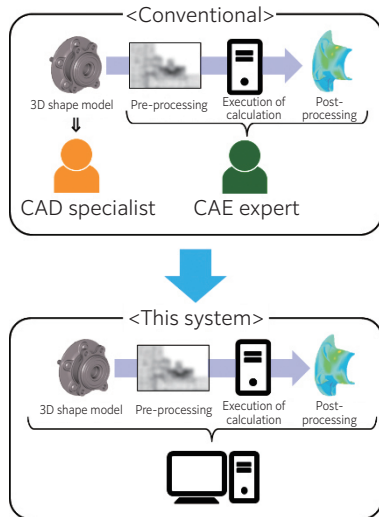


Fig. 9 FEM analysis work

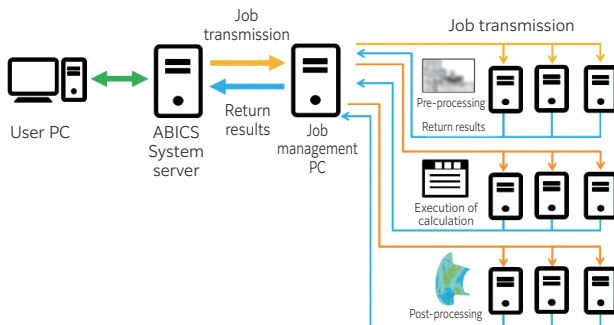


Fig. 10 FEM analysis job management system

3.6 Data management function

All ABICS usage information (input/output results, etc.) is stored and managed in a database. Information designed with ABICS can thus be capitalized on and used effectively. The search function makes it easy to view past design results, while the input data used in calculations can be reused, enabling efficient redesign when improving products.

In addition, design reports can be automatically generated based on the stored input/output results, reducing the time spent by designers and shortening lead times.

4. Conclusion

This paper introduces the integrated technical calculation system SharcNT, which is used to evaluate the performance of rolling bearings, and the integrated calculation automation system ABICS, which automates the design work of GEN3 hub bearings.

Going forward, NTN will continue to research, develop, and utilize CAE technology to further enhance the sophistication and efficiency of product development operations. As we do so, we will build a structure that will enable us to quickly bring to market the bearings that the market demands.

References

- 1) An Introduction to the CAE R&D Center, NTN TECHNICAL REVIEW, No. 87, (2019) Back cover.
- 2) Rolling Bearing Theory and Practice Guidebook (Cat. No. 9600/J), NTN, (2022) 254-255.
- 3) Rolling Bearing Theory and Practice Guidebook (Cat. No. 9600/J), NTN, (2022) 253.
- 4) Makoto Seki, History of Development of Axle Bearing Aiming at Low Fuel Consumption, NTN TECHNICAL REVIEW, No. 87, (2019) 55-58.
- 5) A. Imoo, FEM Analysis of Hub Bearing, NTN TECHNICAL REVIEW, No.70, (2002) 70-73.

Photo of authors



Tomomi ISHIKAWA
CAE R&D Center



Hiroyasu HIRUKAWA
CAE R&D Center



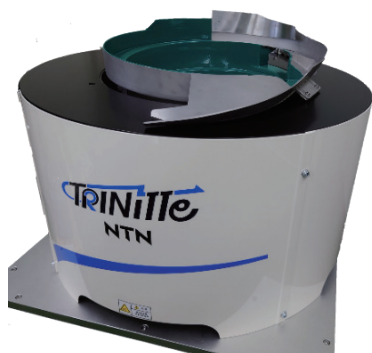
Mariko IZUMI
CAE R&D Center



Cedric BURNET
NTN-SNR
ROULEMENTS
Research, Innovation
& Development

Development of Feeder “TRINITTE” for Picking Robots

Shuhei MATSUI*



NTN has developed a new parts feeder (TRINITTE) that combines a conventional parts feeder and a rotating disk and is developing it into a field that transcends the field of the conventional parts feeder. In this article, I will explain the outline, features and specifications of TRINITTE.

1. Introduction

There has been a rapid expansion in automation and manpower reduction globally using industrial robots with the aim of increasing productivity at the manufacturing site. This situation has occurred because of the diversification of consumer needs, and the shift from mass production to “high-mix low-volume production”. For parts feeders, there is a need to reduce production changeover time due to the support for a wide variety of workpieces, and a need to decrease brief stoppages in production due to workpiece jamming (improve availability factor).

For the conventional parts feeder and picking robot combination, the workpieces are selected and sorted in a bowl feeder were stored in straight feeders, a delivery mechanism used to deliver each workpiece, and then the workpieces were picked up by a picking robot. This setup had issues, which were that only certain workpieces could be handled, many working components were required, and workpieces became jammed when sorting or storing them inside feeders.

However, parts supply devices are now being sold for robots on the premise that sensing technology is used in combination with picking robots. Parts supply devices for robots use 3-axis vibration technology to change the posture of workpieces in the picking area and to separate workpieces if they are too close to each other, and a camera is used to detect the workpiece position so that the picking robot can pick up the workpiece. The issue with this setup is that if a workpiece with a pickable posture is not present in the picking area, the machine operates to change the posture, so the robot stops during this time.

NTN has developed TRINITTE to solve these issues.

2. Overview

Fig. 1 shows the system configuration. TRINITTE comprises a motor-driven rotating disk arranged on the outer circumference of a conventional bowl feeder, and an encoder attached to the rotating disk. A camera and picking robot are connected to the system so that the picking robot can import pulse signals output from TRINITTE and image processing signals obtained from the camera.

The following explains the full sequence of the picking system that combines TRINITTE with a robot.

Workpieces deposited in the bowl are sorted in a single-row single-layer arrangement by the bowl feeder, then supplied onto the rotating disk. The workpieces supplied onto the rotating disk are picked up without stopping the rotating disk using a robot arc conveyor tracking function^{*1}, then supplied to the next process. Any workpieces that could not be picked up are also collected inside the bowl feeder via a workpiece collection opening located on the rotating disk. These recovered workpieces are once again supplied via the bowl feeder onto the rotating disk.

*1 Vision sensors are used to detect the position of a workpiece at any position on the rotating disk. This information and information from the encoder is used by the robot so that it can follow the rotating disk and pick up the workpiece from the disk.

* NTN Technical Service Corp., Precision Equipment Division

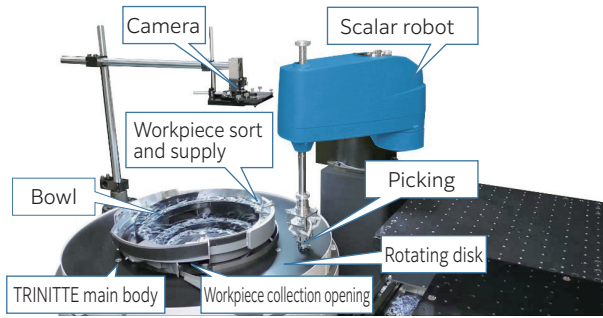


Fig. 1 System configuration

3. Features

TRINITTE has the following features.

(1) Saves space

TRINITTE is different to conventional parts feeders and uses a rotating disk to supply workpieces, so it does not require a straight feeder, a chute or a workpiece separating mechanism. Therefore, as shown in **Fig. 2**, the number of working components can be reduced to cut the footprint by approximately 30 %.

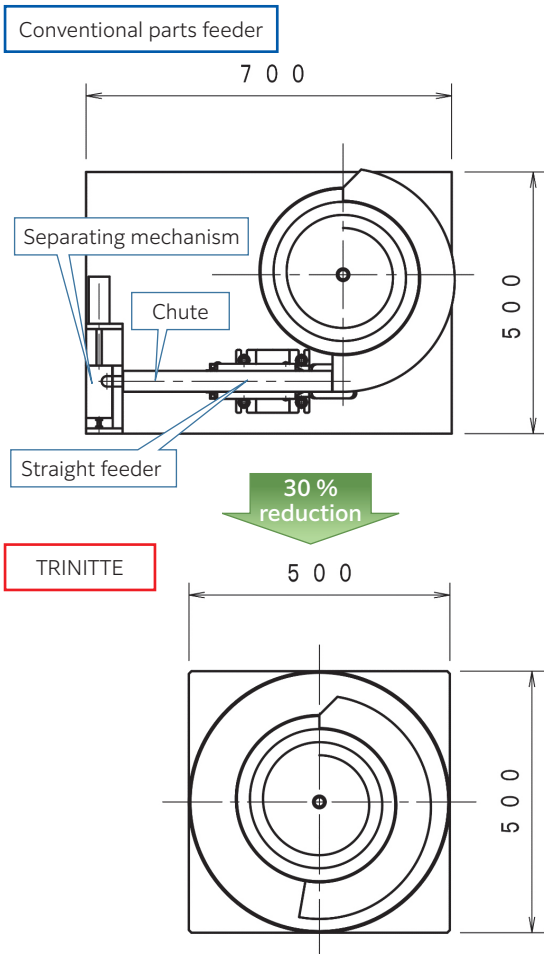
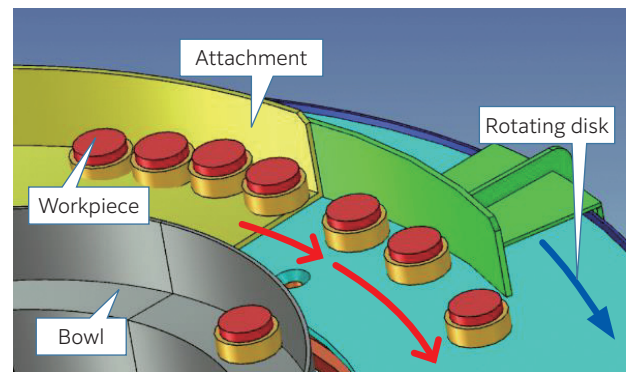


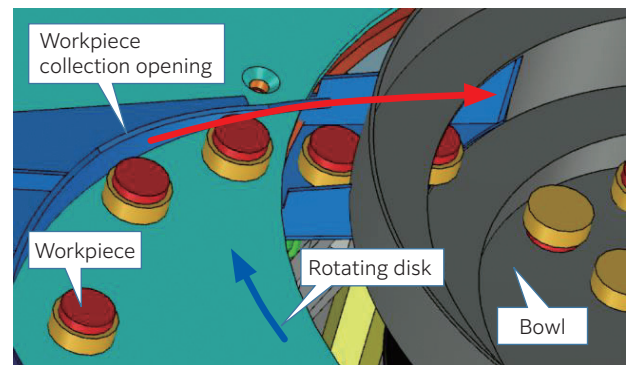
Fig.2 Comparison of size between conventional parts feeder and TRINITTE

In addition to supplying workpieces to the robot using the rotating disk, this product has a simple and compact structure that can also separate workpieces and recover unpicked workpieces, enabling it to perform three tasks in a single unit.

Increasing the rotational speed of the rotating disk more than the supply speed of the bowl feeder enables workpieces that are ejected in a joined manner to be separated, making it easier for the robot to pick up. Workpieces that could not be picked up by the robot are also collected inside the bowl so that they can be supplied once again onto the rotating disk (**Fig. 3**).



(a) Workpiece separation



(b) Workpiece recovery

Fig. 3 Workpiece separation and recovery

(2) Reduces brief stoppages

Conventional parts feeders use an attachment with a complex structure installed on the bowl feeder to arrange the posture of workpieces in the bowl feeder. This complex structure makes it easy for workpieces to become jammed when they are caught on the attachment, etc.

TRINITTE links the vision system and picking robot together so that the attachment installed on the bowl feeder has only a simple structure to perform tasks such as aligning the orientation of workpieces. Since the attachment can be simplified, continuous supply of stable parts is achieved.

(3) Reduces robot wait time

TRINITTE ensures that workpieces are aligned so that their orientation matches in a single-row

Development of Feeder “TRINITTE” for Picking Robots

single-layer arrangement and enables a continuous supply of workpieces at the picking area of the picking robot. Therefore, workpieces on the rotating disk can always be picked up and the robot can continue picking up workpieces. Furthermore, as mentioned previously, the use of an arc conveyor tracking function on the picking robot enables constant operation without stopping the rotating disk, so this increases the equipment availability factor.

(4) Improves versatility

TRINITTE can simplify the attachment installed on the bowl feeder, which makes it possible to support a wide variety of workpieces (**Fig. 4**) by making simple adjustments only, without changing the bowl feeder. This can reduce the time required for production changeover.

Additionally, workpieces that could not be stored and could not be supported with conventional parts feeders, or irregular-shaped workpieces can now be supported, demonstrating that this is a device with high versatility.

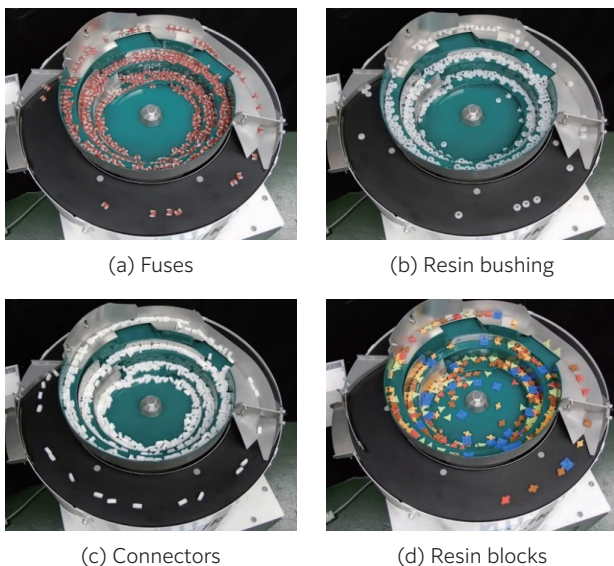


Fig. 4 A wide variety of workpieces are supported using the same bowl

Photo of author



Shuhei MATSUI

NTN Technical
Service Corp.,
Precision Equipment
Division

4. Specifications

TRINITTE has a lineup of 3 distinct types of bowl sizes according to the size of the workpiece. **Table 1** shows the main specifications.

Table 1 Specifications

Part number	K-UP301	K-UP302	K-UP303	
Dimensions	Length 350 mm Width 350 mm Height 320 mm	Length 500 mm Width 500 mm Height 370 mm	Length 700 mm Width 700 mm Height 510 mm	
Bowl diameter	φ190 mm	φ320 mm	φ420 mm	
Power supply voltage	AC200 V 50/60 Hz			
Mass	38 kg	85 kg	200 kg	
Rotating disk	Outer diameter	φ344 mm	φ494 mm	φ694 mm
	Rotational count	1.3 to 6.5 min ⁻¹		
	Rotational speed	0.05 to 0.20 m/s		0.05 to 0.30 m/s
Part number of controller for bowl feeder (manufactured by NTN)	K-ECL25		K-ECH45	
Part number of controller for motor (Manufactured by Oriental Motor)	DSCD15JC			
Encoder part number (Manufactured by Omron)	E6B2-CWZ1X 1000P/RO.5M			

5. Summary

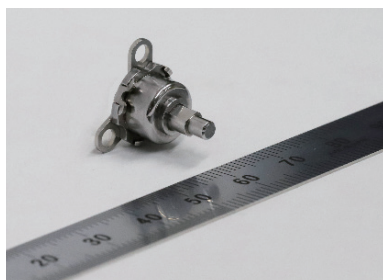
This paper explained the outline, features, and specifications of TRINITTE.

In the future, we will investigate new applications of use, such as special uses that match user requirements and the development of new sizes.

The Precision Equipment Division will work on supporting the changing situation in which workpieces are becoming more diverse, such as their increasing miniaturization and complexity, and achieve stable and continuous operation for the supply of parts so that we can continue to contribute towards the automation of production equipment using robots.

Product Introduction of Compact Torque Diode (TDL8)

Masayuki OHARA *



NTN manufactures a “torque diode” that transmits rotation torque from the input shaft to the output shaft. But does not transmit the torque from the output shaft, which is the reverse input, to the input shaft. This article introduces the technology of the compact and lightweight torque diode “TDL8” which has an outer ring diameter of 1/3 (10 mm) and a weight of 1/14 (5 g) as compared with conventional product “TDL28”.

1. Introduction

NTN produces a torque diode used in reverse input prevention mechanisms and drop prevention mechanisms. This product is used between two power transmission shafts such as a motor and transmission. This is a reverse input blocking clutch that transmits the running torque from the input shaft to the output shaft and locks the running torque from the output shaft, preventing it from being transmitted to the input shaft. Due to this ability, it has been given the name “torque + diode” from the rectifying action of the torque. Since it does not require electric power when compared with an electromagnetic brake, this enables energy to be saved at mounted machinery. It is also unaffected by power outages which is an excellent safety feature. The torque diode (hereafter, TDL) is introduced below (Fig. 1).

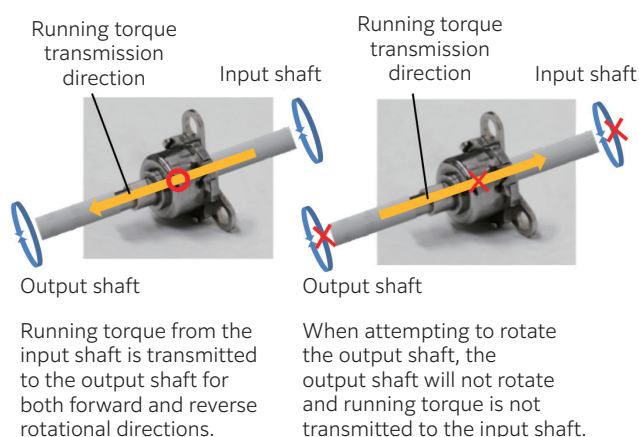


Fig. 1 TDL function

2. Torque diode structure and features

TDL comprises an outer ring, inner ring, cage, rollers, spring and side plate, and is used with an input shaft prepared by the user (Fig. 2). The running torque of the input shaft is transmitted to the output shaft integrated with the inner ring (hereafter, output shaft). The rollers and spring lock the output shaft when the input shaft is not rotating to block reverse input.

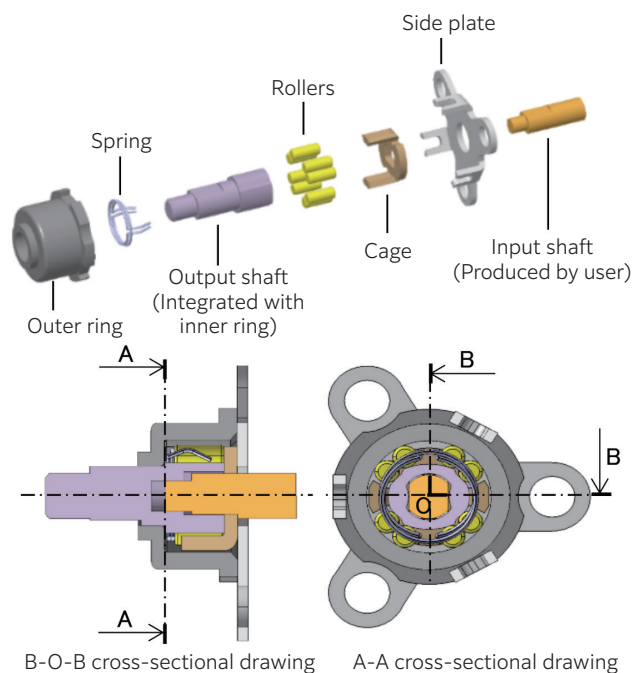


Fig. 2 TDL structure

* Product Design Dept., Industrial Business Headquarters

3. Operating principle

This section explains the operating principle of how TDL transmits running torque from the input shaft to the output shaft. It also uses a structural drawing of a conventional product "TDL28" to show how the rollers lock the output shaft (Fig. 3).

When the input shaft is motionless and not rotating, there is clearance between the input shaft and output shaft. The rollers are making contact with the outer ring bore diameter and the output shaft so there is no rotation (Fig. 3 (a)).

When the input shaft rotates from a motionless state, 1) the cage connected to the input shaft pushes the rollers to release the lock. Then 2) the input shaft and output shaft make contact, and 3) the output shaft rotates (Fig. 3 (b)).

When attempting to rotate from the output shaft, the spring pushes two rollers against a wedge formed by the outer ring bore diameter and output shaft cam surface. This locks rotation in both the forward and reverse directions and prevents the shaft from rotating (Fig. 3 (c)).

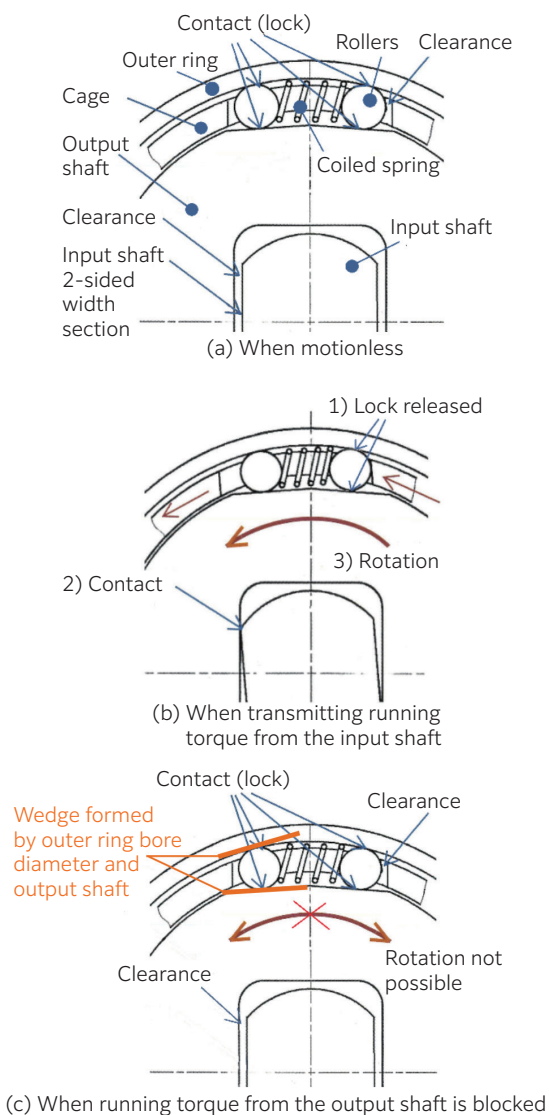


Fig. 3 TDL operating principle

4. TDL8 structure and features

Fig. 4 shows the structure of the compact and lightweight torque diode "TDL8". "TDL8" uses a proprietary shaped C-type spring that enables it to save more space than "TDL28", a conventional product that uses a coiled spring. This enables smaller rollers to be used because many rollers can be inserted. This achieves a 10 mm outer ring outer diameter that is 1/3 the size and a 5 g weight that is 1/14 that of the conventional product "TDL28", while still maintaining the allowable load torque.

The structure and features of the compact and lightweight torque diode "TDL8" are listed below against the conventional product "TDL28".

1. Changed from a coiled spring to a proprietary shaped C-type spring.
2. Many rollers are inserted, enabling smaller roller sizes, which reduces the overall size and weight of TDL.

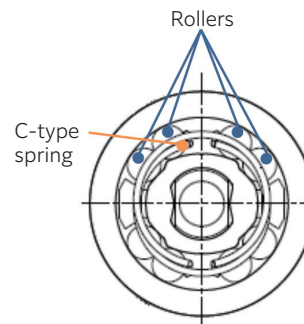


Fig. 4 TDL8 structure

5. Example of application

TDL is used in as applications like reverse input prevention mechanisms. This will prevent unintended rotation from the output shaft and drop prevention mechanisms (Fig. 5) for the purpose of maintaining safety when stopping rotation from the input shaft at the time of a power outage, etc.

It is also installed in automobile seat lifter mechanisms (Fig. 6). These systems are used to lift or lower an automobile seat surface by operating a lever when adjusting the height of the seat. It will also allow a user to maintain the height of the seat when not operating the lever.

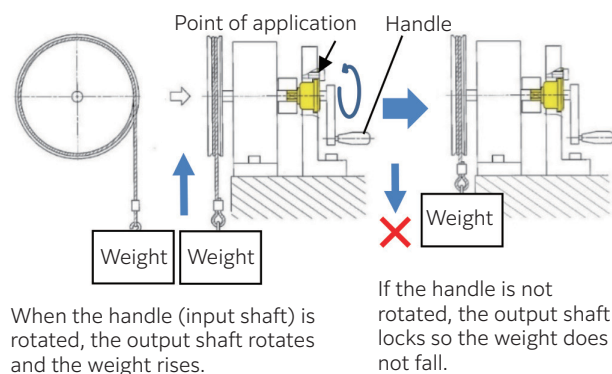
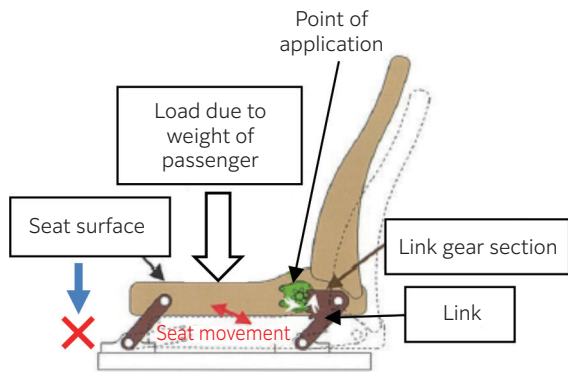


Fig. 5 Example of application in drop prevention mechanism



The torque diode prevents the link from falling over to maintain the seat position.

Fig. 6 Example of application on automobile seat

6. Summary

The compact and lightweight torque diode “TDL8” achieves a significantly smaller and lighter product in comparison with the conventional product “TDL28”, and is a product that contributes towards making mounted machinery smaller, lighter and require less energy.

In the future, **NTN** will continue to aim to make this product more compact, lightweight and provide higher efficiency, and also achieve a sustainable “NAMERAKA Society” by saving energy.

References

- 1) NTN Catalog Clutch Related Products CAT. No.6405/J.

Photo of author



Masayuki OHARA

Product Design
Dept.,
Industrial Business
Headquarters

Application Examples of the Wrist Joint Module “i-WRIST™”



Yuzuru TANAKA*



NTN developed an angle control equipment system applying a parallel link mechanism, a constant velocity joint¹⁾⁻⁷⁾. We started mass production under the product name of the “i-WRIST™” in August 2018⁸⁾. We have improved its functions to meet the needs of customers and have launched it on the market with the target of automating and reducing manual work⁹⁾. The features of the i-WRIST™ like “high-speed angle control” are useful in the appearance inspection process of complex-shaped parts. We would like to introduce application examples that show such advantageous features of the i-WRIST™.

1. Introduction

Due to the reduction in the working population, aging of skilled workers, and rise in personnel expenses, the range of application for robots has spread from work mostly involving tasks that placed a heavy load on operators and extremely dangerous work, such as transporting heavy objects and welding, to more detailed manual labor work. Among these more detailed jobs, appearance inspection still relies heavily on manual labor, and there is an increased demand to automate this type of work. However, conventional robots cannot achieve the speed of visual checks performed by humans, and the automation of appearance inspection for complex shaped parts is particularly lagging.

NTN has proposed the application of Wrist Joint Module “i-WRIST™” to automate tasks handled by humans. i-WRIST™ has received high praise for its strength in “high-speed angle control”, and examples of its use in projects to automate visual inspection have increased.

2. i-WRIST™ overview

i-WRIST™ is a robotic module product that achieves smooth movement like a human wrist. **Fig. 1** shows a schematic drawing of the i-WRIST™ unit. The i-WRIST™ unit comprises a parallel link mechanism and drive mechanism. The drive mechanism determines angle orientation in 2degrees of freedom (bending angle and swing angle) at the parallel link mechanism for high-speed and high precision positioning within hemispherical areas. Furthermore, cables can be passed through the internal space of the parallel link mechanism, so the cables do not become twisted even when swing operation is repeated in the same direction.

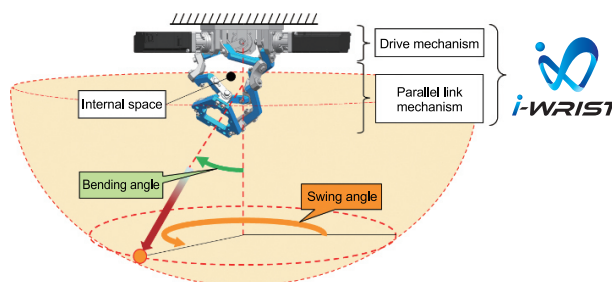


Fig. 1 Schematic drawing of i-WRIST™ unit

3. Features of i-WRIST™ in use at the production site

The use of robots at the production site poses problems for some managers who give comments such as “we installed robots but are not satisfied with the cycle time”, “robots are difficult to operate and hard to master” and “we have no space to install robots.” To solve these problems, NTN proposes a configuration⁹⁾ that combines i-WRIST™ with a linear actuator or rotation actuator. The features of this are shown below.

(1) Fast motion

The moment of inertia at the entire movable section is small, and the robot can move to the target orientation along the shortest route. Therefore, this setup can be particularly effective for work that requires fine movement, something that conventional robots do not do well.

(2) Easy of use

Even operators who do not have expert knowledge of robot language can easily operate this setup using a dedicated console.

* Robotics & Sensing Engineering Dept., Industrial Business Headquarters

(3) No singularity point

There is no need to create an operation program to avoid the singularity point, as is the case with articulated robots.

(4) Offline teaching

NTN provides a PC-based teaching tool to specify points on a 3D model and configure operating patterns⁹⁾.

(5) Space-saving

In combination with a linear actuator or rotation actuator, the machine can be compactly configured, which allows this setup to be installed in a space where an operator worked⁹⁾.

Fig. 2 shows examples of application for i-WRIST™. Among such applications, i-WRIST™ is often used in appearance inspection machines equipped with cameras and lighting. An example of this is shown below.

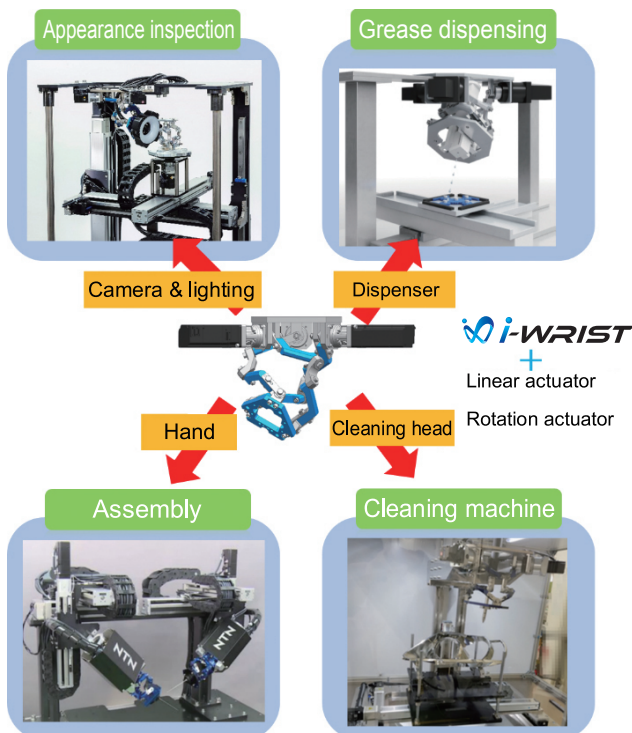


Fig. 2 Example of applications for i-WRIST™

4. Example of applications for i-WRIST™ in appearance inspection

During appearance inspection of workpieces that have a 3D shape or complex shape, such as casting parts and resin molded parts, humans can quickly and skillfully visually inspect multiple locations of the workpiece from various angles while changing how lighting is shone onto the workpiece and the angle of the workpiece. This type of high-speed inspection is exceedingly difficult to automate. However, many examples exist in which this difficulty has been

resolved using the features of i-WRIST™. For example, as shown in **Fig. 3**, inspection processes that have so far required the use of two robots can now be configured using a single i-WRIST™ unit, and this has been evaluated as achieving the required cycle time and has been adopted for use. Below introduces more specific examples of the application in appearance inspection.

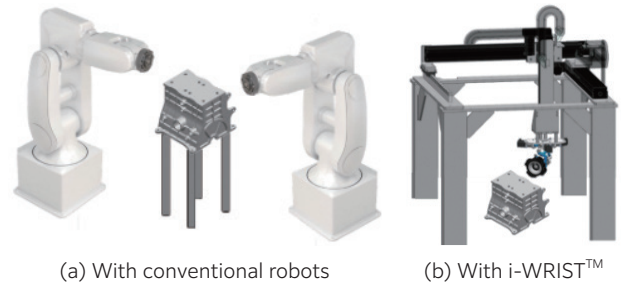


Fig. 3 Example of application at the production site

4.1 Example of application for casting parts

During appearance inspection of small casting parts, such as for an automotive compressor as shown in **Fig. 4 (a)**, appearance inspection of 0.2 seconds per single point -- about 2.5 times the speed of conventional robots -- was achieved. **Fig. 5** shows an example of the configuration for this system. This configuration involves mounting a camera onto i-WRIST™ and controlling the angle, while a rotation actuator and linear actuators are used to position the workpiece. The rotation actuator rotates the workpiece while images are captured from multiple directions. This enables high-speed inspection for defects such as surface scratches, dents, and residual debris inside bore holes. This configuration can also make the machine more compact.

During appearance inspection of large casting parts such as for an engine block or transmission case as shown in **Fig. 4 (b)**, appearance inspection of 0.3 seconds per single point was achieved. **Fig. 6** shows an example of the configuration for this system. This configuration involves mounting a camera onto i-WRIST™ installed at an incline and using a rotation actuator and linear actuators to position the workpiece. Installing i-WRIST™ at an incline enables images to be taken of the workpiece while looking up at the workpiece from below. This enables high-speed inspection for defects such as scratches on uneven surfaces at the side of the workpiece, dents, and residual debris inside bore holes.

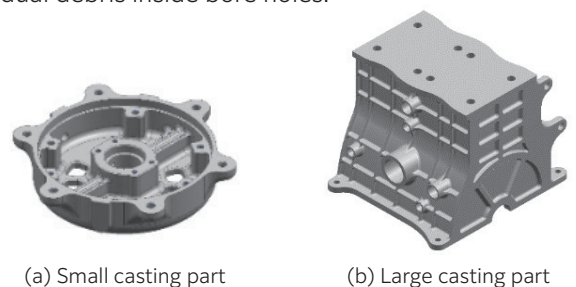


Fig. 4 Casting parts

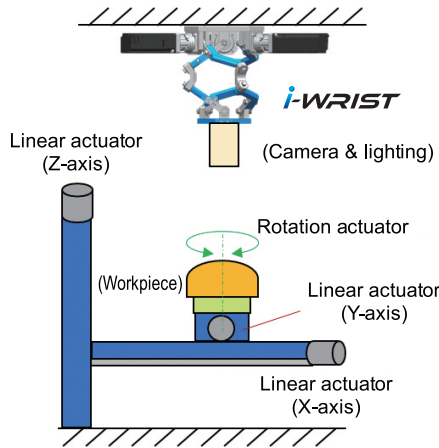


Fig. 5 System configuration example (1)

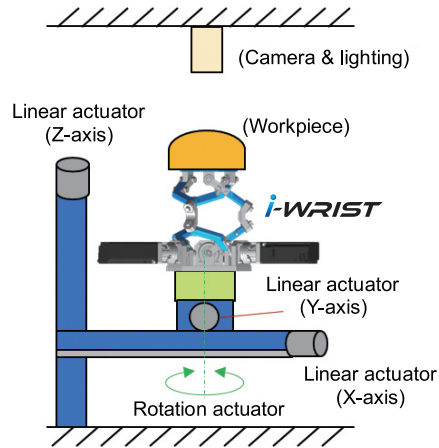


Fig. 8 System configuration example (3)

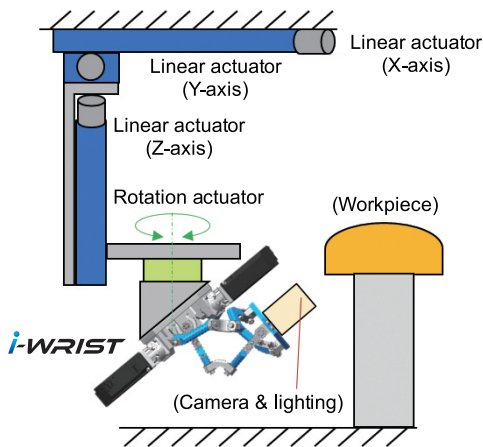


Fig. 6 System configuration example (2)

4.2 Example of application for automotive resin molded parts

During appearance inspection of automotive resin molded parts integrated with various sensors as shown in Fig. 7, visual inspection of 0.3 seconds per single point was achieved. Fig. 8 shows an example of the configuration for this system. This configuration involves fixing the camera and lighting while a chuck mounted onto i-WRIST™ holds the workpiece. The workpiece is positioned using i-WRIST™, a linear actuator and a rotation actuator. The use of a rotation actuator achieves a compact system configuration that can minutely change the positioning of the workpiece while rotating it for a single revolution at the same position. This configuration enables the system to inspect the appearance of surface (for scratches, bubbles and burrs) and check whether any connector pins and sensor parts are missing.



Fig. 7 Resin molded part

4.3 Example of application for automotive electronic control unit

With the electronification of automobiles, examples of appearance inspection have increased for automotive electronic control units, such as gear boxes integrated with electronic circuit boards as shown in Fig. 9. This type of unit has sections where images are difficult to capture, such as the back of circuit boards, so a person visually inspects blind spots that are difficult to see while changing the angle. The system configuration shown in Fig. 6 enables images to be captured of electronic control units, including the back of circuit boards from multiple directions. The illumination angle can be finely adjusted onto the circuit board using i-WRIST™ so that light shines onto blind spots. This enables inspection of blind spots at the back of the circuit board (the soldered surface) as shown in Fig. 10. In this example an inspection speed of 0.3 seconds per single point was achieved to check for missing parts on electronic circuit boards, and for appearance defects on the resin surface such as scratches, dents, and burrs.

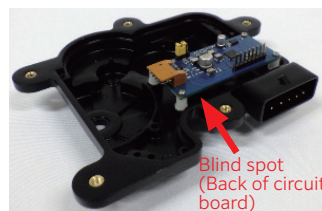


Fig. 9 Electronic control unit



Fig. 10 Example of captured image (back of circuit board)

4.4 Through-hole and screw-hole internal inspection

There is also a high demand for automating inspection of burrs and residual debris inside through-holes and screw-holes. Using the pivot movement of the i-WRIST™ enables the angle to be changed while maintaining working distance from the camera to the reference point by linked i-WRIST™ and linear actuators. Using this action enables images to be captured as shown in Fig. 11. This can make it easy to inspect the entire inside diameter surface of a hole.

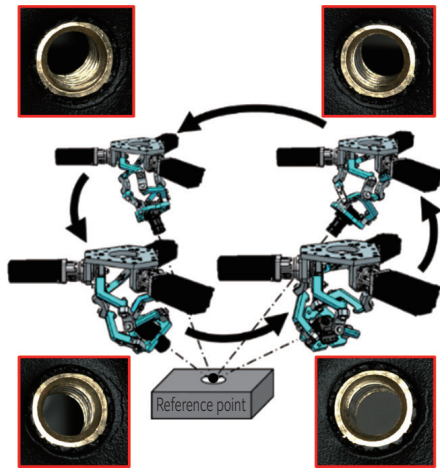


Fig. 11 Pivot movement

5. Efforts to increase the range of application for i-WRIST™

Amid the launch of i-WRIST™ to the market, we received praise for i-WRIST™ high speed operation, and its excellent ability to work without singularity points, which is a challenge for conventional robots. At the same time, we received many requests for i-WRIST™ to handle similar payloads as conventional robots and have investigated methods to achieve this.

Until now, maximum load capacity was restricted to 1 kg so that i-WRIST™ could be used at high speed. However, we developed a new grade that increases the maximum payload to 3 kg by establishing a mode that optimizes the control method to match the load capacity. As a result, it is now possible to mount large-scale lighting and multiple lighting onto i-WRIST™ for appearance inspection. Using large-scale lighting enables images to be captured over a large area in a single shot, and this reduces the number of inspection points, which leads to a shorter cycle time. Furthermore, using multiple lighting increases the variation of how lighting can be shone onto a work piece being inspected. This provides support for work pieces that are difficult to inspect.

In addition to appearance inspection applications, i-WRIST™ can be applied to such as the deburring process in which the machining load acts on the end effector, and the welding process in which the end effector weight is large.

6. Summary

This paper introduced examples of appearance inspection using high-speed angle control, which is a strength of i-WRIST™. Using i-WRIST™ can replace sight checks that are difficult to automate and achieve a cycle time that cannot otherwise be achieved with conventional robots.

In the future, there will be greater demand for automating complex work performed by humans, such as deburring and assembly to accompany the decrease in the working population. i-WRIST™ introduced here is a robotic module product that can achieve automation of manual work at a work speed and smooth movement like human hands. NTN will continue to improve performance

and create examples of applications to contribute to automating and optimizing the production site and stabilize quality.

References

- 1) Keisuke Sone, Hiroshi Isobe, Koji Yamada, Wide Angle Active Link Equipment, NTN TECHNICAL REVIEW, No. 71, (2003) 70-73.
- 2) Hiroshi Isobe, Yukihiko Nishio, Parallel Link High Speed Angle Control Equipment (PHACE), NTN TECHNICAL REVIEW, No. 80, (2012) 42-47.
- 3) Hiroshi Isobe, Yukihiko Nishio, Keisuke Sone, Hiroyuki Yamada, Yoshio Fujikawa, Parallel Link High Speed Angle Control Equipment, Proceedings of the Japan Society for Precision Engineering Spring Meeting in 2013, (2013) 809- 810.
- 4) Hiroshi Isobe, Yukihiko Nishio, Seigo Sakata, Naoya Konagai, Hiroyuki Yamada, Yoshio Fujikawa, Parallel Link High Speed Angle Control Equipment - Implementation on Grease Application Equipment -, Proceedings of the Japan Society for Precision Engineering Spring Meeting in 2014, (2014) 1087-1088.
- 5) Naoya Konagai, Hiroshi Isobe, Seigo Sakata, Kenzou Nose, Hiroyuki Yamada, Yoshio Fujikawa, Parallel Link High Speed Angle Control Equipment, Proceedings of the Japan Society for Precision Engineering Spring Meeting in 2015, (2015) 605-606.
- 6) Kenzou Nose, Hiroshi Isobe, Seigo Sakata, Naoki Marui, Naoya Konagai, Parallel Link High Speed Angle Control Equipment - Enhancement of Performance by Improvement, Proceedings of the Japan Society for Precision Engineering Spring Meeting in 2016, (2016) 483-484.
- 7) Kenzou Nose, Hiroshi Isobe, Seigo Sakata, Speeding Up of Parallel Link Angle Control Equipment, NTN TECHNICAL REVIEW, No. 84, (2016) 96-101.
- 8) Keisuke Kazuno, Hiroshi Isobe, Jun Midoumae, Yuki Shimura, Masayuki Ohara, Development of "i-WRIST™" Wrist Joint Module, NTN TECHNICAL REVIEW, No. 86, (2018) 22-27.
- 9) Keisuke Kazuno, Hiroshi Isobe, Masaki Kagami, Jun Midoumae, Yuki Shimura, Seigo Sakata, Yukihiko Nishio, Naoki Marui, Application Examples and Function Improvements of the Wrist Joint Module "i-WRIST™", NTN TECHNICAL REVIEW, No.88, (2020) 105-110.

Photo of author



Yuzuru TANAKA

Robotics & Sensing
Engineering Dept.,
Industrial Business
Headquarters

Low Friction HUB Bearing III

Makoto SEKI

1. Introduction

The “Low Friction HUB Bearing III”¹⁾, which reduces rotational friction while driving by 62 % compared with conventional products, received the 2020 “CHO” MONODZUKURI Innovative Parts and Components Award, Mobility Components Award sponsored by MONODZUKURI. Nippon. Conference and Nikkan Kogyo Shimbun, Ltd.

NTN developed bearing internal grease in pursuit of low friction, and combined with the latest low friction seals, was able to reduce rotational friction by 62 % when compared with conventional products²⁾. Using this product on the wheels at both sides of a vehicle is expected to improve vehicle fuel efficiency by approximately 0.53 %.

2. Structure

Fig. 1 shows a schematic drawing of Low Friction HUB Bearing III.

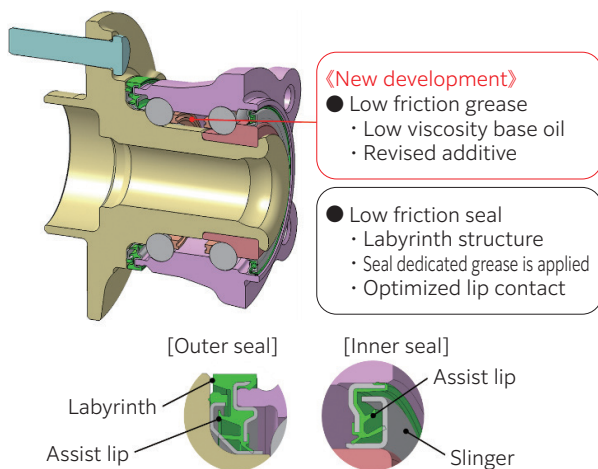


Fig. 1 Structure of Low Friction HUB Bearing III

3. Features

The following are the features of Low Friction HUB Bearing III.

- (1) Application of newly developed low friction grease
- (2) Application of new seal structure with labyrinth
- (3) Application of seal dedicated grease
- (4) Optimization of seal lip contact surface

As shown in Fig. 2, these features reduce bearing friction and outer/inner seal friction to achieve a running torque reduction of 62 % for the entire hub bearing.

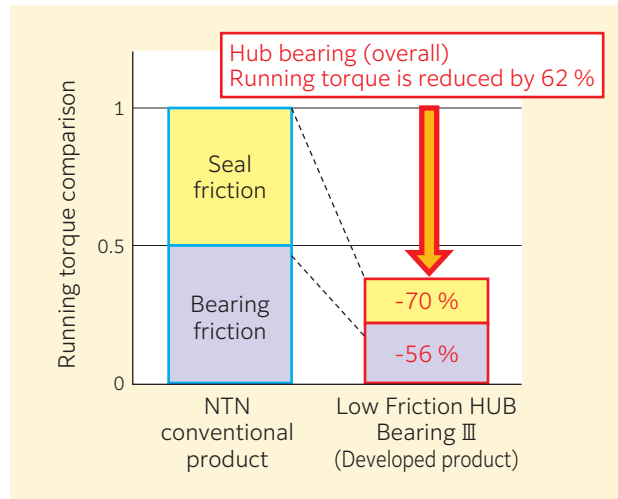


Fig. 2 Hub bearing running torque comparison (an example)

4. Summary

To support stricter emission regulations on CO₂ and improve vehicle fuel efficiency throughout the world, NTN has developed a hub bearing with significantly lower friction over conventional products while meeting the requirements for service life and strength. NTN will continue to develop the market for this product, which is expected to improve vehicle fuel and power consumption efficiency, and also contribute towards reducing the impact on the global environment.

References

- 1) Makoto Seki, Low Friction HUB Bearing III, NTN TECHNICAL REVIEW, No.87, (2019) 63-67.
- 2) Makoto Seki, Low Friction HUB Bearing, NTN TECHNICAL REVIEW, No.85, (2017) 67-71.

Photo of author



Makoto SEKI

Axle Unit Products
Development Dept.,
Axle Products Unit,
Automotive Business
Headquarters

Development of Super Long-Life Tapered Roller Bearings for Automobile

Hiroki FUJIWARA Takashi KAWAI Chikara OHKI

1. Introduction

NTN has developed “Super Long-Life” Tapered Roller Bearings that can be used on automobile transmissions and differentials as well as in electric drive devices (reducers for e-Axle). This product received the 2020 Technology Award from the Japanese Society of Tribologists.

This bearing has an increased resistance to misalignment and contamination and a higher allowable speed. These advancements are possible due to improvements made to the shape of sliding contact areas, the heat treatment method for grain refinement of crystal grain in bearing steel, and the technology used to design the shape of rollers that minimizes the contact stress at the rolling contact surface of roller elements and the raceway surface. These factors enable the automobile drive device to be more compact and lighter in weight, which has been praised for its ability to improve both fuel and power consumption efficiency.

The product that received the award was commercialized as “ULTAGE Tapered Roller Bearing for Automotive Application” (Fig. 1).



Fig. 1 ULTAGE Tapered Roller Bearing for Automotive Application

2. Structure

Fig. 2 shows a schematic drawing of ULTAGE Tapered Roller Bearing for Automotive Application.

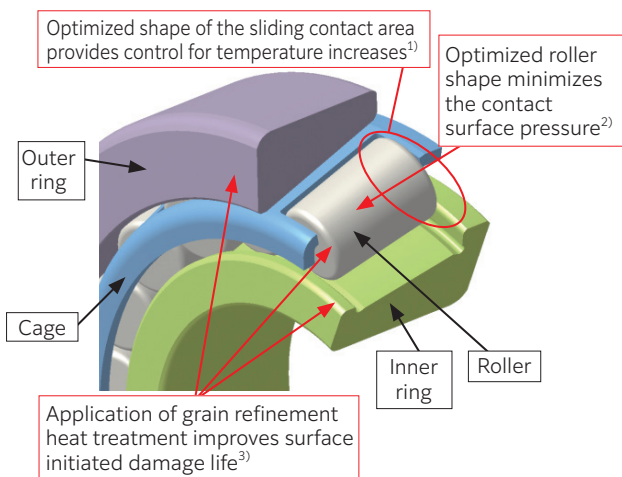


Fig. 2 Structure of ULTAGE Tapered Roller Bearing for Automotive Application

3. Features

- (1) The world’s highest level in high-load capacity
: Basic dynamic load rating⁴⁾ 1.3 times
- (2) Long operating life (comparing basic rating life⁴⁾)
: Standard heat treated type 2.5 times or more
: Grain refinement heat treated type 3.8 times or more
- (3) The world’s highest level in high rotational speed performance
: Allowable speed⁵⁾ Improvement of approx. 10 %
- (4) Allowable misalignment⁵⁾ (misalignment amount)
: Allowable misalignment Up to 4 times

4. Summary

This product was developed to allow for longer operating life for tapered roller bearings. The bearing can also be made smaller dimensionally and achieve the same previous service life. This contributes to making automobile drive devices smaller and lighter, and can also make automobiles more efficient in terms of fuel and power consumption. Furthermore, the longer operating life technology we have developed for this product can also be applied to other areas, which we hope will greatly contribute towards higher optimization of various machines and achieve carbon neutrality.

References

- 1) Yasuhito Fujikake, Takanori Ishikawa, Susumu Miyairi, ULTAGE Tapered Roller Bearing for Automotive Application, NTN TECHNICAL REVIEW, No. 85, (2017) 51-55.
- 2) H. Fujiwara et al., Optimized Logarithmic Roller Crowning Design of Cylindrical Roller Bearings and Its Experimental Demonstration, Tribol. Trans., 53 (2010) 909-916.
- 3) C. Ooki, Improving Rolling Contact Fatigue Life of Bearing Steels Through Grain Refinement, SAE Technical Paper Series, 2004-01-0634.
- 4) JIS B 1518 (2013)
- 5) NTN “Ball and Roller Bearings Catalog” (CAT. No. 2203/J)

Photo of authors



Hiroki FUJIWARA
CAE R&D Center

Takashi KAWAI
Automotive Bearing
Engineering Dept.,
Automotive Bearing Products Unit,
Automotive Business Headquarters

Chikara OHKI
Advanced
Technology R&D
Center

Low Friction Technology of Sealed Ball Bearings for Transmission

Tomohiro SUGAI Katsuaki SASAKI Takahiro WAKUDA

1. Introduction

Lower torque and long operating life are needed for automotive transmission bearings to achieve carbon neutrality. The lubricating oil inside a transmission has contaminants such as gear wear debris which can cause the service life of a rolling bearing to decline. Therefore, countermeasures are provided using methods such as ① preventing contaminants from entering the bearing using a contact seal and ② applying special heat treatment to the rolling bearing ring to improve the service life against contaminants. However, ① places restrictions on the allowable speed due to increased running torque due to the seal and heat generated at the seal. Furthermore, ② is not sufficiently effective at suppressing the decline in service life in comparison with the bearing service life in an environment with no contaminants.

To respond to these issues, NTN has developed technology to reduce running torque while maintaining sufficient service life even when contaminants are present in the lubricating oil^{1,2)}. This technology received the “2021 Japanese Society of Tribologists Technology Award”, which is given for excellent new technology in the field of tribology. This paper introduces this technology.

2. Overview of award-winning technology

With conventional contact seals, the seal sliding surface contacts the inner ring and because a sufficient oil film does not form at the operational speed range, there is a comparatively high drag resistance torque at the seal. In contrast, this technology provides arc-shaped micro convexities on the contact seal sliding surface as shown in **Fig. 1**. These micro convexities generate a fluid film due to the “wedge film effect” between the seal sliding surface and inner ring under oil lubrication. This results in a fluid lubrication state at the operational speed range which reduces the running torque by 80 % when compared to conventional contact seals, as shown in **Fig. 2**. This can achieve the same low torque performance as a non-contact seal despite it being a contact seal. Furthermore, the convexities are of a micro height so they can prevent contaminants of sizes that would cause the service life to decline from entering the bearing. This enables the bearing to maintain a service life equal to a bearing used in an environment with no contaminants.

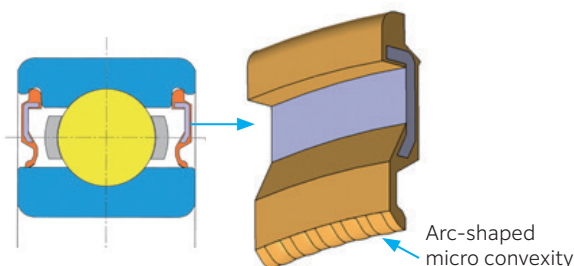


Fig. 1 Schematic drawing of developed seal

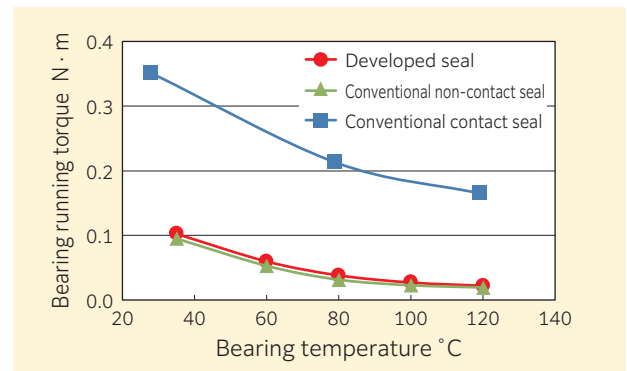


Fig. 2 Bearing running torque experimental results

Additionally, this seal reduces sliding heat generated at the seal contact area so it can also be used under peripheral speed conditions that are two or more times greater than that of a conventional contact seal.

3. Summary

This technology can reduce the running torque of transmission bearings while maintaining sufficient service life even with contaminants in the lubricating oil. This can contribute towards better fuel economy in automobiles. Furthermore, the bearing size can be smaller due to improved reliability which can make automobiles lighter in weight. It can also respond to the demand for speed increases that accompany the electrification of vehicles.

References

- 1) Katsuaki Sasaki, Takahiro Wakuda, Tomohiro Sugai, Ultra-Low Friction Sealed Ball Bearing for Transmission, NTN TECHNICAL REVIEW, No.85, (2017) 62-66.
- 2) Tomohiro Sugai, Katsuaki Sasaki, Takahiro Wakuda, Low Friction Technology of Sealed Ball Bearings for Transmission, Tribology Congress, 2022 Spring Tokyo Proceedings, (2022) B6 85-86.

Photo of authors



Tomohiro SUGAI

Advanced
Technology R&D
Center

Katsuaki SASAKI

Automotive Bearing
Engineering Dept.,
Automotive Bearing
Products Unit,
Automotive Business
Headquarters

Takahiro WAKUDA

Automotive Bearing
Engineering Dept.,
Automotive Bearing
Products Unit,
Automotive Business
Headquarters

Estimation Method of Micropitting Life from $S-N$ Curve Established by Residual Stress Measurements and Numerical Contact Analysis

Naoya HASEGAWA Takumi FUJITA Michimasa UCHIDATE Masayoshi ABO Hiroshi KINOSHITA

1. Introduction

The above-mentioned paper¹⁾ submitted to the Japanese Society of Tribologists (non-profit organization) academic journal "Tribology Online" received the 2021 Best Paper Award. The content of this paper is introduced below.

2. Overview

Peeling (referred to as micropitting in the paper) is the typical damage seen on bearings under severe lubrication conditions. It refers to a concentration of micro spalling caused by cyclic contact of projections on rough surface. This paper proposed a new peeling life estimation method utilizing experimental results.

This method estimates the peeling life using the following procedure.

- 1) A rolling fatigue test is conducted under various operating conditions. Time series data (hereafter, stress history) for cyclic stress at areas of projection contact and peeling life during each test is acquired. The stress history is estimated using the measurement results of surface roughness and residual stress during the operation.
- 2) Regression analysis is performed on the obtained data, and a $S-N$ curve that shows the relationship between cyclic stress and peeling life is created.
- 3) A preliminary test simulating the subject operating conditions is conducted. Stress history under those conditions is obtained. The peeling life is then estimated using the $S-N$ curve created in 2) above and Miner's rule.

To estimate peeling life under various conditions, actual measured data was utilized to increase the precision of life estimation. Furthermore, another feature of this method is that it considers the effect of residual stress on life, something that was difficult to do in the past. However, it must be noted that the application range of this estimation method is limited to pure rolling and boundary lubrication conditions.

Fig. 1¹⁾ shows the relationship between the actual life L_{act} and the peeling life L_{est} estimated using this method. The median, minimum value and maximum

value of the life ratio (L_{act} / L_{est}) is 0.89, 0.49 and 1.82 respectively. This precision is comparable to or better than the generally used spalling life estimation of the rolling bearing. This method is considered sufficiently applicable as an estimation method for peeling life.

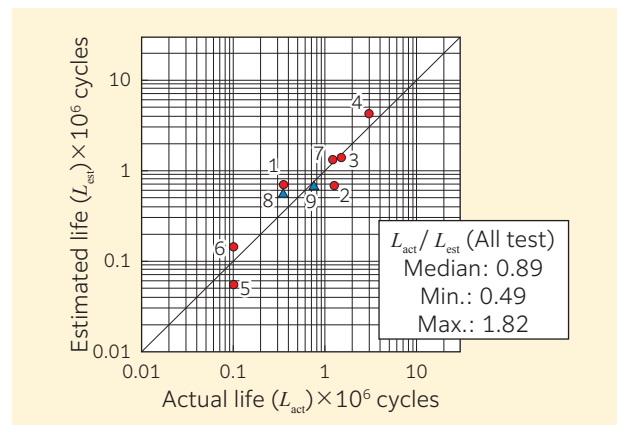


Fig. 1 Relationship between estimated life and actual life¹⁾

3. Summary

Even greater progress is expected in the future to achieve higher efficiency of machines for achieving carbon neutrality by lowering the viscosity of lubricating oils. This increases the likelihood of bearings being used under thin lubrication conditions. Life estimation under conditions similar to those used in this study will become an important technology for maintaining the reliability of bearing life prediction. In the future, **NTN** will strive to increase the application range of this estimation method and further improve its accuracy.

References

- 1) N. Hasegawa, T. Fujita, M. Uchidate, M. Abo & H. Kinoshita: Estimation Method of Micropitting Life from $S-N$ Curve Established by Residual Stress Measurements and Numerical Contact Analysis, Tribology Online, 14, 3 (2019) 131.

Photo of authors



Naoya HASEGAWA

Advanced
Technology R&D
Center



Takumi FUJITA

Product and Business
Strategic Planning
Dept.



Michimasa UCHIDATE

Faculty of Science and
Engineering,
Iwate University



Masayoshi ABO

School of
Engineering,
University of Hyogo



Hiroshi KINOSHITA

School of
Engineering,
University of Hyogo

DLC Coating Spherical Roller Bearing for Wind Turbine Main Shaft

Kazumasa SEKO Takashi YAMAMOTO Masaki NAKANISHI

1. Introduction

“DLC Coating Spherical Roller Bearing for Wind Turbine Main Shaft” received the “New Energy Foundation Chairman Award (products and services category)” of the 2021 New Energy Awards sponsored by the New Energy Foundation.

The award-winning product substantially improves the wear resistance of the raceway surface and rolling contact surface of rolling elements by applying a DLC (diamond-like carbon) coating* to the rolling contact surface of rolling elements. This has been highly regarded for its significant contribution towards improving the reliability of wind turbines.

* A hard film consisting of a mixture of a diamond structure and graphite structure

2. Structure

Fig. 1 shows the structure of the DLC Coating Spherical Roller Bearing for Wind Turbine Main Shaft.

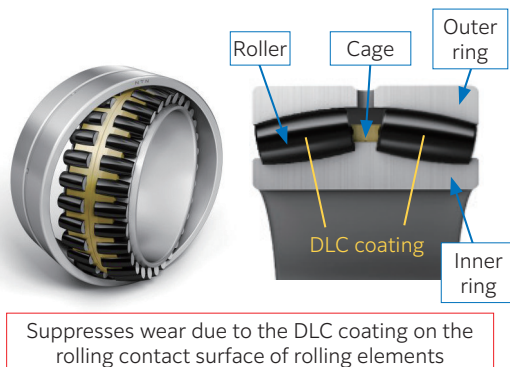


Fig. 1 DLC Coating Spherical Roller Bearing for Wind Turbine Main Shaft

3. Features

When there is insufficient lubrication during operation with conventional spherical roller bearings, metal on the roller raceway surface and rolling contact surface of rolling elements makes contact, resulting in wear on the raceway surface. This contact and resultant wear causes spalling and cracks to occur.

The DLC Coating Spherical Roller Bearing for Wind Turbine Main Shaft can suppress wear on the raceway surface even under harsh lubrication conditions by applying a DLC coating. The DLC coating has a 3-layer structure that provides excellent adhesion to the base material on the rolling contact surface of rolling elements.

During a wear test on smaller sized bearings, NTN

confirmed that wear depth on the outer ring raceway surface was suppressed by 1/9 or less in comparison with a conventional product (Fig. 2).

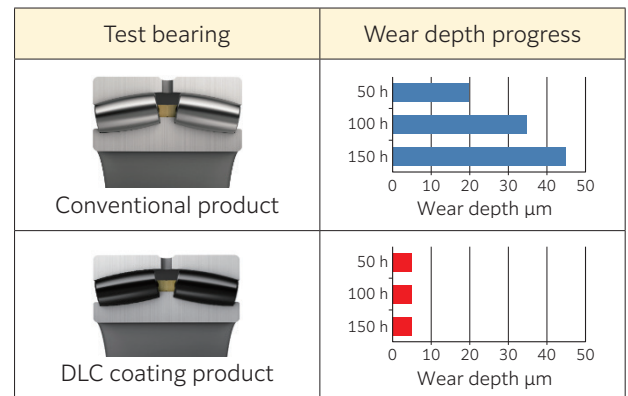


Fig. 2 Wear test results

4. Summary

The main bearings on a wind turbine repeatedly rotate and stop based on wind conditions, and are used under harsh lubrication conditions. Moreover, replacing the main bearings is not an easy task. Therefore, it is necessary to avoid spalling and cracks due to wear on the main bearings because such factors are directly linked to a drop in the reliability of wind turbines.

DLC Coating Spherical Roller Bearing for Wind Turbine Main Shaft is a product that responds to these issues, and can contribute towards improving the reliability of wind turbines by developing the market for this type of product.

References

- 1) Michio Hori, Yusuke Yamada, New Products and Improved Reliability of Main Bearings for Wind Turbine Generators, NTN TECHNICAL REVIEW, No.88, (2021) 15-20.

Photo of authors



Kazumasa SEKO
Application
Engineering Dept.,
Industrial Business
Headquarters

Takashi YAMAMOTO
Product Design
Dept.,
Industrial Business
Headquarters

Masaki NAKANISHI
Advanced
Technology R&D
Center

NTN TECHNICAL REVIEW No.89

Printed and published in December 25, 2023

Editor **Masaki EGAMI**

Published by **NTN Corporation**
Daibiru-Honkan Bldg., 3-6-32, Nakanoshima,
Kita-Ku, Osaka 530-0005, Japan

Publisher **Tatsuo NAGAO**

Printed by Daishinsha Delight Inc.

No part of this publication may be reprinted
or reproduced without the prior permission
of the copyright owner.

Sales Network



